TECHNISCHE UNIVERSITÄT MÜNCHEN

Lehrstuhl für Steuerungs- und Regelungstechnik

Performance-Oriented Distributed Control Design for Interconnected Systems

Azwirman Gusrialdi

Vollständiger Abdruck der von der Fakultät für Elektrotechnik und Informationstechnik der Technischen Universität München zur Erlangung des akademischen Grades eines

Doktor-Ingenieurs (Dr.-Ing.)

genehmigten Dissertation.

Vorsitzender: Univ.-Prof. Dr. rer. nat. Th. Hamacher

Prüfer der Dissertation:

1. Univ.-Prof. Dr.-Ing. S. Hirche

2. Prof. Dr.-Eng. M. Fujita
   Tokyo Institute of Technology / Japan

Die Dissertation wurde am 11.06.2012 bei der Technischen Universität München eingereicht und durch die Fakultät für Elektrotechnik und Informationstechnik am 21.08.2012 angenommen.

Acknowledgements

This dissertation would not have been possible without the support of many people. First of all, I would like to express my gratitude to my advisor, Prof. Sandra Hirche for giving me a controllable freedom to conduct my research on the topics that I am interested in. I really enjoyed the time I spent on discussing a variety of topics with her. I would also like to thank Sandra for the opportunity so that I could conduct my research in an excellent environment in which I could learn a lot of things outside the domain of my research area.

I would also like to thank my collaborators during my Ph.D. journey. Especially, I am grateful to work with Junqi Liu on the control of power systems which resulted in one paper included in this dissertation. My research topic was also inspired during our discussion on his master thesis. In addition, I would like to thank Dr. Changbin Yu for his hospitality during my visit to ANU, Australia and also for the discussion we had which contributed to one chapter of my dissertation. My thanks also go to Huang-Huang for our collaboration during my short, but fruitful visit at ANU, Risvan Dirza for his support on the simulation of coverage control problem, Alexander Moertl and Tamara Lorenz for our collaboration on human-human coordination project and Jun Li for our collaboration on human reaching movement modeling. Collaborating with them really enriched my knowledge.

My life in Munich would not be colorful without my colleagues. I would like to thank my colleagues and the staffs at LSR, especially the Murola group in which I spent the first year of my Ph.D, the Network Control Systems group, in particular Adam Molin, Iason Vittorias and Herbert Mangesius for helping me with all the German-related documents and matters during my stay in Munich. My special thanks go to Vicky Koropouli and Wei Wang for the wonderful time we had during the lunch break and also the culinary adventure. I also extend my sincere thanks to the Indonesian community and my friends (B.S. Darwanto's family, E. Sunarkito's family, D. T. Nugraha's family, Syaiful Rahman, Ferizal Ramli, Afandi, Winnu, Eriza, Rizqy, Nisa, Angga, Adam Hermawan, just to name a few) in Munich for making me always feel like being at home whenever I miss my home country. Last but not least, I would like to thank my parents and brother for their unconditional support and trust on me during my stay abroad in the last 11 years. I believe that without their invisible hand, I would not reach this step.

Munich, June 2012 Azwirman Gusrialdi

to my parents ...

Abstract

The control of complex dynamical systems, such as power networks, is a very challenging task due to its complexity in terms of the number of subsystems and their interconnections. This limits the use of conventional centralized control method and motivates the development of decentralized control method. The basic idea is to design the control law based only on local model obtained from the decomposition of the weakly interconnected subsystems. However, this method may not work when the coupling between the subsystems is not weak and suffers from performance degradation compared to the centralized one. Digital communication networks allow the communication between the subsystems and thereby provide a larger flexibility for control design: instead of only local subsystem information also neighboring subsystems states can be used for the control, known as distributed control. As a result, typically a better performance is achieved compared to the decentralized approach. Additionally, the information exchange can also be utilized to stabilize the interconnected system when no stabilizing decentralized control law exists.

Despite the advantages of distributed control, its design poses several new challenges. The objective function of the distributed optimal control problem is in general non-convex. Furthermore, the incorporation of communication topology into the control design increases the problem complexity due to the combinatorial search that has to be performed. Another challenge is the unavailability of the entire model of the interconnected system in reality for designing the control law. Finally, while the use of communication network may improve the system performance, it comes at the price that the system may become unstable under permanent communication link failures.

This dissertation focuses on the design of distributed control for interconnected systems such that the overall system performance is optimized. So far unique is the exploitation of the additional degree of freedom offered by the communication network in designing the distributed control law, namely taking into account the communication topology and the information that needs to be exchanged between the local controllers. Specifically, the contributions of this dissertation are summarized as follows. First, a novel two-layer control architecture which is a combination of decentralized and distributed control is proposed that allows to jointly improve the system performance and guarantee its stability under permanent communication link failures. Following this, explicit solutions for topology design of distributed control law are studied and discussed here for the first time. The unique approach lies in the utilization of eigenvalue sensitivity analysis to transform the original combinatorial problem into the one which allows for more insightful analysis. Furthermore, a novel coordination algorithm based on decomposition of a global objective function is developed to design distributed control in the absence of global plant model information. Finally, an innovative approach to design distributed control for a coverage control problem which guarantees that the system avoids undesired local optima of a non-convex objective function is proposed by exploiting the use of information which can be communicated.

Zusammenfassung

Die Regelung komplexer dynamscher Systeme, wie es zum Beispiel elektrische Energieversorgungsnetze sind, ist eine äusserst anspruchsvolle Aufgabe. Systemkomplexität bezieht sich hierbei auf die hohe Anzahl von Untersystemen und die Art wie diese miteinander verbunden sind und somit wechselwirken. Aufgrund dieser Charakteristik ist der erfolgreiche Einsatz klassischer, zentralisierter Regelungsverfahren begrenzt, worin gleichzeitig die Motivation für dezentrale Regelungsstrategien liegt. Der Grundgedanke ist es den Regler auf Basis lokaler Modelle, die aus der Zerlegung schwach wechselwirkender Untersysteme gewonnen werden, zu entwerfen. Verglichen mit zentralen Regelungsverfahren kann eine dezentrale Regelungsmethode im Falle nichtschwacher wechselseitiger Kopplung allerdings zum Abfall der Regelgüte führen. Digitale Kommunikationsnetze ermöglichen Kommunikation zwischen Untersystemen, woraus sich Flexibilität (durch zusätzliche Freiheitsgrade) im Reglerentwurf ergibt: Zustände benachbarter Untersysteme können für die lokale Regelung ebenfalls zunutze gemacht werden, anstatt lediglich lokale Information zu gebrauchen, was als verteilte Regelung bekannt ist. Infolgedessen kann im Vergleich zu dezentralen Methoden typischerweise eine verbesserte Regelgüte erzielt werden. Zudem ermöglicht eine angemessene Verwendung von Informations- und Nachrichtenaustausch eine Stabilisierung von vernetzten Systemen auch wenn kein stabilisierendes dezentrales Regelgesetz existiert.

Den Vorteilen verteilter Regelungseinrichtungen stehen neuartige Herausforderungen im erforderlichen Entwurfsprozess gegenüber. Die Zielfunktion des verteilten optimalen Regelungsproblems ist im Allgemeinen nichtkonvex. Wird zudem der Entwurf der Kommunikationstopologie berücksichtigt, so erhöht sich die Komplexität des Entwurfsproblems um den Aufwand einer notwendigen kombinatorischen Suche. Schließlich kommt der Nutzen einer Verwendung von Kommunikationsnetzen hinsichtlich der Regelungsgüte auf Kosten möglicher Instabilität im Falle andauernden Ausfalls von Nachrichtenverbindungen.

Diese Dissertation behandelt den Entwurf verteilter Regelungsgesetze für vernetzte Systeme mit dem Ziel des Erreichens einer optimalen Performanz des Gesamtsystems. Eine grundlegende Neuerung im Entwurf eines verteilten Regelungsgesetzes ist die Nutzung des Komunikationsnetzes als zusätzlichen Freiheitsgrad; die Struktur der Kommunikationstopologie und die spezifische lokale Information, die unter lokalen Reglern wechselseitig ausgetauscht wird, findet dabei Berücksichtigung. Im Speziellen ist der Beitrag dieser Dissertation wie folgt zusammengefasst: Zunächst wird eine neuartige zweischichtige Regelungsarchitektur als Kombination von dezentraler und verteilter Regelung vorgestellt, die eine Performanzverbesserung unter garantierter Wahrung der Gesamtsystemstabilität ermöglicht bei anhaltendem Ausfall von Nachrichtenverbindungen. Dann werden explizite Lösungen für den Topologieentwurf in verteilten Regelungseinrichtungen zum ersten Mal studiert und diskutiert. Als Ansatz zum überwinden der kombinatorischen Natur des Problems dient eine Eigenwertsensitivitätsanalyse, die eine einsichtsvollere Analyse erlaubt. Darüberhinaus wird ein neuartiger Algorithmus zum koordinierten Berechnen verteilter Regelgesetze, welche nicht über vollständige Modellinformation verfügen, hergeleitet, basierend auf einer Zerlegung der globalen Zielfunktion. Abschließend ist ein innovatives Verfahren zum Entwurf verteilter Regelungsgesetze in einem "Coverage"-Problem vorgestellt. Hierbei kann durch gezieltes Austauschen von Information das Erreichen ungewünschter lokaler Optima einer nichtkonvexen Zielfunktion unter Garantie vermieden werden.

Contents

1 Introduction **1**
- 1.1 Challenges . . . 3
- 1.2 Related Work . . . 4
- 1.3 Main Contributions and Outline of Dissertation . . . 7

2 Modeling of Interconnected Systems **10**
- 2.1 Power System . . . 10
  - 2.1.1 Generator and Exciter System Model . . . 11
  - 2.1.2 Network Model . . . 11
  - 2.1.3 State Space Model . . . 12
- 2.2 Thermal Model of Large Buildings . . . 13
  - 2.2.1 Heat Transfer . . . 13
  - 2.2.2 State Space Model . . . 15
- 2.3 Deformable Mirrors . . . 17
  - 2.3.1 Dynamic Deformable Mirrors . . . 18
  - 2.3.2 State Space Model . . . 19
- 2.4 Summary and Discussion . . . 20

3 Two-layer Control Architecture for Interconnected Systems **21**
- 3.1 Problem Formulation . . . 22
- 3.2 Two-layer Control Architecture . . . 23
  - 3.2.1 Decentralized Control Design . . . 24
  - 3.2.2 Joint Distributed Control Gain-Communication Topology Design . 26
  - 3.2.3 Evaluation . . . 28
- 3.3 Two-layer Control Architecture for Time-Delay Systems . . . 33
  - 3.3.1 Distributed Control Design . . . 35
  - 3.3.2 Evaluation . . . 36
- 3.4 Application to Power Systems . . . 37
  - 3.4.1 Distributed Damping Control for Power Systems . . . 38
  - 3.4.2 Evaluation . . . 40
- 3.5 Summary and Discussion . . . 41

4 On the Explicit Solution of Communication Topology Design **46**
- 4.1 Problem Formulation . . . 46
  - 4.1.1 Adding Communication Links is not Always Beneficial . . . 48
- 4.2 Eigenvalue Sensitivity based Approach . . . 49
- 4.3 Explicit Solution for Special Class of Physical Topology . . . 55
  - 4.3.1 Ring Topology Case . . . 55

4.3.2 Star Topology Case . . . 56
4.3.3 Line Topology Case . . . 59
4.4 Explicit Solution for Multidimensional Subsystems . . . 61
4.5 Explicit Solution for Multiple Communication Links . . . 63
4.6 Explicit Solution for Complex Physical Topology . . . 64
4.7 Eigenvalue Sensitivity for Distributed Control with Time Delay . . . 68
4.7.1 Sensitivity to Communication Link . . . 69
4.7.2 Sensitivity to Time Delay . . . 70
4.8 Evaluation . . . 70
4.8.1 Single Communication Link . . . 70
4.8.2 Multiple Communication Links . . . 71
4.9 Summary and Discussion . . . 72

5 Distributed Control Design under Limited Model Information 74
5.1 Problem Formulation . . . 75
5.2 Proposed Distributed Algorithms . . . 78
5.2.1 Two-layer Control Architecture . . . 79
5.2.2 Cost Function Decomposition . . . 80
5.2.3 Distributed Control Design - Single Communication Link . . . 83
5.2.4 Distributed Control Design - Multiple Communication Links . . . 86
5.2.5 Complexity of the Proposed Approach . . . 87
5.3 Evaluation . . . 87
5.4 Summary and Discussion . . . 90

6 Performance-Oriented Distributed Coverage Control for Robotic Sensor Networks 92
6.1 Problem Formulation . . . 94
6.1.1 Region of Interest . . . 94
6.1.2 Sensor Model . . . 94
6.1.3 Communication Graph . . . 96
6.1.4 Optimal Coverage Formulation . . . 96
6.1.5 Distributed Coverage Algorithm . . . 97
6.2 Proposed Coverage Algorithm . . . 97
6.2.1 Global Leader based Algorithm . . . 98
6.2.2 Local Leader based Algorithm . . . 100
6.2.3 Leader Election's Complexity . . . 106
6.3 Evaluation . . . 107
6.4 Summary and Discussion . . . 108

7 Conclusions and Future Directions 115
7.1 Concluding Remarks . . . 115
7.2 Outlook . . . 117

A Power systems simulation parameters 118

B Proofs **119**
B.1 Proof of Proposition 4.3.1 119
B.2 Proof of Proposition 4.3.2 120
B.3 Proof of Lemma 4.3.4 127
B.4 Proof of Proposition 4.4.1 129
B.5 Proof of Proposition 4.4.2 129
B.6 Proof of Lemma 4.7.1 130
B.7 Proof of Lemma 4.7.3 130

Notations

Abbreviations

LTI	Linear Time Invariant
LMI	Linear Matrix Inequality
BMI	Bilinear Matrix Inequality
DFM	Decentralized Fixed Mode
AVR	Automatic Voltage Regulator
PSS	Power System Stabilizers
PMU	Phasor Measurement Units
WAMS	Wide-Area Measurement Systems
WACS	Wide-Area Control Systems
FACTS	Flexible AC Transmission System
LQR	Linear Quadratic Regulator
LQG	Linear Quadratic Gaussian
MISDP	Mixed Integer Semidefinite Program

Conventions

Scalars, Vectors, and Matrices

Scalars are denoted by upper and lower case letters in italic type. Vectors are denoted by lower case letters in boldface type, and a vector $\boldsymbol{x}$ is composed of elements x_i. Matrices are denoted by upper case letters in boldface type.

x	scalar
$\boldsymbol{x}$	vector
$\boldsymbol{X}$	matrix
$f(\cdot)$	scalar function
$\dot{\boldsymbol{x}}$	equivalent to $\frac{\mathrm{d}}{\mathrm{d}t}\boldsymbol{x}$
$\boldsymbol{x}^*$	complex conjugate transpose of vector $\boldsymbol{x}$
$\boldsymbol{X}^T$	transposed of matrix $\boldsymbol{X}$
$\boldsymbol{X}^{-1}$	inverse of matrix $\boldsymbol{X}$
$\lvert\boldsymbol{X}\rvert$	determinant of $\boldsymbol{X}$

Symbols

Subscripts and Superscripts

$\lambda_{\max}(\cdot)$	largest real part of the eigenvalues
$\tau_{\max}$	performance-guaranteed time delay bound
α_τ	delay decay rate
$\boldsymbol{w}_i$	left eigenvector w.r.t. the $i-$th eigenvalue
$\boldsymbol{v}_i$	right eigenvector w.r.t. the $i-$th eigenvalue
$\boldsymbol{v}_r$	left eigenvector w.r.t. the largest real part of the eigenvalue

General

$\boldsymbol{I}_n$	$n \times n$ identity matrix
$\boldsymbol{O}_n$	$n \times n$ zero matrix
$\text{diag}(\boldsymbol{x})$	diagonal matrix with $\boldsymbol{x}$ as the main diagonal entries
$\|\| \cdot \|\|$	Euclidean norm
$\|\| \cdot \|\|_2$	second norm
$\lambda(\cdot)$	eigenvalue
$\kappa_2(\cdot)$	condition number
$\mathcal{X}$	set
$\|\mathcal{X}\|$	cardinality of the set $\mathcal{X}$
$\mathbb{R}$	real numbers
$\mathbb{R}_+$	positive real numbers
τ	time delay
σ	real part of eigenvalue
β	imaginary part of eigenvalue
$\otimes$	Kronecker product
$\lfloor x \rfloor$	the largest integer not greater than x
$\lceil x \rceil$	the smallest integer not less than x
$\text{sign}(x)$	sign function, $\text{sign}(x) = \begin{cases} 1 & \text{for } x > 0 \\ -1 & \text{for } x < 0 \end{cases}$

Graph Theory

$\mathcal{G} = (\mathcal{V}, \mathcal{E})$	graph $\mathcal{G}$ with vertices $\mathcal{V}$ and edges $\mathcal{E}$
$\deg(i)$	degree of node i in the graph
$D_{\mathcal{G}}(i, j)$	distance between nodes i and j in graph $\mathcal{G}$

Power System

$\Delta[\bullet]$	increments of the variables
δ_i	rotor angle of i-th machine [rad]
ω_i	rotor speed of i-th machine [rad/s]
E'_{qi}	internal transient voltage in q-axis of i-th machine [p.u.]
M_i	inertia constant of i-th machine [s]
Z_i	damping power coefficient of i-th machine [p.u.]
X_{di}	synchronous reactances in d-axis of i-th machine [p.u.]
X'_{di}	transient reactance in d-axis of i-th machine [p.u.]
T'_{doi}	open-circuit d-axis transient time constant of i-th machine [s]
P_{ei}	active power delivered at the terminals of i-th machine [p.u.]
E_{fi}	electromotive force [p.u.]
$b_{1i}, b_{0i}, c_{1i}, c_{0i}$	coefficients of the transfer function of the voltage control and excitation systems
H_{ij}, L_{ij}	transfer conductance and susceptance between buses i and j respectively [p.u.]
ξ	relative damping ratio

Thermal Model of Large Buildings

q_x	heat transfer rate
T_h	high temperature
T_l	low temperature
L	length of material
k	thermal conductivity
R_{th}	thermal resistance
q	convective heat transfer
T_s	surface temperature
T_∞	fluid temperature
A	surface area
h	convection heat transfer coefficient
R_{cv}	thermal resistance for convection
q_{rad}	net heat radiation transfer
ϵ	emissivity of the surface
σ	Stefan-Boltzman constant
T_{sur}	surrounding temperature
C_i	thermal capacity
ρ_a	density of air at room temperature
V_i	volume of room i

Deformable Mirrors

Δ	smallest distance between actuators
η	relative material damping
ζ	relative actuator damping
E	Young's modulus
k	thermal conductivity
$\mathcal{G}$	finite difference operator
I	moment of inertia
N	number of actuators
$\mathcal{P}_N$	pattern matrix of size $N \times N$
$S_{1/2}$	shift operator along principal axis $s_{1/2}$
c	actuator stiffness
d	actuator damping
f_i	force supplied by actuator i
h	plate thickness
p	actuator pressure
s_1, s_2	principal axis in hexagonal grid
w	deflection of the mirror
ρ	density

Coverage Control

$\mathcal{Q}$	region of interest
$\phi(\cdot)$	density function
$\boldsymbol{s}_i$	position of sensor i
d_i	distance between sensor i and point of interest
R	sensing range of the sensor
R_c	communication range of the sensor
p_i	detection probability of an event by sensor i
I_i	information value of sensor i
h_{ij}	distance between sensor i and sensor j
P	joint detection probability
F	coverage objective function
l^g	global leader
l	local leader(s)
$\mathcal{G}$	communication topology of the sensors
$\mathcal{G}^s$	core structure of the sensors which is a spanning tree

List of Figures

1.1 Examples of large-scale systems: (a) smart grid [3]; (b) wireless sensor networks [1]; (c) traffic network [2]; (d) water distribution network [4]. 1
1.2 Three different control architectures for interconnected systems. Left: centralized control architecture; middle: decentralized control architecture; right: distributed control architecture with information exchange between the local controllers. 2
1.3 Outline of the dissertation. 8

2.1 Automatic voltage regulator model. 11
2.2 Equivalent thermal circuit of heat transfer through a plane wall. 15
2.3 Simple two-room building. 17
2.4 An adaptive optics mirror. Each circle contains an actuator. 17
2.5 A deformable mirror with a thin plate membrane suspended by springs with stiffness c and dampers with damping d and controller by force actuators. . 18
2.6 Infinite hexagonal grid, schematized as $\mathbb{Z}^2$. 19

3.1 An interconnected system with distributed control architecture. 22
3.2 Two-layer control architecture. The decentralized control law stabilizes the interconnected system while the distributed control law improves the overall system performance. 23
3.3 An interconnected system consisting of 20 subsystems. 29
3.4 Optimal communication topology for $\gamma_{ij} = 1, c = 15$. As can be seen, only 14 communication topology is used. This means that adding more communication links will not improve the overall system performance. The solid and dashed lines represent the physical and communication links respectively. 31
3.5 The convergence rate of the interconnected system with the distributed control law and the decentralized control law. Furthermore, as can be seen from the figure, by using the proposed two-layer control architecture, the stability of the overall system is guaranteed under permanent communication link failures. 32
3.6 The convergence rate of the interconnected system with different number of communication links. As can be seen, from a certain number of communication links, the performance improvement becomes smaller. 33
3.7 An interconnected system with distributed control architecture. The communication network has a constant and identical time-delay τ. 34
3.8 Interconnection system consisting of ten subsystems. The solid and dash lines represent the physical interconnection and the optimal communication topology for number of links equal to 2 respectively. 36

3.9 The convergence of the interconnected system with the distributed control law and the decentralized control law. 37
3.10 A five machine power system for case study. 38
3.11 (a) Interconnected system used in the simulation; (b) the optimal communication topology. 40
3.12 Response to disturbance of the generator G_1. 42
3.13 Response to disturbance of the generator G_2. 42
3.14 Response to disturbance of the generator G_3. 43
3.15 Response to disturbance of the generator G_4. 43
3.16 Response to disturbance of the generator G_5. 44

4.1 An example of a plant graph. The edges represent the physical interconnection between the subsystems/nodes. 48
4.2 Largest eigenvalue and Gershgorin discs. 49
4.3 An example of movements of the largest and the second largest eigenvalue of a matrix due to a perturbation which degrade the overall system's performance. 53
4.4 Sufficient condition for the distributed control gain such that the overall system performance is improved, i.e. the largest eigenvalue $\lambda_{\max}$ should move at most distance of $|\lambda_{\max} - \lambda_m|$. 55
4.5 Physical topology of the interconnected system investigated in the dissertation: ring, star and line topology. The physical interconnection between the subsystems are identical. 56
4.6 (a) Disconnected two-star topology with equal number of subsystems $\bar{N}$; (b) Interconnected system whose physical topology is given by a two-star network. 65
4.7 Plant graphs for interconnected system with star topology. The solid line represents the physical interconnection and the dashed line represents the communication link. 71
4.8 (a) The elements of eigenvector corresponding to the largest eigenvalue for interconnected system with ring topology with $N = 20$; (b) The optimal communication topology for number of links equal to 5. The solid line represents the physical interconnection and the dashed line represents the communication link. 72

5.1 (a) Centralized design method where a central computer collects the information of the whole interconnected system and compute the distributed control law based on the information gathered; (b) Proposed distributed design method where the design is performed in each subsystem's local computer by coordinating with its neighbors' local computer. Each local computer only has limited model information on the plant, i.e. its own local dynamics, its neighbors' local dynamics and the interconnection between them. 76
5.2 Example of physical interconnected system. 77

5.3 Limited model information for each subsystem in interconnected system shown Fig. 5.2. Each subsystem has the knowledge of its physical neighbors' local dynamics and the interconnection between them. 78
5.4 Proposed distributed design method. First, the global cost function is decomposed into the summation of local cost functions. The optimization is then solved for each local cost function. Finally, a voting is conducted to obtain a global solution from the solution of the local optimization problems. 79
5.5 Examples of the optimal communication link resulted from the voting. The dashed line represents the optimal communication link. The first case is when the optimal link comes from subproblem 1 and the second case when it comes from subproblem 2. 84
5.6 Interconnected system consists of ten subsystems. The solid lines represent the physical interconnection. The dash and dash-dot lines represent the optimal communication topology for number of links equal to two by means of centralized and distributed design respectively. 88

6.1 The region of interest $\mathcal{Q}$ and its density function $\phi(\boldsymbol{q})$. Regions with a high value of ϕ are regions of higher chances of finding a point of interest. In general, there are some regions in $\mathcal{Q}$ where $\phi(\boldsymbol{q}) = 0$. 95
6.2 Example of communication graph of the sensor networks. The dashed circles represent the communication range and the solid lines represent the communication links. 96
6.3 Example of (a) global leader and (b) local leaders case. For the global leader case, a leader is elected among all sensors in the network while for the local leader case, each sensor assigned himself either as a leader of follower to the other by comparing its information value with its neighbors. The sensor with outgoing arrow is a follower to its local leader, that is the sensor with ingoing arrow as shown in (b). Moreover, as can be seen from (b), sensor 4 acts as a follower and also a local leader for sensor 3 and sensor 5. 102
6.4 (a) Communication topology of the sensors; (b) Core structure which is a spanning tree whose connectivity needs to be maintained by the mobile sensors. 103
6.5 Example of worst case scenario. At the initial deployment, the distance between the sensors is closed to the limitation of the communication range R_c of its neighbors. Furthermore, only sensor 1 which is not an isolated sensor, i.e. $I_1 > 0$ while the other sensors are isolated ones, i.e. $I_i = 0, i \neq 1$. Using the standard algorithm [84] no sensors participate in the coverage task. 106
6.6 Simulation results using the proposed algorithm based on both the global and local leader and the standard algorithm [84] for different value of $\boldsymbol{p}_t$: (a) final value of the objective function. Higher value of F means better coverage performance; (b) time-step until all sensors converge to the final configuration. As can be seen from (a), both the proposed algorithms outperform the standard algorithm. The local leader based algorithm results in a lower final objective function and a slower convergence time compared to one with the global leader. 110

6.7 Final configuration of the sensors by using (a) the standard algorithm in [84]; (b) the proposed algorithm with local leader. The area inside the dashed circle has higher density function. As can be seen from (a), by using the standard algorithm, only sensor 1 which could participate in the coverage task since the rest do not have sufficient information. Thus in the final configuration, there exists several isolated sensors. Meanwhile, as can be observed from (b), by using the proposed algorithm, all sensors participate in the coverage task, i.e., there is no isolated sensors in the final configuration. 111

6.8 Objective function of the coverage problem. The solid, dashed-dot and dashed line represent the evolution of the objective function by using the proposed algorithm with local leader, the proposed algorithm with global leader and the standard algorithm in [84] respectively. As can be seen, both the proposed algorithms result in a better coverage performance compared to the standard coverage algorithm in [84] indicated by a higher value of the objective function. The proposed algorithm with local leader achieves a lower final objective function value and converges slower compared to the algorithm with the global leader. This is due to that for the global leader case, the communication range is assumed to be unlimited so that the sensors do not need to maintain the connectivity among themselves. . 112

6.9 Connectivity between the sensors during the deployment. The solid and dashed line represent the connectivity between the mobile sensors with the proposed algorithm and with the proposed algorithm without considering connectivity maintenance. As can be seen, without the connectivity maintenance, the topology between the sensors will be disconnected, indicated by the algebraic connectivity value equals to 0. 112

6.10 (a) Trajectories of the mobile sensors during the deployment using the proposed algorithm with a global leader and (b) The information value of each sensor and the time of switching into a pure coverage algorithm for the followers. The solid line in (b) represents the evolution of the information value of each sensor over the time. 113

6.11 Snapshots of the deployment of the sensors with unlimited communication range using the proposed algorithm with a global leader at: (a) Initial Condition; (b) Step = 100; (c) Step = 150; (d) Final Condition. The area inside the dashed circle has higher density function. The lines connecting the sensors represent the communication graph between the sensors. 113

6.12 (a) Trajectories of the mobile sensors during the deployment using the proposed algorithm with local leader and (b) The information value of each sensor and the time of switching into autonomous deployment mode for the followers. The solid line in (b) represents the evolution of the information value of each sensor over the time. 114

6.13 Snapshots of the deployment of the sensors using the proposed algorithm with local leader at: (a) Initial Condition; (b) Step = 200; (c) Step = 300; (d) Final Condition. The area inside the dashed circle has higher density function. The lines connecting the sensors represent the communication graph between the sensors. As can be seen, there is no isolated sensors in the final configuration. 114

List of Tables

3.1 The largest eigenvalue for different number of communication links 30
3.2 Eigenvalue analysis of the test system 41
3.3 Squared integrated control error of the rotor angle deviations 41

5.1 The optimal link for each local subproblem ($c = 1$) 89
5.2 The optimal link for each local subproblem ($c = 2$) 89
5.3 Optimal links for centralized and distributed design 89
5.4 Cost comparison between centralized and distributed design 90

6.1 Comparison between global leader and local leader(s) 101

A.1 Generator parameters 118
A.2 Generator operating points 118
A.3 Parameters of transmission lines [p.u.] 118

List of Algorithms

1 Joint control gain-communication topology design-single link case 85
2 Joint control gain-communication topology design-multiple links case . . . 86

3 Proposed distributed algorithm with a global leader 100
4 Proposed distributed algorithm for sensor i ($i \in \{1, \cdots, N\}$) 104

1 Introduction

The design of control algorithms for complex dynamical systems has become a vibrant part of research due to their wide applicability and impact in applications ranging from smart power grids [145], water distribution [105], traffic systems [14] to large arrays of micro-electro-mechanical systems (MEMS), formation of vehicles [9], and sensor actuator networks [146] as illustrated in Fig. 1.1. One of the key challenges for the control of

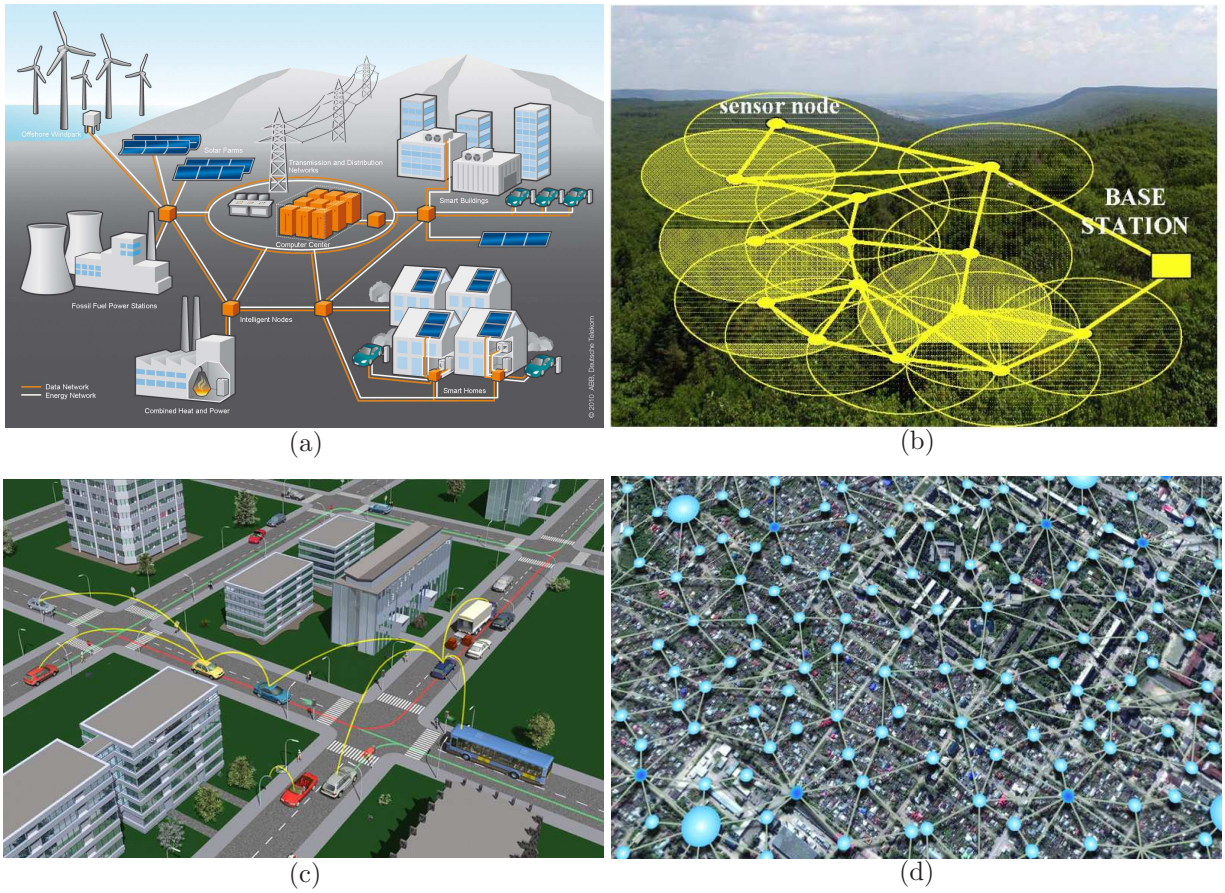

(a) (b)

(c) (d)

Figure 1.1: Examples of large-scale systems: (a) smart grid [3]; (b) wireless sensor networks [1]; (c) traffic network [2]; (d) water distribution network [4].

complex dynamical systems is the complexity, i.e. dimensionality of the overall system in terms of the number of subsystems and their interconnections [147]. In order to control such systems, centralized or conventional control synthesis methods which assume that a single centralized control has access to all measurements instantaneously, as depicted in Fig. 1.2, become infeasible. To illustrate this issue, let us consider the power network as an example of complex dynamical systems which consists of tens-of-thousands of components such as generators, transmission lines, etc. In order to optimally regulate the voltage, power

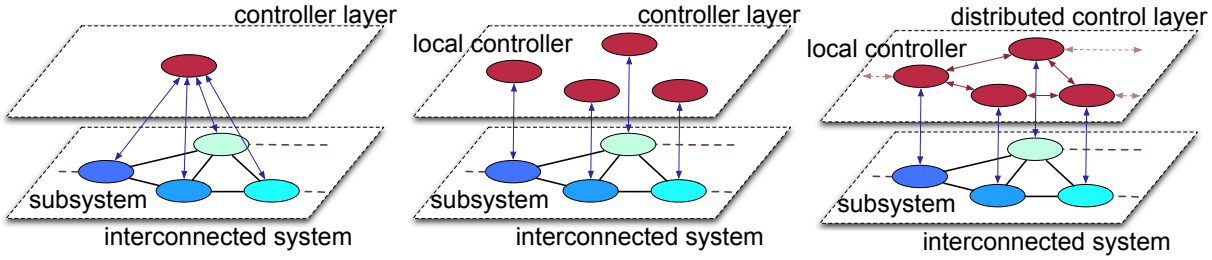

Figure 1.2: Three different control architectures for interconnected systems. Left: centralized control architecture; middle: decentralized control architecture; right: distributed control architecture with information exchange between the local controllers.

and frequency of the power network, a variety of sensors are employed to measure voltage, frequency and power of the network and all of these measurements have to be transmitted to the control stations over a communication network. However, the complexity of the grid makes is extremely difficult to gather the total information. Furthermore, even if one could gather and use this information in order to design a control law, due to for example, the geographical distances, all measurements cannot instantaneously be available to all the controllers of the system, i.e. it might require a very long time and, by then, the information might be outdated which could lead to instability of the closed-loop system.

Preliminary results addressing the dimensional complexity of large-scale systems have been achieved within the *decentralized control* framework developed in the seventies [11]. The fundamental idea in this method is to adopt a "divide and conquer" strategy which decomposes the system into a number of interconnected subsystems. After partitioning the system, the control problems are then solved locally on the level of subsystems and these solutions are furthermore combined with the interconnections to provide a stable feedback law for the overall system as illustrated in Fig. 1.2. In order for this approach to be effective, one of the main challenges is to develop systematic and computationally efficient procedures for decomposing large dynamical systems [147]. An obvious and intuitive way to achieve this goal would be to "tear" the system along certain natural boundaries that are defined by its physical properties. This physical decomposition strategy is characterized by two main advantages. First, by doing so, it is possible to obtain important insights into the interplay between the subsystems and their interconnections. In addition, important "physical" interpretations of the local control actions in terms of global outcomes can also be obtained. However, physical decompositions are neither straightforward nor optimal in general, since there are cases of many practical models in which it is difficult if not impossible, to identify the "natural" boundaries of the subsystems. It is clear in such cases that a physical decomposition is not a suitable strategy. The potential shortages of physical decompositions have triggered the development of powerful numerical decompositions which utilize only the mathematical description of the system such as the well-known Epsilon decomposition which mainly exploits the fact that complex systems often contain a large number of variables which are weakly coupled, if they are coupled at all [147]. For example, in a typical large Linear Time-Invariant (LTI) system, a high percentage of the coefficients in the system matrix are apparently to be small numbers. Therefore, by using this observation, it is possible to perform a permutation on the matrix so that the

off-diagonal blocks are limited to consist of elements that are smaller than the prescribed threshold value Epsilon. The stability of the diagonal blocks can then guarantee the stability of the overall matrix if this Epsilon value is sufficiently small. Although decentralized control has been successfully applied in many engineering problems, it should be noted that it has some inherent weaknesses. One of the most prominent ones is that feedback laws of this type rule out any form of information exchange between the subsystems. As a result, such a control strategy may be ineffective for certain types of models, particularly those where the coupling between individual subsystems is not weak. Furthermore, even though a stabilizing decentralized control law exists, performance might be significantly degraded compared to a centralized approach since only the local subsystem information is used for the design of the control law.

Advances in digital communication networks allow for the communication between subsystems and, thereby, provide a larger flexibility with respect to the control design: instead of only local subsystem information, neighboring subsystems' states can be used for the control as well. These novel approaches are also known under the notion of *distributed control*[1] [10], see Fig. 1.2. As a result, a better performance is typically achieved compared to the decentralized approach. In addition, an additional merit of using information from neighboring subsystems is that this information can be employed to stabilize the interconnected systems when no stabilizing decentralized control law exists, as it happens for example in the presence of decentralized fixed modes (DFM) in a system [134].

1.1 Challenges

Despite the advantages of distributed control, i.e. control law with a certain structural constraint for interconnected systems, the design of distributed control law poses several challenges compared to the conventional centralized and decentralized control. In this section, some of these challenges which will be investigated in the rest of the dissertation, are presented.

i. *Non-convexity:* It was shown by Witsenhausen that the constraint on the structure of the control law can make the problem intractable even in rather simple cases [142]. Furthermore, the objective function of the distributed or decentralized optimal control problem is, in general, non-convex with respect to the control law.

ii. *Combinatorial problem:* Most of the results on distributed control design assume that the structure of the control law is given a priori. The introduction of communication networks, on the other hand, provides an additional degree of freedom to the control design by jointly designing the distributed control gain together with the communication topology with a view of further improving the performance of the overall system. However, this generally results in a mixed-integer optimization formulation, which is hard to solve for a large number of subsystems. In addition, the combinatorial formulation which stems from the nature of the problem makes it difficult to get an explicit solution and also an insightful analysis on the solution.

[1] In some literatures, e.g. [121], the distributed control is also called as partially decentralized control

iii. *Limited model information:* Mainly, when designing a distributed control law, a common assumption is that the system-wide information or the full knowledge of the plant model is available to the designer. However, this assumption is far from being warranted in practice. In real world applications, it is often difficult, if not impossible, to have the whole system information due to the geographical constraints or privacy reasons where the subsystems do not wish to provide their complete description to the designer. Therefore, it is necessary to develop a method in order to design distributed control laws using only limited model information about the interconnected systems.

iv. *Robustness:* It has been shown in many literature that compared to the decentralized control, exchanging local information via the communication network may improve the performance of the interconnected systems. However, the stability of the interconnected system under permanent communication link failures may not always be guaranteed by the standard design procedure in the known literature.

1.2 Related Work

The design of distributed control for interconnected systems has received considerable attention in recent years [12,13,30,31,41,66,68,76,102,130,136,137,139,149,152]. Research efforts have focused on two major issues, namely, the design of the optimal control under a priori specified structural constraints and the design of communication architectures of the distributed control.

Since Witsenhausen's work, much research related to the design of optimal distributed control has been focused on characterizing a class of easily solvable problems. One of the positive results showing that the problem for some cases becomes tractable is the work of Ho and Chu [61] where a class of information structures, called *partially nested*, is defined for which an optimal control law for the LQG problem is linear. Briefly speaking, a plant-controller system is partially connected if controller C_1 has access to all information available to controller C_2 whenever the decision made by C_2 affects the information available to C_1. Rotkowitz and Lall [120] show that the class of *quadratically invariant* problems may be easily solvable via convex programming algorithms [18]. This is one of the largest classes of tractable problems and it includes many previously known tractable cases. In addition, the authors in [136] show conditions where quadratic invariance holds for some sparsity structures, even in cases when the sparsity structures of the plant and the controller differ and provide a specific analytical relationship between quadratic invariance and adjacency matrices. The authors in [129] suggest an independent approach to decentralized control which employs the theory of partially ordered sets to model communication constraints between subsystems. An interesting result regarding interconnection topology is reported in [78] which suggests that if the communication between the controllers incurs some cost, then, adding communication channels may degrade the system performance. Characterizing the structural properties of optimal distributed control law constitutes another important question. For spatially invariant systems, it is shown in [12] that the linear quadratic controllers are also spatially invariant and the measurements from other subsystems are exponentially discounted with the distance between the con-

troller and the subsystems. This spatial decaying property is further extended to systems on graphs in [102] which motivates the search for inherently localized control law. The design of optimal control for spatially invariant systems can also be cast into a convex problem if the information in the controllers propagates at least as fast as in the plant as reported in [13, 139].

It should be noted that the aforementioned work have a common feature: the structure of the control law has to be specified in advance, that is, they do not consider the problem of structure design, but only the design of the control gain itself. The introduction of communication network, however, offers an additional degree of freedom in designing the distributed control by jointly considering the control gain and its structure, i.e. the communication topology which also serves as design variables. Recently, some work have been devoted to designing the distributed control gain together with the communication topology for interconnected systems. The authors in [122] consider the problem of maximization of the degree of decentralization, i.e. minimizing the number of communication links between the subsystems and the state feedback control laws subject to a given error performance in term of the H_∞-norm between the centralized and the decentralized closed loop. The results are extended to the case of dynamic output feedback in [121] by means of a weighted l_1 relaxation and the development of an iterative algorithm based on LMIs to deal with the relaxed decentralized control problem. The authors in [42] consider a linear quadratic optimal control problem with an additional penalty on the number of communication links in the distributed control law. The combinatorial problem is reformulated as a sequence of weighted l_1 problems by utilizing the weighted l_1 norm to approximate the counting of the communication links. Furthermore, a class of systems is identified for which the weighted l_1 problem can be reformulated as a semidefinite program, and thus, the solution can be computed efficiently. Apart from the systems which are interconnected through the dynamics, there are also contributions in multi-agent systems corresponding to communication topology design in recent years [29, 33, 47, 65, 115, 128, 148]. Algebraic connectivity which is the second smallest eigenvalue of the Laplacian matrix is an important performance metric related to the convergence rate of multi-agent systems and its value depends on the communication topology of the network. In [108], it is shown that the connectivity of the agents could improve the convergence rate of the whole system to attain a desired behavior while decreasing the robustness of the systems with respect to time delay. The authors in [47] study the problem of adding edges to a graph from a set of candidate edges so as to maximize its algebraic connectivity. They develop a greedy heuristic for this problem based on the Fiedler vector which can be applied to very large graphs. The problem of finding the optimal graph and the weights of the communication links for a class of directed graphs is solved in [115] by formulating the problem as a *Mixed Integer Semidefinite Program (MISDP)*. Furthermore, the authors in [29] present the optimal network design for consensus based systems using a variety of optimal based methods and categorize the problem into three categories, namely, the construction of optimal non-geometric networks, time-invariant geometric networks and time-varying geometric networks. The authors in [65] consider the problem of optimal local leader selection of a leader-first follower minimally persistent formation system such that the convergence rate is optimized. The proposed approach is first to solve the combinatorial problem in a

continuous domain to obtain the optimal solutions. Then, the actual optimal pair of local leaders is selected from the discrete candidate local leader using the gradient method and the matrix perturbation theory. The problem of designing communication topology has also been studied in the area of sensor networks where the goal is to minimize the sensors' power consumption while maintaining the connectivity of the network [72]. Note that most of the works end up in an optimization problem without providing explicit solutions on the problem.

Most of the work on distributed control design rely on a common assumption: the design can be performed in a centralized manner with full knowledge of the whole plant model. However, this assumption is far from being warranted in practice. This generates a new class of problems, namely distributed control design under a limited model information. There has been some interesting approaches for tackling limited model information based control design problem, although not specifically tailored for it. For example, references [46, 126, 127] introduce methods for designing sub-optimal decentralized control without a global dynamical model of the system. In these works, one key assumption is that the plant consists of an interconnection of weakly coupled subsystems. Then, under this assumption, an optimal control is designed for each subsystem using only the corresponding local model information and the obtained subcontrollers are connected to construct a global control law. In addition, the authors show that, when the coupling is negligible, this control law is satisfactory in terms of closed-loop stability and performance. However, as coupling strength increases, even closed-loop stability guarantees are lost. Note that the motivation behind their studies has been to design fully decentralized near-optimal control for large-scale dynamical systems and to avoid numerical complications stemming from the high dimension of the system, by splitting the original problem into several smaller ones. Other approaches such as in [37] are based on receding horizon control and use decomposition methods to solve each step's optimization problem in a decentralized manner with only limited information exchange between subsystems. Another work on distributed design method for distributed control of identical and dynamically decoupled systems is considered in [15]. Dual decomposition is used for distributed optimization of local controllers in [96, 116]. On the analysis part, the authors in [83] derive scalable decentralized conditions that can guarantee robust stability for networks of linear interconnected, stable, linear time invariant systems. It is shown that robust stability of the entire network is guaranteed by satisfying local rules that only involve an agent and its neighboring dynamics. Recently, the authors in [43, 44] present a rigorous characterization of the best closed-loop performance which can be attained through limited model information design and, furthermore, they study the trade-off between the closed-loop performance and the amount of exchanged information based on the work presented in [77]. Most of the results, however, assume that the structure of the control law is given a priori.

The last, but yet important issue is the robustness of the whole system in the presence of interconnection failures. The authors in [25, 26] present a method for synthesis of decentralized control for multiple subsystems interconnected on a graph. They develop a synthesis procedure for control laws which stabilize the system for any graph topology satisfying given degree bounds, independent of the size of the graph. In other words, the stability of the interconnected systems using the designed control laws can be guaranteed in

the presence of physical interconnection failures. However, no communication is considered and no stability guarantee is provided under permanent communication link failures.

1.3 Main Contributions and Outline of Dissertation

The present dissertation focuses on the design of distributed control laws for interconnected systems where the goal is to improve and optimize the overall system performance. At the same time, various challenges mentioned previously are investigated which have not been addressed in-depth in the existing literature. So far unique is the exploitation of the additional degree of freedom offered by the communication network in the design of the distributed control law, namely taking into account the communication structure and considering the information that needs to be exchanged among the local controllers in order to achieve the objective of the task. The main contributions of this dissertation are fourfold. The first contribution is the development of a novel two-layer control architecture by combining the advantages of decentralized and distributed control law. The proposed control architecture allows to jointly improve the performance of the interconnected system and guarantee the stability of the interconnected system under permanent communication link failures. The developed architecture is not only well suited for ideal communication network, but also can be extended in a straightforward manner to deal with non-ideal communication network. Second, explicit solutions on the communication topology design for distributed control of interconnected systems with certain physical structure are derived here for the first time. A third contribution is the development of a novel coordination algorithm for the design of distributed control together with its communication topology of interconnected systems, given only limited plant model information. Finally, an innovative approach to design distributed control law for a coverage control problem is proposed by exploiting the use of information that can be exchanged via the communication network, which guarantees that the system avoids undesired local optima stemming from the non-convex objective function.

This dissertation is mainly separated into two parts according to the associated interconnected systems which are considered. The first part deals with dynamical systems which are interconnected via the states, inputs and the objective function. The objective here is to improve the system performance by jointly designing the control gain and the communication topology of the distributed control law under a given constraint on the communication network while guaranteeing their stability under permanent communication link failures. The second part is concerned with systems which are coupled via the (non-convex) objective function exemplified by coverage control of mobile sensor networks. Here, the objective is to develop a distributed control law which guarantees that mobile sensor networks avoid certain local optima of the objective function. The results and primary work of this dissertation are published in [51, 53–55, 87]. The structure of this dissertation is given in Fig. 1.3. The associated outline of the presented results is given in the following.

In Chapter 3, a novel two-layer control architecture for interconnected systems is proposed. While the known literature considers the problem of designing optimal distributed control law and robust distributed control law with respect to interconnection failures sep-

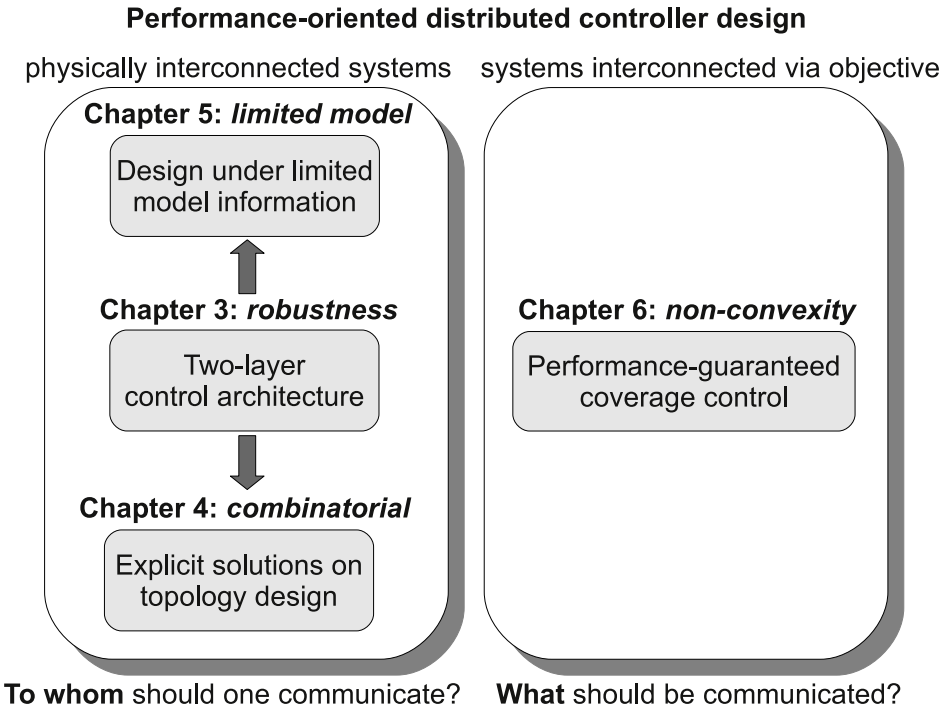

Figure 1.3: Outline of the dissertation.

arately, the developed two-layer control architecture allows the designer to consider this problem in a unified fashion. This results in that the performance of the overall system can be optimized, and at the same time, its stability is guaranteed under permanent communication link failures, which cannot be achieved by the standard design procedure. The innovative strategy is to combine the advantages of decentralized and distributed control laws, i.e. first to design the decentralized control law that stabilizes the interconnected systems, and then, improve the overall system performance by designing the distributed control law together with its communication topology, under a given communication network constraint. Communication topology design of distributed control reported in the existing literature so far assumes an ideal communication network. In this chapter, it is further demonstrated that the novel two-layer control architecture is not only suited for ideal communication network, but also can be extended into the case where constant and identical time delay exists in the communication network. Another innovation in this chapter is the investigation via numerical simulations on how the addition of communication links influences the performance of the interconnected system, which is still far from being understood. Finally, the proposed method is applied to the design of a novel distributed damping control for power systems.

While the results of joint distributed control gain-communication topology design reported in the known literature, including the one presented in Chapter 3 end-up in an optimization formulation, Chapter 4 provides for the first time the explicit solutions on communication topology design problem with a fixed control gain for interconnected systems with certain class of physical structure, namely ring, star and line topology. As a unique approach, the eigenvalue sensitivity analysis is utilized by treating the distributed

control as a perturbation influencing the interconnected system and investigating how the structure of the control law influences the movement of the eigenvalues. The analysis starts with the case of interconnection of identical scalar subsystems and a single communication link. The results are then extended into interconnected systems with non-scalar subsystems, multiple communication links and also more complex topology which can be decomposed into rings, stars or lines. In addition, some new insights in terms of explicit relation between the heterogeneity of the subsystems local dynamics, the strength of the physical interconnection, the size of the network and the optimal communication topology are introduced. Finally, the novel approach based on eigenvalue sensitivity is applied to the case where time delay exists in the communication network to investigate how the communication topology and time delay influence the performance of the interconnected systems.

The proposed method in Chapter 3 and Chapter 4 requires system-wide information in order to compute the control law even though the control law is implemented in a distributed fashion. In real world applications, however it is difficult, if not impossible, to obtain the whole system information due to the geographical constraints or privacy reasons in which the subsystems may not wish to provide a complete description of themselves to the designer. Therefore, in Chapter 5 a novel algorithm is developed in order to design distributed control for interconnected systems under a limited plant model information. In contrast to existing related literature where the structure of the control law is fixed and given a priori, here the design of communication topology is also taken into account. Specifically, it is assumed that each subsystem only has the information about its physical neighbors' local dynamics and the interconnection between them. The novel strategy is to decompose and assign the design problem to each subsystem and then each subsystem solves the design problem by coordinating with its neighbors, thus the joint distributed control gain-communication topology design can be performed in a distributed fashion.

Finally, Chapter 6 deals with distributed control design for coverage control of mobile sensor networks. It is known that the coverage control or deployment problem is a non-convex optimization problem. In this chapter, an innovative approach to design distributed control law which guarantees that the sensors avoid undesired local optima is proposed. The unique strategy is to characterize, for the first time, the undesired local optima where it is shown that one of them is caused by the existence of sensors which do not participate in the coverage due to lack of information that the sensors sense. In order to avoid the undesired local optima, as an intuitive strategy the standard coverage control law based on a gradient method is combined with the leader-following algorithm which can be viewed as a perturbation influencing the gradient-based term where the leaders are defined as sensors with the most available information. The sensors provided with no information follow the leaders until they gain some information about the region of interest by exploiting the use of information that can be exchanged between them. The proposed novel algorithm is advantageous compared to the other non-gradient based approaches in the sense that it is more intuitive and is proven to guarantee that the sensors avoid the undesired local optima, which cannot be achieved by other approaches reported in related literature.

This dissertation is concluded in Chapter 7 where a summary and discussion about potential future directions are presented.

2 Modeling of Interconnected Systems

A model is a mathematical representation of a physical system which allows us to reason about a system, make prediction about its behavior and design a control law to manipulate its behavior. In general, there is a trade-off between the accuracy of the selected models and the complexity of the control design. For example, general nonlinear models can be very accurate in describing the behavior of a dynamical system, however, are difficult to analyze and apply in model based control schemes. Therefore, it is important to choose the models that are simple, but still can capture the behavior of the real dynamical systems. In this dissertation, we choose to use linear time invariant (LTI) systems to model the interconnected systems and design the distributed control law based on the corresponding model. This chapter provides some background on the modeling of interconnected systems and shows that a variety of interconnected systems found in the real world applications can be modeled as the interconnection of a number of LTI subsystems. We consider three real examples of interconnected systems, namely: power systems, temperature regulation in large buildings and deformable mirrors in adaptive optics. For each interconnected system, we derive the ordinary differential equations which is a common class of mathematical models for dynamical systems and based on these equations, the state space system is constructed which will be used as a model of the interconnected system for the distributed control design in the remaining of the dissertation.

2.1 Power System

Generally, a power system is an interconnected system and its model consists of differential and algebraic equations describing the generator dynamics, controllers, networks and loads. Power system dynamics can be divided into four groups depending on its time scale, namely: wave dynamics which are the fastest, electromagnetic dynamics, electromechanical dynamics and thermodynamics which are the slowest [95]. In this dissertation, we consider the small-signal stability defined as the ability of power systems to maintain synchronism under small disturbances. Specifically, we aim at designing a damping control for low-frequency oscillations. This kind of stability problem belongs to the categories of electromechanical dynamics whose time scale varies from seconds to minutes. Since the disturbance is assumed to be small, a linearized model including the generator dynamics and an equivalent transfer network model is considered. The equivalent transfer network is a reduced network model in which all load nodes are eliminated and all generator nodes are directly connected with each other, see e.g. [95]. The power system considered in this dissertation consists of the generator, excitation system with voltage control and the network described in the following.

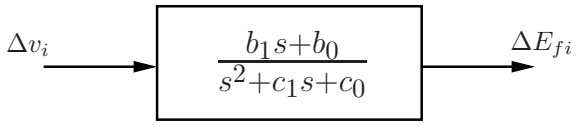

Figure 2.1: Automatic voltage regulator model.

2.1.1 Generator and Exciter System Model

A linearized third order generator model with an excitation system as introduced in [95] is used here as the model of i-th generator in the system.

- Generator dynamic equations is given by

$$\begin{aligned} \Delta\dot{\delta}_i &= \Delta\omega_i, && (2.1)\\ M_i\Delta\dot{\omega}_i &= -Z_i\Delta\omega_i - \Delta P_{ei}, && (2.2)\\ T'_{doi}\Delta\dot{E}'_{qi} &= -\Delta E'_{qi} + (X_{di} - X'_{di})\Delta I_{di} + \Delta E_{fi} && (2.3) \end{aligned}$$

  where δ_i, ω_i are the rotor angle and speed, M_i denotes the inertia constant, Z_i represents the damping coefficient, P_{ei} is the active power delivered at the terminals, T'_{doi} is the time constant, E'_{qi} denotes the internal voltage, X_{di} denotes the reactance and I_{di}, E_{fi} are the currents and the electromotive force of the $i-$th machine. A second-order transfer function is used to represent the Automatic Voltage Regulator (AVR) for the generator exciter as shown in Fig. 2.1. An AVR controls the excitation current, and consequently the generators terminal voltage.

- Excitation system and automatic voltage control can be written as

$$\begin{aligned} \dot{z}_{2i} &= -c_{1i}z_{2i} - c_{0i}z_{1i} + \Delta v_i, && (2.4)\\ \dot{z}_{1i} &= z_{2i}, && (2.5)\\ \Delta E_{fi} &= b_{1i}z_{2i} + b_{0i}z_{1i} && (2.6) \end{aligned}$$

  where z_{1i} and z_{2i} are the internal states of the AVR.

The linearized state dynamic $\boldsymbol{x}_i$ of the i-th synchronous generator is then given by

$$\boldsymbol{x}_i = \begin{bmatrix}\Delta\delta_i & \Delta\omega_i & \Delta E'_{qi} & z_{2i} & z_{1i}\end{bmatrix}^T \quad (2.7)$$

and the control input signal is denoted by Δv_i.

2.1.2 Network Model

In general, the network model of a power system is represented by the algebraic nodal equations describing the relation between the current injections and the voltages of all generation and load nodes via the admittance matrix. As discussed in [95], eliminating the load nodes leads to an equivalent transfer network in which the generator nodes are

directly connected with each other. After the elimination of all the load nodes, including the generation terminal nodes, the d-axis currents I_{di} and the electrical power P_{ei} of the i-th generator can be expressed in terms of its variables, in this case the rotor angle δ_i and the transient voltage E'_{qi} according to

$$I_{di} = \sum_{j=1}^{N} E'_{qi}[L_{ij}\cos(\delta_i - \delta_j) - H_{ij}\sin(\delta_i - \delta_j)], \tag{2.8}$$

$$P_{ei} = E'_{qi}\sum_{j=1}^{N}[L_{ij}\sin(\delta_i - \delta_j) + H_{ij}\cos(\delta_i - \delta_j)]E'_{qj} \tag{2.9}$$

where N is the total number of generators in the system and $i, j \in \{1 \cdots N\}$, L_{ij} and H_{ij} are the imaginary and the real part of a network admittance Y_{ij}.

Linearizing the equations (2.8) and (2.9), the power increment ΔP_{ei} in (2.2) and the current increment ΔI_{di} in (2.3) are given by

$$\Delta P_{ei} = \begin{bmatrix} \frac{\partial P_{ei}}{\partial \boldsymbol{\delta}} & \frac{\partial P_{ei}}{\partial \mathbf{E}'_q} \end{bmatrix} \begin{bmatrix} \Delta\boldsymbol{\delta} \\ \Delta\mathbf{E}'_q \end{bmatrix}, \quad \Delta I_{di} = \begin{bmatrix} \frac{\partial I_{di}}{\partial \boldsymbol{\delta}} & \frac{\partial I_{di}}{\partial \mathbf{E}'_q} \end{bmatrix} \begin{bmatrix} \Delta\boldsymbol{\delta} \\ \Delta\mathbf{E}'_q \end{bmatrix} \tag{2.10}$$

with $\Delta\boldsymbol{\delta}$ consists of the rotor angle deviations and $\Delta\mathbf{E}'_q$ consists of the transient voltage deviations of all generators in the power systems.

2.1.3 State Space Model

Combining equations (2.1)-(2.6) and (2.10), the small-signal dynamics of a generator connected to the power system can be written as

$$\dot{\boldsymbol{x}}_i = \boldsymbol{A}_i\boldsymbol{x}_i + \boldsymbol{B}_i u_i + \sum_{j\in\mathcal{N}_i} \boldsymbol{A}_{ij}\boldsymbol{x}_j \tag{2.11}$$

where $u_i = \Delta v_i$ and $\mathcal{N}_i$ represents the set of the generators that are physically connected with the i-th generator. The matrices $\boldsymbol{A}_i \in \mathbb{R}^{5\times5}, \boldsymbol{B}_i \in \mathbb{R}^{5\times1}, \boldsymbol{A}_{ij} \in \mathbb{R}^{5\times5}$ are given by

$$\boldsymbol{A}_i = \begin{bmatrix} 0 & 1 & 0 & 0 & 0 \\ -\frac{1}{M_i}\frac{\partial P_{ei}}{\partial \delta_i} & -\frac{D_i}{M_i} & -\frac{1}{M_i}\frac{\partial P_{ei}}{\partial E'_{qi}} & 0 & 0 \\ \eta_i\frac{\partial I_{di}}{\partial \delta_i} & 0 & -\frac{1}{T'_{doi}} + \eta_i\frac{\partial I_{di}}{\partial E'_{qi}} & \frac{b_{1i}}{T'_{doi}} & \frac{b_{0i}}{T'_{doi}} \\ 0 & 0 & 0 & -c_{1i} & -c_{0i} \\ 0 & 0 & 0 & 1 & 0 \end{bmatrix},$$

$$\boldsymbol{B}_i = \begin{bmatrix} 0 & 0 & 0 & 1 & 0 \end{bmatrix}^T,$$

$$\boldsymbol{A}_{ij} = \begin{bmatrix} 0 & 0 & 0 & 0 & 0 \\ -\frac{1}{M_i}\frac{\partial P_{ei}}{\partial \delta_j} & 0 & -\frac{1}{M_i}\frac{\partial P_{ei}}{\partial E'_{qj}} & 0 & 0 \\ \eta_i\frac{\partial I_{di}}{\partial \delta_j} & 0 & -\frac{1}{T'_{doi}} + \eta_i\frac{\partial I_{di}}{\partial E'_{qj}} & \frac{b_{1i}}{T'_{doi}} & \frac{b_{0i}}{T'_{doi}} \\ 0 & 0 & 0 & 0 & 0 \\ 0 & 0 & 0 & 0 & 0 \end{bmatrix}$$

with $\eta_i = \frac{X_{di}-X'_{di}}{T'_{doi}}$. Therefore, the linearized power system can be expressed by an LTI interconnected systems given by

$$\dot{\boldsymbol{x}} = \boldsymbol{A}\boldsymbol{x} + \boldsymbol{B}\boldsymbol{u} \tag{2.12}$$

where $\boldsymbol{x} \in \mathbb{R}^{5N\times 1}$ and $\boldsymbol{u} \in \mathbb{R}^{N\times 1}$ are the states and input signals of all N generators in the power system respectively and the matrices $\boldsymbol{A} \in \mathbb{R}^{5N\times 5N}, \boldsymbol{B} \in \mathbb{R}^{5N\times N}$ are given by

$$\boldsymbol{A} = \begin{bmatrix} \boldsymbol{A}_1 & \boldsymbol{A}_{12} & \cdots & \boldsymbol{A}_{1N} \\ \boldsymbol{A}_{21} & \boldsymbol{A}_2 & \cdots & \boldsymbol{A}_{2N} \\ \vdots & \vdots & \ddots & \vdots \\ \boldsymbol{A}_{N1} & \boldsymbol{A}_{N2} & \cdots & \boldsymbol{A}_N \end{bmatrix}, \quad \boldsymbol{B} = \begin{bmatrix} \boldsymbol{B}_1 & \boldsymbol{0} & \cdots & \boldsymbol{0} \\ \boldsymbol{0} & \boldsymbol{B}_2 & \ddots & \vdots \\ \vdots & \ddots & \ddots & \boldsymbol{0} \\ \boldsymbol{0} & \cdots & \boldsymbol{0} & \boldsymbol{B}_N \end{bmatrix}.$$

Remark 1 Similar state space model can also be derived for the case of water distribution network, see e.g. [39, 81] for the details.

2.2 Thermal Model of Large Buildings

The building sector consumes about 40% of the energy used in the United States [98]. Therefore, it is economically and environmentally significant to reduced the energy consumption of buildings. Furthermore, according to the September 2008 report of American Physical Society [5], a large fraction of the energy delivered to buildings is wasted because of inefficient building technologies. Real time monitoring and control is thus likely to play a more significant role in operating the HVAC (Heating, Ventilation, and Air Conditioning) equipment in buildings than it has played so far. Mathematical models of thermal transport, especially the dynamics of temperature evolution, in large building is an important key to develop an effective control and monitoring systems. The temperatures in the rooms of a building depend on the thermal interaction between rooms and the outside via the walls, heat transport by supplied conditioned air as well as the solar radiation through the windows. Furthermore, the complexity in the dynamics of temperature evolution in a room comes from the thermal interaction between the rooms and the outside which can be either via conduction through the walls, or convective air exchange among rooms. To summarize, the thermal properties of a building is composed of heat transmission. Before deriving the dynamics of the temperature evolution in a building, we first review the basic equations to describe the heat transmission.

2.2.1 Heat Transfer

Heat transfer takes place via the conduction, convection and radiation described briefly in the following [94].

Conduction

Conduction is the process of heat transfer through a substance such as a wall, from higher to lower temperatures. It is possible to quantify the heat transfer process in terms of rate

equations. The rate equation for heat conduction is known as Fourier's law. Under steady state and for one-dimensional plane wall, the Fourier's equation is given by

$$q_x = kA\frac{\Delta T}{\Delta x} = kA\frac{T_h - T_l}{L} \tag{2.14}$$

where q_x (W) is the heat transfer rate in the x direction, T_h, T_l (K) are the high and low temperatures respectively, $L(m)$ is the length/thickness of material and k (W/mK) is the thermal conductivity of the material. Note that equivalent to electric circuit, a thermal resistance R_{th} may be associated with the conduction of heat which is given by

$$R_{th} = \frac{T_h - T_l}{q_x} = \frac{L}{kA}. \tag{2.15}$$

Convection

Convection is the heat transfer between a surface and fluid or gas by the movement of the fluid or gas. The rate equation for heat convection transfer process is given by

$$q = hA(T_s - T_\infty) \tag{2.16}$$

where q (W) is the convective heat transfer, T_s, T_∞ (K) are the surface and fluid temperatures respectively, A (m^2) is the surface area and h (W/m^2K) is the convection heat transfer coefficient which are influenced for example by surface geometry or the nature of the fluid motion. Similar to conduction, we can define the thermal resistance for convection R_{cv} as

$$R_{cv} = \frac{T_s - T_\infty}{q} = \frac{1}{hA}. \tag{2.17}$$

Radiation

Radiation is the energy emitted by matter transported by electromagnetic waves. While the transfer of energy by conduction or convection requires the presence of a material medium, radiation does not and even occurs most efficiently in a vacuum. Radiation may also be incident on a surface from its surroundings. The radiation may originate from a special source, such as the sun. The net radiation heat transfer from the surface is given by the Stefan-Boltzman law

$$q_{\text{rad}} = \epsilon\sigma(T_s^4 - T_{\text{sur}}^4) \tag{2.18}$$

where ϵ is the emissivity of the surface whose values $0 \leq \epsilon \leq 1$, σ is the Stefan-Boltzman constant, T_s, T_{sur} are the surface and surroundings temperatures. Eq. (2.18) describes the difference between thermal energy that is released due to radiation emission and that which is gained due to radiation absorption.

Thermal Capacitance

Thermal capacitance is the capacity of a body to store heat. In order to compute the thermal capacitance, we consider the following assumptions.

- The air in a room has one temperature across its volume.
- The specific heat of air, c_p, is constant.
- All rooms are at the same pressure.
- The radiative coupling between inner building walls can be ignored.

Therefore, the thermal capacity of room i, denoted by C_{ri} is given by

$$C_{ri} = \rho_a V_i c_{pa} \tag{2.19}$$

where ρ_a is the density of air at room temperature and V_i is the volume of room i. A similar equation can also be derived for the walls.

2.2.2 State Space Model

Circuit representations provide a useful tool for quantifying heat transfer problems. The equivalent thermal circuit for the plane wall with convection surface conditions is depicted in Fig. 2.2 whose heat transfer rate can be expressed by

$$q_x = \frac{T_{\infty,1} - T_{\infty,2}}{R_{tot}}, \quad R_{tot} = \frac{1}{h_1 A} + \frac{L}{kA} + \frac{1}{h_2 A}.$$

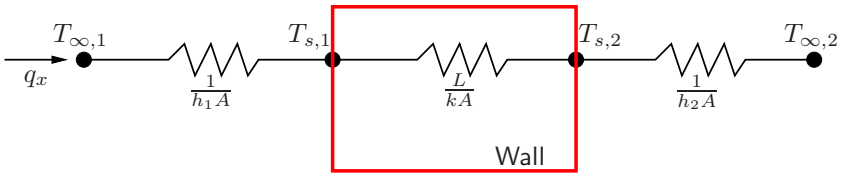

Figure 2.2: Equivalent thermal circuit of heat transfer through a plane wall.

For the sake of simplicity and clarity, we consider a building consists of two rooms as shown in Fig. 2.3. The thermal influences between rooms of the same building occur through internal walls, i.e. the internal walls isolation is weak [100]. Furthermore, the coupling is assumed to be caused only between two adjacent rooms through walls. Each room is also equipped with an independent converter heater as the control input. Each wall and room is represented as nodes. Since the thermal model is an RC network, as mentioned previously, its dynamics is described by a system of coupled first order linear differential equations of the form $C_i \frac{dT_i}{dt} = q_i$ where C_i is the thermal capacitance of node i and q_i is the net heat flow into node i through the resistive elements connected to it [35]. Therefore, we can write the following dynamics for wall w_1

$$\frac{T_\infty - T_{w_1}}{\bar{R}_1} + \frac{T_1 - T_{w_1}}{\tilde{R}_1} + \alpha A_1 q_{\mathrm{rad}_1} = C_{w_1} \frac{d(T_{w_1})}{dt}$$

where $\bar{R}_1 = R_o^1 + \frac{R_w}{2}, \tilde{R}_1 = R_i^1 + \frac{R_w}{2}$ and R_w, R_o^1, R_i^1 denote the total thermal resistance of the wall, the external and internal sides of the peripheral walls respectively. The first term represents the heat transfer from outside to the wall while the second term describes the heat transfer from the air in room number 1 to the wall. Moreover, the term αq_{rad_1} is the portion of the radiation heat from the sun absorbed by the wall, where α is the absorptivity coefficient of the wall. Similar equations can also be obtained for walls w_2, w_3, w_4, w_5, w_6. On the other hand, we have the following dynamics for wall w_7.

$$\frac{T_1 - T_{w_7}}{\bar{R}_7} + \frac{T_2 - T_{w_7}}{\tilde{R}_7} = C_{w_7} \frac{d(T_{w_7})}{dt}.$$

Using the similar analysis, the dynamics for rooms number 1 and 2 can be written as follows.

$$\begin{aligned}
\frac{T_{w_1} - T_1}{\tilde{R}_1} + \frac{T_{w_2} - T_1}{\tilde{R}_2} + \frac{T_{w_7} - T_1}{\tilde{R}_7} + \frac{T_{w_6} - T_1}{\tilde{R}_6} + Q_1 &= C_{r_1} \frac{d(T_1)}{dt}, \\
\frac{T_{w_4} - T_2}{\tilde{R}_4} + \frac{T_{w_5} - T_2}{\tilde{R}_5} + \frac{T_{w_7} - T_2}{\tilde{R}_7} + \frac{T_{w_3} - T_2}{\tilde{R}_3} + Q_2 &= C_{r_2} \frac{d(T_2)}{dt}
\end{aligned}$$

where Q_1, Q_2 are the input to the rooms. The state space representation of room number 1 can then be written as follows.

$$\underbrace{\begin{bmatrix} \dot{T}_1 \\ \dot{T}_{w_1} \\ \dot{T}_{w_2} \\ \dot{T}_{w_6} \\ \dot{T}_{w_7} \end{bmatrix}}_{\dot{\boldsymbol{x}}_1} = \underbrace{\begin{bmatrix} a & \frac{1}{\bar{R}_1 C_{r_1}} & \frac{1}{\bar{R}_2 C_{r_1}} & \frac{1}{\bar{R}_6 C_{r_1}} & \frac{1}{\bar{R}_7 C_{r_1}} \\ \frac{1}{\tilde{R}_1 C_{w_1}} & -\frac{1}{\tilde{R}_1 C_{w_1}} & 0 & 0 & 0 \\ \frac{1}{\tilde{R}_2 C_{w_2}} & 0 & -\frac{1}{\tilde{R}_2 C_{w_2}} & 0 & 0 \\ \frac{1}{\tilde{R}_6 C_{w_6}} & 0 & 0 & -\frac{1}{\tilde{R}_6 C_{w_6}} & 0 \\ \frac{1}{\tilde{R}_7 C_{w_7}} & 0 & 0 & 0 & -\frac{1}{\tilde{R}_7 C_{w_7}} \end{bmatrix}}_{\boldsymbol{A}_1} \underbrace{\begin{bmatrix} T_1 \\ T_{w_1} \\ T_{w_2} \\ T_{w_6} \\ T_{w_7} \end{bmatrix}}_{\boldsymbol{x}_1} + \underbrace{\begin{bmatrix} 1 \\ 0 \\ 0 \\ 0 \\ 0 \end{bmatrix}}_{\boldsymbol{b}_{1,1}} \underbrace{Q_1}_{u_1} +$$

$$\underbrace{\begin{bmatrix} 0 \\ 0 \\ 0 \\ 0 \\ \frac{1}{\tilde{R}_7 C_{w_7}} \end{bmatrix}}_{\boldsymbol{b}_{1,2}} \underbrace{T_2}_{y_2} + \underbrace{\begin{bmatrix} 0 \\ \frac{\alpha A_1 q_{\text{rad}_1}}{C_{w_1}} + \frac{T_\infty}{\bar{R}_1 C_{w_1}} \\ \frac{\alpha A_2 q_{\text{rad}_2}}{C_{w_2}} + \frac{T_\infty}{\bar{R}_2 C_{w_2}} \\ \frac{\alpha A_6 q_{\text{rad}_6}}{C_{w_6}} + \frac{T_\infty}{\bar{R}_6 C_{w_6}} \\ 0 \end{bmatrix}}_{\boldsymbol{d}_1}$$

$$\underbrace{T_1}_{y_1} = \underbrace{[1\ 0\ 0\ 0\ 0]}_{\boldsymbol{c}_1^T} \begin{bmatrix} T_1 \\ T_{w_1} \\ T_{w_2} \\ T_{w_6} \\ T_{w_7} \end{bmatrix}$$

where $a = \frac{-1}{C_{r_1}} \left(\frac{1}{\bar{R}_1} + \frac{1}{\bar{R}_2} + \frac{1}{\bar{R}_6} + \frac{1}{\bar{R}_7} \right)$ and $\frac{1}{\bar{R}_i} = \frac{1}{R_i} + \frac{1}{\tilde{R}_i}$. A similar state space representation can also be obtained for room number 2. As can be observed from the above state space representation, the dynamics of room number 1 is influenced, i.e. coupled by room number

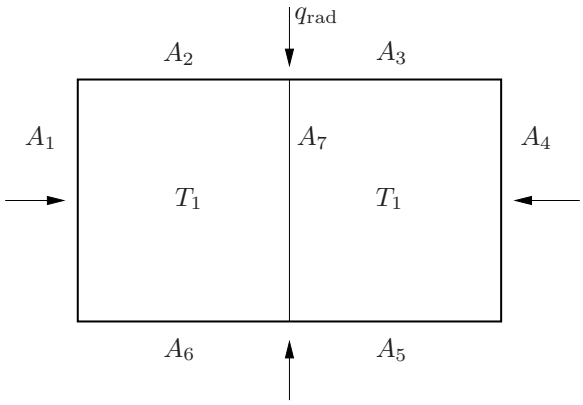

Figure 2.3: Simple two-room building.

2 via the temperature, i.e. T_2. The state space representation for room i without any external disturbance, i.e. $\boldsymbol{d}_i = 0$ can then be generalized in the following form [101]

$$\begin{aligned} \dot{\boldsymbol{x}}_i &= \boldsymbol{A}_i \boldsymbol{x}_i + \sum_{j \in \mathcal{H}_i} \boldsymbol{b}_{i,j} y_j + \boldsymbol{b}_{i,i} u_i, \\ y_i &= \boldsymbol{c}_i^T \boldsymbol{x}_i \end{aligned}$$

where $\mathcal{H}_i$ is the set of adjacent rooms of room i.

2.3 Deformable Mirrors

Since the turbulent nature of the atmosphere, light from distant stars and planets is distorted before being received by ground-based telescopes. These distortions can be compensated by means of adaptive optics. In adaptive optics systems, a deformable mirrors is controlled by changing its shapes to counteract the spatially-distributed wavefront distortion with a spatial resolution equivalent to the strength of the turbulence. Feedback is provided by a sensor array that measures local gradients of the incoming wavefront.

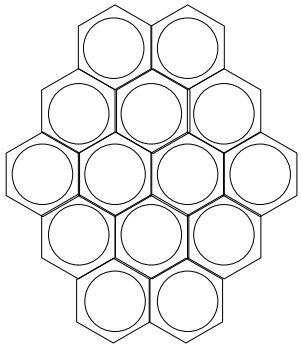

Figure 2.4: An adaptive optics mirror. Each circle contains an actuator.

2.3.1 Dynamic Deformable Mirrors

In this section, the case of hexagonal pattern, which is common for deformable mirrors is considered as illustrated in Fig 2.4 [45]. Deformable mirrors are typically made of a thin reflective membrane or plate that can be shaped by means of an array of linear actuators. In this section, it is assumed that the deflection $w(x, y, t)$ of the mirror can be described by the thin plate partial differential equation given by

$$\left(EI\nabla^4\left(1+\eta\frac{\partial}{\partial t}\right)+\rho h\frac{\partial^2}{\partial t^2}\right)w(x,y,t)=p(x,y,t) \tag{2.20}$$

where $\nabla^4 = (\frac{\partial^4}{\partial x^4} + 2\frac{\partial^4}{\partial x^2\partial y^2} + \frac{\partial^4}{\partial y^4})$ is the biharmonic operator, E denotes the Young's modulus, $I = \frac{h^3}{12}$ represents the moment of inertia, η is a material damping parameter, ρ is the density, h denotes the thickness of the plate and $p(x, y, t)$ is the pressure excerted by the actuators [45]. The actuators are distributed over a spatial grid with equidistant spacing. Furthermore, each actuator consists of a parallel connection of a spring with stiffness c, a damper with damping constant $d = \zeta c$ which are assumed to be identical for all actuators and a force f_i of actuator i which can be controlled, see Fig. 2.5. By

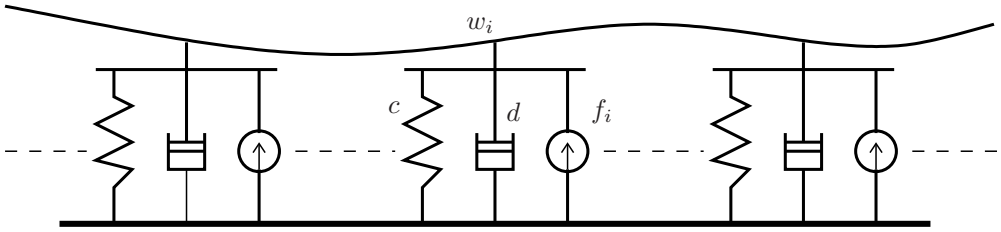

Figure 2.5: A deformable mirror with a thin plate membrane suspended by springs with stiffness c and dampers with damping d and controller by force actuators.

assuming that the distance Δ between the actuators to be small, the finite-difference discretization of Eq. (2.20) over the hexagonal grid results in a sufficiently accurate model. The finite-difference of the biharmonic operator over the grid with a unit distance between two neighboring points is given by

$$\begin{aligned}\mathcal{G}(S_1,S_2) &= \frac{4}{9}(42-10(S_1+S_1^{-1}+S_1S_2^{-1}+S_1^{-1}S_2+S_2+S_2^{-1})\\ &\quad +2(S_1^2S_2^{-1}+S_1^{-2}S_2+S_1S_2+S_1^{-1}S_2^{-1}+S_1S_2^{-2}+S_1^{-1}S_2^2)\\ &\quad +(S_1^2+S_1^{-2}+S_1^2S_2^{-2}+S_1^{-2}S_2^2+S_2^2+S_2^{-2})\end{aligned} \tag{2.21}$$

where S_1 and S_2 are the unit shift operators along two principal axis s_1 and s_2 of the grid, as shown in Fig. 2.6. The finite-difference discretization of Eq. (2.20) interconnected with the actuators is given as follows.

$$\left(\frac{AEI}{\Delta^4}\mathcal{G}(S_1,S_2)\left(1+\eta\frac{\partial}{\partial t}\right)+c\left(1+\zeta\frac{\partial}{\partial t}\right)+\rho Ah\frac{\partial^2}{\partial t^2}\right)w(i,j,t)=f(i,j,t) \tag{2.22}$$

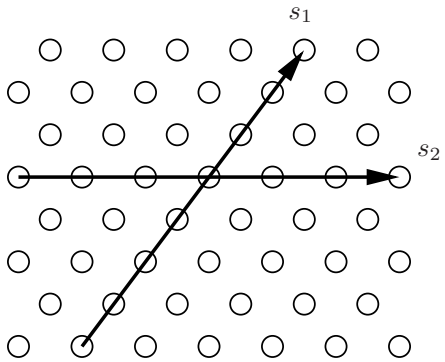

Figure 2.6: Infinite hexagonal grid, schematized as $\mathbb{Z}^2$.

where $w(i,j,t), f(i,j,t)$ are the displacement and force at point with discrete index (i,j) respectively and $A = \frac{3\sqrt{3}}{8}\Delta^2$ denotes the surface area of one element corresponding with one actuator. In addition, it is assumed that $w(i,j,t) = 0$ for points (i,j) outside the dimensions of the mirror which corresponds with the clamped boundary condition.

2.3.2 State Space Model

The deformable mirror described by Eq. (2.22) can be written as an interconnected of a series of equal and small size subsystems where the interconnection pattern is determined by the finite-difference operator given by Eq. (2.21). In order to show this, Eq. (2.22) is re-written in the following state-space form.

$$\begin{aligned}
\begin{bmatrix} \dot{w}(i,j,t) \\ \ddot{w}(i,j,t) \end{bmatrix} &= \begin{bmatrix} 0 & 1 \\ -\left(\frac{Eh^2\mathcal{G}(S_1,S_2)}{12\rho\Delta^4} + \frac{8c}{3\sqrt{3}\rho\Delta^2 h}\right) & -\left(\frac{\eta Eh^2\mathcal{G}(S_1,S_2)}{12\rho\Delta^4} + \frac{8\zeta c}{3\sqrt{3}\rho\Delta^2 h}\right) \end{bmatrix} \begin{bmatrix} w(i,j,t) \\ \dot{w}(i,j,t) \end{bmatrix} \\
&\quad + \begin{bmatrix} 0 \\ \frac{8}{3\sqrt{3}\rho\Delta^2 h} \end{bmatrix} f(i,j,t) \\
w(i,j,t) &= [1\ 0] \begin{bmatrix} w(i,j,t) \\ \dot{w}(i,j,t) \end{bmatrix}
\end{aligned}$$

where $\dot{w} = \frac{\partial w}{\partial t}, \ddot{w} = \frac{\partial^2 w}{\partial t^2}$ and we use $A = \frac{3\sqrt{3}}{8}\Delta^2$ and $I = \frac{h^3}{12}$. By stacking the values of $w(i,j,t), f(i,j,t)$ and the local state $\boldsymbol{x}(i,j,t) = [w(i,j,t)\ \dot{w}(i,j,t)]^T$ at N grid points (i,j) into $\boldsymbol{w}(t) \in \mathbb{R}^N, \boldsymbol{f}(t) \in \mathbb{R}^N$ and $\boldsymbol{x}(t) \in \mathbb{R}^{2N}$, the global deformable mirror model for N grid points can then be written as

$$\begin{aligned}
\dot{\boldsymbol{x}}(t) &= (\boldsymbol{I}_N \otimes \boldsymbol{A}_{a,c} + \mathcal{P}_N \otimes \boldsymbol{A}_{b,c})\boldsymbol{x}(t) + (\boldsymbol{I}_N \otimes \boldsymbol{B}_{a,c})\boldsymbol{f}(t) \\
\boldsymbol{w}(t) &= (\boldsymbol{I}_N \otimes \boldsymbol{C}_{a,c})\boldsymbol{x}(t)
\end{aligned}$$

where

$$\boldsymbol{A}_{a,c} = \begin{bmatrix} 0 & 1 \\ -\frac{8c}{3\sqrt{3}\rho\Delta^2 h} & -\frac{8\zeta c}{3\sqrt{3}\rho\Delta^2 h} \end{bmatrix},\ \boldsymbol{A}_{b,c} = \begin{bmatrix} 0 & 0 \\ -\frac{Eh^2}{12\rho\Delta^4} & -\frac{\eta Eh^2}{12\rho\Delta^4} \end{bmatrix},\ \boldsymbol{B}_{a,c} = \begin{bmatrix} 0 \\ \frac{8c}{3\sqrt{3}\rho\Delta^2 h} \end{bmatrix},\ \boldsymbol{C}_{a,v} = [1\ 0].$$

Furthermore, $\mathcal{P}_N$ is a (sparse) pattern matrix where the non-zero elements on each row correspond to the coefficients of the operator $\mathcal{G}(S_1, S_2)$ in Eq. (2.21) which represents the coupling between the sub-elements.

2.4 Summary and Discussion

This chapter discusses the modeling of interconnected systems. It is demonstrated that a variety of interconnected systems found in real world applications such as power systems, temperature regulation in large buildings and adaptive optics can be simply modeled as linear time invariant systems under several assumptions. Other examples which are not discussed in this chapter include water distributed network [39] and web processing lines [110]. Based on this observation, in the presented dissertation, we consider interconnected systems modeled as an interconnection of LTI subsystems. The utilized model provides us with the first step in analyzing the dynamical systems and designing the control law based on the established theorem of linear dynamical systems. In the future, it is necessary to employ more general models, for example by considering the nonlinear models in order to obtain more accurate models of the interconnected systems.

3 Two-layer Control Architecture for Interconnected Systems

The introduction of communication network provides an additional degree of freedom for the structural design of distributed control in terms of its communication topology. The joint distributed control gain-communication topology design has been investigated recently, for example in [122] where structure optimization is done in terms of a minimization of the required communication links and subject to a predefined bound on the tolerable loss of the achieved H_∞-performance of the decentralized control compared to an H_∞-optimal centralized control. The authors in [90] consider the synchronization of identical networked systems by introducing a distributed control where the control gain and structure are optimized subject to a constraint on the number of links that can be added. Even though adding communication links results in a performance improvement compared to the decentralized control [34, 106], the interconnected system may become unstable under communication link failures. This issue has not been considered in the known literature so far. Furthermore, all of the works mentioned above assume an ideal communication network. The use of communication networks comes, however, at the price of non-ideal signal transmission: the data sent through the networks experience time delay or suffer transmission data losses which is a source of instability and deteriorates the control performance [49].

The major innovation in this chapter is the development of a novel two-layer control architecture which enables the designer to improve the performance of the overall interconnected system while guaranteeing, at the same time, its stability in the presence of permanent communication link failures. The source of inspiration is a combination of the advantages of decentralized and distributed control. First, decentralized control law is designed to stabilize the overall interconnected system. Additionally, the overall system performance, which is the convergence rate, is improved by designing a control law, together with its structure, i.e. the communication topology, which uses the state information from other subsystems under a given communication network constraint. Furthermore, it is demonstrated that the approach is also well suited for the case of non-ideal communication network where the communication link is affected by constant and identical time delay. Another part of innovation in this chapter is the investigation via numerical simulations on the impact of the number of communication topology utilized for the control on the performance improvement of the overall interconnected system.

The remainder of this chapter is organized as follows. After formulating the problem in Section 3.1, we develop a novel two-layer control architecture in Section 3.2 which guarantees the stability of the overall system in the presence of permanent communication link failures by combining the decentralized and distributed control. Furthermore, the two-layer control architecture and the joint distributed control gain-communication topology design are extended to the case of non-ideal communication network, i.e. when the communica-

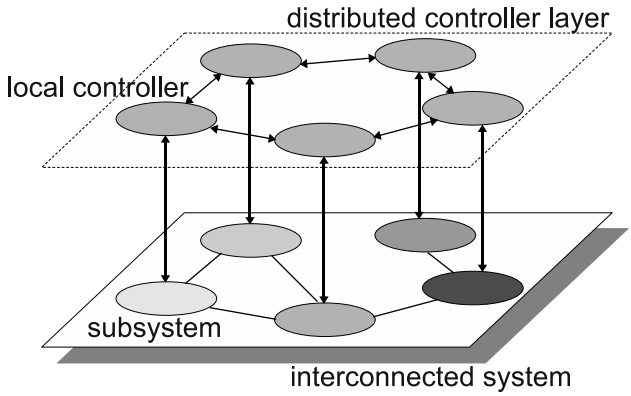

Figure 3.1: An interconnected system with distributed control architecture.

tion network is affected by time delay in Section 3.3. Finally, the proposed approach is tested for designing a novel distributed damping control of power systems in Section 3.4.

3.1 Problem Formulation

Consider an interconnected system of N heterogeneous linear time invariant (LTI) subsystems described by the following differential equations

$$\dot{\boldsymbol{x}}_i = \boldsymbol{A}_i\boldsymbol{x}_i + \sum_{j\in\mathcal{N}_i} \boldsymbol{A}_{ij}\boldsymbol{x}_j + \boldsymbol{B}_i\boldsymbol{u}_i, \quad \boldsymbol{x}_i(t_0) = \boldsymbol{x}_0^i \tag{3.1}$$

where $i = 1, 2, ..., N$ denotes the $i-$th subsystem, $\boldsymbol{x}_i \in \mathbb{R}^n$, $\boldsymbol{u}_i \in \mathbb{R}^p$ are the state of subsystem i and the control input to subsystem i, and $\boldsymbol{A}_i, \boldsymbol{A}_{ij} \in \mathbb{R}^{n\times n}$, $\boldsymbol{B}_i \in \mathbb{R}^{n\times p}$. The term $\sum_{j\in\mathcal{N}_i} \boldsymbol{A}_{ij}\boldsymbol{x}_j$ represents the physical interconnection between the subsystems where $\mathcal{N}_i$ is the set of subsystems to which subsystem i is physically connected. Here we consider a state feedback control for which the control law can be written as follows

$$\boldsymbol{u}_i = \boldsymbol{K}_i\boldsymbol{x}_i + \sum_{j\in\mathcal{G}_i} \boldsymbol{K}_{ij}\boldsymbol{x}_j \tag{3.2}$$

which is known as *distributed* control law since the control law for each subsystem does not only depend on its own states but also the states of the other subsystems. Here $\mathcal{G}_i$ represents a set of subsystems to which controller i could communicate, i.e. exchange information via the network. The interconnected system with its distributed controller is illustrated in Fig. 3.1. If $\boldsymbol{K}_{ij} = 0, \forall i$ and $\forall j \in \mathcal{G}_i$, then the control law (3.2) is called a *decentralized* control law. The overall dynamics of the interconnected system can then be written as

$$\dot{\boldsymbol{x}} = \boldsymbol{A}\boldsymbol{x} + \boldsymbol{B}\boldsymbol{u}, \quad \boldsymbol{x}(t_0) = \boldsymbol{x}_0 \tag{3.3}$$

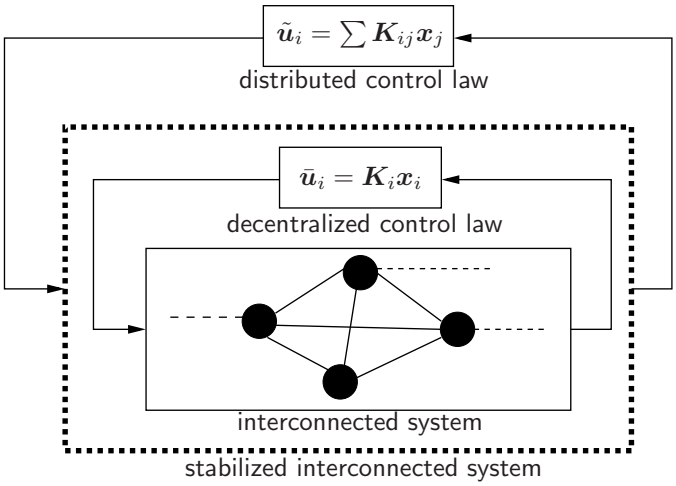

Figure 3.2: Two-layer control architecture. The decentralized control law stabilizes the interconnected system while the distributed control law improves the overall system performance.

where $\boldsymbol{x} = [\boldsymbol{x}_1, \boldsymbol{x}_2, \cdots, \boldsymbol{x}_N]^T$, $\boldsymbol{u} = [\boldsymbol{u}_1, \boldsymbol{u}_2, \cdots, \boldsymbol{u}_N]^T$ and

$$\boldsymbol{A} = \begin{bmatrix} \boldsymbol{A}_1 & \boldsymbol{A}_{12} & \cdots & \boldsymbol{A}_{1N} \\ \boldsymbol{A}_{21} & \boldsymbol{A}_2 & \cdots & \boldsymbol{A}_{2N} \\ \vdots & \vdots & \ddots & \vdots \\ \boldsymbol{A}_{N1} & \boldsymbol{A}_{N2} & \cdots & \boldsymbol{A}_N \end{bmatrix} \in \mathbb{R}^{nN \times nN}, \quad \boldsymbol{B} = \begin{bmatrix} \boldsymbol{B}_1 & 0 & \cdots & 0 \\ 0 & \boldsymbol{B}_2 & \cdots & 0 \\ \vdots & \vdots & \ddots & \vdots \\ 0 & 0 & \cdots & \boldsymbol{B}_N \end{bmatrix} \in \mathbb{R}^{nN \times pN}.$$

The goal is to design the distributed control law (3.2) together with the communication topology such that

- the overall system performance is improved and the stability of the system is guaranteed,
- the stability of the interconnected system w.r.t. the permanent communication link failures is guaranteed.

As a performance metric, in this chapter the convergence rate of the overall interconnected system is considered.

3.2 Two-layer Control Architecture

In order to achieve the goals, in this section a novel two-layer control architecture as illustrated in Fig. 3.2 is proposed. As an idea, first, a decentralized control law is designed that guarantees the stability of the whole interconnected system. The performance of the overall system is then improved by designing a distributed control law, i.e. the second term of (3.2) together with the communication topology $\mathcal{G}_i, \forall i$.

3.2.1 Decentralized Control Design

As a first step, the decentralized control law that stabilizes the interconnected system (3.1) is designed. Let us first investigate the stability of the following interconnected system.

$$\dot{\boldsymbol{x}}_i = \boldsymbol{A}_i x_i + \sum_{j \in \mathcal{N}_i} \boldsymbol{A}_{ij} \boldsymbol{x}_j. \tag{3.4}$$

Proposition 3.2.1 If there exists positive constants $\epsilon_i > 0$ such that the following N linear matrix inequalities have symmetrically positive definite solutions $\boldsymbol{P}_i \in \mathbb{R}^{n \times n}$,

$$\begin{bmatrix} \boldsymbol{A}_i \boldsymbol{F}_i + \boldsymbol{F}_i \boldsymbol{A}_i^T + \frac{1}{\epsilon_i}(\sum_{j \in \mathcal{N}_i} \boldsymbol{A}_{ij} \boldsymbol{A}_{ij}^T) & \boldsymbol{F}_i \\ \boldsymbol{F}_i & -\frac{1}{\epsilon_i (N-1)} \boldsymbol{I}_n^{-1} \end{bmatrix} < 0 \tag{3.5}$$

where $\boldsymbol{F}_i = \boldsymbol{P}_i^{-1}$ and $\boldsymbol{I}_n$ is the identity matrix with dimension of n, then the interconnected system (3.4) is asymptotically stable.

In order to prove the proposition, we need the following lemma.

Lemma 3.2.2 [17] Let $\boldsymbol{X}, \boldsymbol{Y}$ be two matrices of appropriate dimension. Then, for any $\epsilon > 0$, the following inequality holds.

$$\boldsymbol{X}^T \boldsymbol{Y} + \boldsymbol{Y}^T \boldsymbol{X} \leq \epsilon \boldsymbol{X}^T \boldsymbol{X} + \frac{1}{\epsilon} \boldsymbol{Y}^T \boldsymbol{Y}.$$

We are now ready to prove the proposition.

Proof: The proof is similar to the one discussed in [135]. First, let us consider the following Lyapunov function

$$V(\boldsymbol{x}) = \sum_{i=1}^{N} \boldsymbol{x}_i^T \boldsymbol{P}_i \boldsymbol{x}_i.$$

Taking the derivative of $V(\boldsymbol{x})$ along (3.4) gives:

$$\dot{V}(\boldsymbol{x}) = \sum_{i=1}^{N} \dot{\boldsymbol{x}}_i^T \boldsymbol{P}_i \boldsymbol{x}_i + \boldsymbol{x}_i^T \boldsymbol{P}_i \dot{\boldsymbol{x}}_i. \tag{3.8}$$

Substituting (3.4) into the above equation gives

$$\begin{aligned} \dot{V}(\boldsymbol{x}) &= \sum_{i=1}^{N} \left[(\boldsymbol{A}_i \boldsymbol{x}_i + \sum_{j \in \mathcal{N}_i} \boldsymbol{A}_{ij} \boldsymbol{x}_j)^T \boldsymbol{P}_i \boldsymbol{x}_i + \boldsymbol{x}_i^T \boldsymbol{P}_i (\boldsymbol{A}_i \boldsymbol{x}_i + \sum_{j \in \mathcal{N}_i} \boldsymbol{A}_{ij} \boldsymbol{x}_j) \right] \\ &= \sum_{i=1}^{N} \boldsymbol{x}_i^T (\boldsymbol{A}_i^T \boldsymbol{P}_i + \boldsymbol{P}_i \boldsymbol{A}_i) \boldsymbol{x}_i + (\sum_{j \in \mathcal{N}_i} \boldsymbol{A}_{ij} \boldsymbol{x}_j)^T \boldsymbol{P}_i \boldsymbol{x}_i + \boldsymbol{x}_i^T \boldsymbol{P}_i \sum_{j \in \mathcal{N}_i} \boldsymbol{A}_{ij} \boldsymbol{x}_j \end{aligned}$$

and applying Lemma 1 yields

$$\begin{aligned}\dot{V}(\boldsymbol{x}) &\leq \sum_{i=1}^{N} \boldsymbol{x}_i^T(\boldsymbol{A}_i^T\boldsymbol{P}_i + \boldsymbol{P}_i\boldsymbol{A}_i)\boldsymbol{x}_i + \frac{1}{\epsilon}\boldsymbol{x}_i^T\boldsymbol{P}_i(\sum \boldsymbol{A}_{ij}\boldsymbol{A}_{ij}^T)\boldsymbol{P}_i\boldsymbol{x}_i + \epsilon\sum_{j\neq i}\boldsymbol{x}_j^T\boldsymbol{x}_j \\ &\leq \sum_{i=1}^{N} \boldsymbol{x}_i^T\left[\boldsymbol{A}_i^T\boldsymbol{P}_i + \boldsymbol{P}_i\boldsymbol{A}_i + \frac{1}{\epsilon}\boldsymbol{P}_i(\sum_{j\in\mathcal{N}_i}\boldsymbol{A}_{ij}\boldsymbol{A}_{ij}^T)\boldsymbol{P}_i + \epsilon(N-1)\boldsymbol{I}_n\right]\boldsymbol{x}_i. \qquad (3.9)\end{aligned}$$

If $\forall i$, $\boldsymbol{A}_i^T\boldsymbol{P}_i+\boldsymbol{P}_i\boldsymbol{A}_i+\frac{1}{\epsilon}\boldsymbol{P}_i(\sum_{j\in\mathcal{N}_i}\boldsymbol{A}_{ij}\boldsymbol{A}_{ij}^T)\boldsymbol{P}_i+\epsilon(N-1)\boldsymbol{I}_n<0$, then $\dot{V}(\boldsymbol{x})$ is negative definite. Therefore, the interconnected system (3.4) is stable. Furthermore, pre- and post-multiply (3.9) by $\boldsymbol{P}_i^{-1}$ respectively gives

$$\boldsymbol{A}_i\boldsymbol{F}_i + \boldsymbol{F}_i\boldsymbol{A}_i^T + \epsilon_i\boldsymbol{F}_i(N-1)\boldsymbol{I}_n\boldsymbol{F}_i + \frac{1}{\epsilon_i}(\sum_{j\in\mathcal{N}_i}\boldsymbol{A}_{ij}\boldsymbol{A}_{ij}^T) < 0. \qquad (3.10)$$

Finally, applying Schur complement to (3.10) results in (3.5). ■

Next, we consider the decentralized control law synthesis for the interconnected system (3.1) with the control input given by

$$\boldsymbol{u}_i = \bar{\boldsymbol{u}}_i = \boldsymbol{K}_i\boldsymbol{x}_i. \qquad (3.11)$$

Let $\boldsymbol{A}_i + \boldsymbol{B}_i\boldsymbol{K}_i = \bar{\boldsymbol{A}}_i$ and we will have a similar expression as in (3.5) given by

$$\begin{bmatrix}\bar{\boldsymbol{A}}_i\boldsymbol{F}_i + \boldsymbol{F}_i\bar{\boldsymbol{A}}_i^T + \frac{1}{\epsilon_i}(\sum_{j\in\mathcal{N}_i}\boldsymbol{A}_{ij}\boldsymbol{A}_{ij}^T) & \boldsymbol{F}_i \\ \boldsymbol{F}_i & -\frac{1}{\epsilon_i(N-1)}\boldsymbol{I}_n^{-1}\end{bmatrix} < 0. \qquad (3.12)$$

The difficulty in solving the feedback gain $\boldsymbol{K}_i$ in the matrix inequality (3.12) is that it involves the nonlinear terms, i.e. $\bar{\boldsymbol{A}}_i\boldsymbol{F}_i$, thus it cannot be considered as an LMI problem. However, by restricting the solution space of $\boldsymbol{F}_i$, the nonlinear terms can be eliminated and the LMI problem is recovered. By using Proposition 3.2.1, the decentralized control law synthesis can be computed as follows.

Proposition 3.2.3 If there exists positive constants $\epsilon_i > 0$ such that the following N linear matrix inequalities have symmetric solutions $\boldsymbol{F}_i > 0$ and $\boldsymbol{Y}_i$,

$$\begin{bmatrix}\boldsymbol{A}_i\boldsymbol{F}_i + (\boldsymbol{A}_i\boldsymbol{F}_i)^T + \boldsymbol{B}_i\boldsymbol{Y}_i + (\boldsymbol{B}_i\boldsymbol{Y}_i)^T + \frac{1}{\epsilon_i}(\sum_{j\in\mathcal{N}_i}\boldsymbol{A}_{ij}\boldsymbol{A}_{ij}^T) & \boldsymbol{F}_i \\ \boldsymbol{F}_i & -\frac{1}{\epsilon_i(N-1)}\boldsymbol{I}_n^{-1}\end{bmatrix} < 0$$

where $\boldsymbol{F}_i = \boldsymbol{P}_i^{-1}$, then the decentralized control law in (3.11) is given by $\boldsymbol{K}_i = \boldsymbol{Y}_i\boldsymbol{F}_i^{-1}$.

Remark 2 In this dissertation, it is assumed that all the decentralized fixed modes (DFMs), if any, are in the open left half plane. The problem with unstable DFMs is beyond the scope of this dissertation.

3.2.2 Joint Distributed Control Gain-Communication Topology Design

After the overall interconnected system (3.1) has been stabilized by the decentralized control law, i.e. the first term of (3.2), the second step in the two-layer control architecture is to improve the system performance by designing the distributed control law, i.e. the feedback gain and the communication topology under a given communication network constraint. Here the convergence rate of the overall system is considered as a performance metric. However, the proposed approach can also be applied to other performance metrics.

The closed loop expression of the interconnected system (3.1) with the decentralized control law (3.11) can be written as

$$\dot{\boldsymbol{x}} = \boldsymbol{A}_{\text{dec}} x, \quad \boldsymbol{x}(t_0) = \boldsymbol{x}_0 \tag{3.14}$$

where

$$\boldsymbol{A}_{\text{dec}} = \begin{bmatrix} \bar{\boldsymbol{A}}_1 & \boldsymbol{A}_{12} & \cdots & \boldsymbol{A}_{1N} \\ \boldsymbol{A}_{21} & \bar{\boldsymbol{A}}_2 & \cdots & \boldsymbol{A}_{2N} \\ \vdots & \vdots & \ddots & \vdots \\ \boldsymbol{A}_{N1} & \boldsymbol{A}_{N2} & \cdots & \bar{\boldsymbol{A}}_N \end{bmatrix} \in \mathbb{R}^{nN \times nN}.$$

It is well known that the solution of (3.14) is given by $\boldsymbol{x}(t) = e^{\boldsymbol{A}_{\text{dec}}(t-t_0)}\boldsymbol{x}_0$ and the state norm satisfies

$$\|\boldsymbol{x}(t)\| \leq e^{\{\lambda_{\max}(\boldsymbol{A}_{\text{dec}})(t-t_0)\}}\|\boldsymbol{x}_0\|, \forall t \geq t_0 \tag{3.15}$$

where $\lambda_{\max}(\boldsymbol{A}_{\text{dec}}) \in \mathbb{R}$ represents the largest real part of the eigenvalues of $\boldsymbol{A}_{\text{dec}}$.

The objective is to improve the performance of the overall system, i.e. increase the convergence rate by designing the second term of (3.2) given by the following control law

$$\bar{\boldsymbol{u}}_i = \sum_{j \in \mathcal{G}_i} d_{ij} \boldsymbol{K}_{ij} \boldsymbol{x}_j \tag{3.16}$$

where $d_{ij} \in \{0, 1\}$ is a binary number that denotes the possibility to perform the state information exchange between controllers i and j, i.e. $d_{ij} = 1$ means that a communication link is added between controllers i and j and vice versa. The new closed loop expression of (3.1) with the addition of control law (3.16) is given by

$$\dot{\boldsymbol{x}} = \bar{\boldsymbol{A}}\boldsymbol{x}, \quad \boldsymbol{x}(t_0) = \boldsymbol{x}_0 \tag{3.17}$$

where

$$\begin{aligned} \bar{\boldsymbol{A}} &= \begin{bmatrix} \bar{\boldsymbol{A}}_1 & \boldsymbol{A}_{12} & \cdots & \boldsymbol{A}_{1N} \\ \boldsymbol{A}_{21} & \bar{\boldsymbol{A}}_2 & \cdots & \boldsymbol{A}_{2N} \\ \vdots & \vdots & \ddots & \vdots \\ \boldsymbol{A}_{N1} & \boldsymbol{A}_{N2} & \cdots & \bar{\boldsymbol{A}}_N \end{bmatrix} + \begin{bmatrix} 0 & \bar{\boldsymbol{A}}_{12} & \cdots & \bar{\boldsymbol{A}}_{1N} \\ \bar{\boldsymbol{A}}_{21} & 0 & \cdots & \bar{\boldsymbol{A}}_{2N} \\ \vdots & \vdots & \ddots & \vdots \\ \bar{\boldsymbol{A}}_{N1} & \bar{\boldsymbol{A}}_{N2} & \cdots & 0 \end{bmatrix}, \\ \bar{\boldsymbol{A}} &= \boldsymbol{A}_{\text{dec}} + \boldsymbol{A}_{\text{dist}} \end{aligned} \tag{3.18}$$

and the term $\bar{\boldsymbol{A}}_{ij}$ is defined as $\bar{\boldsymbol{A}}_{ij} = d_{ij}\boldsymbol{B}_i\boldsymbol{K}_{ij}$. Furthermore, it is assumed that not

arbitrary many links can be added, i.e. the number is limited by an upper bound induced by the communication constraint

$$\sum_{1\leq i\leq j\leq N} \gamma_{ij} d_{ij} \leq c \tag{3.19}$$

where $c > 0$ is the total cost constraint on the communication network, and γ_{ij} represents a cost to establish a link between subsystem i and j. This cost is typically related to factors such as hardware costs, energy consumption for communicating information, the distance between the subsystems or the number of hops in a multi-hop wireless network.

The problem can then be formulated as finding the control gain and communication topology of the distributed control law such that the convergence rate of the interconnected system is optimized under a given communication constraint. The solution of joint distributed control gain and communication topology design problem is given by the following proposition.

Proposition 3.2.4 Consider an interconnected system (3.17). If there exists a solution of the optimization problem

$$\begin{aligned} \underset{\boldsymbol{K}_{ij}, d_{ij}}{\text{minimize}} \quad & \lambda_{\max}(\bar{\boldsymbol{A}}) \\ \text{subject to} \quad & \lambda_{\max}(\bar{\boldsymbol{A}}) < \lambda_{\max}(\boldsymbol{A}_{\text{dec}}), \\ & \sum_{1\leq i\leq j\leq N} \gamma_{ij} d_{ij} \leq c, \\ & d_{ij} \in \{0, 1\}, \end{aligned} \tag{3.20}$$

then the convergence rate of the interconnected system with the distributed control law (3.2) is higher than with the decentralized control law (3.11) and the overall system remains stable.

Proof: Here we prove that the system remains stable if a solution of the optimization problem (3.20) exists. Since the overall interconnected system is stabilized by the decentralized control, then $\lambda_{\max}(\boldsymbol{A}_{\text{dec}}) < 0$. This yields

$$\lambda_{\max}(\bar{\boldsymbol{A}}) < \lambda_{\max}(\boldsymbol{A}_{\text{dec}}) < 0,$$

i.e. the interconnected system with the distributed control law is stable. Moreover, since $\lambda_{\max}(\bar{\boldsymbol{A}}) < \lambda_{\max}(\boldsymbol{A}_{\text{dec}})$, the convergence rate of the interconnected system with the distributed control is higher than with the decentralized control. ■

The optimization problem (3.20) is a mixed integer optimization problem since it is solved with respect to both the feedback gain and the communication topology of the distributed control law. Furthermore, the objective function, i.e. the spectral abscissa $\lambda_{\max}$ is non-convex and non-smooth since in general the matrix $\bar{\boldsymbol{A}}$ is nonsymmetric. Therefore, finding global optimum of the spectral abscissa is hard. Some numerical methods have been developed in order to solve the optimization of the spectral abscissa, for example the method proposed in [20]. However, when the matrix $\bar{\boldsymbol{A}}$ is symmetric, the objective function

becomes convex and the problem can be reformulated into the Mixed Integer Semidefinite Program (MISDP) as demonstrated in [115, 131].

Another important issue related to the optimization problem (3.20) is the combinatorial problem stemmed from the communication topology design. For the sake of clarity, let us assume that $\gamma_{ij} = 1$. The complexity of the design approach for a given communication links c in terms of the number of combinations that has to be performed is given by $\binom{c_{\max}}{c} = \frac{c_{\max}!}{c!(c_{\max}-c)!}$ where $c_{\max} = \frac{N}{2}(N-1)$. Even though the optimization (3.20) can be solved using well-known techniques such as relaxation and decomposition techniques or cutting planes approaches [73], solving (3.20) for a large number of subsystems may become very hard. However, as will be shown later in Chapter 4, for a special class of systems, the combinatorial problem cannot only be solved efficiently, but the closed-loop solution can also be obtained. An alternative method to deal with the combinatorial aspect of this problem is by formulating the integer problem using l_0 norm, and then relaxing the combinatorial problem using (weighted) l_1 norm as discussed in [121, 122].

In the following, it is shown that by using the two-layer control architecture developed previously, the stability of the interconnected system is guaranteed in the presence of permanent communication link failures as stated in the following Proposition.

Proposition 3.2.5 The stability of the interconnected system (3.17) is guaranteed under any combination of permanent communication link failures.

Proof: Since the maximum and minimum value of $\lambda_{\max}(\bar{\boldsymbol{A}})$ are given by Propositions 3.2.1 and 3.2.4 respectively, the maximum eigenvalue of the whole system under any combination of communication link failures, i.e. $\lambda_{\max}(\tilde{\boldsymbol{A}})$ will satisfy $\lambda_{\max}(\bar{\boldsymbol{A}}) < \lambda_{\max}(\tilde{\boldsymbol{A}}) < \lambda_{\max}(\boldsymbol{A}_{\text{dec}}) < 0$. ■

Remark 3 Even though the proposed two-layer control architecture guarantees the stability of the interconnected system under permanent communication link failures, it may lead to a reduced system performance since the design of the decentralized control law is not considered in the optimization problem (3.20).

3.2.3 Evaluation

In this section, the proposed two-layer control architecture is evaluated via numerical examples. Furthermore, the impact of the addition of communication links on the system performance improvement is investigated for the first time. For the sake of clarity, an interconnection of scalar subsystems is considered which can be found for example in temperature regulation problem in large building as described in Chapter 2 [43]. Specifically, we consider an interconnected system consisting of 20 scalar subsystems whose physical interconnection is shown in Fig. 3.3. It is assumed that the overall system has been stabilized by using decentralized control law and the closed loop dynamics with the decentralized

control law is given by:

$$\boldsymbol{A}_{\text{dec}} = \begin{bmatrix}
-15 & 2 & 0 & 0 & 3 & 0 & 0 & 0 & 4 & 0 & 0 & 0 & 0 & 0 & 0 & 0 & 0 & 0 & 0 & 0 \\
2 & -10 & 0 & 0 & 0 & 0 & 0 & 0 & 0 & 0 & 0 & 0 & 0 & 0 & 0 & 0 & 0 & 3 & 0 & 0 \\
0 & 0 & -12 & 1 & 0 & 0 & 0 & 0 & 0 & 0 & 0 & 5 & 0 & 0 & 0 & 0 & 0 & 0 & 0 & 0 \\
0 & 0 & 1 & -13 & 3 & 0 & 0 & 0 & 0 & 0 & 10 & 0 & 0 & 0 & 0 & 0 & 0 & 2 & 0 & 0 \\
3 & 0 & 0 & 3 & -15 & 2 & 0 & 0 & 0 & 0 & 0 & 0 & 0 & 4 & 0 & 0 & 0 & 0 & 0 & 0 \\
0 & 0 & 0 & 0 & 2 & -8 & 0 & 0 & 0 & 0 & 0 & 0 & 0 & 0 & 0 & 0 & 0 & 0 & 0 & 3 \\
0 & 0 & 0 & 0 & 0 & 0 & -7 & 4 & 0 & 2 & 0 & 0 & 0 & 0 & 0 & 0 & 0 & 0 & 0 & 0 \\
0 & 0 & 0 & 0 & 0 & 0 & 4 & -15 & 0 & 0 & 0 & 0 & 0 & 0 & 3 & 0 & 0 & 0 & 0 & 0 \\
4 & 0 & 0 & 0 & 0 & 0 & 0 & 0 & -10 & 0 & 0 & 0 & 0 & 0 & 0 & 0 & 0 & 0 & 1 & 0 \\
0 & 0 & 0 & 0 & 0 & 0 & 2 & 0 & 0 & -10 & 4 & 0 & 0 & 0 & 0 & 1 & 0 & 0 & 0 & 0 \\
0 & 0 & 0 & 10 & 0 & 0 & 0 & 0 & 0 & 4 & -15 & 0 & 0 & 0 & 0 & 1 & 0 & 0 & 0 & 0 \\
0 & 0 & 5 & 0 & 0 & 0 & 0 & 0 & 0 & 0 & 0 & -15 & 2 & 0 & 0 & 0 & 0 & 0 & 0 & 0 \\
0 & 0 & 0 & 0 & 0 & 0 & 0 & 0 & 0 & 0 & 0 & 2 & -9 & 0 & 0 & 0 & 3 & 0 & 0 & 4 \\
0 & 0 & 0 & 0 & 4 & 0 & 0 & 0 & 0 & 0 & 0 & 0 & 0 & -10 & 0 & 0 & 0 & 0 & 0 & 0 \\
0 & 0 & 0 & 0 & 0 & 0 & 0 & 3 & 0 & 0 & 0 & 0 & 0 & 0 & -15 & 3 & 0 & 0 & 0 & 0 \\
0 & 0 & 0 & 0 & 0 & 0 & 0 & 0 & 0 & 1 & 1 & 0 & 0 & 0 & 3 & -11 & 0 & 0 & 0 & 0 \\
0 & 0 & 0 & 2 & 0 & 0 & 0 & 0 & 0 & 0 & 0 & 0 & 3 & 0 & 0 & 0 & -12 & 0 & 0 & 0 \\
0 & 3 & 0 & 0 & 0 & 0 & 0 & 0 & 0 & 0 & 0 & 0 & 0 & 0 & 0 & 0 & 0 & -15 & 0 & 0 \\
0 & 0 & 0 & 0 & 0 & 0 & 0 & 0 & 1 & 0 & 0 & 0 & 0 & 0 & 0 & 0 & 0 & 0 & -19 & 0 \\
0 & 0 & 0 & 0 & 0 & 3 & 0 & 0 & 0 & 0 & 0 & 0 & 4 & 0 & 0 & 0 & 0 & 0 & 0 & -15
\end{bmatrix}$$

where its largest real part of the eigenvalues is given by $\lambda_{\max}(\boldsymbol{A}_{\text{dec}}) = -1.89$.

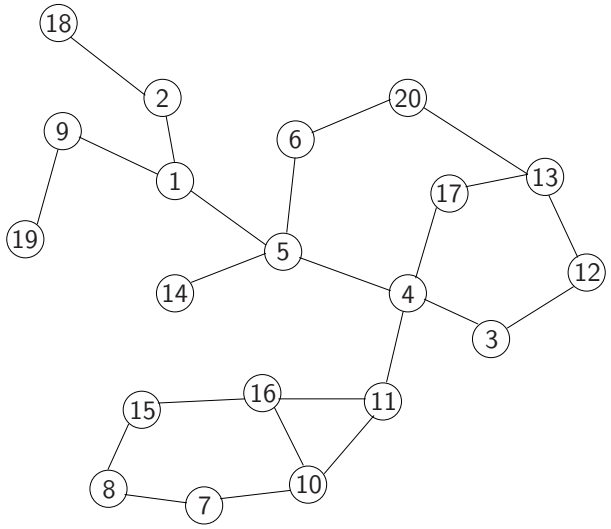

Figure 3.3: An interconnected system consisting of 20 subsystems.

Joint Control Gain-Communication Topology

First, the performance of the overall system is improved by designing the distributed control law, i.e. the second term of (3.2) together with the communication topology by solving the optimization problem (3.20). In addition, it is assumed that $\gamma_{ij} = 1$. The simulations are performed by solving (3.20) using the YALMIP toolbox [92] for the maximum number of allowable communication links c equal to 1,2,3 and 15. The results are summarized in Table 3.1.

It can be observed from the simulations that for the case of $c = 1$, the communication link is added between the local controllers of subsystems 4 and 11. Next, we set $c = 2$

Table 3.1: The largest eigenvalue for different number of communication links

maximum number of links (c)	used communication links	$\lambda_{\max}(\boldsymbol{A})$
1	1	-4.26
2	2	-4.56
3	3	–4.56
15	14	-7

which results in $\lambda_{\max} = -4.56$ and $\boldsymbol{A}_{\text{dist}}$ is given by

$$\boldsymbol{A}_{\text{dist}} = \begin{bmatrix}
0 & 0 & 0 & 0 & 0 & 0 & 0 & 0 & 0 & 0 & 0 & 0 & 0 & 0 & 0 & 0 & 0 & 0 & 0 & 0 \\
0 & 0 & 0 & 0 & 0 & 0 & 0 & 0 & 0 & 0 & 0 & 0 & 0 & 0 & 0 & 0 & 0 & 0 & 0 & 0 \\
0 & 0 & 0 & 0 & 0 & 0 & 0 & 0 & 0 & 0 & 0 & 0 & 0 & 0 & 0 & 0 & 0 & 0 & 0 & 0 \\
0 & 0 & 0 & 0 & 0 & 0 & 0 & 0 & 0 & 0 & \mathbf{-10} & 0 & 0 & 0 & 0 & 0 & 0 & 0 & 0 & 0 \\
0 & 0 & 0 & 0 & 0 & 0 & 0 & 0 & 0 & 0 & 0 & 0 & 0 & 0 & 0 & 0 & 0 & 0 & 0 & 0 \\
0 & 0 & 0 & 0 & 0 & 0 & 0 & 0 & 0 & 0 & 0 & 0 & 0 & 0 & 0 & 0 & 0 & 0 & 0 & 0 \\
0 & 0 & 0 & 0 & 0 & 0 & 0 & 0 & 0 & \mathbf{-2.1225} & 0 & 0 & 0 & 0 & 0 & 0 & 0 & 0 & 0 & 0 \\
0 & 0 & 0 & 0 & 0 & 0 & 0 & 0 & 0 & 0 & 0 & 0 & 0 & 0 & 0 & 0 & 0 & 0 & 0 & 0 \\
0 & 0 & 0 & 0 & 0 & 0 & 0 & 0 & 0 & 0 & 0 & 0 & 0 & 0 & 0 & 0 & 0 & 0 & 0 & 0 \\
0 & 0 & 0 & 0 & 0 & 0 & \mathbf{-2.1225} & 0 & 0 & 0 & 0 & 0 & 0 & 0 & 0 & 0 & 0 & 0 & 0 & 0 \\
0 & 0 & 0 & \mathbf{-10} & 0 & 0 & 0 & 0 & 0 & 0 & 0 & 0 & 0 & 0 & 0 & 0 & 0 & 0 & 0 & 0 \\
0 & 0 & 0 & 0 & 0 & 0 & 0 & 0 & 0 & 0 & 0 & 0 & 0 & 0 & 0 & 0 & 0 & 0 & 0 & 0 \\
0 & 0 & 0 & 0 & 0 & 0 & 0 & 0 & 0 & 0 & 0 & 0 & 0 & 0 & 0 & 0 & 0 & 0 & 0 & 0 \\
0 & 0 & 0 & 0 & 0 & 0 & 0 & 0 & 0 & 0 & 0 & 0 & 0 & 0 & 0 & 0 & 0 & 0 & 0 & 0 \\
0 & 0 & 0 & 0 & 0 & 0 & 0 & 0 & 0 & 0 & 0 & 0 & 0 & 0 & 0 & 0 & 0 & 0 & 0 & 0 \\
0 & 0 & 0 & 0 & 0 & 0 & 0 & 0 & 0 & 0 & 0 & 0 & 0 & 0 & 0 & 0 & 0 & 0 & 0 & 0 \\
0 & 0 & 0 & 0 & 0 & 0 & 0 & 0 & 0 & 0 & 0 & 0 & 0 & 0 & 0 & 0 & 0 & 0 & 0 & 0 \\
0 & 0 & 0 & 0 & 0 & 0 & 0 & 0 & 0 & 0 & 0 & 0 & 0 & 0 & 0 & 0 & 0 & 0 & 0 & 0 \\
0 & 0 & 0 & 0 & 0 & 0 & 0 & 0 & 0 & 0 & 0 & 0 & 0 & 0 & 0 & 0 & 0 & 0 & 0 & 0
\end{bmatrix}.$$

Furthermore, solving (3.20) for the maximum number of allowable communication links $c = 3$ yields

$$\boldsymbol{A}_{\text{dist}} = \begin{bmatrix}
0 & 0 & 0 & 0 & 0 & 0 & 0 & 0 & 0 & 0 & 0 & 0 & 0 & 0 & 0 & 0 & 0 & 0 & 0 & 0 \\
0 & 0 & 0 & 0 & 0 & 0 & 0 & 0 & 0 & 0 & 0 & 0 & 0 & 0 & 0 & 0 & 0 & 0 & 0 & 0 \\
0 & 0 & 0 & 0 & 0 & 0 & 0 & 0 & 0 & 0 & 0 & 0 & 0 & 0 & 0 & 0 & 0 & 0 & 0 & 0 \\
0 & 0 & 0 & 0 & 0 & 0 & 0 & 0 & 0 & 0 & \mathbf{-10} & 0 & 0 & 0 & 0 & 0 & 0 & 0 & 0 & 0 \\
0 & 0 & 0 & 0 & 0 & 0 & 0 & 0 & 0 & 0 & 0 & 0 & 0 & 0 & 0 & 0 & 0 & 0 & 0 & 0 \\
0 & 0 & 0 & 0 & 0 & 0 & 0 & 0 & 0 & 0 & 0 & 0 & 0 & 0 & 0 & 0 & 0 & 0 & 0 & 0 \\
0 & 0 & 0 & 0 & 0 & 0 & 0 & \mathbf{-4} & 0 & \mathbf{-2} & 0 & 0 & 0 & 0 & 0 & 0 & 0 & 0 & 0 & 0 \\
0 & 0 & 0 & 0 & 0 & 0 & \mathbf{-4} & 0 & 0 & 0 & 0 & 0 & 0 & 0 & 0 & 0 & 0 & 0 & 0 & 0 \\
0 & 0 & 0 & 0 & 0 & 0 & 0 & 0 & 0 & 0 & 0 & 0 & 0 & 0 & 0 & 0 & 0 & 0 & 0 & 0 \\
0 & 0 & 0 & 0 & 0 & 0 & \mathbf{-2} & 0 & 0 & 0 & 0 & 0 & 0 & 0 & 0 & 0 & 0 & 0 & 0 & 0 \\
0 & 0 & 0 & \mathbf{-10} & 0 & 0 & 0 & 0 & 0 & 0 & 0 & 0 & 0 & 0 & 0 & 0 & 0 & 0 & 0 & 0 \\
0 & 0 & 0 & 0 & 0 & 0 & 0 & 0 & 0 & 0 & 0 & 0 & 0 & 0 & 0 & 0 & 0 & 0 & 0 & 0 \\
0 & 0 & 0 & 0 & 0 & 0 & 0 & 0 & 0 & 0 & 0 & 0 & 0 & 0 & 0 & 0 & 0 & 0 & 0 & 0 \\
0 & 0 & 0 & 0 & 0 & 0 & 0 & 0 & 0 & 0 & 0 & 0 & 0 & 0 & 0 & 0 & 0 & 0 & 0 & 0 \\
0 & 0 & 0 & 0 & 0 & 0 & 0 & 0 & 0 & 0 & 0 & 0 & 0 & 0 & 0 & 0 & 0 & 0 & 0 & 0 \\
0 & 0 & 0 & 0 & 0 & 0 & 0 & 0 & 0 & 0 & 0 & 0 & 0 & 0 & 0 & 0 & 0 & 0 & 0 & 0 \\
0 & 0 & 0 & 0 & 0 & 0 & 0 & 0 & 0 & 0 & 0 & 0 & 0 & 0 & 0 & 0 & 0 & 0 & 0 & 0 \\
0 & 0 & 0 & 0 & 0 & 0 & 0 & 0 & 0 & 0 & 0 & 0 & 0 & 0 & 0 & 0 & 0 & 0 & 0 & 0 \\
0 & 0 & 0 & 0 & 0 & 0 & 0 & 0 & 0 & 0 & 0 & 0 & 0 & 0 & 0 & 0 & 0 & 0 & 0 & 0 \\
0 & 0 & 0 & 0 & 0 & 0 & 0 & 0 & 0 & 0 & 0 & 0 & 0 & 0 & 0 & 0 & 0 & 0 & 0 & 0
\end{bmatrix}$$

which surprisingly, results in a similar performance value as $c = 2$, i.e. $\lambda_{\max} = -4.56$. It should be noted that the optimal communication topology for $c = 2$ is the subset of the optimal topology for $c = 3$.

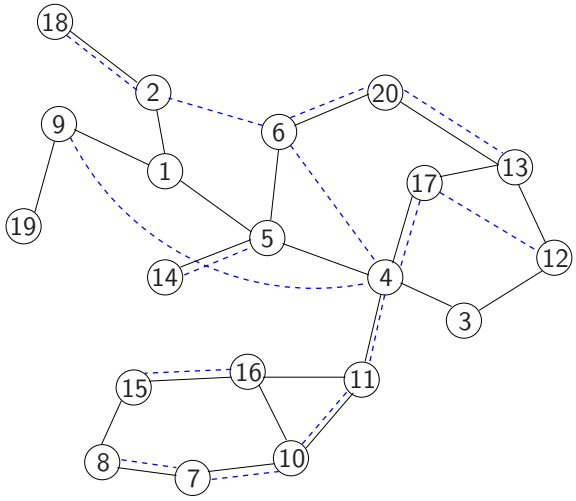

Figure 3.4: Optimal communication topology for $\gamma_{ij} = 1, c = 15$. As can be seen, only 14 communication topology is used. This means that adding more communication links will not improve the overall system performance. The solid and dashed lines represent the physical and communication links respectively.

Discussion

The results indicate that by increasing the number of communication links, the system performance may not always be improved. Additionally, when the maximum number of allowable communication links is increased to 15 links, as can be observed from Table 3.1, only 14 out of 15 allowable communication links are utilized. In other words, by increasing the number of maximum allowable communication links more than 14 links, the optimal solution will be similar to the case of $c = 14$, i.e. the system performance cannot be further improved. One of the possible reasons is that the distributed control gain is exploited to improve the overall system performance without the need of having more communication links. The optimal communication topology for the case of $c = 15$ is shown in Fig. 3.4, and the trajectories of $||\boldsymbol{x}||$ are shown in Fig. 3.5 for a random initial states. As can be seen from Fig. 3.5, the distributed control improves the performance of the overall system. Furthermore, the robustness of the two-layer control architecture proposed in this chapter is investigated by randomly deleting 4 communication links, in this case, communication links between the local controllers of subsystems 4-9,13-20,17-4,7-8. As depicted in Fig. 3.5, the overall interconnected system remains stable and the decay rate is still higher than the decentralized control. Furthermore, the stability of the interconnected systems is also guaranteed under permanent communication link failures which demonstrates the efficacy of the proposed control architecture.

Impact of Number of Links on the Overall Performance

Next, the impact of addition of communication links on the system performance improvement is investigated. Since we are interested in the impact of the utilization of communication links, the distributed control gain is assumed to be fixed and identical for all communication links, i.e. the optimization problem is solved only with respect to the

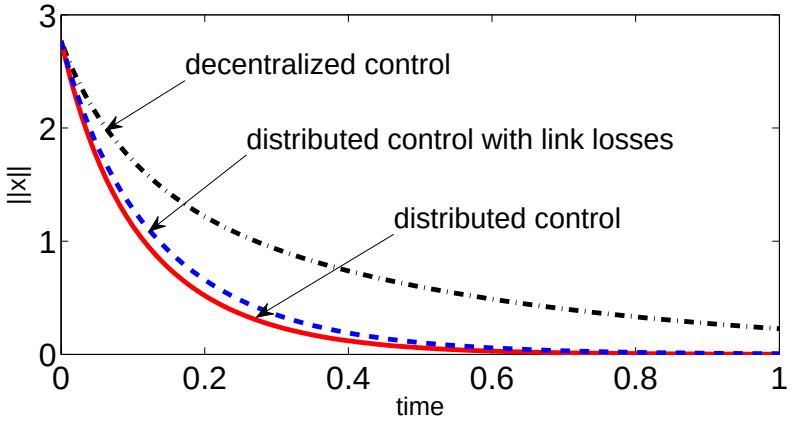

Figure 3.5: The convergence rate of the interconnected system with the distributed control law and the decentralized control law. Furthermore, as can be seen from the figure, by using the proposed two-layer control architecture, the stability of the overall system is guaranteed under permanent communication link failures.

communication topology. In the simulations, the distributed control gain is set equally to -2, i.e. $\boldsymbol{K}_{ij} = -2, \forall i, j, i \neq j$. The optimization is solved for maximum allowable number of communication links $c = 1, 2, 3, 4, 5, 6, 7, 8, 9, 15, 20$, and the results are summarized in Fig. 3.6.

Discussion

As can be observed from Fig. 3.6, for a small number of communication links, the system performance is significantly improved. However, when the number of communication links becomes larger, the performance improvement becomes smaller and the largest eigenvalue of the closed loop with distributed control law is approximately constant when the number of links is larger than 9. The simulation results for this specific setup indicate that adding more than 9 communication links may not be beneficial to the performance improvement of the interconnected system. It should be noted that similar results are also observed in the consensus problem of multiagent systems. The algebraic connectivity, i.e. the second smallest eigenvalue of the Laplacian matrix is known as a performance metric which describes the convergence rate for reaching consensus, and its value depends on the topology of the communication graph between the agents. While adding a communication link into a graph may not decrease the algebraic connectivity, it is reported in [115] that by increasing the maximum allowable communication cost, the algebraic connectivity is not always improved. One of the conditions that results in the circumstance as discussed in [19,47] is that when the second smallest eigenvalue of the original graph has multiplicity r, then exactly r links are needed to be added before the algebraic connectivity increases from its current value.

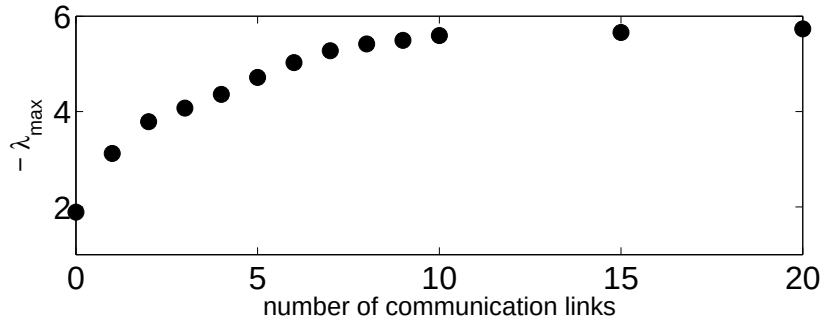

Figure 3.6: The convergence rate of the interconnected system with different number of communication links. As can be seen, from a certain number of communication links, the performance improvement becomes smaller.

3.3 Two-layer Control Architecture for Time-Delay Systems

Next, we investigate a more realistic case by considering non-ideal communication networks where the information exchange is afflicted by time delay $\tau > 0$ which is assumed to be constant and identical for all communication links as illustrated in Fig. 3.7. The distributed control law (3.2) can then be written as

$$\boldsymbol{u}_i = \boldsymbol{K}_i \boldsymbol{x}_i + \sum_{j \in \mathcal{G}_i} \boldsymbol{K}_{ij} (\boldsymbol{x}_j - \tau). \tag{3.22}$$

From Eq. (3.22), the closed loop expression (3.1) with constant and identical time delay τ can be written as

$$\begin{aligned} \dot{\boldsymbol{x}}(t) &= \boldsymbol{A}_{\text{dec}} \boldsymbol{x}(t) + \boldsymbol{A}_{\text{dist}} \boldsymbol{x}(t-\tau), \\ \boldsymbol{x}(\theta) &= \boldsymbol{x}_0, \ \forall \theta \in [-\tau, 0]. \end{aligned} \tag{3.23}$$

Before proceeding, let us recall the following theorem on the exponential stability of time-delay system [89]. For the sake of convenience, the notation in [89] is adopted into the ones used in this section. Consider the time-delay system (3.23) utilizing the following transformation

$$\boldsymbol{z}(t) = \mathrm{e}^{\alpha_\tau t} \boldsymbol{x}(t) \tag{3.24}$$

where $\alpha_\tau > 0$ is the delay decay rate, that is the convergence rate of time-delay system (3.23), to transform (3.23) into

$$\dot{\boldsymbol{z}}(t) = (\boldsymbol{A}_{\text{dec}} + \alpha_\tau \boldsymbol{I}) \boldsymbol{z}(t) + \boldsymbol{A}_{\text{dist}} \mathrm{e}^{\alpha_\tau \tau} \boldsymbol{z}(t-\tau). \tag{3.25}$$

First, we introduce the following theorem on the stability of time-delay systems (3.25).

Theorem 3.3.1 [89] Consider the time-delay system (3.25) with delay time $\tau > 0$ and delay decay rate α_τ. This system is exponentially stable with decay rate α_τ if there exists symmetric and positive-definite matrices $\boldsymbol{P} > 0, \boldsymbol{F} > 0$ such that the following inequality

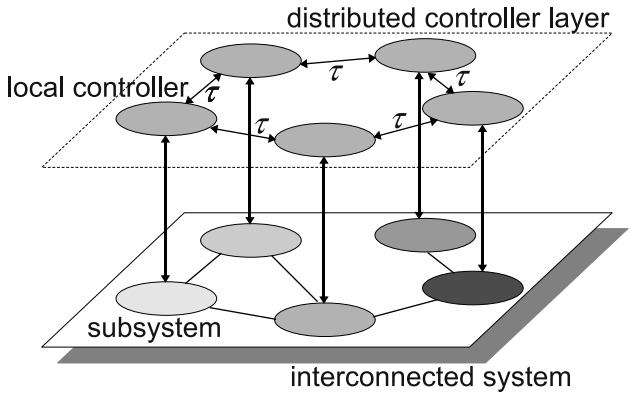

Figure 3.7: An interconnected system with distributed control architecture. The communication network has a constant and identical time-delay τ.

holds

$$\boldsymbol{S}_1 = \begin{bmatrix} \hat{\boldsymbol{A}}^T\boldsymbol{P} + \boldsymbol{P}\hat{\boldsymbol{A}} + \tau\boldsymbol{F} & \tau \mathrm{e}^{\alpha_\tau \tau}\hat{\boldsymbol{A}}^T\boldsymbol{P}\boldsymbol{A}_{\mathrm{dist}} \\ \tau \mathrm{e}^{\alpha_\tau \tau}\boldsymbol{A}_{\mathrm{dist}}^T\boldsymbol{P}\hat{\boldsymbol{A}} & -\tau\boldsymbol{F} \end{bmatrix} < 0 \tag{3.26}$$

where $\hat{\boldsymbol{A}} = \boldsymbol{A}_{\mathrm{dec}} + \alpha_\tau \boldsymbol{I} + \boldsymbol{A}_{\mathrm{dist}}\mathrm{e}^{\alpha_\tau \tau}$.

Since in general time delay deteriorates the performance of the overall system, first the following practically relevant question is addressed: given a pre-designed distributed control under a given communication network constraint and without consideration of time delay using the approach in Section 3.2.2, up to which time delay value a communication network is still beneficial in terms of the convergence rate of the overall system. In this section, we refer to the corresponding time delay as a performance-guaranteed time delay bound. Specifically, the performance-guaranteed time delay bound $\tau_{max} \in [0, \infty)$ is defined as follows.

$$\begin{aligned} &\max \tau \\ &\text{s.t. } \alpha_\tau \geq |\lambda_{\max}(\boldsymbol{A}_{\mathrm{dec}})| \end{aligned} \tag{3.27}$$

where $\lambda_{\max}(\boldsymbol{A}_{\mathrm{dec}})$ denotes the decay rate of the interconnected system with the decentralized control law.

From Theorem 3.3.1 and Eq. (3.27), the performance-guaranteed time delay bound $\tau_{\max}$ for time-delay system (3.23) is given by the solution of the following optimization problem.

$$\begin{aligned} &\underset{\tau}{\text{maximize}} \quad \tau \\ &\text{subject to} \quad \boldsymbol{S}_1 < 0 \text{ with } \alpha_\tau = |\lambda_{\max}(\boldsymbol{A}_{\mathrm{dec}})|. \end{aligned} \tag{3.28}$$

Note that α_τ is set to $|\lambda_{\max}(\boldsymbol{A}_{\mathrm{dec}})|$ which is the convergence rate of the overall system with the decentralized control law (3.11) since it is desired that the convergence rate by using the distributed control law (3.22) to be higher than with the decentralized one. In particular, the performance-guaranteed time delay bound can be calculated by increasing τ until the positive definiteness conditions of $\boldsymbol{P}, \boldsymbol{F}$ are violated.

Remark 4 A less conservative result on the performance-guaranteed time delay bound $\tau_{\max}$ can be achieved using the result on the exponential stability of time-delay systems, e.g. [24].

3.3.1 Distributed Control Design

Next, the following problem is considered: given a constant, identical time delay τ for all communication links, design the distributed control law (3.2), if any, such that the performance of the whole system is improved and the stability of the system is guaranteed. Combining Theorem 3.3.1 and the results for performance-guaranteed time delay bound derived previously, the distributed control design is given by

Proposition 3.3.2 Consider an interconnected time-delay system (3.23) with a given constant and identical time delay τ for all communication links. If there exists a solution to the optimization problem

$$\begin{aligned} \underset{\boldsymbol{K}_{ij},d_{ij}}{\text{maximize}} \quad & \alpha \\ \text{subject to} \quad & \boldsymbol{S}_1 < 0, \\ & \alpha > |\lambda_{\max}(\boldsymbol{A}_{\text{dec}})|, \\ & \sum_{1\le i\le j\le N} \gamma_{ij} d_{ij} \le c, \\ & d_{ij} \in \{0,1\}, \end{aligned} \tag{3.29}$$

then the convergence rate of the interconnected time-delay system (3.23) with the distributed control law (3.22) is higher than with the decentralized control law (3.11) and the whole system remains stable.

Proof: the proof is straightforward from Theorem 3.3.1 and the definition of performance-guaranteed time delay bound. ■

Remark 5 The first constraint in (3.29) is not an LMI problem due to the nonlinear terms $\boldsymbol{P}\hat{\boldsymbol{A}}$ and $\hat{\boldsymbol{A}}\boldsymbol{P}\boldsymbol{A}_{\text{dist}}$ in (3.26). However, the optimization problem can be solved using numerical BMI techniques.

Next we have the following result on the stability of the interconnected time-delay system in the presence of permanent communication link failures.

Proposition 3.3.3 The stability of the interconnected system (3.23) is guaranteed under any combination of permanent communication link failures.

Proof: Since the convergence rate of the interconnected system (3.23) with distributed control law (3.22) is higher than with the decentralized control law (3.11), we have $\lambda_{\max}(\bar{\boldsymbol{A}}) < \lambda_{\max}(\boldsymbol{A}_{\text{dec}}) < 0$. Furthermore, due to the local continuity of each eigenvalue w.r.t. the parameter [99], the rightmost eigenvalue of the overall system under any combination of communication link failures, i.e. $\lambda_{\max}(\tilde{\boldsymbol{A}})$ will be $\lambda_{\max}(\bar{\boldsymbol{A}}) < \lambda_{\max}(\tilde{\boldsymbol{A}}) < \lambda_{\max}(\boldsymbol{A}_{\text{dec}}) < 0$. ■

3.3.2 Evaluation

Let us consider an interconnected system consisting of 10 scalar subsystems as shown in Fig. 3.8. Furthermore, it is assumed that $\gamma_{ij} = 1$, time delay $\tau = 0.01$ and the distributed control gain is set to 1. The closed-loop system with the decentralized control law, i.e. $\boldsymbol{A}_{\text{dec}}$ in Eq. (3.23) is given by

$$\boldsymbol{A}_{\text{dec}} = \begin{bmatrix} -5 & 0 & 0 & 3 & 4 & 0 & 0 & 0 & 0 & 0 \\ 0 & -25 & 6 & 0 & 3 & 0 & 0 & 0 & 0 & 0 \\ 0 & 6 & -3 & 1 & 0 & 0 & 2 & 0 & 0 & 0 \\ 3 & 0 & 1 & -10 & 0 & 0 & 0 & 0 & 0 & 0 \\ 4 & 3 & 0 & 0 & -6 & 1 & 0 & 0 & 0 & 0 \\ 0 & 0 & 0 & 0 & 1 & -7 & 0 & 0 & 0 & 8 \\ 0 & 0 & 2 & 0 & 0 & 0 & -9 & 0 & 1 & 0 \\ 0 & 0 & 0 & 0 & 0 & 0 & 0 & -8 & 2 & 5 \\ 0 & 0 & 0 & 0 & 0 & 0 & 1 & 2 & -15 & 0 \\ 0 & 0 & 0 & 0 & 0 & 8 & 0 & 5 & 0 & -20 \end{bmatrix}.$$

First, the case of $c = 2$ is considered. The optimal communication topology and the convergence of the system are illustrated in Fig. 3.8 and Fig. 3.9 respectively.

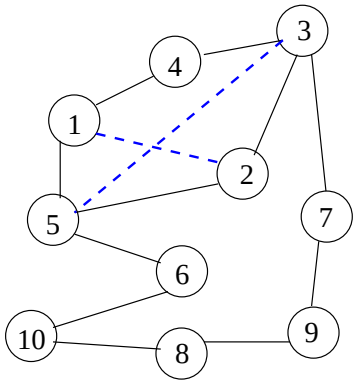

Figure 3.8: Interconnection system consisting of ten subsystems. The solid and dash lines represent the physical interconnection and the optimal communication topology for number of links equal to 2 respectively.

Discussion

As can be observed from Fig. 3.9, the interconnected system with the distributed control law (3.22) converges faster than with the decentralized control law (3.11). Furthermore, by solving the optimization problem (3.28) using the YALMIP toolbox [92], the performance-guaranteed time delay bound for the resulting topology is $\tau_{\max} = 0.91$. Next, the optimal topology for $c = 43$ is computed. The optimal topology is obtained without connecting local controller of subsystems 3,5 and 3,6 from 45 links needed to make a complete graph while the performance is shown in Fig. 3.9. and the time delay bound is $\tau_{\max} = 0.11$. Furthermore, in order to investigate the relation between $\tau_{\max}$ and the number of allowable

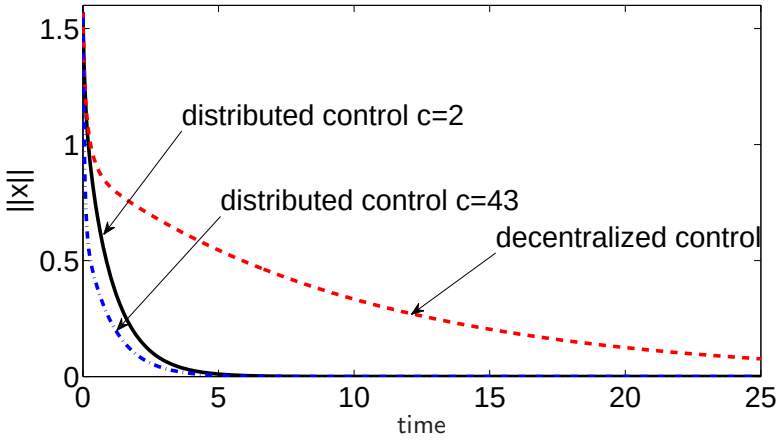

Figure 3.9: The convergence of the interconnected system with the distributed control law and the decentralized control law.

communication links c, Monte Carlo simulation is performed with respect to the interconnected system dynamics and the physical topology. The simulation results indicate that having more communication links may result in a lower $\tau_{\max}$ which also indicates that the number of links should be reduced when τ becomes large.

3.4 Application to Power Systems

With the deregulation and integration of large amount of distributed generation units, power systems are increasingly driven to operate closer to their operating and stability limits. Under critical operation conditions in which the possibility of low-frequency oscillations rises, the small-signal stability of the system has to be guaranteed for secure operation. These low-frequency oscillation modes have to be well damped by applying advanced control strategies in order to avoid fatal contingencies such as blackouts.

The contemporary solution is the combined Automatic Voltage Regulator (AVR) - Power System Stabilizers (PSS) approach with the support of wide-area signals. Such control laws are usually designed based on pole placement and phase compensation technique in terms of increasing the damping ratio or the decay rate of the system in response to small disturbances. The development and deployment of Wide-Area Measurement System (WAMS) based on the synchronized phasor measurement units (PMU) technology [112], [32] enables the remote measurement and transmission of the synchronized system dynamic data such as voltage, angle, frequency from and to different locations. Wide-Area Control System (WACS) using the PMU measurements for the oscillation damping have been widely investigated. It is shown that with the remote measured signals, the wide-area control improves the damping performance and the stability of the power system [119], [6], [144], [133].

Different control architectures have been proposed for the WACS design. In [133], [107], [144] a centralized control have been designed as a supervisory instance to collect remote signals from each local measurement units and send the processed control signals back to local AVR of the generators. Two-level hierarchical control have also been widely investi-

gated, see e.g. [69], [150], [36], [59]. In such architecture, a decentralized control serves as the first level, comprehending the local controller at generators or FACTS (Flexible AC Transmission System) equipments, and provides the stabilizing action for local oscillation modes for which global information may not be necessary. It also ensures the system stability during events of loss of communication links or of failure that makes the central instance unavailable. A centralized control, as the second control level, collects and processes the wide-area measurement data. Its output is transmitted to the local controllers of the generators in order to improve the global system performance. In any case, reliable and efficient communication networks are required for enabling the WAMS and the WACS. In the aforementioned works, the topology of the communication network is fixed for the control design. The integration of communication technologies into the power system gives though an additional degree of freedom in designing the distributed control for the interconnected systems and can be used to improve the performance of the overall system under a given communication network constraint.

In the remaining of this chapter, the theoretical analysis in the previous sections is applied to design a novel distributed damping control of a wide-area power system from a new perspective, i.e. by jointly designing the control gain and communication topology such that the overall system performance is improved and its stability in the presence of the permanent communication link failures is guaranteed. In this section, a five-machine power system [143] is considered as a case study as shown in Fig. 3.10 whose dynamics is derived in Chapter 2.

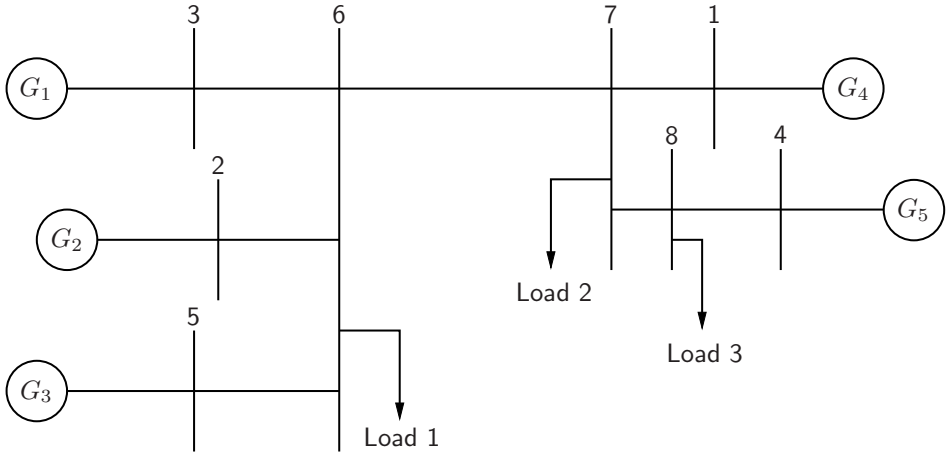

Figure 3.10: A five machine power system for case study.

3.4.1 Distributed Damping Control for Power Systems

The conventional method for damping control is based on the modal analysis since the oscillation modes are characterized by the eigenvalues of the linearized power system as formalized in (2.12). Let $\lambda_i = \sigma_i + j\beta_i$ be the $i-th$ eigenvalue of the state matrix $\boldsymbol{A}$ in (2.12) where

- σ_i shows the damping or decay rate,

- β_i denotes the frequency of the oscillation,

- the relative damping ratio is given by

$$\xi_i = \frac{-\sigma_i}{\sqrt{\sigma_i^2 + \beta_i^2}}. \tag{3.30}$$

The contemporary solution is usually realized based on pole placement and phase lead compensation. The control goal can be formulated as to improve the decay rate of the system oscillations by shifting the real part of the eigenvalue σ_i towards the left half complex plane that also means to minimize σ_i which is negative in a system with a stabilizing control law. This method of pole shifting can also be formulated as an optimization problem as in (3.20).

Remark 6 The decay rate of the overall system that is $\lambda_{\max}$ is chosen as a performance metric in this section since it influences the relative damping ratio of the power system as will be shown later. Moreover, $\lambda_{\max}$ also plays a dominant role in the dynamic responses of the power system [64].

On the other hand, the eigenvalue assignment is proved to be complicated, while the optimal linear quadratic (LQ) control provides a systematic way of designing the feedback control for the complex systems with high order. Moreover, the resulting LQ control law is guaranteed to stabilize the system with sufficient margins [8].

Using the proposed design procedure introduced in Section 3.2, first a decentralized LQ control is designed using the approach discussed in [88] that stabilizes the system and provides a minimum damping performance. Then, the distributed control together with the optimized communication structure under a given communication network constraint is designed by solving the mixed-integer optimization problem (3.20) that improves the decay rate, i.e. the damping performance of the overall system. In contrast to the conventional supervisory centralized control of the whole system, e.g. [144], [133], the central instance in the proposed approach is only responsible for the optimization of the communication topology, i.e. solving the optimization problem (3.20). After the optimization is performed, the generators with local controllers can operate autonomously while exchanging information with each other. Since it is possible to use any of the variables from the generators, e.g. the generator rotor speeds, angles, voltages or other variables [59], in this section it is assumed that the local controller of the generators could measure all of its dynamic states and exchange them with each other via the communication links. Since AVR control loop with wide-area signals could provide relatively good damping performance for the inter-area oscillations of the power system as discussed in [144], [133], we consider in this section that each generator is equipped with a local AVR but no PSS which could further improve the damping performance of the system. However, this does not affect the applicability of the design principle of the proposed approach. The inclusion of PSS is beyond the scope of this dissertation.

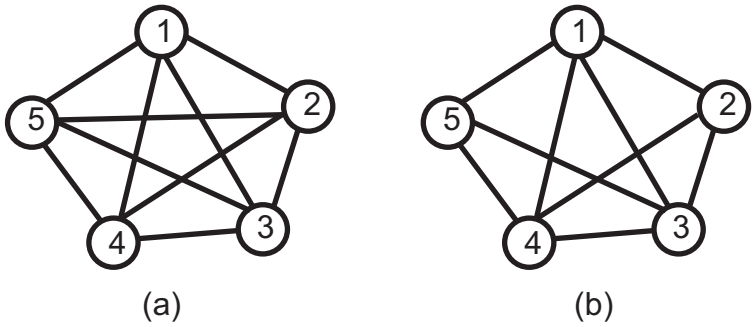

Figure 3.11: (a) Interconnected system used in the simulation; (b) the optimal communication topology.

3.4.2 Evaluation

The proposed distributed control is evaluated via a numerical simulation using MATLAB for the power system shown in Fig. 3.10 by considering the linearized model in (2.1)-(2.12). The parameters are chosen as in [143] and listed in Appendix.

The system turns out to have a fully connected physical structure, i.e. all the five generators are physically coupled with each other as shown in Fig. 3.11a. The γ_{ij} and c in (3.19) are equal to 1 and 9 respectively. This means that only 9 communication links are available for the overall system. Solving the optimization problem (3.20) using the YALMIP toolbox [92] gives the optimal topology as shown in Fig. 3.11b, where all local controllers communicate with each other except between the local controller of generator 2 and 5.

The eigenvalue analysis of the inter-area oscillations of the test system is compared in Table 3.2 in terms of the damping ratio and frequencies in the case of with and without the obtained control law. The analysis shows that compared to the open loop, the decentralized control improved slightly the decay rates and the damping ratios. Note that according to the optimization problem (3.20), only the maximal real part of the eigenvalues is taken into account to be minimized, which does not necessarily mean that the real parts of all eigenvalues will be minimized, for example the second eigenvalue of the distributed control case in Table 3.2 is larger than the second one of the decentralized control. However, it is observed that with the proposed distributed control, the damping ratios of all the oscillation modes are improved compared to the system with decentralized control. It is interesting in the future to investigate this effect based on modal analysis of the system and to perform the optimization by including all the eigenvalues and use different performance metric such as the damping ratio.

Furthermore, the damping performance of the decentralized control and the proposed distributed control in terms of the rotor angle deviations $\Delta\delta_i$ and rotor speed deviations $\Delta\omega_i$ of each generator is also compared when a sudden load change of the load 3 is simulated as a small disturbance to the power system starting at $t = 0.5$ and lasting for $1s$ as shown in Fig. 3.12 - 3.16.

In consistence with the eigenvalue analysis in Table 3.2, it is observed that all the rotor angle deviations $\Delta\delta_i$ are damped much faster by the distributed control compared to the

Table 3.2: Eigenvalue analysis of the test system

Case	Eigenvalues	Damping Ratio	Freq. [Hz]
Open Loop	$-0.339 \pm 4.818j$	0.0703	0.7668
	$-0.405 \pm 3.265j$	0.1230	0.5196
	$-0.354 \pm 2.615j$	0.1344	0.4157
Decentralized Control	$-0.352 \pm 4.813j$	0.0730	0.7666
	$-0.411 \pm 3.260j$	0.1251	0.5188
	$-0.355 \pm 2.609j$	0.1347	0.4152
Distributed Control	$-0.355 \pm 4.769j$	0.0743	0.7590
	$-0.409 \pm 2.860j$	0.1414	0.4553
	$-0.363 \pm 2.377j$	0.1509	0.3783

one with the decentralized control. Moreover, the damping of the rotor speed deviations are also increased for some of the generators. It can also be observed that the oscillation of the generator G_3 and G_4 have larger amplitude than the other three generators due to the assumption in the simulation that the fault occurs at the load 3 which is physically located closer to the generator G_3 and G_4.

The integrated squared control error of the rotor angle deviations $\Delta\delta_i$ is shown in Table 3.3. It is obvious that the distributed control achieves smaller integrated errors than the decentralized ones except for the $\Delta\delta_4$ of the generator G_4. This might be due to the fact that only the largest eigenvalue is considered in the optimization problem that leads to the performance degradation of a subset of the generators. A similar effect is also observed for the squared integrated control errors of the rotor speed deviations $\Delta\omega_i$.

Table 3.3: Squared integrated control error of the rotor angle deviations

Integrated error	$\Delta\delta_1$	$\Delta\delta_2$	$\Delta\delta_3$	$\Delta\delta_4$	$\Delta\delta_5$
Dec. Control	0.0200	0.0174	0.0173	0.0357	0.0155
Dist. Control	0.0089	0.0003	0.0002	0.0441	0.0004

3.5 Summary and Discussion

While exchanging some information between the local controllers may improve the performance of the interconnected system, the system may not be guaranteed to be robust with respect to permanent communication link failures. In this chapter, a novel two-layer control architecture is proposed in order to guarantee the stability of the interconnected system while optimizing a given performance metric. The proposed control architecture allows the designer to jointly consider the optimality and robustness aspects of distributed control design. The innovative approach is first by designing decentralized control which stabilizes the interconnected system and then improving the overall system performance by

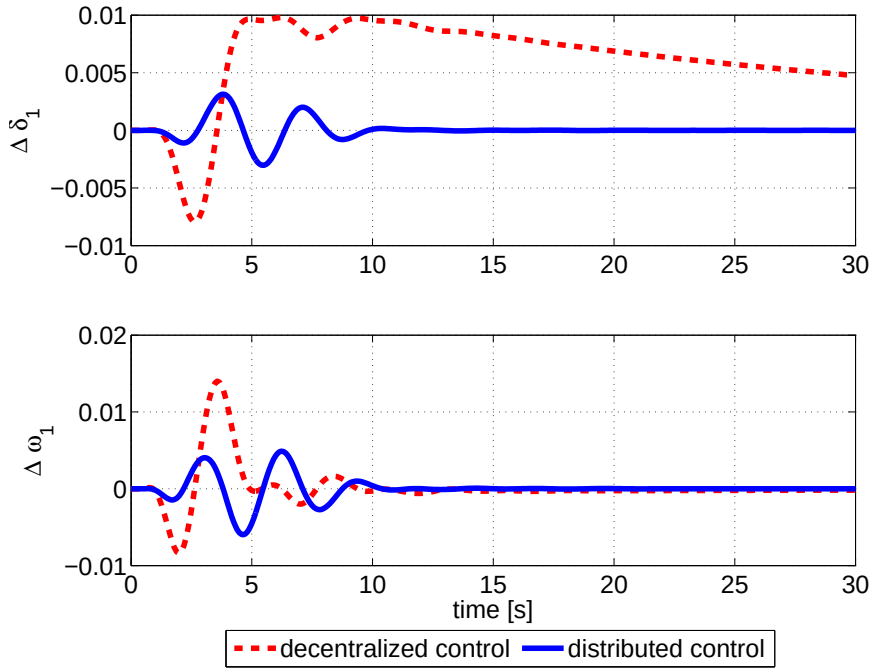

Figure 3.12: Response to disturbance of the generator G_1.

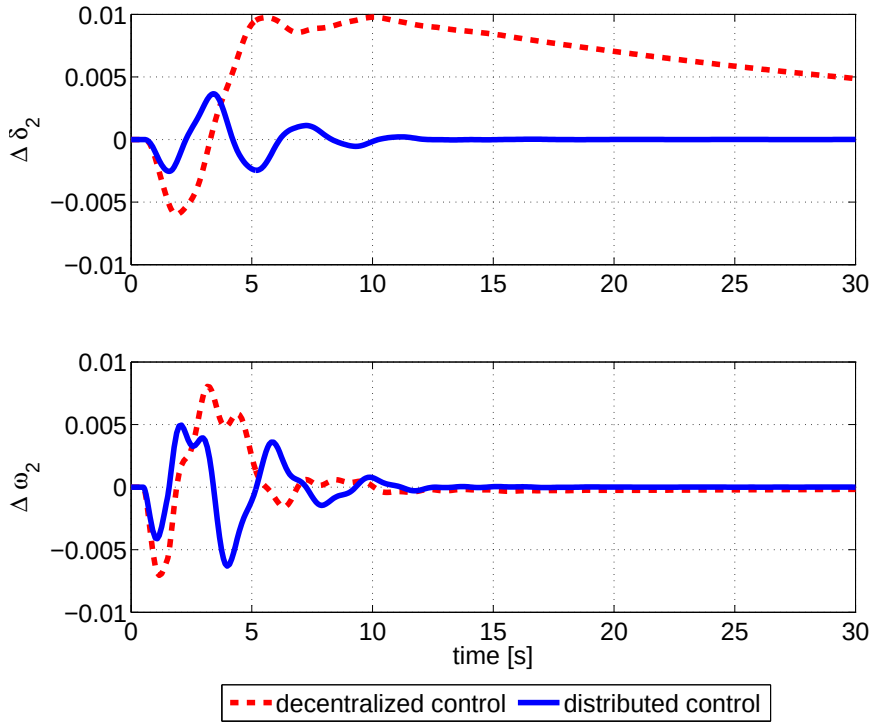

Figure 3.13: Response to disturbance of the generator G_2.

designing the distributed control together with its communication topology under a given network cost, i.e. by exploiting the additional degree of freedom offered by the introduction

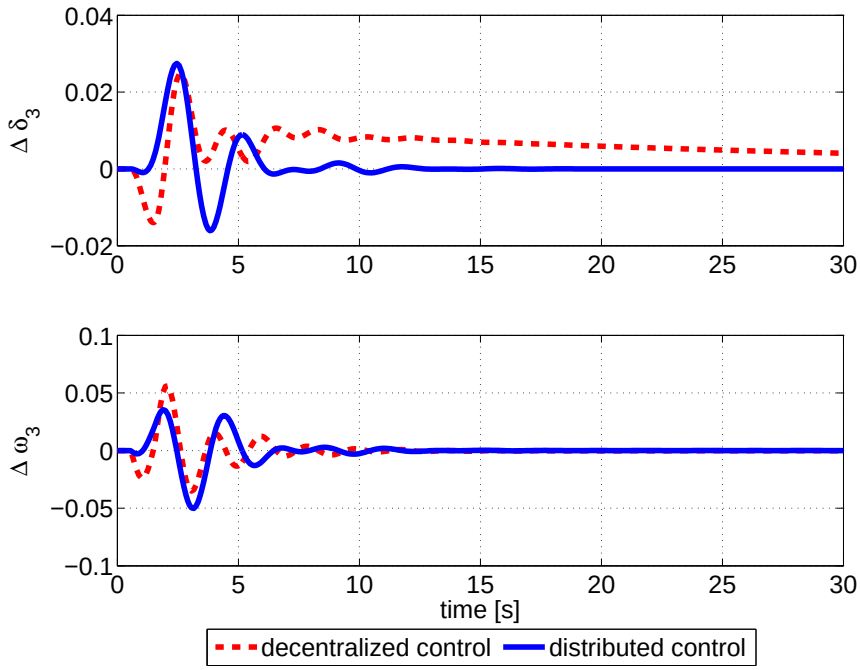

Figure 3.14: Response to disturbance of the generator G_3.

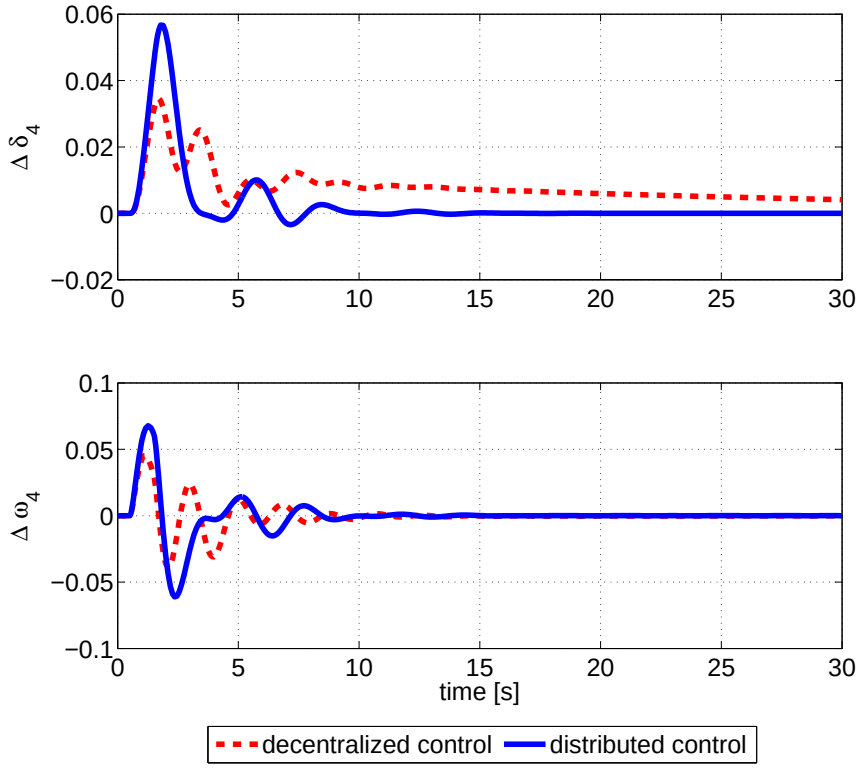

Figure 3.15: Response to disturbance of the generator G_4.

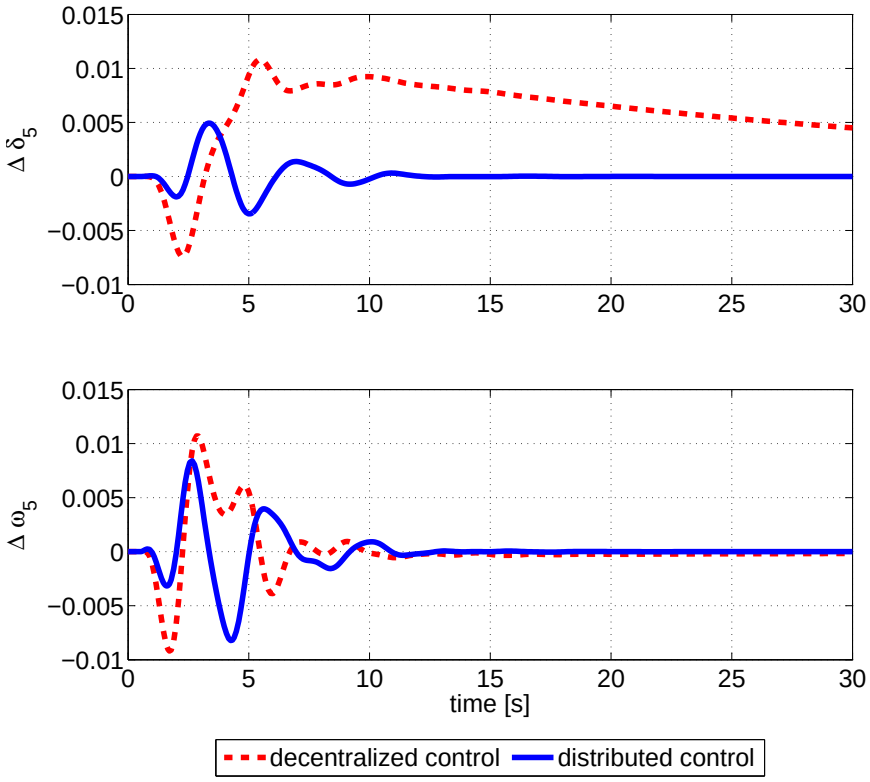

Figure 3.16: Response to disturbance of the generator G_5.

of communication network. The problem is formulated as a mixed integer optimization. Furthermore, it is demonstrated that the novel two-layer control architecture is also well suited for the case when constant and identical time delay exists in the communication links, i.e. for non-ideal communication network. It is also investigated via numerical simulations on the influence of addition of communication links on the performance improvement of the interconnected system. It is indicated from the simulation results that adding more links may not always result in the system performance improvement. It is observed that the performance is drastically improved when few links are added and the improvement gradually gets smaller as the number of links becomes larger. In addition, when constant and identical time delay exists in the communication links, the simulation results suggest that the number of communication links should be reduced when the time delay is large. The simulation results provide a preliminary rule-of-thumb on the design of distributed control law with respect to the number of communication links that has to be utilized in order to obtain a good trade-off between optimal performance and network cost. The proposed two-layer architecture can be applied to a variety of interconnected systems. One of the examples is to design a novel distributed damping control of power systems as discussed in this chapter. It should be noted that even though in this chapter the decay rate of the overall system is used as a performance metric, the proposed two-layer control architecture can also be applied to other performance metrics.

The novel two-layer control architecture proposed in this chapter heavily relies on the assumption that a stabilizing decentralized control law exists. However, when the in-

terconnection between the subsystems is strong, this assumption may not always hold. Furthermore, even though the proposed two-layer control architecture guarantees the stability of the interconnected system under permanent communication link failures, it may lead to a reduced performance since the design of decentralized control law is not considered in the optimization problem. Another important issue is the election of the objective function in order to have the optimization problem efficiently solvable. In this chapter, the decay rate of the overall system is chosen as a performance metric which, as discussed previously, in general results in a non-convex and non-smooth objective function. However, as shown in the following chapter, for a certain class of interconnected systems, the chosen objective function in this chapter becomes convex and furthermore, it is possible to obtain a closed-loop solution of the optimization problem with some insights. Additionally, for the case of non-ideal communication network, it is assumed in this chapter that the time delay in the communication links is constant and identical, which is not always the case in real world applications. These lead to the following problems which require further investigations in the future:

- Convex relaxation of the objective function and the relaxation of the binary decision variables introduced by the design of communication topology. One possible approach in order to relax the binary decision variables is to utilize l_0 norm relaxation method as proposed and discussed in the known literature, e.g. [122].
- Extension of joint distributed control gain-communication topology design for non-ideal communication network where non-identical and time-varying delay exists in the communication links.
- A rigorous analysis on the impact of the addition of communication links on the improvement of overall system performance.

4 On the Explicit Solution of Communication Topology Design

Most of the work on communication topology design, e.g. [47, 115, 122] ends up in an optimization formulation and lacks of explicit solutions. Having an explicit solution on communication topology design provides the designer additional information about the relation between the subsystem dynamics, strength of physical interconnection and the resulting communication topology. This information can be exploited in designing the interconnected system, given the constraint on the network cost. However, the explicit solutions on topology design problem is in general hard to derive due to its combinatorial formulation.

The major innovation in this chapter is to study for the first time the explicit solutions of communication topology design for distributed control of interconnected systems. The unique strategy is to employ the eigenvalue sensitivity analysis in order to investigate the influence of the structure of the distributed control law, i.e. the communication topology, on the overall system performance. In this chapter, the analysis focuses on interconnected systems with a special class of physical interconnection topology, namely ring, star and line topology. First, the explicit solutions of a single communication link for an interconnected system with homogeneous interacting scalar subsystems are derived. Additionally, some new insights are obtained on how the heterogeneity of the subsystem local dynamics affects the optimal communication topology. The results are then extended to the case of interconnection of homogeneous non-scalar subsystems, multiple communication links and interconnected system with more complex physical interconnection topology. The eigenvalue sensitivity based approach is furthermore employed to distributed control with time delay, where the results can be used to investigate how the communication topology and time delay influence the performance of the interconnected system.

The remainder of this chapter is organized as follows: After formulating the problem in Section 4.1, the communication topology design is reformulated using eigenvalue sensitivity approach in Section 4.2. Explicit solutions on the single communication link design for interconnected systems with interacting scalar subsystems are presented in Section 4.3. The results are then extended to the case of non-scalar subsystems, multiple communication links and more complex physical topology in Sections 4.4, 4.5 and 4.6 respectively. The proposed method is also applied to distributed control with time delay in Section 4.7.

4.1 Problem Formulation

Let us first recall the problem formulation and optimization problem presented in Chapter 3. Consider N LTI subsystems described by

$$\dot{\boldsymbol{x}}_i = \boldsymbol{A}_i\boldsymbol{x}_i + \sum_{j\in\mathcal{N}_i} \boldsymbol{A}_{ij}\boldsymbol{x}_j + \boldsymbol{B}_i\boldsymbol{u}_i, \quad \boldsymbol{x}_i(t_0) = \boldsymbol{x}_0^i \tag{4.1}$$

with the control input is given by

$$\boldsymbol{u}_i = \boldsymbol{K}_i \boldsymbol{x}_i + \sum_{j \in \mathcal{G}_i} \boldsymbol{K}_{ij} \boldsymbol{x}_j. \tag{4.2}$$

The closed loop expression of the interconnected system (4.1) with the distributed control law (4.2) can be written as

$$\dot{\boldsymbol{x}} = \bar{\boldsymbol{A}} \boldsymbol{x}, \quad \boldsymbol{x}(t_0) = \boldsymbol{x}_0 \tag{4.3}$$

where $\bar{\boldsymbol{A}}$ is given by

$$\begin{aligned} \bar{\boldsymbol{A}} &= \begin{bmatrix} \bar{\boldsymbol{A}}_1 & \boldsymbol{A}_{12} & \cdots & \boldsymbol{A}_{1N} \\ \boldsymbol{A}_{21} & \bar{\boldsymbol{A}}_2 & \cdots & \boldsymbol{A}_{2N} \\ \vdots & \vdots & \ddots & \vdots \\ \boldsymbol{A}_{N1} & \boldsymbol{A}_{N2} & \cdots & \bar{\boldsymbol{A}}_N \end{bmatrix} + \begin{bmatrix} 0 & \bar{\boldsymbol{A}}_{12} & \cdots & \bar{\boldsymbol{A}}_{1N} \\ \bar{\boldsymbol{A}}_{21} & 0 & \cdots & \bar{\boldsymbol{A}}_{2N} \\ \vdots & \vdots & \ddots & \vdots \\ \bar{\boldsymbol{A}}_{N1} & \bar{\boldsymbol{A}}_{N2} & \cdots & 0 \end{bmatrix}, \\ \bar{\boldsymbol{A}} &= \boldsymbol{A}_{\text{dec}} + \boldsymbol{A}_{\text{dist}} \end{aligned} \tag{4.4}$$

where $\bar{\boldsymbol{A}}_i = \boldsymbol{A}_i + \boldsymbol{K}_i$, $\bar{\boldsymbol{A}}_{ij} = d_{ij} \boldsymbol{B}_i \boldsymbol{K}_{ij}$.

The goal in general is to design the control gain and also the communication topology of the control law, i.e. the graph $\mathcal{G}_i$ which can be formulated as the following mixed-integer optimization problem.

$$\begin{aligned} \underset{\boldsymbol{K}_i, \boldsymbol{K}_{ij}, d_{ij}}{\text{minimize}} \quad & \lambda_{\max}(\bar{\boldsymbol{A}}) \\ \text{subject to} \quad & \lambda_{\max}(\bar{\boldsymbol{A}}) < 0, \\ & \sum_{1 \le i \le j \le N} \gamma_{ij} d_{ij} \le c, \\ & d_{ij} \in \{0, 1\} \end{aligned} \tag{4.5}$$

where the second constraint represents the communication network constraint. In contrast to the work in the known literature which focuses on the computation of the optimal control gain for a given control law structure, in this chapter it is assumed that the control gain $\boldsymbol{K}_i, \boldsymbol{K}_{ij}$ are fixed. Furthermore, for the sake of clarity, it is assumed that the interconnected system is stable so that we can set $\boldsymbol{K}_i = \boldsymbol{0}, \forall i$ and $\boldsymbol{A}_{\text{dec}} = \boldsymbol{A}$. The only design parameter is thus the communication topology $\mathcal{G}_i$. The goal of this chapter is to find the analytical solution of the communication topology $\mathcal{G}_i$, i.e. the binary variable d_{ij} in the following optimization problem.

$$\begin{aligned} \underset{d_{ij}}{\text{minimize}} \quad & \lambda_{\max}(\bar{\boldsymbol{A}}) \\ \text{subject to} \quad & \lambda_{\max}(\bar{\boldsymbol{A}}) < \lambda_{\max}(\boldsymbol{A}), \\ & \sum_{1 \le i \le j \le N} \gamma_{ij} d_{ij} \le c, \\ & d_{ij} \in \{0, 1\}. \end{aligned} \tag{4.6}$$

The condition on $\boldsymbol{K}_{ij}$ such that the optimization problem (4.6) has feasible solutions will be discussed in the subsequent section. Before proceeding, we introduce the following definitions. Let us represent the structure of the interconnected system, i.e. the structure

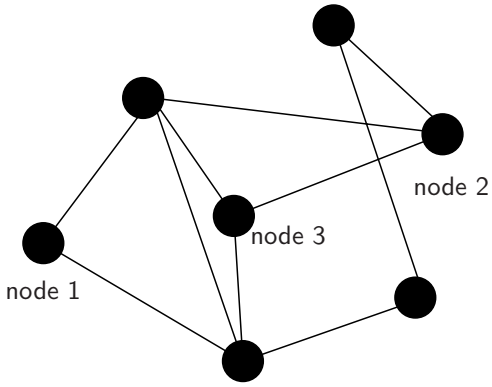

Figure 4.1: An example of a plant graph. The edges represent the physical interconnection between the subsystems/nodes.

of matrix $\boldsymbol{A}$ in (4.4) by a plant graph $\mathcal{G}_P = (\mathcal{V}_p, \mathcal{E}_p)$ comprising a set $\mathcal{V}_P = \{1, \cdots, N\}$ of vertices or subsystems and a set $\mathcal{E}_P = \{(j,i)|e_{ij} \neq 0\}$ of edges where $e_{ij} \neq 0$ means that subsystem j is (physically) affecting subsystem i. In this chapter it is assumed that the graph $\mathcal{G}_P$ is undirected. Moreover, when $e_{ij} \neq 0$, we call vertices i, j are adjacent. Next we review the definitions of path, distance and degree of a graph.

Definition 4.1.1 [48] A path of length r from i to j in a graph is a sequence of $r+1$ distinct vertices starting with i and ending with j such that consecutive vertices are adjacent.

Definition 4.1.2 [48] The distance $D_{\mathcal{G}_P}(i,j)$ between subsystem i and j in a graph $\mathcal{G}_P$ is the length of the shortest path from i to j.

Definition 4.1.3 [48] The degree of node i, i.e. $\deg(i)$ of a graph is the number of edges incident to node i, i.e. the number of physical neighbors of node i.

Example 1 The distance between node 1 and node 2 of the plant graph depicted in Fig. 4.1 is $D_{\mathcal{G}_P}(1,2) = 2$ and the degree of node 3 is $\deg(3)$=3.

4.1.1 Adding Communication Links is not Always Beneficial

First, we discuss that adding communication links is not always beneficial by finding a counterexample using eigenvalue perturbation theory. Before proceeding we review the well-known Gershgorin theorem. Consider a complex $n \times n$ matrix $\boldsymbol{A}$ with entries a_{ij}. For $i \in \{1, \cdots, n\}$ write $R_i = \sum_{j \neq i} |a_{ij}|$ and let $D(a_{ii}, R_i)$ be the disc centered at a_{ii} with radius R_i. Such a disc is called Gershgorin disc. We have the following theorems related to the eigenvalue of a matrix and its Gershgorin disc.

Theorem 4.1.4 [62] Every nonzero eigenvalue of $\boldsymbol{A}$ lies within at least one of the Gerhgorin discs $D(a_{ii}, R_i)$, i.e. every $\lambda_i(\boldsymbol{A})$ satisfies $|\lambda_i - a_{ii}| \leq R_i$ for some a_{ii}.

Theorem 4.1.5 [62] If the union of k discs is disjoint from the union of the other $n-k$ discs, then the former union contains exactly k and the latter $n-k$ eigenvalues of $\boldsymbol{A}$.

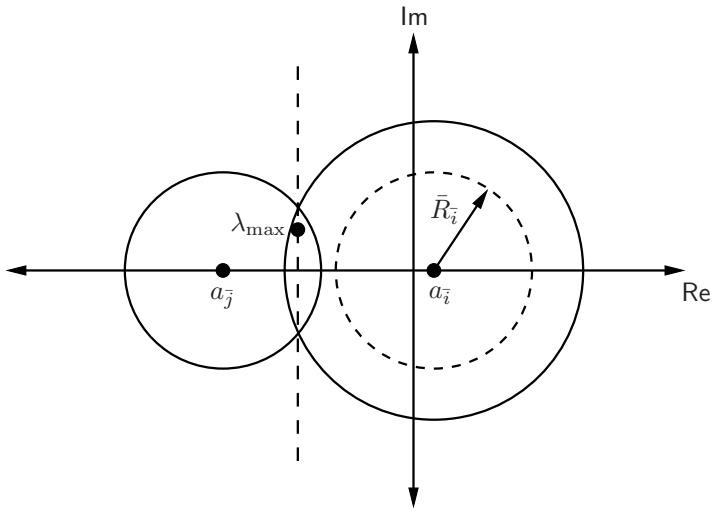

Figure 4.2: Largest eigenvalue and Gershgorin discs.

Recall Eq. (4.4) given by $\bar{\boldsymbol{A}} = \boldsymbol{A} + \boldsymbol{A}_{\text{dist}}$. The term $\boldsymbol{A}_{\text{dist}}$ can be seen as a perturbation working on the matrix $\boldsymbol{A}$. In order to show that adding communication links is not always beneficial, we need to show that the perturbation $\boldsymbol{A}_{\text{dist}}$ can possibly result in that the convergence rate of the overall system with matrix $\bar{\boldsymbol{A}}$ is lower than with matrix $\boldsymbol{A}$, i.e. $\lambda_{\max}(\bar{\boldsymbol{A}}) > \lambda_{\max}(\boldsymbol{A})$. Consider a case where $\boldsymbol{A}$ is stable and its largest eigenvalue lies between the $\bar{i}$-th and $\bar{j}$-th Gershgorin disc centered at $a_{\bar{i}}$ and $a_{\bar{j}}$, $a_{\bar{i}} > a_{\bar{j}}$ respectively as illustrated in Fig. 4.2. Now we would like to improve the performance by adding communication links between the subsystems under a given constraint on the total number of links. Here we assume directed communication links. Adding communication links into the i-th row means that only the i-th controller could receive information from the other controllers. Assume that the communication links are added only into the $\bar{i}$-th row of matrix $\boldsymbol{A}_{\text{dist}}$. From Theorem 4.1.4 and since the perturbation is only working on the non-diagonal elements of $\bar{\boldsymbol{A}}$, the new Gershgorin discs have the same centers and the radius are scaled with the perturbation. Moreover, since the perturbations only influence the $\bar{i}$-th row of the matrix $\bar{\boldsymbol{A}}$, only the radius of the $\bar{i}$-th Gerhgorin disc changes. Therefore, a combination of communication links together with the corresponding gain can be selected such that the $\bar{i}$-th Gershgorin disc is disjoint from the other as illustrated in Fig. 4.2 and the new radius is less than the distance from its center to the largest eigenvalue of the non-perturbed matrix $\boldsymbol{A}$, i.e. $\bar{R}_{\bar{i}} \leq \|a_{\bar{i}} - \lambda_{max}(\boldsymbol{A})\|$. From Theorem 4.1.5, it is clear that the $\bar{i}$-th Gershgorin disc has one eigenvalue inside and since $a_{\bar{i}} > a_{\bar{j}} > \cdots > a_N$, the corresponding eigenvalue is thus the largest eigenvalue of the perturbed matrix. This yields $\lambda_{\max}(\bar{\boldsymbol{A}}) > \lambda_{\max}(\boldsymbol{A})$.

4.2 Eigenvalue Sensitivity based Approach

In the previous section it has been discussed that the addition of communication links is not always beneficial since it could deteriorate the performance of the whole system. In this section we derive an explicit solution on how to add the communication links, i.e.

which controllers should communicate in order to improve the performance of the whole system for a given number of available communication links. In general, it is hard to derive the explicit solution to the optimization problem (4.6). Therefore, in order to analyze the optimal topology design, we constrain ourselves for the remainder of this section by the following assumptions.

A1 The subsystems are scalar, i.e. $x_i \in \mathbb{R}$.

A2 The physical interconnection is symmetric, i.e. $\boldsymbol{A}^T = \boldsymbol{A}$.

A3 The communication is bidirectional, i.e. $\boldsymbol{A}_{\text{dist}}^T = \boldsymbol{A}_{\text{dist}}$.

A4 The distributed control gains are fixed and equal, i.e. $K_{ij} = K$.

The objective function in optimization problem (4.6) under Assumptions A1-A4 is convex and can be solved by relaxing the binary variable into $d_{ij} = [0, 1]$ and reformulating it into a semi-definite programming (SDP) problem as discussed in [131]. However, since we are interested in obtaining the explicit solution, an alternative approach is proposed based on eigenvalue sensitivity analysis. Eigenvalue sensitivity gives an insight on the behavior of the eigenvalues of a matrix when the matrix is perturbed, in our case, when the distributed control law is applied to the interconnected system. Moreover, the magnitude of the eigenvalue sensitivity informs about the size of the eigenvalue displacement in the complex plane [93]. Assume that the matrix $\boldsymbol{A}$ is perturbed by a matrix $\boldsymbol{M} = [m_{ij}]$ with identical entries equal to m, i.e., $m_{ij} = m$, $\forall i, j$. Then the change of each eigenvalue of the matrix $\boldsymbol{A}$ is given by [138]

$$\frac{\partial \lambda_i}{\partial m} = \frac{\boldsymbol{v}_i^T \frac{\partial \bar{\boldsymbol{A}}}{\partial m} \boldsymbol{w}_i}{\boldsymbol{v}_i^T \boldsymbol{w}_i} \tag{4.7}$$

where $\bar{\boldsymbol{A}} = \boldsymbol{A} + \boldsymbol{M}$, $\boldsymbol{v}_i$ and $\boldsymbol{w}_i$ are the right and left eigenvector of the matrix $\boldsymbol{A}$ corresponding to the eigenvalue λ_i.

Next we present the results on where to add the communication links and how to choose the feedback gain. For the simplicity of analysis and clarity of the result, it is assumed that $\gamma_{ij} = 1, \forall i, j$ and $c = 1$, i.e. only one link is allowed to be added. The perturbation matrix $\boldsymbol{M}$ can be seen as a distributed control given by $\boldsymbol{A}_{\text{dist}} = [K_{ij}]$ where $K_{ij} = K$ by Assumption A4. Let $\boldsymbol{v}_r = [v_{r_1}, \cdots, v_{r_N}]^T$ be the eigenvector corresponding to $\lambda_{\max}(\boldsymbol{A})$.

Proposition 4.2.1 Consider an interconnected system (4.3) under Assumptions A1-A4. The optimization problem (4.6) is minimized by adding a communication link between the $i-$th and $j-$th controller that solves the following optimization problem

$$\underset{i,j}{\text{maximize}} \; |v_{r_i} v_{r_j}| \tag{4.8}$$

and the sign of the feedback gain is chosen according to the following rules.

$$K = \begin{cases} > 0 & \text{if } \text{sign}(v_{r_i}.v_{r_j}) < 0 \\ < 0 & \text{if } \text{sign}(v_{r_i}.v_{r_j}) > 0. \end{cases} \tag{4.9}$$

Proof: In order to find the optimal communication topology that minimizes $\lambda_{\max}$, first we need to investigate the condition that results in $\lambda_{\max}(\bar{\boldsymbol{A}}) < \lambda_{\max}(\boldsymbol{A})$, i.e. $\frac{\partial \lambda_{\max}}{\partial K} < 0$. Next, we find the structure of perturbation, i.e. the distributed control $\boldsymbol{A}_{\text{dist}}$ that results in the largest displacement of $\lambda_{\max}$ or maximizes $|\lambda_{\max}(\bar{\boldsymbol{A}}) - \lambda_{\max}(\boldsymbol{A})|$.

The derivation of $\lambda_{\max}$ w.r.t. perturbation K is given by

$$\frac{\partial \lambda_{\max}}{\partial K} = \frac{\boldsymbol{v}_r^T \frac{\partial \bar{\boldsymbol{A}}}{\partial K} \boldsymbol{w}_r}{\boldsymbol{v}_r^T \boldsymbol{w}_r} \tag{4.10}$$

where $r = \arg\max_i \lambda_i$. From Assumption A2, $\boldsymbol{v}_r = \boldsymbol{w}_r = [v_{r_1}, \cdots, v_{r_N}]^T$. This results in

$$\frac{\partial \lambda_{\max}}{\partial K} = \frac{\boldsymbol{v}_r^T \frac{\partial \bar{\boldsymbol{A}}}{\partial K} \boldsymbol{v}_r}{\|\boldsymbol{v}_r\|^2}. \tag{4.11}$$

Assume that the perturbation K works on A_{ij} and A_{ji} of $\boldsymbol{A}$. Since $\|\boldsymbol{v}_r\|^2 = 1$, we have

$$\frac{\partial \lambda_{\max}}{\partial K} = \begin{bmatrix} v_{r_1} \cdots v_{r_N} \end{bmatrix} \frac{\partial \bar{\boldsymbol{A}}}{\partial K} \begin{bmatrix} v_{r_1} \\ \vdots \\ v_{r_N} \end{bmatrix}$$

where

$$\frac{\partial \bar{\boldsymbol{A}}}{\partial K} = \begin{bmatrix} 0 & 0 & \cdots & 0 & 0 & \cdots & 0 \\ 0 & 0 & \cdots & \operatorname{sign}(K) & 0 & \cdots & 0 \\ \vdots & \vdots & \ddots & \vdots & \vdots & \ddots & \vdots \\ 0 & \operatorname{sign}(K) & \cdots & 0 & 0 & \cdots & 0 \\ 0 & 0 & \cdots & 0 & 0 & \cdots & 0 \\ \vdots & \vdots & \ddots & \vdots & \vdots & \ddots & \vdots \\ 0 & 0 & \cdots & 0 & 0 & \cdots & 0 \end{bmatrix},$$

i.e. $\left[\frac{\partial \bar{\boldsymbol{A}}}{\partial K}\right]_{ij} = \left[\frac{\partial \bar{\boldsymbol{A}}}{\partial K}\right]_{ji} = \operatorname{sign}(K)$ and are equal to 0 otherwise. After a straightforward calculation, we have

$$\frac{\partial \lambda_{\max}}{\partial K} = 2\operatorname{sign}(K) v_{r_i} v_{r_j}. \tag{4.13}$$

In order to have $\frac{\partial \lambda_{\max}}{\partial K} < 0$, the sign of K has to be selected as in (4.9).

We have guaranteed that $\lambda_{\max}$ is always decreasing. Next, we investigate the structure of $\boldsymbol{A}_{\text{dist}}$ that minimizes $\lambda_{\max}$ or maximizes $|\lambda_{\max}(\bar{\boldsymbol{A}}) - \lambda_{\max}(\boldsymbol{A})|$. Therefore, the optimization problem (4.6) can be reformulated as to find the structure of the distributed control law $\boldsymbol{A}_{\text{dist}}$ that results in the largest displacement of $\lambda_{\max}$. In other words, we would like to solve the following optimization problem.

$$\underset{i,j}{\text{maximize}} \ \left| \frac{\partial \lambda_{\max}}{\partial K} \right|. \tag{4.14}$$

From (4.13), the problem (4.14) can be written as

$$\underset{i,j}{\text{maximize}} \ |v_{r_i} v_{r_j}|.$$

This completes the proof. ■

Remark 7 Proposition 4.2.1 is easier to solve for a large number of subsystems than (4.6) since the eigenvector can be computed in a decentralized manner [70]. Moreover it also

provides the relation between the communication topology and the eigenvector w.r.t. the rightmost eigenvalue of the interconnected system.

Note that for $c > 1$, the formulation as in Eq. (4.8) and Eq. (4.9) in Proposition 4.2.1 will become more complicated. However, by considering an additional assumption given by

A5 $A_i < 0, A_{ij} > 0$ and $K < 0$,

the communication topology design can be simply formulated as follows.

Proposition 4.2.2 Consider an interconnected system (4.3) under assumption A1-A5. The optimal communication topology for a given number c of links to be added can be reformulated as to find c pairs of links between the $i-$th and the $j-$th controller such that the following optimization problem is solved

$$\underset{(i,j),\cdots,(h,l)}{\text{maximize}} \overbrace{|v_{r_i}v_{r_j}| + \cdots + |v_{r_h}v_{r_l}|}^{c \text{ pairs}}. \tag{4.16}$$

Proof: First, we show that under $A_i < 0, A_{ij} > 0$ and $K < 0$, the eigenvector corresponding to $\lambda_{\max}$ has all positive or negative entries, i.e. $v_{r_i} > 0$ or $v_{r_i} < 0, \forall i$. From the definition of eigenvector we have

$$\boldsymbol{A}\boldsymbol{v}_r = \lambda_{\max}\boldsymbol{v}_r. \tag{4.17}$$

The $i-$th row of (4.17) can be written as

$$A_i v_{r_i} + \sum_{j\neq i} A_{ij} v_{r_j} = \lambda_{\max} v_{r_i}$$

where $A_i < 0, \lambda_{\max} < 0$ and $A_{ij} > 0$. Rearranging the above equation yields

$$(A_i - \lambda_{\max})v_{r_i} = -\sum_{j\neq i} A_{ij} v_{r_j}. \tag{4.19}$$

Now let us assume that $v_{r_i} < 0$ and $v_{r_j} > 0, \forall j \neq i$. Therefore, in order (4.19) to be satisfied, the inequality $A_i - \lambda_{\max} > 0$ must hold. Assume that $A_i > \lambda_{\max}$. It is known that

$$\begin{aligned} \text{trace}(\boldsymbol{A}) &= \sum \lambda_i(\boldsymbol{A}), \\ \lambda_{\max} + \sum_{i\neq r} \lambda_i &= NA_i. \end{aligned}$$

Since $\lambda_{\max} > \lambda_i > \cdots > \lambda_N$, we always have

$$\lambda_{\max} + \sum_{i\neq r} \lambda_i < NA_i.$$

Thus, (4.19) will never hold. Therefore, it can be concluded that $\text{sign}(v_{r_i}) = \text{sign}(v_{r_j}), \forall i, j$.

The derivation of $\lambda_{\max}$ is given by

$$\frac{\partial \lambda_{\max}}{\partial K} = \sum \left[\text{sign}(K) v_{r_i} v_{r_j}\right]. \tag{4.21}$$

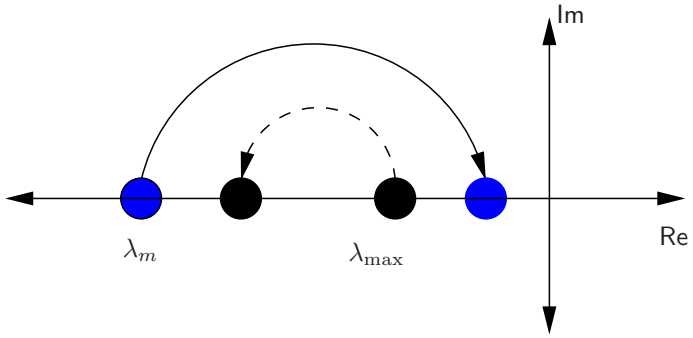

Figure 4.3: An example of movements of the largest and the second largest eigenvalue of a matrix due to a perturbation which degrade the overall system's performance.

Since $\text{sign}(v_{r_i}) = \text{sign}(v_{r_j}), \forall i, j$ and $K < 0$, $\frac{\partial \lambda_{\max}}{\partial K} < 0$. Therefore, the combination of local controllers that results in the largest displacement can be computed by solving (4.16). ■

Remark 8 Systems that satisfy Assumption A5 is known as positive systems and can be found in many important application areas, such as mechanical systems, transportation network, vehicle formation and electrical power transmission [117].

The assumption in Proposition 4.2.1 is that the feedback gain for the distributed control law is fixed. However, how to choose this gain is not a trivial problem. From $\text{trace}(\bar{\boldsymbol{A}}) = \sum \lambda_i(\bar{\boldsymbol{A}})$ we have $\sum \frac{\partial \lambda_i}{\partial K} = 0$. This means that when $\frac{\partial \lambda_{\max}}{\partial K} < 0$, there exists at least one eigenvalue of $\boldsymbol{A}$ denoted by $\lambda_m(\boldsymbol{A})$ such that $\frac{\partial \lambda_m}{\partial K} > 0$. Therefore, for a certain value of K, it is possible that $\lambda_m(\bar{\boldsymbol{A}}) > \lambda_{\max}(\boldsymbol{A})$, i.e. the system with distributed control performs worse as illustrated in Fig. 4.3. Therefore, in order to guarantee the improvement of the performance by using the distributed control law, we derive the upper bound for the distributed feedback gain. First, we introduce the following Lemma.

Lemma 4.2.3 Consider an interconnected system (4.3) under Assumptions A1-A4. Let $\boldsymbol{V}$ be a matrix of the right eigenvectors of $\boldsymbol{A}$ in (4.3). The condition number of $\boldsymbol{V}$ denoted by $\kappa_2(\boldsymbol{V})$ is one, i.e. $\kappa_2(\boldsymbol{V}) = 1$.

Proof: The condition number is given by

$$\kappa_2(\boldsymbol{V}) = \|\boldsymbol{V}\|_2 \|\boldsymbol{V}^{-1}\|_2. \tag{4.22}$$

From the definition of eigenvalue and eigenvector we have

$$\boldsymbol{A}\boldsymbol{V} = \boldsymbol{V}\text{diag}(\lambda_i). \tag{4.23}$$

Taking the transpose and from the assumption $\boldsymbol{A} = \boldsymbol{A}^T$ yields

$$\boldsymbol{V}^T\boldsymbol{A} = \text{diag}(\lambda_i)\boldsymbol{V}^T. \tag{4.24}$$

From (4.24) we have $\text{diag}(\lambda_i) = \boldsymbol{V}^T\boldsymbol{A}(\boldsymbol{V}^T)^{-1}$. Substituting this into (4.23) gives

$$\boldsymbol{A}\boldsymbol{V} = \boldsymbol{V}\boldsymbol{V}^T\boldsymbol{A}(\boldsymbol{V}^T)^{-1}. \tag{4.25}$$

Eq. (4.25) is satisfied if and only if $\boldsymbol{V}\boldsymbol{V}^T = \boldsymbol{I}$ and $\boldsymbol{V} = (\boldsymbol{V}^T)^{-1}$. Therefore, we have $\boldsymbol{V}^T = \boldsymbol{V}^{-1}$.

Finally (4.22) can be computed as

$$\begin{aligned}\kappa_2(\boldsymbol{V}) &= \left[\lambda_{\max}(\boldsymbol{V}^T\boldsymbol{V})\right]^{\frac{1}{2}} \left[\lambda_{\max}((\boldsymbol{V}^{-1})^T(\boldsymbol{V}^{-1}))\right]^{\frac{1}{2}} \\ &= 1\end{aligned}$$

which completes the proof. ■

Before proceeding, we review the Bauer-Fike Theorem [62] which bounds the maximum movement of all eigenvalues of a matrix when it is perturbed in some region. According to the Bauer-Fike Theorem, when the matrix $\boldsymbol{A}$ with eigenvalue λ_i is perturbed by the matrix $\boldsymbol{A}_{\text{dist}}$ where the resulting eigenvalues are given by $\bar{\lambda}_i$, the movement of the eigenvalues are bounded by

$$|\lambda_i - \bar{\lambda}_i| < \kappa_2(\boldsymbol{V})\|\boldsymbol{A}_{\text{dist}}\|_2 \tag{4.26}$$

where $\boldsymbol{V}$ is the eigenvector matrix of $\boldsymbol{A}$. Using (4.26), the upper bound for the distributed feedback gain with a single communication link such that the improvement of the performance for the whole system is guaranteed is given as follows.

Proposition 4.2.4 Consider an interconnected system (4.3) under assumption A1-A5 and $c = 1$. Let $\lambda_m(\boldsymbol{A})$ be the largest eigenvalue of $\boldsymbol{A}$ that satisfies $\frac{\partial \lambda_m}{\partial K} > 0$. If the feedback gain K satisfies

$$|K| < |\lambda_{\max}(\boldsymbol{A}) - \lambda_m(\boldsymbol{A})|, \tag{4.27}$$

then the performance of (4.3) with distributed control is guaranteed to be better than the decentralized one.

Proof: From (4.26) and Lemma 4.2.3 we have

$$\begin{aligned}|\lambda_i - \bar{\lambda}_i| &< \kappa_2(\boldsymbol{V})\|\boldsymbol{A}_{\text{dist}}\|_2, \\ |\lambda_i - \bar{\lambda}_i| &< \|\boldsymbol{A}_{\text{dist}}\|_2\end{aligned} \tag{4.28}$$

where $\bar{\lambda}_i$ are the perturbed eigenvalues. The $\|\boldsymbol{A}_{\text{dist}}\|_2$ can be computed as

$$\|\boldsymbol{A}_{\text{dist}}\|_2 = \left[\lambda_{\max}(\boldsymbol{A}_{\text{dist}}^T\boldsymbol{A}_{\text{dist}})\right]^{\frac{1}{2}} = \left[\lambda_{\max}(\boldsymbol{A}_{\text{dist}}\boldsymbol{A}_{\text{dist}})\right]^{\frac{1}{2}}. \tag{4.29}$$

Assume that we add the communication links between the $k-$th and $l-$th controllers, i.e. $\bar{A}_{kl} = \bar{A}_{lk} = K$. Since $[\boldsymbol{A}_{\text{dist}}\boldsymbol{A}_{\text{dist}}]_{ij} = \sum_{s=1}^{N} \bar{A}_{is}\bar{A}_{sj}$, we have $[\boldsymbol{A}_{\text{dist}}\boldsymbol{A}_{\text{dist}}]_{ij} = 0$ except for $[\boldsymbol{A}_{\text{dist}}\boldsymbol{A}_{\text{dist}}]_{kk} = K^2$ and $[\boldsymbol{A}_{\text{dist}}\boldsymbol{A}_{\text{dist}}]_{ll} = K^2$. The eigenvalues of $\boldsymbol{A}_{\text{dist}}\boldsymbol{A}_{\text{dist}}$, i.e. λ_i are the solutions of $(\lambda - K^2)^2(\lambda)^{N-2} = 0$. Therefore, $\lambda_{\max}(\boldsymbol{A}_{\text{dist}}\boldsymbol{A}_{\text{dist}}) = K^2$ and $\|\boldsymbol{A}_{\text{dist}}\|_2 = |K|$. Then Eq. (4.28) becomes

$$|\lambda_i - \bar{\lambda}_i| < |K|.$$

The above inequality informs us that the movement of any eigenvalues are bounded by the magnitude of the perturbation to the system. Thus in order to guarantee $\lambda_m(\bar{\boldsymbol{A}}) < \lambda_{\max}(\boldsymbol{A})$, a sufficient condition is that the distance of the movement of the largest eigenvalue

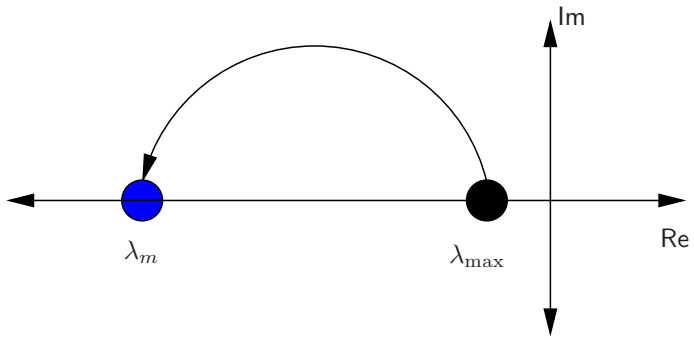

Figure 4.4: Sufficient condition for the distributed control gain such that the overall system performance is improved, i.e. the largest eigenvalue $\lambda_{\max}$ should move at most distance of $|\lambda_{\max} - \lambda_m|$.

$\lambda_{\max}$ has to be at most $|\lambda_{\max} - \lambda_m|$ as illustrated in Fig. 4.4. In other words,

$$|\lambda_{\max} - \bar{\lambda}_{\max}| < |K| < |\lambda_{\max} - \lambda_m|.$$

Therefore the feedback gain has to be chosen according to (4.27). This completes the proof. ■

4.3 Explicit Solution for Special Class of Physical Topology

Next, we present the explicit solution on where to add the communication link such that the overall system performance is optimized for a given control gain based on the eigenvalue sensitivity analysis presented in the previous section. In Section 4.2, the optimization problem (4.6) is reformulated as finding the elements of eigenvector corresponding to the largest eigenvalue for a given control gain. However, in general the closed form are not available for the generic case. Therefore, in this chapter as a first step we focus on interconnected system with three different physical topology namely ring, star and line structure as illustrated in Fig. 4.5. We start the investigation for scalar subsystems and $c = 1$, i.e. we consider the case of a single communication link. The results are then extended to the case of non-scalar subsystems, multiple communication links and more complex physical topology.

4.3.1 Ring Topology Case

First, we present the explicit solution of communication topology design for interconnected system whose physical topology has a ring structure and identical local dynamics.

Proposition 4.3.1 Consider an interconnected system (4.3) under Assumptions A1-A5 with a ring physical topology. In addition, it is assumed that the local dynamics of the subsystems are identical, i.e. $A_i = A_j = a, i \neq j$ and $A_{ij} = b, \forall i, j$. Then the solution of (4.8) is $d_{i^\star j^\star}$ where $(i^\star, j^\star) = \operatorname{argmax} D_{\mathcal{G}_P}(i, j)$.

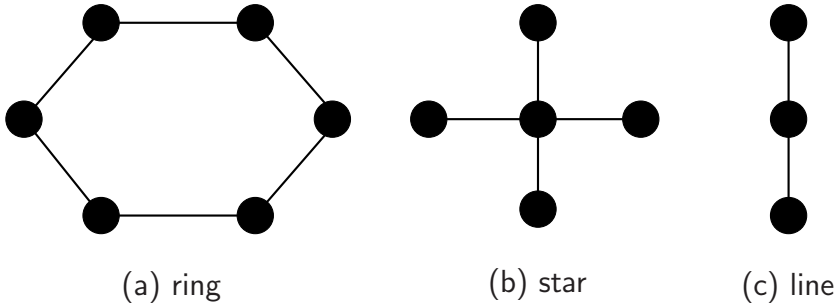

Figure 4.5: Physical topology of the interconnected system investigated in the dissertation: ring, star and line topology. The physical interconnection between the subsystems are identical.

Proof: See Appendix B.1. ■

Next we investigate how the heterogeneity of the local dynamics affects the solution by replacing one subsystem with different local dynamics.

Proposition 4.3.2 Consider an interconnected system (4.3) under Assumptions A1-A5 with a ring physical topology. It is assumed that the local dynamics of the subsystems are identical except for the local dynamics of subsystem m, i.e. $A_m = g, A_i = A_j = a$ where $i, j \neq m$. Furthermore, assumed that $A_{ij} = b, \forall i, j$. Then, the solution of (4.8) is $d_{i^\star j^\star}$ where

- $i^\star = m$ and $D_{\mathcal{G}_P}(m, j^\star) = 1$ when $|g| < |a|$
- $D_{\mathcal{G}_P}(i^\star, m) > D_{\mathcal{G}_P}(k, m)$ and $D_{\mathcal{G}_P}(j^\star, m) > D_{\mathcal{G}_P}(k, m)$, $\forall k, k \neq i^\star, j^\star$ and $i^\star \neq j^\star$, otherwise.

Proof: See Appendix B.2. ■

Discussion

As shown in the above proposition, the optimal communication link for homogeneous scalar subsystems with ring physical topology results in a high network cost under assumption that the cost is proportional to the distance between the local controller. On the other hand, unlike the case of homogeneous subsystems where the communication topology does not depend on the local dynamics and the strength of physical interconnection, when the subsystems of an interconnected system with ring physical topology are not identical, the local dynamics affects the resulting communication topology, as shown in the above proposition.

4.3.2 Star Topology Case

Next, we present the explicit solution of communication topology design for the interconnected system whose physical topology has a star structure.

Proposition 4.3.3 Consider an interconnected system (4.3) under Assumptions A1-A5 with a star physical topology. Under the assumption that the local dynamics of the subsystems are identical except for subsystem m with the largest degree, i.e. $A_m = g$, where $\deg(m) = N-1$ and $A_i = A_j = a$ where $i, j \neq m$. Furthermore, we assume that $A_{ij} = b, \forall i, j$. Then the solution of (4.8) is $d_{i^\star j^\star}$ where

- $i^\star = m$ and $D_{\mathcal{G}_P}(i^\star, j^\star) = 1$ when $g - a > b(2-N)$,
- $D_{\mathcal{G}_P}(i^\star, j^\star) = 2$, otherwise.

Remark 9 Note that the result can be extended in a straightforward manner for the case of $\deg(m) = 1$.

Before proving the aforementioned proposition, we first introduce the following Lemma.

Lemma 4.3.4 The eigenvalues of the $N \times N$ matrix

$$\boldsymbol{A} = \begin{bmatrix} g & b & b & \cdots & b \\ b & a & 0 & & 0 \\ b & 0 & a & & \vdots \\ \vdots & \vdots & & \ddots & 0 \\ b & 0 & \cdots & 0 & a \end{bmatrix} \tag{4.31}$$

where $a, g < 0$ and $b > 0$ are given by

$$\begin{aligned} \lambda_1 &= \frac{a+g+\sqrt{(a+g)^2 - 4\left(ag-(N-1)b^2\right)}}{2} \\ \lambda_2 &= \frac{a+g-\sqrt{(a+g)^2 - 4\left(ag-(N-1)b^2\right)}}{2} \\ \lambda_3 &= \cdots = \lambda_N = a. \end{aligned}$$

Proof: See Appendix B.3. ∎

We are now ready to prove Proposition 4.3.3.

Proof: With no loss of generality, we re-order the numbering of subsystems where the subsystem with the largest degree, i.e. subsystem m as subsystem 1 and the others in clockwise direction as subsystem $2, \cdots, N$. The overall dynamics of the interconnected system with star topology can then be written as

$$\boldsymbol{A} = \begin{bmatrix} g & b & b & \cdots & b \\ b & a & 0 & & 0 \\ b & 0 & a & & \vdots \\ \vdots & \vdots & & \ddots & 0 \\ b & 0 & \cdots & 0 & a \end{bmatrix}. \tag{4.32}$$

The eigenvector corresponding to the largest eigenvalue λ_r can be computed by

$$\begin{bmatrix} g & b & b & \cdots & b \\ b & a & 0 & & 0 \\ b & 0 & a & & \vdots \\ \vdots & \vdots & & \ddots & 0 \\ b & 0 & \cdots & 0 & a \end{bmatrix} \begin{bmatrix} v_{r_1} \\ v_{r_2} \\ \vdots \\ v_{r_{N-1}} \\ v_{r_N} \end{bmatrix} = \lambda_r \begin{bmatrix} v_{r_1} \\ v_{r_2} \\ \vdots \\ v_{r_{N-1}} \\ v_{r_N} \end{bmatrix}.$$

The above equation can be re-written as

$$\begin{aligned} gv_{r_1} + bv_{r_2} + \cdots + bv_{r_N} &= \lambda_r v_{r_1} \\ bv_{r_1} + av_{r_2} &= \lambda_r v_{r_2} \\ &\vdots \\ bv_{r_1} + av_{r_N} &= \lambda_r v_{r_N}. \end{aligned}$$

Then, it can be computed that

$$v_{r_2} = \cdots = v_{r_N} = \frac{b}{\lambda_r - a} v_{r_1}. \tag{4.33}$$

From Lemma 4.3.4, $\lambda_r = \lambda_1$, then we have

$$v_{r_2} = \cdots = v_{r_N} = \frac{2b}{g - a + \sqrt{(a+g)^2 - 4\left(ag - (N-1)b^2\right)}} v_{r_1}.$$

With no loss of generality, taking $v_{r_2} = \cdots = v_{r_N} = 1$ we have

$$v_{r_1} = \frac{g - a + \sqrt{(a+g)^2 - 4\left(ag - (N-1)b^2\right)}}{2b}. \tag{4.34}$$

The optimal communication link is formulated as the optimization problem (4.8) whose solution is given by $i^\star = 1$, $j^\star \neq 1$ when $v_{r_1} > 1$ and $i^\star, j^\star \neq 1$ when $v_{r_1} < 1$. Next, the condition for $v_{r_1} > 1$ can be computed as follows

$$\begin{aligned} v_{r_1} &> 1 \\ \sqrt{(a+g)^2 - 4\left(ag - (N-1)b^2\right)} &> 2b - (g-a) \\ \sqrt{(g-a)^2 + 4(N-1)b^2} &> \sqrt{(g-a)^2 + 4(N-1)b^2} \\ 4(N-1)b^2 &> 4\left[b^2 - b(g-a)\right] \\ Nb - b &> b - (g-a) \\ g - a &> b(2-N). \end{aligned}$$

This completes the proof. ■

Additionally, we have the following corollary for the case of interconnected system with identical local dynamics.

Corollary 4.3.5 Consider an interconnected system (4.3) under Assumptions A1-A5 with

a star physical topology. In addition we assume that the local dynamics of the subsystems are identical, i.e. $A_i = A_j = a, i \neq j$ and $A_{ij} = b, \forall i, j$. Then the solution of (4.8) is $d_{i^\star j^\star}$ where $i^\star = m$ and $D_{\mathcal{G}_P}(i^\star, j^\star) = 1$.

Proof: Since the subsystems are identical, i.e. $a = g$, Eq. (4.34) becomes

$$v_{r_1} = \sqrt{N-1} > 1. \tag{4.35}$$

Therefore, the solution of optimization problem (4.8) is given by $i^\star = 1$ and $j^\star \neq 1$. This completes the proof. ■

Discussion

It is interesting to note that for interconnected systems consists of heterogeneous scalar subsystems with a star physical topology, the resulting topology does not depend only on the difference of local dynamics, but also on the strength of the physical interconnection and the number of subsystems, i.e. the size of the network. On the other hand, for homogeneous subsystems under a similar physical topology, the communication topology neither depends on the local dynamics nor the strength of the physical interconnection.

4.3.3 Line Topology Case

Finally, we present the explicit solution of communication topology design for interconnected system whose physical topology has a line structure.

Proposition 4.3.6 Consider an interconnected system (4.3) under Assumptions A1-A5 with a line physical topology. We assume that the local dynamics of the subsystems are identical, i.e. $A_i = A_j = a, i \neq j$ and $A_{ij} = b, \forall i, j$. Furthermore, with no loss of generality, the numbering of subsystems is re-ordered from left to right or up to down as $1, 2, \cdots, N$. Then the solution of (4.8) is $d_{i^\star j^\star}$ where

- $j^\star = \frac{N+1}{2}$ and $i^\star = \frac{N+1}{2} + 1$ or $i^\star = \frac{N+1}{2} - 1$ when N is odd
- $j^\star = \frac{N}{2}$ and $i^\star = \frac{N}{2} + 1$ when N is even.

Proof: With no loss of generality, we re-order the numbering of subsystems from left to right or up to down as $1, 2, \cdots, N$. The overall dynamics of the interconnected system with line topology can then be written as

$$\boldsymbol{A} = \begin{bmatrix} a & b & & & \\ b & a & b & & \\ & \ddots & \ddots & \ddots & \\ & & b & a & b \\ & & & b & a \end{bmatrix}. \tag{4.36}$$

In order to prove the statement, first we need to compute the largest eigenvalue and the corresponding eigenvector of (4.36). In general, the eigenvalue of the matrix $\boldsymbol{A}$ in (4.36)

is given by [16]

$$\lambda_j = a + 2|b| \cos\left(\frac{j}{N+1}\pi\right), \quad j = 1, \cdots, N \tag{4.37}$$

while the corresponding eigenvector is given by

$$\boldsymbol{v}_j = y_j[\Delta \boldsymbol{u}_j], j = 1, \cdots, N \tag{4.38}$$

where

$$\begin{aligned} \boldsymbol{u}_j &= \left(\frac{2}{N+1}\right)^{\frac{1}{2}} \left[\sin\left(\frac{j\pi}{N+1}\right), \cdots, \sin\left(\frac{Nj\pi}{N+1}\right)\right]^T, \\ \Delta &= \mathrm{diag}(1, \cdots, 1), \\ y_j &= \left(\frac{2}{N+1}\sum_{i=1}^{N} \sin^2\left(\frac{ij\pi}{N+1}\right)\right)^{-\frac{1}{2}}. \end{aligned}$$

From (4.37), the largest eigenvalue, i.e. $j = 1$ can be computed as

$$\lambda_{\max} = a + 2|b| \cos\left(\frac{1}{N+1}\pi\right) \tag{4.39}$$

and the corresponding eigenvector

$$\begin{aligned} \boldsymbol{v}_1 &= y_1[\Delta \boldsymbol{u}_1] \\ &= \left(\sum_{i=1}^{N} \sin^2\left(\frac{i\pi}{N+1}\right)\right)^{-\frac{1}{2}} \mathrm{diag}(1, \cdots, 1) \\ &\quad \left[\sin\left(\frac{1\pi}{N+1}\right), \cdots, \sin\left(\frac{N\pi}{N+1}\right)\right]^T. \end{aligned}$$

It is known that

$$\sum_{i=1}^{N} \sin^2(ix) = \frac{1}{4}\{1 + 2N - \csc(x)\sin[x(1+2N)]\}.$$

Taking $x = \frac{\pi}{N+1}$, we have

$$\sum_{i=1}^{N} \sin^2\left(\frac{i\pi}{N+1}\right) = \frac{N+1}{2}.$$

Therefore, the eigenvector corresponding to $\lambda_{\max}$ is given by

$$\boldsymbol{v}_1 = \sqrt{\frac{2}{N+1}} \left[\sin\left(\frac{1\pi}{N+1}\right), \cdots, \sin\left(\frac{N\pi}{N+1}\right)\right]^T.$$

The maximum value of the element of $\boldsymbol{v}_1$ is equal to 1 which occurs at

$$\sin\left(\frac{j\pi}{N+1}\right) = \sin\left(\frac{\pi}{2}\right) \Leftrightarrow j = \frac{N+1}{2}. \tag{4.40}$$

The optimal communication link is formulated as the optimization problem (4.8) whose solution is then given by

- $j^\star = \frac{N+1}{2}$ and $i^\star = \frac{N+1}{2} + 1$ or $i^\star = \frac{N+1}{2} - 1$ when N is odd
- $j^\star = \frac{N}{2}$ and $i^\star = \frac{N}{2} + 1$ when N is even.

In other words, the communication link is added between local controller in the middle and its neighbor. This completes the proof. ■

4.4 Explicit Solution for Multidimensional Subsystems

In this section, the results in section 4.3 are extended into the case of multidimensional subsystems. Specifically, we investigate the following question: for which class of interconnected system do the results for the scalar case still hold? We consider an interconnected system given by the following assumptions.

V1 The state of subsystem i, i.e. $\boldsymbol{x}_i \in \mathbb{R}^n$.

V2 Matrix $\boldsymbol{A}_i$ is real symmetric, i.e. $\boldsymbol{A}_i = \boldsymbol{A}_i^T$ and $\lambda_{\max}(\boldsymbol{A}_i) < 0$.

V3 The physical interconnections are identical, i.e. $\boldsymbol{A}_{ij} = \boldsymbol{A}_{ks}$, $i \neq j, k \neq s$ and $\boldsymbol{A}_{ij} = \boldsymbol{A}_{ij}^T$, $\boldsymbol{A}_{ij} = l\boldsymbol{A}_i, l < 0 \in \mathbb{R}$.

V4 The communication is bidirectional and the distributed control gains are fixed and equal. Moreover $\boldsymbol{B}_i\boldsymbol{K}_{ij} = k\boldsymbol{J}_n$ where $k \in \mathbb{R}, k < 0$ and $\boldsymbol{J}_n$ is a unit matrix of size n.

Let us consider an interconnected system (4.3) under Assumptions V1-V4 where the local dynamics of the subsystems are identical, i.e. $\boldsymbol{A}_i = \boldsymbol{A}_j = \hat{\boldsymbol{A}}, i \neq j$. Next let us compute the change of the largest eigenvalue of the matrix $\boldsymbol{A}$ when it is perturbed by the matrix $\boldsymbol{K} = [\boldsymbol{B}_i\boldsymbol{K}_{ij}] \in \mathbb{R}^{Nn\times Nn}$ where $\boldsymbol{B}_i\boldsymbol{K}_{ij} \in \mathbb{R}^{n\times n}$ is given by Assumption V4. Without loss of generality, it is assumed that the physical interconnection topology is given by a ring and the communication link is added between the local controller of subsystem i and j. Eq. (4.10) can then be computed as

$$\frac{\partial \lambda_{\max}}{\partial k} = \boldsymbol{v}_r^T \begin{bmatrix} \boldsymbol{O}_n & \boldsymbol{O}_n & \cdots & \boldsymbol{O}_n & \boldsymbol{O}_n & \cdots & \boldsymbol{O}_n \\ \boldsymbol{O}_n & \boldsymbol{O}_n & \cdots & -\boldsymbol{J}_n & \boldsymbol{O}_n & \cdots & \boldsymbol{O}_n \\ \vdots & \vdots & \ddots & \vdots & \vdots & \ddots & \vdots \\ \boldsymbol{O}_n & -\boldsymbol{J}_n & \cdots & \boldsymbol{O}_n & \boldsymbol{O}_n & \cdots & \boldsymbol{O}_n \\ \boldsymbol{O}_n & \boldsymbol{O}_n & \cdots & \boldsymbol{O}_n & \boldsymbol{O}_n & \cdots & \boldsymbol{O}_n \\ \vdots & \vdots & \ddots & \vdots & \vdots & \ddots & \vdots \\ \boldsymbol{O}_n & \boldsymbol{O}_n & \cdots & \boldsymbol{O}_n & \boldsymbol{O}_n & \cdots & \boldsymbol{O}_n \end{bmatrix} \boldsymbol{v}_r \tag{4.41}$$

where $\boldsymbol{v}_r = [v_{r_1}, v_{r_2}, \cdots, v_{r_n}, v_{r_{n+1}}, \cdots, v_{r_{Nn}}]^T$. After straightforward computation, Eq. (4.41) becomes $\frac{\partial \lambda_{\max}}{\partial k} = -2v_r^i v_r^j$ where

$$v_r^i = \sum_{p=(i-1)n+1}^{in} v_{r_p}. \tag{4.42}$$

Next we compute the eigenvector of $\boldsymbol{A}$ corresponding to the largest eigenvalue $\lambda_{\max}$. The matrix $\boldsymbol{A}$ can be written as

$$\boldsymbol{A} = \boldsymbol{C} \otimes -\hat{\boldsymbol{A}}$$

where $\otimes$ describes the Kronecker product and the matrix $\boldsymbol{C} \in \mathbb{R}^{N\times N}$ is given by

$$\boldsymbol{C} = \begin{bmatrix} -1 & \bar{l} & 0 & & \bar{l} \\ \bar{l} & -1 & \bar{l} & & \\ & \ddots & \ddots & \ddots & \\ & & \bar{l} & -1 & \bar{l} \\ \bar{l} & & 0 & \bar{l} & -1 \end{bmatrix}$$

where $\bar{l} = -l$. The Nn eigenvalues of $\boldsymbol{C} \otimes -\hat{\boldsymbol{A}}$ are then given by [79]

$$\lambda_1(\boldsymbol{C})\lambda_1(-\hat{\boldsymbol{A}}), \cdots, \lambda_1(\boldsymbol{C})\lambda_n(-\hat{\boldsymbol{A}}), \lambda_2(\boldsymbol{C})\lambda_1(-\hat{\boldsymbol{A}}), \cdots, \lambda_2(\boldsymbol{C})\lambda_n(-\hat{\boldsymbol{A}}), \cdots, \lambda_N(\boldsymbol{C})\lambda_n(-\hat{\boldsymbol{A}}).$$

Therefore, under Assumption V2, the largest eigenvalue of $\boldsymbol{A}$ can be computed as $\lambda_{\max}(\boldsymbol{A}) = \lambda_{\max}(\boldsymbol{C})\lambda_{\max}(-\hat{\boldsymbol{A}})$ or $\lambda_{\max}(\boldsymbol{A}) = \lambda_{\max}(\boldsymbol{C})\alpha_{\min}(-\hat{\boldsymbol{A}})$. Furthermore, if $\boldsymbol{z}_1, \cdots, \boldsymbol{z}_N$ are linearly independent right eigenvectors of $\boldsymbol{C}$ corresponding to $\lambda_1(\boldsymbol{C}), \cdots, \lambda_N(\boldsymbol{C})$ and $\boldsymbol{w}_1, \cdots, \boldsymbol{w}_n$ are linearly independent right eigenvectors of $-\hat{\boldsymbol{A}}$ corresponding to $\lambda_1(-\hat{\boldsymbol{A}}), \cdots, \lambda_n(-\hat{\boldsymbol{A}})$, then $\boldsymbol{z}_i \otimes \boldsymbol{w}_j \in \mathbb{R}^{Nn}$ are linearly independent right eigenvectors of $\boldsymbol{C} \otimes -\hat{\boldsymbol{A}}$ corresponding to $\lambda_i(\boldsymbol{C})\lambda_j(-\hat{\boldsymbol{A}})$ [79]. The right eigenvectors of $\boldsymbol{A}$ corresponding to the largest eigenvalue $\lambda_{\max}$ is thus given by $\boldsymbol{v}_r = \boldsymbol{z}_r \otimes \boldsymbol{w}_r$ or $\boldsymbol{v}_r = \boldsymbol{z}_r \otimes \boldsymbol{w}_1$. Then, Eq. (4.42) can be re-written as

$$v_r^i = z_{r_i} \sum_{j=1}^{n} w_{r_j} \text{ or } v_r^i = z_{r_i} \sum_{j=1}^{n} w_{1_j}$$

where $\boldsymbol{w}_r = [w_{r_1}, \cdots, w_{r_n}]^T$, $\boldsymbol{w}_1 = [w_{1_1}, \cdots, w_{1_n}]^T$. Then we have

$$\frac{\partial \lambda_{\max}}{\partial k} = -2 z_{r_i} z_{r_j} \underbrace{\left| \sum_{j=1}^{n} w_{r_j} \right|^2}_{\text{constant}} \text{ or } \frac{\partial \lambda_{\max}}{\partial k} = -2 z_{r_i} z_{r_j} \underbrace{\left| \sum_{j=1}^{n} w_{1_j} \right|^2}_{\text{constant}}.$$

Therefore, it can be concluded that $\frac{\partial \lambda_{\max}}{\partial k} \sim -2 z_{r_i} z_{r_j}$. It is clear that the optimization problem is reduced to the case of the scalar case by finding a pair of elements of eigenvector corresponding to the largest eigenvalue of matrix $\boldsymbol{C}$.

Remark 10 The similar results can be obtained for the case $\boldsymbol{B}_i \boldsymbol{K}_{ij} = k \boldsymbol{I}_n$.

Similar results can be obtained for non-identical subsystems where one subsystem is substituted by another subsystem with different local dynamics and also for the non-scalar subsystems with a star physical topology, as summarized in the following propositions.

Proposition 4.4.1 Consider an interconnected system (4.3) under Assumptions V1-V4 with a ring physical topology. In addition it is assumed that the local dynamics of the subsystems are identical except for the local dynamics of subsystem m where $\boldsymbol{A}_m = \zeta \boldsymbol{A}_i$, $i, j \neq m$ and $\zeta > 0 \in \mathbb{R}$. Then the solution of (4.8) is $d_{i^\star j^\star}$ where

- $i^\star = m$ and $D_{\mathcal{G}_P}(m, j^\star) = 1$ when $\zeta < 1$
- $D_{\mathcal{G}_P}(i^\star, m) > D_{\mathcal{G}_P}(k, m)$ and $D_{\mathcal{G}_P}(j^\star, m) > D_{\mathcal{G}_P}(k, m)$, $\forall k, k \neq i^\star, j^\star$ and $i^\star \neq j^\star$, otherwise.

Proof: See Appendix B.4. ■

Proposition 4.4.2 Consider an interconnected system (4.3) under Assumptions V1-V4 with a star physical topology. Under the assumption that the local dynamics of the subsystems are identical except for subsystem m with the largest degree where $\boldsymbol{A}_m = \zeta A_i, \deg(m) = N - 1$, $i, j \neq m$ and $\zeta > 0 \in \mathbb{R}$. Then the solution of (4.8) is $d_{i^\star j^\star}$ where

- $i^\star = m$ and $D_{\mathcal{G}_P}(i^\star, j^\star) = 1$ when $\zeta - 1 > \bar{l}(2 - N)$,
- $D_{\mathcal{G}_P}(i^\star, j^\star) = 2$, otherwise.

Proof: See Appendix B.5. ■

Remark 11 As mentioned previously, the results for multidimensional subsystems under Assumptions V1-V4 also hold for an interconnected system with star and line physical topologies.

4.5 Explicit Solution for Multiple Communication Links

In this section, we discuss the case where multiple communication links are going to be added, i.e. $\gamma_{ij} = 1, c > 1$. Without loss of generality we consider the scalar subsystems. The results also hold for non-scalar case under Assumptions V1-V4. First, we introduce the following Lemmas for interconnected system consists of identical local dynamics.

Lemma 4.5.1 Consider an interconnected system (4.3) under Assumptions A1-A5 with identical subsystems and a star physical topology. In addition, we assume that the subsystem with degree $N - 1$ as subsystem 1 and the others in clockwise direction as subsystem $2, \cdots, N$. Then $v_{r_i} > 0$ is the concave function of i and $\operatorname{argmax}_i v_{r_i} = 1$.

Proof: It is obvious from (4.33) and (4.35). ■

Lemma 4.5.2 Consider an interconnected system (4.3) under Assumptions A1-A5 with identical subsystems and a line physical topology. In addition we re-order the numbering of subsystems from left to right or up to down as $1, 2, \cdots, N$. Then $v_{r_i} > 0$ is the concave function of i and

$$\underset{i}{\operatorname{argmax}}\, v_{r_i} = \begin{cases} \frac{N+1}{2} & \text{if } N \text{ is odd} \\ \frac{N}{2}, \frac{N+1}{2} & \text{if } N \text{ is even.} \end{cases}$$

Proof: It is clear from the proof of Proposition 4.3.6 that

$$\boldsymbol{v}_r = \sqrt{\frac{2}{N+1}} \left[\sin\left(\frac{1\pi}{N+1}\right), \cdots, \sin\left(\frac{N\pi}{N+1}\right) \right]^T.$$

■

Furthermore we also have the following Lemmas.

Lemma 4.5.3 Consider an interconnected system (4.3) under Assumptions A1-A5 with ring physical topology. Furthermore, let us assume that the local dynamics of the subsystems are identical except for subsystem 1 and the subsystems are numbered in a clockwise direction as $1, 2, \cdots, N$. Then $v_{r_i} > 0$ is a concave (resp. convex) function of i if $|A_1| > |A_j|, j \neq 1$ (resp. $|A_1| < |A_i|, j \neq 1$) and $\operatorname{argmax}_i v_{r_i} = \left\lfloor \frac{N}{2} \right\rfloor + 1$ (resp. $\operatorname{argmax}_i v_{r_i} = 1$).

Proof: The proof is straightforward from Lemma B.2.1 and Eq. (B.15) or Eq. (B.14). ■

Lemma 4.5.4 Consider an interconnected system (4.3) under Assumptions A1-A5 with star physical topology. Furthermore, let us assume that the local dynamics of the subsystems are identical except for subsystem with degree $N-1$ and the subsystems are numbered such that subsystem with degree $N-1$ as subsystem 1 and the others in clockwise direction as subsystem $2, \cdots, N$. Then v_{r_i} is a concave (resp. convex) function of i if $A_1 - A_j < A_{ij}(2-N), j \neq 1$ (resp. $A_1 - A_j > A_{ij}(2-N), j \neq 1$) and $\operatorname{argmax}_i v_{r_i} = i \neq 1$ (resp. $\operatorname{argmax}_i v_{r_i} = 1$).

Proof: The proof is straightforward from (4.33) and (4.34). ■

The results are intuitive since the minimization of $\lambda_{\max}$ of a symmetric matrix is a convex problem [131]. Therefore, by using Lemmas 4.5.1-4.5.4 and solving the optimization problem (4.16), the optimal communication topology for multiple links case can be computed efficiently as will be demonstrated later via a numerical example.

4.6 Explicit Solution for Complex Physical Topology

In this section, it is demonstrated how the results can be extended to interconnected system with more complex physical topology composed of the basic topologies investigated in Section 4.3, i.e. the star, ring and line topology. For the sake of simplicity and clarity, we consider the interconnected system given by Assumptions A1-A5 and the case of a single communication link. Furthermore, we consider as an example an interconnected system whose physical topology is a two-star network with identical subsystems as shown in Fig. 4.6(b). We thus have the following result.

Proposition 4.6.1 Consider an interconnected system (4.3) under Assumptions A1-A5 with a two-star physical topology and equal number of subsystems. In addition it is assumed that the local dynamics of the subsystems are identical, i.e. $A_i = A_j = a, i \neq j$ and $A_{ij} = b, \forall i, j$. Then the solution of (4.8) is $d_{i^\star j^\star}$ where $\deg(i^\star)$=$\deg(j^\star)$>1.

Proof: With no loss of generality, we re-order the numbering of the subsystems as illustrated in Fig. 4.6(b). The overall dynamics of the interconnected system with two-star

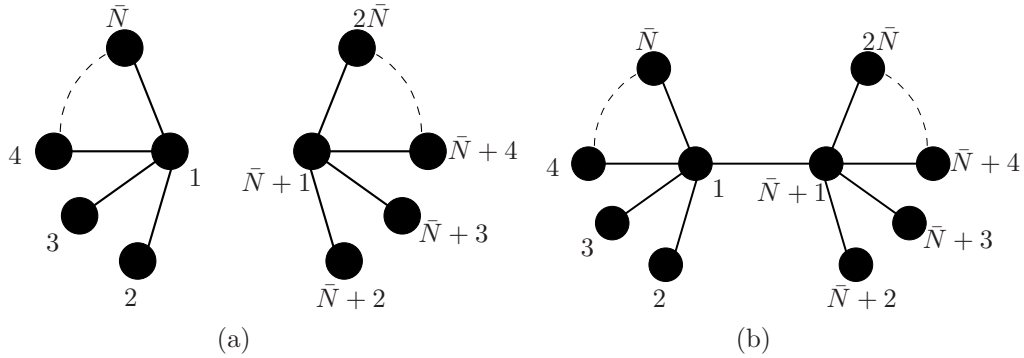

Figure 4.6: (a) Disconnected two-star topology with equal number of subsystems $\bar{N}$; (b) Interconnected system whose physical topology is given by a two-star network.

topology can then be written as

$$\boldsymbol{A} = \begin{bmatrix} a & b & b & \cdots & b & b & 0 & 0 & \cdots & 0 \\ b & a & 0 & & 0 & 0 & 0 & 0 & \cdots & 0 \\ b & 0 & a & & \vdots & \vdots & \vdots & \vdots & \vdots & \vdots \\ \vdots & \vdots & & \ddots & 0 & 0 & 0 & 0 & \cdots & 0 \\ b & 0 & \cdots & 0 & a & 0 & 0 & 0 & \cdots & 0 \\ b & 0 & 0 & \cdots & 0 & a & b & b & \cdots & b \\ 0 & 0 & 0 & \cdots & 0 & b & a & 0 & & 0 \\ \vdots & \vdots & \vdots & \vdots & \vdots & b & 0 & a & & \vdots \\ 0 & 0 & 0 & \cdots & 0 & \vdots & \vdots & & \ddots & 0 \\ 0 & 0 & 0 & \cdots & 0 & b & 0 & \cdots & 0 & a \end{bmatrix} \in \mathbb{R}^{2\bar{N}\times 2\bar{N}}. \tag{4.43}$$

The two-star topology can be obtained by connecting the nodes with the maximum degree of the identical stars topology in Fig. 4.6(a). Eq. (4.43) can then be written as

$$\begin{aligned} \boldsymbol{A} &= \begin{bmatrix} a & b & b & \cdots & b & 0 & 0 & 0 & \cdots & 0 \\ b & a & 0 & & 0 & 0 & 0 & 0 & \cdots & 0 \\ b & 0 & a & & \vdots & \vdots & \vdots & \vdots & \vdots & \vdots \\ \vdots & \vdots & & \ddots & 0 & 0 & 0 & 0 & \cdots & 0 \\ b & 0 & \cdots & 0 & a & 0 & 0 & 0 & \cdots & 0 \\ 0 & 0 & 0 & \cdots & 0 & a & b & b & \cdots & b \\ 0 & 0 & 0 & \cdots & 0 & b & a & 0 & & 0 \\ \vdots & \vdots & \vdots & \vdots & \vdots & b & 0 & a & & \vdots \\ 0 & 0 & 0 & \cdots & 0 & \vdots & \vdots & & \ddots & 0 \\ 0 & 0 & 0 & \cdots & 0 & b & 0 & \cdots & 0 & a \end{bmatrix} + \begin{bmatrix} 0 & 0 & 0 & \cdots & 0 & b & 0 & 0 & \cdots & 0 \\ 0 & 0 & 0 & & 0 & 0 & 0 & 0 & \cdots & 0 \\ 0 & 0 & 0 & & \vdots & \vdots & \vdots & \vdots & \vdots & \vdots \\ \vdots & \vdots & & \ddots & 0 & 0 & 0 & 0 & \cdots & 0 \\ 0 & 0 & \cdots & 0 & 0 & 0 & 0 & 0 & \cdots & 0 \\ b & 0 & 0 & \cdots & 0 & 0 & 0 & 0 & \cdots & 0 \\ 0 & 0 & 0 & \cdots & 0 & 0 & 0 & 0 & & 0 \\ \vdots & \vdots & \vdots & \vdots & \vdots & 0 & 0 & 0 & & \vdots \\ 0 & 0 & 0 & \cdots & 0 & \vdots & \vdots & & \ddots & 0 \\ 0 & 0 & 0 & \cdots & 0 & 0 & 0 & \cdots & 0 & 0 \end{bmatrix} \\ &= \boldsymbol{A}_0 + d\boldsymbol{A}. \end{aligned} \tag{4.44}$$

The matrix $d\boldsymbol{A}$ can be seen as a perturbation working on the matrix $\boldsymbol{A}_0$. Therefore, in the following we investigate how the eigenvector related to the largest eigenvalue of $\boldsymbol{A}_0$

changes due to the perturbation by $d\boldsymbol{A}$. First we compute the eigenvector w.r.t. the largest eigenvalue of $\boldsymbol{A}_0$. The eigenvalues of $\boldsymbol{A}_0$ are given by $\lambda(\boldsymbol{A}_0) = \{\lambda(\boldsymbol{A}^s), \lambda(\boldsymbol{A}^s)\}$ where

$$\boldsymbol{A}^s = \begin{bmatrix} a & b & b & \cdots & b \\ b & a & 0 & & 0 \\ b & 0 & a & & \vdots \\ \vdots & \vdots & & \ddots & 0 \\ b & 0 & \cdots & 0 & a \end{bmatrix} \in \mathbb{R}^{\bar{N}\times\bar{N}}.$$

The largest eigenvalue of $\boldsymbol{A}_0$ is then given by $\lambda_{\max}(\boldsymbol{A}_0) = \lambda_{\max}(\boldsymbol{A}^s)$ and the corresponding eigenvector $\boldsymbol{v}_r$ can be computed as

$$\boldsymbol{A}_0\boldsymbol{v}_r(\boldsymbol{A}_0) = \lambda_{\max}\boldsymbol{v}_r(\boldsymbol{A}_0).$$

From (4.33) and (4.35), $\boldsymbol{v}_r(\boldsymbol{A}_0)$ is then given by $\boldsymbol{v}_r = [v_{r_1}, v_{r_2}, \cdots, v_{r_2}, v_{r_1}, v_{r_2}, \cdots, v_{r_2}]^T$ where $v_{r_1} = \sqrt{N-1}$ and $v_{r_2} = \frac{1}{\sqrt{N-1}}v_{r_1}$. Next we investigate the eigenvector sensitivity of $\boldsymbol{A}$ when $\boldsymbol{A}_0$ is perturbed by $d\boldsymbol{A}$ given by

$$[\boldsymbol{A} - \lambda_{\max}\boldsymbol{I}_N]\frac{d\boldsymbol{v}_r}{db} = -\left[\frac{\partial \boldsymbol{A}}{\partial b} - \lambda'_{\max}\boldsymbol{I}_N\right]\boldsymbol{v}_r(\boldsymbol{A}_0) \tag{4.45}$$

where $\lambda'_{\max} = \frac{\partial\lambda_{\max}}{\partial b}$. The left and right hand side of (4.45) can be computed as

$$[\boldsymbol{A} - \lambda_{\max}\boldsymbol{I}_N]\frac{d\boldsymbol{v}_r}{db} = \begin{bmatrix} \hat{a} & b & b & \cdots & b & b & 0 & 0 & \cdots & 0 \\ b & \hat{a} & 0 & & 0 & 0 & 0 & 0 & \cdots & 0 \\ b & 0 & \hat{a} & & \vdots & \vdots & \vdots & \vdots & \vdots & \vdots \\ \vdots & \vdots & & \ddots & 0 & 0 & 0 & 0 & \cdots & 0 \\ b & 0 & \cdots & 0 & \hat{a} & 0 & 0 & 0 & \cdots & 0 \\ b & 0 & 0 & \cdots & 0 & \hat{a} & b & b & \cdots & b \\ 0 & 0 & 0 & \cdots & 0 & b & \hat{a} & 0 & & 0 \\ \vdots & \vdots & \vdots & \vdots & \vdots & b & 0 & \hat{a} & & \vdots \\ 0 & 0 & 0 & \cdots & 0 & \vdots & \vdots & & \ddots & 0 \\ 0 & 0 & 0 & \cdots & 0 & b & 0 & \cdots & 0 & \hat{a} \end{bmatrix} \frac{d\boldsymbol{v}_r}{db},$$

$$-\left[\frac{\partial \boldsymbol{A}}{\partial b}-\lambda'_{\max}\boldsymbol{I}_N\right]\boldsymbol{v}_r(\boldsymbol{A}_0)=\begin{bmatrix}\lambda'_{\max} & 0 & 0 & \cdots & 0 & -1 & 0 & 0 & \cdots & 0\\ 0 & \lambda'_{\max} & 0 & & 0 & 0 & 0 & 0 & \cdots & 0\\ 0 & 0 & \lambda'_{\max} & & \vdots & \vdots & \vdots & \vdots & \vdots & \vdots\\ \vdots & \vdots & & \ddots & 0 & 0 & 0 & 0 & \cdots & 0\\ 0 & 0 & \cdots & 0 & \lambda'_{\max} & 0 & 0 & 0 & \cdots & 0\\ b & 0 & 0 & \cdots & 0 & \lambda'_{\max} & 0 & 0 & \cdots & 0\\ 0 & 0 & 0 & \cdots & 0 & 0 & 0 & 0 & & 0\\ \vdots & \vdots & \vdots & \vdots & \vdots & 0 & 0 & \lambda'_{\max} & & \vdots\\ 0 & 0 & 0 & \cdots & 0 & \vdots & \vdots & & \ddots & 0\\ 0 & 0 & 0 & \cdots & 0 & 0 & 0 & \cdots & 0 & \lambda'_{\max}\end{bmatrix}\boldsymbol{v}_r(\boldsymbol{A}_0)$$

where $\hat{a}=a-\lambda_{\max}(\boldsymbol{A}_0)=-b\sqrt{N-1}$. Therefore, Eq. (4.45) can be written by N equations given as follows

$$\begin{aligned}\hat{a}q_1+bq_2+\cdots+bq_N &= v_{r_1}(\lambda'_{\max}-1)\\ bq_1+\hat{a}q_2 &= \lambda'_{\max}v_{r_2}\\ &\vdots\\ bq_1+\hat{a}q_{\bar{N}} &= \lambda'_{\max}v_{r_2}\\ bq_1+\hat{a}q_{\bar{N}+1}+\cdots+bq_N &= v_{r_1}(\lambda'_{\max}-1)\\ bq_{\bar{N}+1}+\hat{a}q_{\bar{N}+2} &= \lambda'_{\max}v_{r_2}\\ &\vdots\\ bq_{\bar{N}+1}+\hat{a}q_N &= \lambda'_{\max}v_{r_2}.\end{aligned}$$

where $q_i=\frac{dv_{r_i}}{db}$. Subtracting the $i-$th and $j-$th equation where $2\leq i,j\leq\bar{N}$ results in $q_2=\cdots=q_{\bar{N}}$. Similar result given by $q_{\bar{N}+1}=\cdots=q_N$ is also obtained for $\bar{N}+1\leq i,j\leq N$. Furthermore, subtracting the first and $(\bar{N}+1)-$th equations gives $(\hat{a}-b)(q_1-q_{\bar{N}+1})+(\bar{N}-1)b(q_2-q_{\bar{N}+2})=0$. Applying the similar computation to the second and $(\bar{N}+2)-$th equations gives $b(q_1-q_{\bar{N}+1})+\hat{a}(q_2-q_{\bar{N}+2})=0$. Both equations can then be written as

$$\begin{bmatrix}\hat{a}-b & (\bar{N}-1)b\\ b & \hat{a}\end{bmatrix}\begin{bmatrix}q_1-q_{\bar{N}+1}\\ q_2-q_{\bar{N}+2}\end{bmatrix}=\begin{bmatrix}0\\0\end{bmatrix}.$$

Therefore, we have $q_1=q_{\bar{N}+1}$ and $q_2=q_{\bar{N}+2}$. In other words, the first element and the $(\bar{N}+1)-$th element of the eigenvector has the same sensitivity. The similar result can also be obtained for the rest of the elements of the corresponding eigenvector. The final step is to prove that the first and the $(\bar{N}+1)-$th elements of eigenvector of $\boldsymbol{A}$ is larger than the rest of the elements. Let us recall the definition of eigenvector of $\boldsymbol{A}$ given by

$$\boldsymbol{A}\boldsymbol{v}_r(\boldsymbol{A})=\lambda_{\max}\boldsymbol{v}_r(\boldsymbol{A}).$$

From the above equation, we have the following.

$$v_{r_1}=\left(\frac{\lambda_{\max}(\boldsymbol{A})-a}{b}\right)v_{r_2},$$

$$
\begin{aligned}
v_{r_1} &= \left(\frac{\lambda_{\max}(\boldsymbol{A}_0) + \lambda'_{\max} - a}{b} \right) v_{r_2}, \\
&= \left(\frac{a + b\sqrt{N-1} + (\sqrt{N-1})^2 - a}{b} \right) v_{r_2}, \\
&= \left(\frac{b\sqrt{N-1} + N - 1}{b} \right) v_{r_2}.
\end{aligned}
$$

At the end, we have $v_{r_1} > v_{r_2}$. It can then be concluded that the optimal communication link is obtained by connecting the first local controller and the $(\bar{N}+1)-$th local controller. This completes the proof. ■

Remark 12 It is possible to apply the similar idea to interconnected systems whose topology is given by a two-ring network or combination of stars, rings and lines networks. The main procedure is first to disconnect the topology into several basic topologies, e.g. ring, star and line and then to treat the links connecting the basic topologies as perturbations, as illustrated in Proposition 4.6.1.

4.7 Eigenvalue Sensitivity for Distributed Control with Time Delay

In the following, the eigenvalue sensitivity approach described in the previous section is applied to the interconnected system with time delay discussed in Section 3.3. First, let us recall the closed loop dynamics of the interconnected system with distributed control law where the information exchange is afflicted by constant and identical time delay τ:

$$
\begin{aligned}
&\dot{\boldsymbol{x}}(t) = \boldsymbol{A}_{\text{dec}}\boldsymbol{x}(t) + \boldsymbol{A}_{\text{dist}}\boldsymbol{x}(t-\tau), \\
&\boldsymbol{x}(\theta) = \boldsymbol{x}_0, \ \forall \theta \in [-\tau, 0].
\end{aligned}
\tag{4.46}
$$

Furthermore, for the sake of simplicity, we constrain ourselves for the remainder of this section by the following assumptions.

D1 The subsystems are scalar, i.e. $x_i \in \mathbb{R}$.

D2 The number of communication link $c = 1$ with $\gamma_{ij} = 1$.

D3 The communication is bidirectional.

D4 The distributed control gain K is fixed and equal for all subsystems which results in $\boldsymbol{A}_{\text{dist}}^T = \boldsymbol{A}_{\text{dist}}$.

Note that the approach described in the following can also be extended to the case when $\boldsymbol{x}_i \in \mathbb{R}^n$ and for multiple communication links, i.e. $c > 1$ which however results in a more complicated formulation.

The largest real part of the eigenvalues of (4.46), i.e. $\lambda_{\max}$ determines the decay rate of the whole interconnected system. Therefore, similar to the non-delay case, we are interested in the minimization of the real part of the rightmost eigenvalue $\lambda_{\max}$.

4.7.1 Sensitivity to Communication Link

In this section, the eigenvalue sensitivity is analyzed in order to investigate how the structure of the distributed control law affects $\lambda_{\max}$ of (4.46) for a given time delay τ. The eigenvalues of (4.46) are equivalent to the roots of the characteristic equation

$$\det(\lambda \boldsymbol{I}_N - \boldsymbol{A}_{\text{dec}} - \boldsymbol{A}_{\text{dist}}\, \mathrm{e}^{\lambda\tau}) = 0. \tag{4.47}$$

Note that Eq. (4.47) is a nonlinear eigenvalue problem and has infinitely many solutions. However, the number of eigenvalues to the right of any vertical line, $\mathrm{Re}(\lambda) \geq r$, with $r \in \mathbb{R}$, is finite, and hence $-\infty$ is the only accumulation point for the real parts of the eigenvalues [99]. Before proceeding, let us recall the sensitivity analysis for the nonlinear eigenvalue problem [67]. Consider a nonlinear eigenvalue problem depending on a parameter $h, \boldsymbol{G}_h$. Hence the sensitivity of a solution to the nonlinear eigenvalue problem λ, which is the generalization for the linear case is given by [67]

$$\lambda'(h) = \frac{\boldsymbol{v}^* \frac{\partial \boldsymbol{G}_h}{\partial h}(\lambda)\boldsymbol{w}}{\boldsymbol{v}^*(\boldsymbol{I}_N - \frac{\partial \boldsymbol{G}_h}{\partial \lambda}(\lambda))\boldsymbol{w}} \tag{4.48}$$

where $\boldsymbol{v}$ and $\boldsymbol{w}$ are the left and right eigenvector respectively with normalization $\boldsymbol{v}^*\boldsymbol{w} = 1$ where $\boldsymbol{v}^*$ is the complex conjugate transpose of $\boldsymbol{v}$. Since the goal is to find the communication topology such that the convergence rate of the overall system (4.46) with the distributed control law is higher than the one with the decentralized control, we would like to find the structure of the perturbation to the rightmost eigenvalues $\lambda_{\max}$ of (4.46) such that its sensitivity is negative and the magnitude is maximum. Note that the rightmost eigenvalues of (4.47) can be computed numerically using, e.g. [40]. The function $\boldsymbol{G}_K(\lambda)$ is given as

$$\boldsymbol{G}_K(\lambda) = \boldsymbol{A}_{\text{dec}} + \boldsymbol{A}_{\text{dist}}(K)e^{-\tau\lambda}. \tag{4.49}$$

The sensitivity of the rightmost eigenvalues of (4.46) is then given by the following Lemma.

Lemma 4.7.1 Consider an interconnected system (4.46) under Assumptions D1-D4. The sensitivity of the rightmost eigenvalue $\lambda_{\max}$ w.r.t. the structure of the distributed control, i.e. the communication topology is given by

$$\lambda'_{\max} = \frac{(v^*_{r_i} w_{r_j} + v^*_{r_j} w_{r_i})\ \mathrm{sign}(K)}{e^{\tau\lambda_{\max}} + K\tau(v^*_{r_i} w_{r_j} + v^*_{r_j} w_{r_i})} \tag{4.50}$$

where $\boldsymbol{v}_r, \boldsymbol{w}_r$ are the left and right eigenvector w.r.t. $\lambda_{\max}$.

Proof: See Appendix B.6. ∎

As can be observed from (4.50), the sensitivity of the rightmost eigenvalue depends on the distributed control gain K, time delay τ and also the elements of the eigenvectors corresponding to the rightmost eigenvalue $\lambda_{\max}$. When the rightmost eigenvalue is complex, only the movement along the real axis that needs to be considered. The communication link is then added according to the following proposition.

Proposition 4.7.2 Consider an interconnected system (4.46) under assumption D1-D4 with a constant time delay τ. The convergence rate of the overall system with distributed control law is maximized by adding a communication link between subsystem i and j which is the solution to

$$\begin{aligned} \underset{i,j}{\text{maximize}} \quad & |\lambda'_{\max}| \\ \text{subject to} \quad & \lambda'_{\max} < 0. \end{aligned}$$

Proof: Since we want to have the real part of the rightmost eigenvalue of (4.46) to be smaller than the one with the decentralized control law, it is required that $\lambda'_{\max} < 0$. Moreover, the movement of the real part of the perturbed rightmost eigenvalue has to be maximum in order to have the highest convergence rate of (4.46). ■

4.7.2 Sensitivity to Time Delay

Next the influence of time delay τ on the performance of the whole interconnected system for a given distributed control law with a certain communication topology is investigated. Using the eigenvalue sensitivity analysis, the sensitivity of the rightmost eigenvalue of (4.46) with respect to the time delay is then given by

Lemma 4.7.3 Consider an interconnected system (4.46) under Assumptions D1-D4 where the communication link is added between local controller of subsystem i and j. The sensitivity of the rightmost eigenvalue $\lambda_{\max}$ w.r.t. the time delay τ is given by

$$\lambda'_{\max} = -\frac{\lambda_{\max} K (v^*_{r_i} w_{r_j} + v^*_{r_j} w_{r_i})}{e^{\tau \lambda_{\max}} + K\tau (v^*_{r_i} w_{r_j} + v^*_{r_j} w_{r_i})} \tag{4.51}$$

where $\boldsymbol{v}_r, \boldsymbol{w}_r$ are the left and right eigenvector w.r.t. $\lambda_{\max}$.

Proof: See Appendix B.7. ■

Using (4.51), it can be investigated how the time delay influences the performance of the whole interconnected system for a given communication topology.

4.8 Evaluation

In this section we illustrate our results on the explicit solution of communication topology design using several numerical examples.

4.8.1 Single Communication Link

Consider three different interconnected systems consist of scalar subsystems with a star topology satisfying Assumptions A1-A5 as shown in Fig. 4.7. The dynamics of the whole

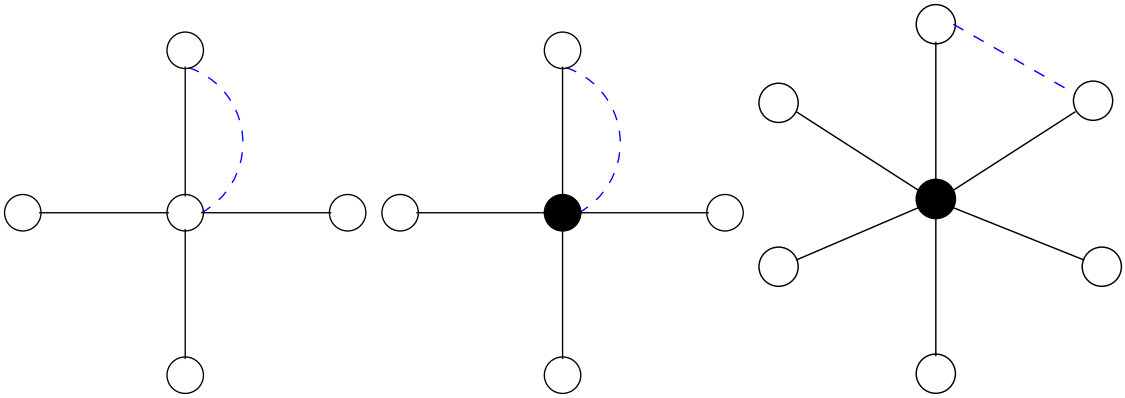

(a) Plant graph G_1 (b) Plant graph G_2 (c) Plant graph G_3

Figure 4.7: Plant graphs for interconnected system with star topology. The solid line represents the physical interconnection and the dashed line represents the communication link.

interconnected system for each topology is given by

$$\boldsymbol{A}_{\mathcal{G}_1} = \begin{bmatrix} -18 & 2 & 2 & 2 & 2 \\ 2 & -18 & 0 & 0 & 0 \\ 2 & 0 & -18 & 0 & 0 \\ 2 & 0 & 0 & -18 & 0 \\ 2 & 0 & 0 & 0 & -18 \end{bmatrix}, \boldsymbol{A}_{\mathcal{G}_2} = \begin{bmatrix} -20 & 2 & 2 & 2 & 2 \\ 2 & -18 & 0 & 0 & 0 \\ 2 & 0 & -18 & 0 & 0 \\ 2 & 0 & 0 & -18 & 0 \\ 2 & 0 & 0 & 0 & -18 \end{bmatrix},$$

$$\boldsymbol{A}_{\mathcal{G}_3} = \begin{bmatrix} -30 & 2 & 2 & 2 & 2 & 2 & 2 \\ 2 & -18 & 0 & 0 & 0 & 0 & 0 \\ 2 & 0 & -18 & 0 & 0 & 0 & 0 \\ 2 & 0 & 0 & -18 & 0 & 0 & 0 \\ 2 & 0 & 0 & 0 & -18 & 0 & 0 \\ 2 & 0 & 0 & 0 & 0 & -18 & 0 \\ 2 & 0 & 0 & 0 & 0 & 0 & -18 \end{bmatrix}.$$

Furthermore, it is assumed that $c = 1, \gamma_{ij} = 1$ and the distributed control gain is equal to -1 for the three cases. Using the results in Proposition 4.3.3 and Corollary 4.3.5, the communication topology can be computed as illustrated in Fig. 4.7. The rightmost eigenvalue with the distributed control law are given by $\lambda_{\max}(\bar{\boldsymbol{A}}_{\mathcal{G}_1}) = -14.3944$, $\lambda_{\max}(\bar{\boldsymbol{A}}_{\mathcal{G}_2}) = -15.2583$ and $\lambda_{\max}(\bar{\boldsymbol{A}}_{\mathcal{G}_3}) = -16.4601$.

4.8.2 Multiple Communication Links

Next, consider an interconnected system with 20 interacting scalar subsystems with a ring physical topology satisfying Assumptions A1-A5 where $g = -11, a = -15$, $b = 5$ and the distributed control gain $K = -2$. Since $|g| < |a|$ and from Proposition 4.3.2 and Lemma 4.5.3, it can be concluded that v_{r_i} is a convex function of the number of subsystem i as illustrated in Fig. 4.8(a). The optimal communication topology is the solution of optimization problem (4.16). By observing the elements of eigenvector v_{r_i}

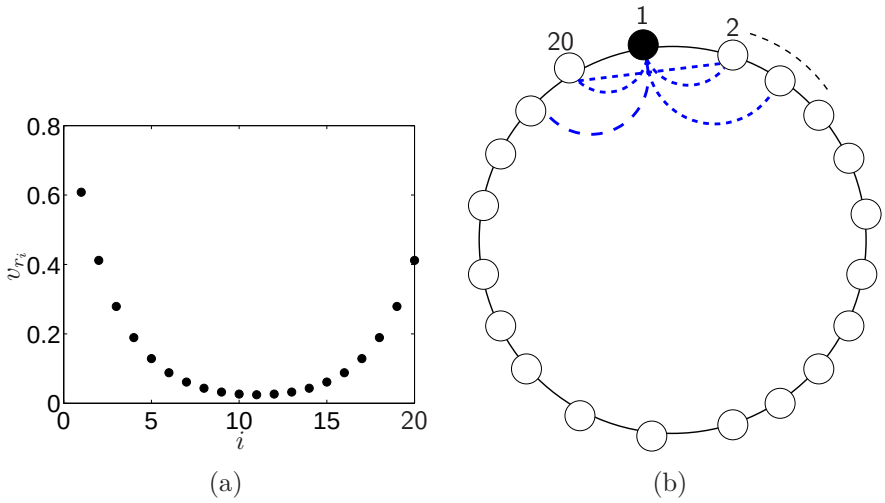

Figure 4.8: (a) The elements of eigenvector corresponding to the largest eigenvalue for interconnected system with ring topology with $N = 20$; (b) The optimal communication topology for number of links equal to 5. The solid line represents the physical interconnection and the dashed line represents the communication link.

shown in Fig. 4.8(a), the optimal communication topology can be computed efficiently. For example, when $\gamma_{ij} = 1$, $c = 5$, the communication topology is depicted in Fig. 4.8(b) which results in $\lambda_{\max}(\bar{\boldsymbol{A}}) = -5.1264$.

4.9 Summary and Discussion

This chapter presents for the first time explicit solutions of communication topology design for distributed control of interconnected systems with special class of physical interconnection topology, namely ring, star and line structure. The innovative approach is mainly based on eigenvalue sensitivity analysis. First, explicit solutions of a single communication link are derived for interconnected system consists of identical scalar subsystems. As can be observed, for the class of systems considered in this chapter with homogeneous subsystems and a single link case, the ring structure results in a communication topology with the highest cost w.r.t. the distance between the controllers. Furthermore, it is investigated how heterogeneity of the subsystems influences the communication topology. It turns out that for the heterogeneous interconnected subsystems with star topology, the number of subsystems also plays a role in the resulting topology, in addition to the local dynamics and the strength of physical interconnection. The results are then extended for the case of interconnected system with non-scalar subsystems by investigating the class of non-scalar subsystems which can be reduced to the scalar case and also for multiple communication links. It is also demonstrated that it is possible to extend the results into more complex physical interconnection topology, which is composed of the ring, star and line networks and where the interconnection is sparse using the idea described in Section 4.6. For a more general physical topology, i.e. topology which cannot be decomposed into ring, star, line, it is difficult to obtain a closed-form on the communication topology. However, the eigen-

value sensitivity analysis can still be used in order to reduce the number of combinations that has to be computed by looking at the sign of the elements of the eigenvector with respect to the largest eigenvalue. Finally, the eigenvalue sensitivity analysis is applied to distributed control with time delay in order to investigate the influence of the communication topology and time delay on the performance of the distributed control. The explicit solutions and new insights on communication topology design introduced in this chapter can be applied to a variety of interconnection systems such as power grid. One of the examples is that the insights on topology design in this chapter can be used to design the physical interconnection structure of the power grid. As shown in this chapter, in order to achieve an optimal performance, choosing a ring structure results in a higher communication cost compared to line and star topologies and will be less robust to time delay, under assumption that the value of time delay is proportional to the distance between the subsystems. Note that it is also possible to utilize the idea of eigenvalue sensitivity analysis in order to investigate the robustness of the physical structure of the interconnected system assuming that the subsystem or the physical interconnection is perturbed by a certain disturbance. This may also serve as a guidance in designing robust physical topology for the interconnected system, given the number of subsystems and the heterogeneity of the subsystems local dynamics.

However, the eigenvalue sensitivity based approach utilized in this chapter also suffers from some disadvantages. The results obtained in this chapter rely on the assumption that the physical interconnection are symmetric. On the other hand, in reality this assumption may not always be satisfied by the interconnected systems. The breaking of symmetry of the physical interconnection results in complex eigenvalues which makes the prediction of their movement become more complicated and challenging, thus limits the use of eigenvalue sensitivity analysis. Furthermore, the results for multiple communication links are also derived by assuming that the distributed control gain are equal for all communication links, which is quite a strong assumption. These lead to the following problems which require further investigations in the future:

- Explicit solutions for the case of interconnected system with non-symmetric physical interconnection.
- Extension of eigenvalue sensitivity analysis in order to deal with distributed control consists of non-identical control gains.
- Explicit solutions of communication topology design for communication links with time delay.
- Insights for interconnected system consists of more heterogeneous local dynamics.
- Investigation on the wider class of non-scalar subsystems whose analysis can be reduced to the scalar case.

5 Distributed Control Design under Limited Model Information

The design of distributed control in most literature, including the results presented in Chapters 3 and 4 is performed in a centralized manner. In other words, system-wide information needs to be collected in a central computer in order to compute the control law, even though the control law is implemented in a distributed fashion. However, this is not a realistic case and is difficult to be implemented in real world applications, for example in the case of power system whose transmission and distribution networks have numerous and geographically dispersed distributed generations. Another reason is due to the privacy reasons in which the subsystems may not wish to provide their complete description to the designer. The authors in [43, 44] present a framework for studying control design under limited plant model information, and investigate the connection between the control performance achieved by a design method and the amount of plant model information available to it. Furthermore, the authors in [15] propose a distributed design of distributed control. However, the subsystems are assumed to be identical and not physically coupled. The authors in [116] propose an optimization-based distributed control design which can be solved in a distributed manner. However, the communication topology in the known literature mentioned previously is assumed to be fixed and given a priori.

The major innovation in this chapter is to develop a novel coordination algorithm in order to design distributed control for interconnected systems under limited plant model information. Specifically, it is assumed that each subsystem only has the information about its physical neighbors local dynamics and the interconnection between them in addition to its own local dynamics. The objective is to design the distributed control law together with the communication topology under the limited model information such that the performance of the overall system, which is the linear quadratic cost, is improved and the stability is guaranteed under permanent communication link failures. The innovative strategy is to distribute the control design among the subsystems. The proposed strategy can be summarized as follows. First, sufficient condition in order to decompose the global cost function into the sum of local cost functions is derived. Each subsystem is then assigned a local cost function and based on the limited plant model information available to it, the optimization problem is solved by coordinating with the neighboring subsystems. Furthermore, the novel two-layer control architecture developed in Chapter 3 is adopted to guarantee the stability of the overall system under permanent communication link failures.

The remainder of this chapter is organized as follows. After formulating the problem in Section 5.1, the proposed novel algorithm for designing the distributed control gain and the communication topology by using limited plant model information is described in Section 5.2. Furthermore, the complexity of the approach is compared to the centralized design proposed in Chapter 3. The proposed approach is finally illustrated through a numerical example in Section 5.3.

5.1 Problem Formulation

Consider an interconnected system of N heterogeneous linear time invariant (LTI) subsystems described by the following differential equations

$$\dot{\boldsymbol{x}}_i = \boldsymbol{A}_i\boldsymbol{x}_i + \sum_{j\in\mathcal{N}_i} \boldsymbol{A}_{ij}\boldsymbol{x}_j + \boldsymbol{B}_i\boldsymbol{u}_i, \quad \boldsymbol{x}_i(t_0) = \boldsymbol{x}_0^i \tag{5.1}$$

where $i = 1, 2, ..., N$ denotes the $i-$th subsystem, $\boldsymbol{x}_i \in \mathbb{R}^n$, $\boldsymbol{u}_i \in \mathbb{R}^p$ are the state of subsystem i and the control input to subsystem i, and $\boldsymbol{A}_i, \boldsymbol{A}_{ij} \in \mathbb{R}^{n\times n}$, $\boldsymbol{B}_i \in \mathbb{R}^{n\times p}$. The term $\sum_{j\in\mathcal{N}_i} \boldsymbol{A}_{ij}\boldsymbol{x}_j$ represents the physical interconnection between the subsystems where $\mathcal{N}_i$ is the set of subsystems to which subsystem i is physically connected. Additionally, we consider a state feedback control for which the control law can be written as

$$\boldsymbol{u}_i = \boldsymbol{K}_i\boldsymbol{x}_i + \sum_{j\in\mathcal{G}_i} \boldsymbol{K}_{ij}\boldsymbol{x}_j \tag{5.2}$$

where $\mathcal{G}_i$ represents a set of subsystems to which controller i can exchange information with via the communication network.

The overall dynamics of the interconnected system can then be written as

$$\dot{\boldsymbol{x}} = \boldsymbol{A}\boldsymbol{x} + \boldsymbol{B}\boldsymbol{u}, \quad \boldsymbol{x}(t_0) = \boldsymbol{x}_0 \tag{5.3}$$

where $\boldsymbol{x} = [\boldsymbol{x}_1, \boldsymbol{x}_2, \cdots, \boldsymbol{x}_N]^T$, $\boldsymbol{u} = [\boldsymbol{u}_1, \boldsymbol{u}_2, \cdots, \boldsymbol{u}_N]^T$ and

$$\boldsymbol{A} = \begin{bmatrix} \boldsymbol{A}_1 & \boldsymbol{A}_{12} & \cdots & \boldsymbol{A}_{1N} \\ \boldsymbol{A}_{21} & \boldsymbol{A}_2 & \cdots & \boldsymbol{A}_{2N} \\ \vdots & \vdots & \ddots & \vdots \\ \boldsymbol{A}_{N1} & \boldsymbol{A}_{N2} & \cdots & \boldsymbol{A}_N \end{bmatrix} \in \mathbb{R}^{nN\times nN}, \boldsymbol{B} = \begin{bmatrix} \boldsymbol{B}_1 & 0 & \cdots & 0 \\ 0 & \boldsymbol{B}_2 & \cdots & 0 \\ \vdots & \vdots & \ddots & \vdots \\ 0 & 0 & \cdots & \boldsymbol{B}_N \end{bmatrix} \in \mathbb{R}^{nN\times pN}.$$

In this chapter, an linear quadratic regulator (LQR) problem is considered for the interconnected system (5.3) with cost function given by

$$J(\boldsymbol{u}, \boldsymbol{x}_0) = \int_0^\infty \left(\boldsymbol{x}^T\boldsymbol{Q}\boldsymbol{x} + \boldsymbol{u}^T\boldsymbol{R}\boldsymbol{u}\right) dt \tag{5.4}$$

where $\boldsymbol{x}_0$ is the initial state, $\boldsymbol{Q} > 0$, $\boldsymbol{R} > 0$ are the weighting matrices with appropriate dimensions and given by

$$\boldsymbol{Q} = \begin{bmatrix} \boldsymbol{Q}_{11} & \boldsymbol{Q}_{12} & \cdots & \boldsymbol{Q}_{1N} \\ \boldsymbol{Q}_{21} & \boldsymbol{Q}_{22} & \cdots & \boldsymbol{Q}_{2N} \\ \vdots & \vdots & \ddots & \vdots \\ \boldsymbol{Q}_{N1} & \boldsymbol{Q}_{N2} & \cdots & \boldsymbol{Q}_{NN} \end{bmatrix}, \quad \boldsymbol{R} = \begin{bmatrix} \boldsymbol{R}_{11} & 0 & \cdots & 0 \\ 0 & \boldsymbol{R}_{22} & \cdots & 0 \\ \vdots & \vdots & \ddots & \vdots \\ 0 & 0 & \cdots & \boldsymbol{R}_{NN} \end{bmatrix}.$$

Similar to Chapter 3, the communication topology, that is $\mathcal{G}_i, \forall i$ of the distributed control law (5.2) is also a design parameter and the number of communication links that can be

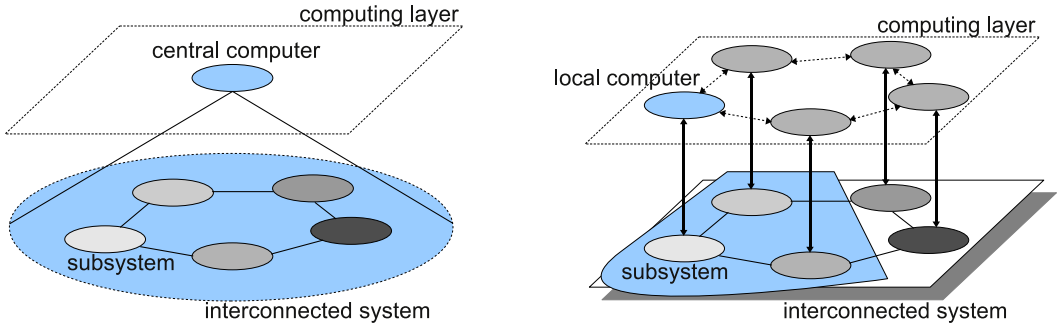

Figure 5.1: (a) Centralized design method where a central computer collects the information of the whole interconnected system and compute the distributed control law based on the information gathered; (b) Proposed distributed design method where the design is performed in each subsystem's local computer by coordinating with its neighbors' local computer. Each local computer only has limited model information on the plant, i.e. its own local dynamics, its neighbors' local dynamics and the interconnection between them.

added is limited by an upper bound induced by the communication constraint

$$\sum_{1\leq i\leq j\leq N} \gamma_{ij} d_{ij} \leq c \tag{5.5}$$

where $d_{ij} \in \{0, 1\}$, $c > 0$ is the total cost constraint on the communication network, and γ_{ij} represents a cost to establish a link between the local controllers of subsystems i and j.

Therefore, by adopting the results in Chapter 3, the distributed control design together with the communication topology can be formulated as the following optimization problem:

$$\begin{aligned} \underset{\boldsymbol{K}_i, \boldsymbol{K}_{ij}, d_{ij}}{\text{minimize}} \quad & J \\ \text{subject to} \quad & \dot{\boldsymbol{x}} = \boldsymbol{A}\boldsymbol{x} + \boldsymbol{B}\boldsymbol{u}, \quad \boldsymbol{x}(t_0) = \boldsymbol{x}_0, \\ & \sum_{1\leq i\leq j\leq N} \gamma_{ij} d_{ij} \leq c, \\ & d_{ij} \in \{0, 1\}. \end{aligned} \tag{5.6}$$

The optimization problem (5.6) is a mixed integer optimization problem since it is solved with respect to both the feedback gain and the communication topology of the distributed control. It should be noted that the optimization problem (5.6) is solved in a centralized fashion, i.e. the global knowledge of the interconnected system is required, see Fig. 5.1(a). However, in real world applications, it is either very hard to obtain the complete model of the interconnected system or the designer does not have access to full model of the systems. The reasons are either because the full plant model is simply not available or the subsystems may not wish to provide their complete description to the designer. In addition, computing the distributed control law in a centralized manner results in that the designer needs to completely recompute the control laws when the model parameters

change or if new subsystems are introduced into the interconnected system.

In this chapter, a method in order to jointly design the control gain together with the communication topology in a distributed fashion is proposed. Instead of computing the distributed control law in a central computer, the computation is distributed among the local controllers in each subsystem, see Fig. 5.1(b). Each local computer only has partial or limited model information of the overall interconnected system. Specifically, it is assumed that each subsystem has the information on the local dynamics of its physical neighbors and also the interconnection matrix between its neighbors in addition to its own local dynamics. In other words, the subsystem i has the following extended dynamics

$$\dot{\hat{\boldsymbol{x}}}_i = \hat{\boldsymbol{A}}_i \hat{\boldsymbol{x}}_i + \hat{\boldsymbol{B}}_i \hat{\boldsymbol{u}}_i, \quad \hat{\boldsymbol{x}}_i(t_0) = \hat{\boldsymbol{x}}_0^i \tag{5.7}$$

where $\hat{\boldsymbol{x}}_i = [\boldsymbol{x}_i, \cdots, \boldsymbol{x}_k]^T$, $\hat{\boldsymbol{u}}_i = [\boldsymbol{u}_i, \cdots, \boldsymbol{u}_k]^T$, $k \in \mathcal{N}_i$. The matrix $\hat{\boldsymbol{A}}_i \in \mathbb{R}^{n(|\mathcal{N}_i|+1)\times n(|\mathcal{N}_i|+1)}$ and $\hat{\boldsymbol{B}}_i \in \mathbb{R}^{n(|\mathcal{N}_i|+1)\times p(|\mathcal{N}_i|+1)}$ in (5.7) is obtained from (5.3).

Example 2 The limited model information of each subsystem from interconnected system depicted in Fig. 5.2 is shown in Fig. 5.3. The extended dynamics of subsystem 1 can then be written as

$$\dot{\hat{\boldsymbol{x}}}_1 = \begin{bmatrix} \boldsymbol{A}_1 & \boldsymbol{A}_{12} & \boldsymbol{A}_{14} & \boldsymbol{A}_{15} \\ \boldsymbol{A}_{21} & \boldsymbol{A}_2 & \boldsymbol{O}_n & \boldsymbol{A}_{25} \\ \boldsymbol{A}_{41} & \boldsymbol{O}_n & \boldsymbol{A}_4 & \boldsymbol{O}_n \\ \boldsymbol{A}_{51} & \boldsymbol{A}_{52} & \boldsymbol{O}_n & \boldsymbol{A}_5 \end{bmatrix} \hat{\boldsymbol{x}}_1 + \begin{bmatrix} \boldsymbol{B}_1 & 0 & 0 & 0 \\ 0 & \boldsymbol{B}_2 & 0 & 0 \\ 0 & 0 & \boldsymbol{B}_4 & 0 \\ 0 & 0 & 0 & \boldsymbol{B}_5 \end{bmatrix} \hat{\boldsymbol{u}}_1$$

where $\hat{\boldsymbol{x}}_1 = [\boldsymbol{x}_1, \boldsymbol{x}_2, \boldsymbol{x}_4, \boldsymbol{x}_5]^T$. It can be observed from the example above that subsystem 1 does not have the complete model information of its neighbors, i.e. subsystems 2, 4 and 5.

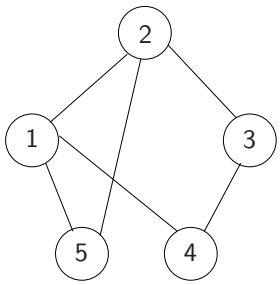

Figure 5.2: Example of physical interconnected system.

Furthermore, for each subsystem with extended dynamics described in (5.7), a local cost function $\hat{J}_i$ is assigned given as follows.

$$\hat{J}_i(\hat{\boldsymbol{u}}, \hat{\boldsymbol{x}}_0) = \int_0^\infty \left(\hat{\boldsymbol{x}}_i^T \hat{\boldsymbol{Q}}_i \hat{\boldsymbol{x}}_i + \hat{\boldsymbol{u}}_i^T \hat{\boldsymbol{R}}_i \hat{\boldsymbol{u}}_i \right) dt \tag{5.8}$$

where $\hat{\boldsymbol{Q}}_i, \hat{\boldsymbol{R}}_i$ are the corresponding weighting matrices with appropriate dimensions. Note that for the remainder of this chapter, the notation ($\hat{}$) is used to refer to the local subproblem solved by the corresponding subsystem.

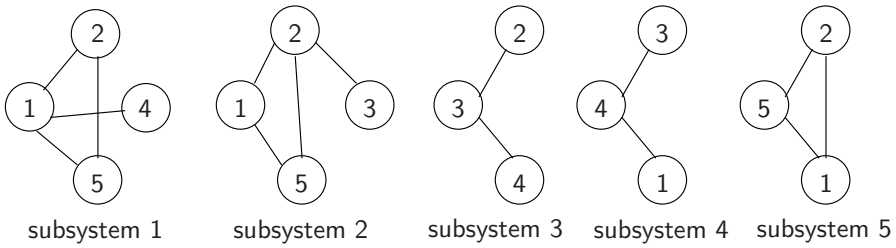

Figure 5.3: Limited model information for each subsystem in interconnected system shown Fig. 5.2. Each subsystem has the knowledge of its physical neighbors' local dynamics and the interconnection between them.

The objective of this chapter is to develop an algorithm in order to design the distributed control law (5.2), including the communication topology by using the limited model information (5.7) and local cost function (5.8) such that:

- the overall system performance is improved, that is the cost function (5.4) is minimized and the stability of the whole system (5.3) is guaranteed,
- the stability of the interconnected system under permanent communication link failures is guaranteed.

Remark 13 The choice of quadratic infinite horizon cost (5.4) as a performance metric results in several advantages compared to the decay rate of the system as used in the previous chapters. First, as will be shown in the next section, it is possible to decompose the global optimization problem into N local optimization problem which can be solved by each subsystem in a distributed manner. Another advantage is that the quadratic infinite horizon cost also considers input costs into the optimization which is not the case for the decay rate.

5.2 Proposed Distributed Algorithms

In this section, we propose a method to design the distributed control, i.e. the control gain and the communication topology by using only the limited model information in each subsystem, instead of designing the distributed control in a centralized fashion. First, in order to guarantee the stability of the interconnected system in the presence of permanent communication link failures, a two-layer control architecture proposed in Chapter 3 is adopted. Next, the algorithm to solve the optimization problem (5.6) in a distributed fashion using only the limited model information in each subsystem is described. Briefly speaking, the design procedure consists of three steps as illustrated in Fig. 5.4. First, sufficient condition that enables to decompose the global cost function (5.6) into the summation of N local cost functions (5.8) is derived. The optimization problem is then solved independently for each local cost function by every subsystem. Finally, the optimal solution of each local optimization problem is aggregated to obtain the global solution.

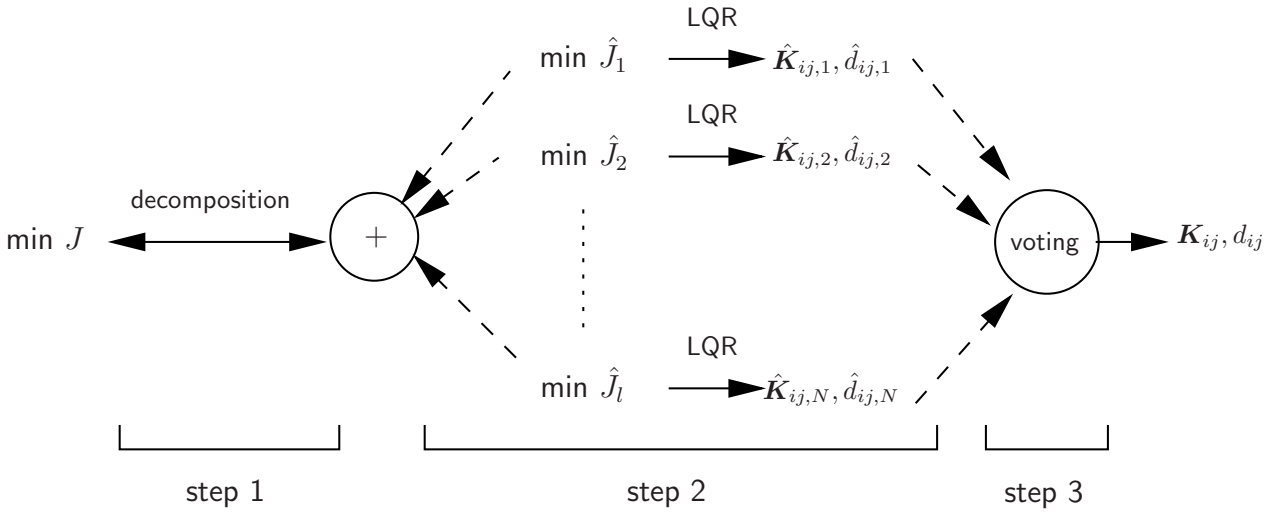

Figure 5.4: Proposed distributed design method. First, the global cost function is decomposed into the summation of local cost functions. The optimization is then solved for each local cost function. Finally, a voting is conducted to obtain a global solution from the solution of the local optimization problems.

5.2.1 Two-layer Control Architecture

In order to guarantee the stability of the interconnected system in the presence of permanent communication link failures, a two-layer control architecture proposed in Chapter 3 is adopted. First, a decentralized control law is designed that guarantees the stability of the interconnected system (5.3) by using, e.g. the method in [71] with the control input given by

$$\bar{\boldsymbol{u}}_i = \boldsymbol{K}_i \boldsymbol{x}_i. \tag{5.9}$$

Remark 14 Similar to Chapter 3, it is assumed that all the decentralized fixed modes (DFM), if any, are in the open left half plane.

The performance is then improved by designing a distributed control law, i.e. the second term of (5.2). The optimization problem (5.6) is then reduced to

$$\begin{aligned} \underset{\boldsymbol{K}_{ij}, d_{ij}}{\text{minimize}} \quad & J \\ \text{subject to} \quad & \dot{\boldsymbol{x}} = \boldsymbol{A}\boldsymbol{x} + \boldsymbol{B}\boldsymbol{u}, \quad \boldsymbol{x}(t_0) = \boldsymbol{x}_0, \\ & \sum_{1 \le i \le j \le N} \gamma_{ij} d_{ij} \le c, \\ & d_{ij} \in \{0, 1\}. \end{aligned} \tag{5.10}$$

Remark 15 Since the first term of (5.2) is designed in advanced and will be fixed in the design of the communication topology, the optimality of the solution from the distributed design approach may be degraded. However, as shown later in this chapter, this will guarantee the stability of the overall system in the presence of permanent communication link failures.

In the following, an algorithm is proposed to solve the optimization problem (5.6) in a distributed manner as illustrated in Fig. 5.4. We first give a sufficient condition that decomposes the global cost function in (5.6) into N local cost functions (5.8).

5.2.2 Cost Function Decomposition

In the distributed design setting, each subsystem needs to solve its own subproblem. We define subproblem i of subsystem i consists of the extended dynamics (5.7) and local cost function (5.8). Before proceeding, let us introduce the following definition in order to express the relation between the non-sparsity structure of two matrices.

Given a matrix $\boldsymbol{Y} \in \mathbb{R}^{m\times n}$ which may be written in term of its columns as $\boldsymbol{Y} = [\boldsymbol{y}_1 \cdots \boldsymbol{y}_n]$ and associated with a vector $\text{vec}(\boldsymbol{Y}) \in \mathbb{R}^{nm\times 1}$ defined by

$$\text{vec}(\boldsymbol{Y}) = \begin{bmatrix} \boldsymbol{y}_1 \\ \vdots \\ \boldsymbol{y}_n \end{bmatrix}.$$

The l_0 norm of a vector is defined as $\|\boldsymbol{x}\|_{l_0} = |\{i : x_i \neq 0\}|$ and counts the non-zero entries in $\boldsymbol{x}$. Thus, for any $m \times n$ matrices $\boldsymbol{X} = [\boldsymbol{X}_{ij}]$ and $\boldsymbol{Y} = [\boldsymbol{Y}_{ij}]$, the non-sparsity structure of $\boldsymbol{X}$ is the subset of that of $\boldsymbol{Y}$ iff $\|\text{vec}(\boldsymbol{X}_{ij})\|_{l_0} = 0$ whenever $\|\text{vec}(\boldsymbol{Y}_{ij})\|_{l_0} = 0$.

Example 3 The non-sparsity structure of matrix $\boldsymbol{X}_1$ below is the subset of that of $\boldsymbol{X}_2$

$$\boldsymbol{X}_1 = \begin{bmatrix} -18 & 1 & 0 & 2 & 0 \\ 1 & -10 & 0 & 0 & 0 \\ 0 & 0 & -12 & 0 & 0 \\ 2 & 0 & 0 & -6 & 0 \\ 0 & 0 & 0 & 0 & -8 \end{bmatrix}, \quad \boldsymbol{X}_2 = \begin{bmatrix} -10 & 2 & 4 & 2 & 3 \\ 2 & -18 & 0 & 0 & 0 \\ 4 & 0 & -6 & 0 & 0 \\ 2 & 0 & 0 & -14 & 0 \\ 3 & 0 & 0 & 0 & -20 \end{bmatrix}.$$

Furthermore, the following assumption is considered.

Assumption 1 The non-sparsity structure of the weighting matrix $\boldsymbol{Q}$ in (5.4) is the subset of that of the physical interconnection, that is the non-sparsity structure of the matrix $\boldsymbol{A}$ in (5.3).

Next, we introduce the following Lemma.

Lemma 5.2.1 Consider an interconnected system whose dynamics given by (5.1). Under Assumption 1, the global cost (5.4) can be decomposed into N local cost (5.8) given by

$$J = \sum_{i=1}^{N} \hat{J}_i \tag{5.11}$$

where the weighting matrices $\hat{\boldsymbol{Q}}_i, \hat{\boldsymbol{R}}_i$ are given by

$$\hat{\boldsymbol{Q}}_i = \begin{bmatrix} \frac{1}{d_i+1}\boldsymbol{Q}_{ii} & \frac{1}{2}\boldsymbol{Q}_{ij} & \cdots & \frac{1}{2}\boldsymbol{Q}_{ik} \\ \frac{1}{2}\boldsymbol{Q}_{ji} & \frac{1}{d_j+1}\boldsymbol{Q}_{jj} & \cdots & \frac{1}{2}\boldsymbol{Q}_{jk} \\ \vdots & \vdots & \ddots & \vdots \\ \frac{1}{2}\boldsymbol{Q}_{ki} & \frac{1}{2}\boldsymbol{Q}_{kj} & \cdots & \frac{1}{d_k+1}\boldsymbol{Q}_{kk} \end{bmatrix}, \hat{\boldsymbol{R}}_i = \begin{bmatrix} \frac{1}{d_i+1}\boldsymbol{R}_{ii} & 0 & \cdots & 0 \\ 0 & \frac{1}{d_j+1}\boldsymbol{R}_{jj} & \cdots & 0 \\ \vdots & \vdots & \ddots & \vdots \\ 0 & 0 & \cdots & \frac{1}{d_k+1}\boldsymbol{R}_{kk} \end{bmatrix}$$

where $j, k \in \mathcal{N}_i$ and $d_i = |\mathcal{N}_i|$.

Proof: For the sake of clarity, first the global cost function J in (5.4) is separated into two parts, namely J_Q and J_R defined as

$$\begin{aligned} J &= \int_0^\infty (\boldsymbol{x}^T \boldsymbol{Q} \boldsymbol{x}) dt + \int_0^\infty (\boldsymbol{u}^T \boldsymbol{R} \boldsymbol{u}) dt, \\ &= J_Q + J_R. \end{aligned}$$

Let $\boldsymbol{Ad}$ be the adjacency matrix of the interconnected system (5.3) and $\boldsymbol{Ad}_{ij} \in \mathbb{R}$ be its i, j element. Then $\boldsymbol{Ad}_{ii} = 0, \forall i = 1, \cdots, N$, $\boldsymbol{Ad}_{ij} = 0$ if $\boldsymbol{A}_{ij} = \boldsymbol{O}_n$ and $\boldsymbol{Ad}_{ij} = 1$ otherwise. Moreover, define the matrix $\boldsymbol{H}$ as $\boldsymbol{H} = \boldsymbol{I}_N + \boldsymbol{Ad}$ where $h_{ij} \in \mathbb{R}$ is its i, j element. The former part J_Q can then be written as

$$\begin{aligned} J_Q &= \int_0^\infty \left(\boldsymbol{x}^T \begin{bmatrix} \boldsymbol{Q}_{11} h_{11} & \boldsymbol{Q}_{12} h_{12} & \cdots & \boldsymbol{Q}_{1N} h_{1N} \\ \boldsymbol{Q}_{21} h_{21} & \boldsymbol{Q}_{22} h_{22} & \cdots & \boldsymbol{Q}_{2N} h_{2N} \\ \vdots & \vdots & \ddots & \vdots \\ \boldsymbol{Q}_{N1} h_{N1} & \boldsymbol{Q}_{N2} h_{N2} & \cdots & \boldsymbol{Q}_{NN} h_{NN} \end{bmatrix} \boldsymbol{x} \right) dt \\ &= \int_0^\infty \left(\sum_{i=1}^N \boldsymbol{x}_i^T \boldsymbol{Q}_{ii} h_{ii} \boldsymbol{x}_i + \sum_{i=1}^N \sum_{j \neq i}^N (\boldsymbol{x}_i^T \boldsymbol{Q}_{ij} h_{ij} \boldsymbol{x}_j) \right) dt \\ &= \int_0^\infty \left(\sum_{i=1}^N \boldsymbol{x}_i^T \boldsymbol{Q}_{ii} \boldsymbol{x}_i + \sum_{i=1}^N \sum_{j \in \mathcal{N}_i} (\boldsymbol{x}_i^T \boldsymbol{Q}_{ij} \boldsymbol{x}_j) \right) dt \\ &= \int_0^\infty \sum_{i=1}^N \left((d_i + 1) \boldsymbol{x}_i^T \frac{1}{d_i + 1} \boldsymbol{Q}_{ii} \boldsymbol{x}_i + \sum_{j \in \mathcal{N}_i} 2 (\boldsymbol{x}_i^T \frac{1}{2} \boldsymbol{Q}_{ij} \boldsymbol{x}_j) \right) dt. \end{aligned}$$

Since the term $\boldsymbol{Q}_{ij}$ is only shared by subsystem i and j and the term $\boldsymbol{Q}_{ii}$ can be found only in the subproblems which consists of the neighbors of subsystem i, the global cost can then be written as

$$\begin{aligned} J_Q = \int_0^\infty \Bigg(& \underbrace{\hat{\boldsymbol{x}}_1^T \begin{bmatrix} \frac{1}{d_1+1} \boldsymbol{Q}_{11} & \frac{1}{2} \boldsymbol{Q}_{1i} & \cdots & \frac{1}{2} \boldsymbol{Q}_{ik} \\ \frac{1}{2} \boldsymbol{Q}_{i1} & \frac{1}{d_i+1} \boldsymbol{Q}_{ii} & \cdots & 0 \\ \vdots & \vdots & \ddots & \vdots \\ \frac{1}{2} \boldsymbol{Q}_{k1} & 0 & \cdots & \frac{1}{d_k+1} \boldsymbol{Q}_{kk} \end{bmatrix} \hat{\boldsymbol{x}}_1}_{\text{subproblem 1 where } i,k \in \mathcal{N}_1} + \\ & + \cdots + \underbrace{\hat{\boldsymbol{x}}_N^T \begin{bmatrix} \frac{1}{d_N+1} \boldsymbol{Q}_{NN} & \frac{1}{2} \boldsymbol{Q}_{Nj} & \cdots & \frac{1}{2} \boldsymbol{Q}_{Nm} \\ \frac{1}{2} \boldsymbol{Q}_{jN} & \frac{1}{d_j+1} \boldsymbol{Q}_{jj} & \cdots & 0 \\ \vdots & \vdots & \ddots & \vdots \\ \frac{1}{2} \boldsymbol{Q}_{mN} & 0 & \cdots & \frac{1}{d_m+1} \boldsymbol{Q}_{mm} \end{bmatrix} \hat{\boldsymbol{x}}_N}_{\text{subproblem } N \text{ where } j,m \in \mathcal{N}_N} \Bigg) dt. \end{aligned}$$

Therefore, J_Q can be written as

$$J_Q = \sum_{i=1}^{N} \int_0^\infty (\hat{\boldsymbol{x}}_i^T \hat{\boldsymbol{Q}}_i \hat{\boldsymbol{x}}_i) dt = \sum_{i=1}^{N} \hat{J}_{Q_i}.$$

A similar procedure can also be applied to J_R as follows.

$$\begin{aligned}
J_R &= \int_0^\infty \begin{bmatrix} \boldsymbol{u}_1 \\ \boldsymbol{u}_2 \\ \vdots \\ \boldsymbol{u}_N \end{bmatrix}^T \begin{bmatrix} \boldsymbol{R}_{11} & 0 & \cdots & 0 \\ 0 & \boldsymbol{R}_{22} & \cdots & 0 \\ \vdots & \vdots & \ddots & \vdots \\ 0 & 0 & \cdots & \boldsymbol{R}_{NN} \end{bmatrix} \begin{bmatrix} \boldsymbol{u}_1 \\ \boldsymbol{u}_2 \\ \vdots \\ \boldsymbol{u}_N \end{bmatrix} dt \\
&= \int_0^\infty (\sum_{i=1}^{N} \boldsymbol{u}_i^T \boldsymbol{R}_{ii} \boldsymbol{u}_i) dt \\
&= \int_0^\infty \sum_{i=1}^{N} \left((d_i+1) \boldsymbol{u}_i^T \frac{1}{d_i+1} \boldsymbol{R}_{ii} \boldsymbol{u}_i \right) dt \\
&= \int_0^\infty \Bigg(\underbrace{\hat{\boldsymbol{u}}_1^T \begin{bmatrix} \frac{1}{d_1+1}\boldsymbol{R}_{11} & 0 & \cdots & 0 \\ 0 & \frac{1}{d_i+1}\boldsymbol{R}_{ii} & \cdots & 0 \\ \vdots & \vdots & \ddots & \vdots \\ 0 & 0 & \cdots & \frac{1}{d_k+1}\boldsymbol{R}_{kk} \end{bmatrix} \hat{\boldsymbol{u}}_1}_{\text{subproblem 1 where } i,k \in \mathcal{N}_1} + \\
&\quad + \cdots + \underbrace{\hat{\boldsymbol{u}}_N^T \begin{bmatrix} \frac{1}{d_N+1}\boldsymbol{R}_{NN} & 0 & \cdots & 0 \\ 0 & \frac{1}{d_i+1}\boldsymbol{R}_{ii} & \cdots & 0 \\ \vdots & \vdots & \ddots & \vdots \\ 0 & 0 & \cdots & \frac{1}{d_m+1}\boldsymbol{R}_{mm} \end{bmatrix} \hat{\boldsymbol{u}}_N}_{\text{subproblem } N \text{ where } j,m \in \mathcal{N}_N} \Bigg) dt \\
&= \sum_{i=1}^{N} \int_0^\infty (\hat{\boldsymbol{u}}_i^T \hat{\boldsymbol{R}}_i \hat{\boldsymbol{u}}_i) dt, \\
&= \sum_{i=1}^{N} \hat{J}_{R_i}.
\end{aligned}$$

By combining both results together, we have

$$J = \sum_{i=1}^{N} \left(\hat{J}_{Q_i} + \hat{J}_{R_i} \right) = \sum_{i=1}^{N} \hat{J}_i.$$

This completes the proof. ∎

Remark 16 The decomposition in (5.11) does not guarantee that $\hat{\boldsymbol{Q}}_i$ is also positive definite. The positive definite of $\hat{\boldsymbol{Q}}_i$ can be guaranteed, for example by choosing $\boldsymbol{Q}$ as a

diagonal dominant matrix.

Under Lemma 5.2.1, the global optimization problem (5.10) can then be written as the summation of the local optimization subproblem given as follows.

$$\min \ J = \min \sum_{i=1}^{N} \ \hat{J}_i = \sum_{i=1}^{N} \min \ \hat{J}_i. \tag{5.12}$$

Subsystem i can then solve the optimization subproblem i independently which results in the optimization of the global problem (5.10), as can be observed from (5.12). Next, the performance is improved by designing jointly the distributed control gain and communication topology, i.e. $\boldsymbol{K}_{ij}$ and $\mathcal{G}_i$ of (5.2) by solving the local subproblem (5.8) under dynamics (5.7). For the remainder of the chapter, without loss of generality, it is assumed that $\gamma_{ij} = 1$, i.e. c is equal to the number of available communication links.

5.2.3 Distributed Control Design - Single Communication Link

For the sake of clarity, we first consider the case when only a single communication link is allowed to be added to the interconnected system, i.e. $c = 1$. Let us define $\mathcal{N}_m^+ = \{m \cup \mathcal{N}_m\}$. Due to the decomposition in (5.12), we can argue on the subproblem level which consists of subsystem and its neighbors. The optimization for subproblem $m = 1, \cdots, N$ (Step 2 in Fig. 5.4) can then be formulated as follows.

$$\begin{aligned}
\underset{\hat{\boldsymbol{K}}_{ij,m}, \hat{d}_{ij,m}}{\text{minimize}} \quad & \hat{J}_m \\
\text{subject to} \quad & \dot{\hat{\boldsymbol{x}}}_m = \hat{\boldsymbol{A}}_m \hat{\boldsymbol{x}}_m + \hat{\boldsymbol{B}}_m \hat{\boldsymbol{u}}_m, \quad \hat{\boldsymbol{x}}_m(t_0) = \hat{\boldsymbol{x}}_0^m, \\
& \hat{J}_m < \hat{J}_m^{\text{dec}}, \\
& \sum_{1 \le i \le j \le N_m} \hat{d}_{ij,m} \le 1, \\
& \hat{d}_{ij,m} \in \{0, 1\}, \\
& (i, j) \in \mathcal{N}_m^+
\end{aligned} \tag{5.13}$$

where $\hat{J}_m^{\text{dec}}$ is the cost of subproblem m with the decentralized control law and $\hat{\boldsymbol{K}}_{ij,m} \in \mathbb{R}^{p \times n}, \hat{d}_{ij,m}$ are the optimal control gain and communication link from subproblem m respectively. The optimal control law for the extended dynamics (5.7) is then given by

$$\hat{\boldsymbol{u}}_m = -\hat{\boldsymbol{R}}_m^{-1} \hat{\boldsymbol{B}}_m^T \hat{\boldsymbol{P}}_m \hat{\boldsymbol{x}}_m = \hat{\boldsymbol{K}}_m \hat{\boldsymbol{x}}_m \tag{5.14}$$

where $\hat{\boldsymbol{K}}_m \in \mathbb{R}^{(|\mathcal{N}_m^+|)p \times (|\mathcal{N}_m^+|)n}$ and $\hat{\boldsymbol{P}}_m$ is the solution of the following algebraic Riccati equation

$$\hat{\boldsymbol{A}}_m^T \hat{\boldsymbol{P}}_m + \hat{\boldsymbol{P}}_m \hat{\boldsymbol{A}}_m - \hat{\boldsymbol{P}}_m \hat{\boldsymbol{B}}_m \hat{\boldsymbol{R}}_m^{-1} \hat{\boldsymbol{B}}_m^T \hat{\boldsymbol{P}}_m + \hat{\boldsymbol{Q}}_m = 0. \tag{5.15}$$

The local cost with the distributed control law obtained from (5.13) is denoted by $\hat{J}_m^{\text{dist}}$ which can be computed as [103]

$$\hat{J}_m^{\text{dist}} = \hat{\boldsymbol{x}}_{0_m}^T \hat{\boldsymbol{P}}_m \hat{\boldsymbol{x}}_{0_m}. \tag{5.16}$$

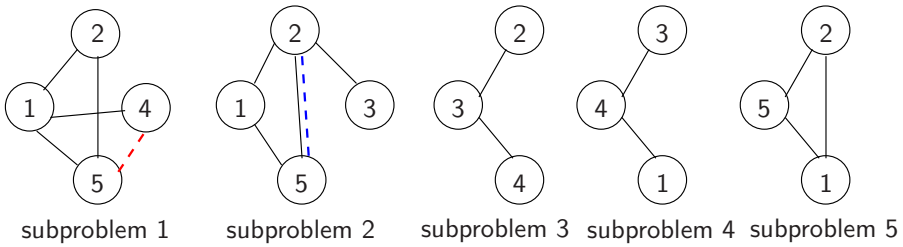

Figure 5.5: Examples of the optimal communication link resulted from the voting. The dashed line represents the optimal communication link. The first case is when the optimal link comes from subproblem 1 and the second case when it comes from subproblem 2.

After the optimal control gain and communication link in each subproblem is computed, the aggregation step, i.e. Step 3 in Fig. 5.4 is performed. A voting is employed among the subsystems in order to select which link has to be used for the global problem, i.e. d_{ij} in (5.10). Since the goal is to improve the performance, i.e. to have a minimum value of J, the voting elects the communication link among the subsystems that results in the smallest cost compared to the cost with the decentralized control law as formulated in the following

$$d_{ij} = \hat{d}_{ij,m^\star} = \arg\max_{\hat{d}_{ij,m}} (\hat{J}_m^{\text{dec}} - \hat{J}_m^{\text{dist}}(\hat{\boldsymbol{K}}_m)). \tag{5.17}$$

Remark 17 The voting can be performed in a distributed manner between the subsystems by using the existing distributed voting algorithm, e.g. [58] or flooding algorithm.

Remark 18 Since the optimal link for each subproblem $\hat{d}_{ij,m}$ can only take value in the set $\mathcal{N}_m^+$, the optimal link resulting from the distributed design, that is d_{ij} in (5.17) may differ from the one of the centralized design in (5.10). This may also result in an optimality loss compared to the centralized design.

After fixing the optimal communication link via a voting, the next step is to choose the optimal control gain obtained from the local optimization problem. Given the optimal link d_{ij} obtained from (5.17), which is the optimal link for subproblem $m^\star$, i.e. $d_{ij} = \hat{d}_{ij,m^\star}$, we first define the following notation.

$$\hat{\mathcal{N}}_{m^\star} = \{k | i, j \in \mathcal{N}_k^+, k \neq m^\star\}. \tag{5.18}$$

When $\hat{\mathcal{N}}_{m^\star} = \emptyset$, i.e. no other subsystems that have both subsystem i and j as their physical neighbors, the optimal gain $\boldsymbol{K}_{ij,m^\star}$ obtained from (5.13) is also the optimal gain for the global problem (5.6), i.e. $\hat{\boldsymbol{K}}_{ij} = \hat{\boldsymbol{K}}_{ij,m^\star}$ since

$$J = \hat{J}_1^{\text{dec}} + \cdots + \hat{J}_{m^\star}^{\text{dist}} + \cdots + \hat{J}_N^{\text{dec}} < \sum_m^N \hat{J}_m^{\text{dec}}. \tag{5.19}$$

Example 4 As shown in Fig. 5.5, when the optimal link for the global problem after the voting is d_{45}, which is the optimal link of subproblem 1, then $\boldsymbol{K}_{45} = \hat{\boldsymbol{K}}_{45,1}$ since $\hat{\mathcal{N}}_1 = \emptyset$.

However, when $\hat{\mathcal{N}}_{m^\star} \neq \emptyset$, the optimal gain $\hat{\boldsymbol{K}}_{ij,m^\star}$ which is the solution of (5.13), (5.17) cannot be directly used since it may destabilize the local interconnected systems in the other local subproblems which share those subsystems, i.e. subproblems $k \in \hat{\mathcal{N}}_{m^\star}$. In order to tackle this problem, the following approach is proposed. The idea is to use the optimal link resulting from the optimization problem (5.17) and then to recompute the optimal gain of the corresponding communication link, while taking into account the stability and performance of the subproblems $k \in \hat{\mathcal{N}}_{m^\star}$.

First, every subproblem $l \in \{m^\star \cup \hat{\mathcal{N}}_{m^\star}\}$ sets $\hat{d}_{ij,l} = d_{ij}, k \in \hat{\mathcal{N}}_i$ and solve the following optimization problem to recompute their optimal gain.

$$\begin{aligned} \underset{\hat{\boldsymbol{K}}_{ij,l}}{\text{minimize}} \quad & \hat{J}_l \\ \text{subject to} \quad & \dot{\hat{\boldsymbol{x}}}_l = \hat{\boldsymbol{A}}_l \hat{\boldsymbol{x}}_l + \hat{\boldsymbol{B}}_l \hat{\boldsymbol{u}}_l, \quad \hat{\boldsymbol{x}}_l(t_0) = \hat{\boldsymbol{x}}_{0,l}, \\ & \hat{J}_l < \hat{J}_l^{\text{dec}}, \forall l \in \{m^\star \cup \hat{\mathcal{N}}_{m^\star}\}. \end{aligned} \tag{5.20}$$

The last constraint guarantees that using the optimal gain $\hat{\boldsymbol{K}}_{ij,l}$ obtained from (5.20), the interconnected system (5.7) for every subproblem $l \in \{m^\star \cup \hat{\mathcal{N}}_{m^\star}\}$ is also stable and the performance is improved compared to the decentralized control law. However, this comes at a price of loosing some optimality for the resulting control gain. Next, the optimal gain computed by subproblems $l \in \{m^\star \cup \hat{\mathcal{N}}_{m^\star}\}$ are compared with each other to decide which gain results in the smallest cost according to

$$\boldsymbol{K}_{ij} = \arg\max_{\hat{\boldsymbol{K}}_{ij,l}} \sum_{l \in \{m^\star \cup \hat{\mathcal{N}}_{m^\star}\}} \left(\hat{J}_l^{\text{dec}} - \hat{J}_l^{\text{dist}}(\hat{\boldsymbol{K}}_l) \right). \tag{5.21}$$

The detail of the proposed approach is shown in Algorithm 1.

Algorithm 1 Joint control gain-communication topology design-single link case

Step 1: Decompose the global cost function into N local cost functions
Step 2: Compute $\hat{\boldsymbol{K}}_{ij,m}, \hat{d}_{ij,m}$ for each subproblems $m = 1, \cdots, N$
Step 3: Compute $d_{ij} = \hat{d}_{ij,m^\star} \arg\max_{\hat{d}_{ij,m}} (\hat{J}_m^{\text{dec}} - \hat{J}_m^{\text{dist}}(\hat{\boldsymbol{K}}_m))$
if $\hat{\mathcal{N}}_{m^\star} = \emptyset$ **then**
  $\boldsymbol{K}_{ij} = \hat{\boldsymbol{K}}_{ij,m^\star}$
else
  For all $l \in \{m^\star \cup \hat{\mathcal{N}}_{m^\star}\}$
  Set $\hat{d}_{ij,l} = d_{ij}$
  Solve (5.20)
  $\boldsymbol{K}_{ij} = \arg\max_{\hat{\boldsymbol{K}}_{ij,l}} \sum_{l \in \{m^\star \cup \hat{\mathcal{N}}_{m^\star}\}} \left(\hat{J}_l^{\text{dec}} - \hat{J}_l^{\text{dist}}(\hat{\boldsymbol{K}}_l) \right)$
end if

Example 5 As shown in Fig. 5.5, when the optimal link for the global problem is d_{25}, which is the optimal link from subproblem 2, then $\hat{\mathcal{N}}_2 = \{1, 5\}$. The subsystem 2 then solves (5.20) by taking into account the stability of interconnected system in subsystems 1 and 5.

5.2.4 Distributed Control Design - Multiple Communication Links

In the following, the approach in the case of a single link described previously will be extended to multiple links case. As can be observed from (5.6), the constraint on the network cost, that is $\sum_{1\leq i\leq j\leq N} d_{ij} \leq c$ is still a global one and couples the whole interconnected system. Therefore, in order to solve this problem, we propose to add the communication link sequentially and solve the optimization problem at each time. Assume that the maximum allowable number of communication links is c. We add the link one after another, that is each optimization subproblem (5.13) is solved at most c times. At each time, the $\hat{J}_m^{\text{dec}}$ (resp. $\hat{J}_l^{\text{dec}}$) in (5.13) (resp. in (5.20)) is updated by $\hat{J}_m^{\text{dist}}$ obtained from the optimization problem in the previous step if a new communication link has been added to the corresponding subproblem m. The optimization (5.13) for each time can then be re-written as

$$
\begin{aligned}
\underset{\hat{\boldsymbol{K}}_{ij,m},\hat{d}_{ij,m}}{\text{minimize}} \quad & \hat{J}_m \\
\text{subject to} \quad & \dot{\hat{\boldsymbol{x}}}_m = \hat{\boldsymbol{A}}_m\hat{\boldsymbol{x}}_m + \hat{\boldsymbol{B}}_m\hat{\boldsymbol{u}}_m, \quad \hat{\boldsymbol{x}}_m(t_0) = \hat{\boldsymbol{x}}_{0,m}, \\
& \hat{J}_m < \begin{cases} \hat{J}_m^{\text{dist}} & \text{if at the previous step } m \in \{m^\star \cup \hat{\mathcal{N}}_{m^\star}\}, \\ \hat{J}_i^{\text{dec}} & \text{otherwise,} \end{cases} \\
& \sum_{1\leq i\leq j\leq N_i} \hat{d}_{ij,m} \leq 1, \\
& \hat{d}_{ij,m} \in \{0,1\}, \\
& (i,j) \in \hat{\mathcal{N}}_m^\star.
\end{aligned}
\tag{5.22}
$$

The detail of the proposed approach for multiple links case is shown in Algorithm 2.

Algorithm 2 Joint control gain-communication topology design-multiple links case

Require: c

```
Decompose the global cost function into N local cost functions
for t = 1 → c do
  Execute Algorithm 1
  if m ∈ {m* ∪ N̂_{m*}} then
    Ĵ_m^dec ← Ĵ_m^dist
  else
    Ĵ_m^dec ← Ĵ_m^dec
  end if
end for
```

Remark 19 Even though adding the communication link sequentially could overcome the global constraint on the network cost, the optimality of the solution may again be degraded compared to the centralized design.

One of the advantages of the two-layer control architecture used in this chapter is that the stability of the whole system is guaranteed under permanent communication link failures as stated in the following proposition.

Proposition 5.2.2 The stability of the interconnected system (5.1) with the control input given by (5.22) is guaranteed under any combination of permanent communication link failures.

Proof: Since from (5.13) and (5.22), the cost is always guaranteed to be improved by the addition of the communication link and the overall system is already stabilized by the decentralized control law which is the worst case when all communication links are failed, then the stability is guaranteed under any permanent communication link failures. ■

Another advantage of designing the distributed control in a distributed manner is its scalability when new subsystems are added into the system. The reason is since only the subsystems which are the physical neighbors of the new subsystem needs to solve its local optimization problem.

5.2.5 Complexity of the Proposed Approach

In this section, a comparison in term of complexity between the centralized approach and the proposed distributed design procedure is discussed. Since it is assumed that $\gamma_{ij} = 1$, the allowable number of links is equal to c. For a given number of subsystems N, the maximum number of communication links $c_{\max}$ can be computed as $c_{\max} = \frac{N}{2}(N-1)$. The complexity of the centralized design approach for a given number of communication links c in term of the number of combinations that has to be carried out is given by $\binom{c_{\max}}{c} = \frac{c_{\max}!}{c!(c_{\max}-c)!}$. On the other hand, the complexity of the distributed approach for each subproblem is depending on the size of each subproblem. Since each subproblem could have a different size, here we consider the worst case by considering the subsystem with the maximum vertex degree $d_{\max}$ defined as

$$d_{\max} = \max_i d_i. \tag{5.23}$$

The complexity of the distributed design for a single link, i.e. $c = 1$ can be computed as $\binom{\bar{c}_{\max}}{1} = \frac{\bar{c}_{\max}}{(\bar{c}_{\max}-1)!}$ where $\bar{c}_{\max} = \frac{d_{\max}}{2}(d_{\max}+1)$. Since in the distributed design the link is added one after another, the total complexity for c number of links is given by $\frac{c\bar{c}_{\max}}{(\bar{c}_{\max}-1)!}$. For large-scale interconnected system whose physical interconnection structure is a sparse matrix such as power networks [109], the distributed design procedure results in a lower complexity compared to the centralized design since $d_{\max} < N$, which results in $\bar{c}_{\max} < c_{\max}$. Furthermore, when a new subsystem is added to the existing interconnected system, the complexity of the centralized design will increase exponentially while the increase of complexity for the distributed design will be linear when $d_{\max}$ is constant.

5.3 Evaluation

In this section, the proposed distributed design is illustrated via a numerical example. For the sake of clarity, an interconnection of scalar subsystems is considered. Specifically, we consider an interconnected system consisting of 10 subsystems as depicted in Fig. 5.6

whose dynamics is given by

$$\boldsymbol{A} = \begin{bmatrix} -5 & 0 & 0 & 3 & 4 & 0 & 0 & 0 & 0 & 0 \\ 0 & -25 & 6 & 0 & 3 & 0 & 0 & 0 & 0 & 0 \\ 0 & 6 & -3 & 1 & 0 & 0 & 2 & 0 & 0 & 0 \\ 3 & 0 & 1 & -10 & 0 & 0 & 0 & 0 & 0 & 0 \\ 4 & 3 & 0 & 0 & -6 & 1 & 0 & 0 & 0 & 0 \\ 0 & 0 & 0 & 0 & 1 & -7 & 0 & 0 & 0 & 8 \\ 0 & 0 & 2 & 0 & 0 & 0 & -9 & 0 & 1 & 0 \\ 0 & 0 & 0 & 0 & 0 & 0 & 0 & -8 & 2 & 5 \\ 0 & 0 & 0 & 0 & 0 & 0 & 1 & 2 & -15 & 0 \\ 0 & 0 & 0 & 0 & 0 & 8 & 0 & 5 & 0 & -20 \end{bmatrix}$$

and $\boldsymbol{B}$ is taken to be identity matrix. The LQR cost (5.4) is considered where the weighting matrices $\boldsymbol{Q}, \boldsymbol{R}$ are assumed to be also identity matrices. Moreover, the maximum number of allowable communication links is set to 2 and $\gamma_{ij} = 1$. After the interconnected system is

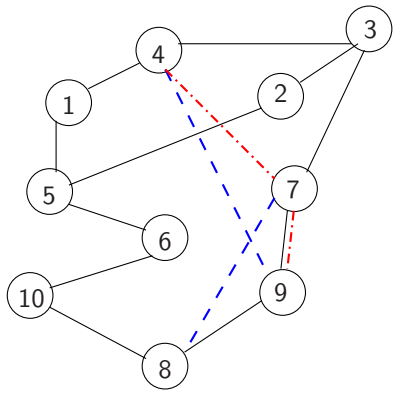

Figure 5.6: Interconnected system consists of ten subsystems. The solid lines represent the physical interconnection. The dash and dash-dot lines represent the optimal communication topology for number of links equal to two by means of centralized and distributed design respectively.

stabilized by the decentralized control law, the interconnected system is then decomposed into 10 subproblems using the result of Lemma 5.2.1. Since for the distributed design the communication link is added one after another, each local subproblem first solves the local optimization (5.13) using the YALMIP toolbox [92] for the addition of a single link. The optimal link for each subproblem is shown in Table 5.1. Since the optimal link from subproblem 9 results in the most improvement of the LQR cost, it is selected as the optimal link for the global problem. The next step is to compute the optimal control gain. Since subsystem 7 and 9 connected by the optimal link are owned by subproblem 7 and 9, i.e. $\hat{\mathcal{N}}_7 = \{9\}$, see Fig. 5.6 and $\hat{d}_{ij,9} = d_{79}$, then subproblems 7 and 9 need to recompute the control gain by taking into account the stability of the interconnected system in subproblem 9 and 7 respectively by solving (5.20) and then compare the resulting gain of each subproblem to select the one which results in the most cost improvement according to (5.21). After computing the optimal link and control gain for a single link case, the

Table 5.1: The optimal link for each local subproblem ($c = 1$)

subproblem i	optimal link $\hat{d}_{ij,i}$	$\hat{J}_i^{\text{dec}} - \hat{J}_i^{\text{dist}}$
1	1-4	22.4909
2	2-5	13.9844
3	4-7	36.2318
4	4-1	27.5482
5	5-1	19.5390
6	5-10	12.1654
7	7-9	42.4931
8	8-9	36.1358
9	9-7	43.2751
10	10-8	15.4705

Table 5.2: The optimal link for each local subproblem ($c = 2$)

subproblem i	optimal link $\hat{d}_{ij,i}$	$\hat{J}_i^{\text{dec}} - \hat{J}_i^{\text{dist}}$
1	1-4	28.3199
2	2-5	15.6788
3	4-7	37.5370
4	4-1	29.0934
5	5-1	22.5657
6	5-10	13.3136
7	7-3	2.5001
8	8-9	37.5062
9	7-8	8.6637
10	10-8	18.6608

optimal link and control gain for the second link is computed by solving (5.22). As can be observed from Table 5.2, since the optimal link of subproblem 3 results in the most cost improvement, thus it is selected as the optimal link for the global problem. Moreover, because no other subsystems own both subsystem 4 and 7, i.e. $\hat{\mathcal{N}}_3 = \emptyset$, the corresponding control gain is then also the optimal control gain for the global problem.

The optimal communication links and the corresponding LQR cost from the centralized and the proposed distributed design can be observed in Tables 5.3 and 5.4 respectively. The complexity can be reduced as much as 96% (from 990 combinations reduced to 30 combinations) for $c = 2$.

Table 5.3: Optimal links for centralized and distributed design

links	centralized design	distributed design
1	7-9	7-9
2	4-9, 7-8	7-9, 4-7

Table 5.4: Cost comparison between centralized and distributed design

links	J^{dec}	centralized	distributed
1	387	259.30	300.45
2	387	168.55	262.91

5.4 Summary and Discussion

The design of distributed control for interconnected systems in the known literature is mainly performed in a centralized fashion, i.e. system-wide information is required to be collected in a central computer to design distributed control law. However, this is not a realistic case and is difficult to be implemented in real world applications due to geographical constraints and privacy reasons. Furthermore, the communication topology of the distributed control law is assumed to be fixed and given a priori.

In this chapter, a novel coordination algorithm is proposed to design distributed control together with its communication topology for interconnected system under a limited plant model information. Here, it is assumed that each subsystem only has the information about its physical neighbors local dynamics and the interconnection between them. As a performance metric, the quadratic infinite horizon cost is considered. The novel idea is to distribute the design of the control law among all subsystems by coordinating with each other, instead of designing it in a central computer. In order to do so, we first give sufficient condition in order to decompose the global cost function into the sum of local cost functions. Each subsystem is then assigned a local cost function and based on the limited plant model information available to it, the optimization problem is solved iteratively by coordinating with the other subsystems. Furthermore, it is demonstrated that it is possible to combine the proposed algorithm with the two-layer control architecture developed in the previous chapter in order to guarantee the stability of the overall system under permanent communication link failures, i.e. enabling the designer to consider jointly performance improvement and robustness issues. As demonstrated from the simulations, the proposed algorithm can reduce the combinatorial search that has to be performed drastically compared to the centralized design approach. The proposed algorithm can be applied in general to a variety of interconnected systems, especially for interconnected systems with a sparse physical network structure such as power networks.

One of the main ingredients of the proposed algorithm is the decomposition of the global objective function into sum of local objective functions. This is one of the reasons of choosing quadratic infinite horizon cost as a performance metric since it can be decomposed under a certain assumption. However, this decomposition strategy may not work for other performance metrics, for example, the decay rate considered in the previous chapters. Furthermore, even though the proposed algorithm can solve the control design in a distributed manner, it suffers from performance degradation compared to the centralized design, which stems from the two-layer control architecture and the iterative process for the case of multiple links. These lead to the following problems that need depth investigations in the future:

- It is significant in the future to investigate analytically how much the performance of the proposed algorithm degrades compared to the centralized design method. The analytical result may be used as a tool to improve the algorithm such that its performance degradation compared to the centralized design method is minimized.
- Extensions of the approach to other performance metrics. Some possible research questions are: For which performance metrics the proposed algorithm can be used in a straightforward manner? How to deal with performance metric which cannot be decomposed in a straightforward fashion?
- It is important to extend the algorithm such that it could deal with the case of addition or removal of subsystems from the interconnected systems, thus enabling a *plug-and-play* control strategy. This will be useful when the algorithm is employed for designing distributed control of a smart power grid where some new distributed generations such as photovoltaic may join and leave the network randomly, and it is not desired to recompute the control law for the whole network.

6 Performance-Oriented Distributed Coverage Control for Robotic Sensor Networks

Stimulated by the technological advances and the development of relatively inexpensive communication, computation, and sensing devices, the interest in the research area of coordinated networked control has increased over the past years, see [97] for an excellent overview. One example is the deployment of autonomous vehicles to perform challenging tasks such as search and recovery operations, manipulation in hazardous environments, surveillance and also environmental monitoring for pollution detection and estimation [82, 111]. Deploying multiple agents to perform tasks is advantageous compared to the single agent case: it provides robustness to agent failure and allows to handle more complex tasks effectively.

In this chapter, we consider a mobile sensing network of vehicles equipped with sensors, known also as robotic sensor network to sample the environment. The goal is to drive the sensors/robots/agents to the position such that a given region is optimally covered by the sensors. There are many approaches proposed in the literature to solve the coverage, i.e. self-deployment problem of mobile sensor network in both centralized and distributed manner [85]. In general there are three main approaches to solve the coverage control problem in a distributed fashion, namely a geometric, probabilistic, and potential field approach [125]. The geometric strategy is based on the Voronoi partition and the continuous version of the Lloyd algorithm, see e.g. [27]. Briefly speaking, the agents partition the given region into subregions given by Voronoi partitions and move towards the centroid of its subregion and adjust their sensing radius until the whole area is covered. The advantage of the Voronoi approach is that the control law is distributed by its nature. Moreover, a lot of variations on the coverage control problem can be addressed and solved in a similar fashion by associating different Voronoi partitions, for example [21, 38, 56, 74, 113]. The probabilistic based strategy is introduced in [84] where the authors consider a probabilistic network model and a density function to represent the frequency of random events taking place over the mission space. The authors formulate an optimization problem that aims at maximizing coverage using sensors with limited range, while minimizing communication cost. A potential-field-based approach to deployment problem in an unknown environment is presented in [63]. A similar approach is proposed in [114] where the area coverage of a mobile sensor network is maximized while satisfying the constraint that every node has at least K neighbors. Moreover, the coverage control problem based on receding horizon control is considered in [7]. A coverage control problem assuming a more realistic sensor model is considered in [28] by introducing "limited-range interactions" of the sensors, that is, the sensing range of the sensor is restricted to a bounded region. Furthermore, coverage algorithms for robotic visual sensor network are proposed in [52, 60, 141] where the sensors have a limited view angle and their sensing performance also depend on their attitude.

As previously mentioned, coverage control problem is generally formulated as to opti-

mize a (non-convex) cost function [27, 84]. The value of the cost function indicates the *coverage performance* of the robotic network which mostly results in a local optimum since most of the distributed control algorithm uses local gradients to compute the movement of the mobile sensors [125]. Some works have been devoted in order to improve the coverage performance, for example by balancing the number of sensors that cover the area with high event density. The authors in [140] develop a task switching-based algorithm in order to improve the coverage performance of the network. First, the agents explore the environment and then switch synchronously the task to coverage which results in an improvement of the coverage performance. The other approaches in order to improve the coverage performance are for example based on distributed annealing algorithm [75] or biologically inspired exploration strategy [124].

Another factor that influences the coverage performance is the participation of the mobile sensors in the coverage task, which is the focus of this chapter. The advantages of using mobile sensors over the static ones are the ability of self-deployment of the sensors and the robustness to sensor failures [85]. However, when the mobile sensors are initially deployed in an unknown environment, for instance air-dropped from an aircraft, some sensors may be initially located far away from the region of interest. Moreover, due to the limited sensing range of the sensors, those sensors may not be able to self-deploy themselves and participate in the coverage task. This will also result in a degradation of the coverage performance by the robotic network, i.e. the agents converge to the undesired local optima. To the best of our knowledge, this fundamental issue has not been considered and discussed in the existing literature so far.

The contribution of this chapter is the development of a novel distributed control law by exploiting the use of information which can be exchanged via the communication network that guarantees the participation of all sensors in the coverage task, i.e. improves the coverage performance of the robotic network, even if some sensors do not sense any event at the initial deployment. The existence of sensors which do not sense any event results in that the system converges to the undesired local optima. Therefore, the objective is to develop a novel distributed control law which guarantees that the agents avoid this undesired local optimal. The innovative idea is to combine the coverage algorithm with the leader-following algorithm where the leader(s), i.e. the sensor(s) who have sufficient information about the environment, is elected by a voting. The sensors acting as leaders will then guide the sensors which do not have information on the environment until they gain sufficient information. First we define a global leader sensor voted only at the initial deployment among all sensors and assume that the communication topology between the mobile sensors is static which implies unlimited communication range. Since the leader is voted only at the initial deployment among all sensors which makes the algorithm computationally expensive when the number of sensors is large and is not robust to sensor failures, we further develop a computationally non-expensive, robust distributed control law with more realistic assumption on the communication range of the sensors. A new leader concept called "local leaders" is introduced in order to reduce the complexity of the algorithm. This local leader is elected locally between each sensor and its neighbors. Moreover, the local leader is re-elected at every time step to increase the robustness with respect to the environment changes and sensor failures. Furthermore, a more realistic case

with limited communication range, resulting in a time-varying topology is considered. A potential-function based algorithm is incorporated in order to maintain the connectivity of the sensors during the deployment. The work in this chapter is based on the framework developed in [84] since it can be generalized to incorporate different sensor model, e.g. visual sensor [52], non-convex environment [57, 151] and also limited energy storage [50]. However, the proposed approach can also be applied to other distributed coverage algorithms, e.g. [27].

This chapter is organized as follows. The problem formulation for the coverage control problem is presented in Section 6.1. Two novel distributed coverage control laws with the global and local leader(s) are proposed and analyzed in Section 6.2. The effectiveness of the proposed control laws are validated through numerical simulations in Section 6.3.

6.1 Problem Formulation

In this section, a condition which results in the convergence of the agents to the undesired local optima is investigated. In order to do so, we first adopt some of the notation and setting described in [84] and in addition introduce a new term called *information value* of a sensor which will be presented in the following.

6.1.1 Region of Interest

Let $\mathcal{Q}$ be a polyhedron in $\mathbb{R}^2$ including its interior. The density function $\phi(q) : \mathcal{Q} \to \mathbb{R}_+$ represents the probability that some event take place in $\mathcal{Q}$. Regions with a large value of ϕ are regions of higher chances of finding a point of interest. The density function $\phi(\boldsymbol{q})$ satisfies $\phi(\boldsymbol{q}) \geq 0$ for all $\boldsymbol{q} \in \mathcal{Q}$ and $\int_{\mathcal{Q}} \phi(\boldsymbol{q}) < \infty$. In general, the region of interest $\mathcal{Q}$ may be very large so that there exists some areas where the value of $\phi(\boldsymbol{q})$ approaches 0 as illustrated in Fig. 6.1.

6.1.2 Sensor Model

We consider a robotic network where each robot is equipped with omnidirectional communication and isotropic sensing capabilities. For the sake of simplicity, it is assumed that all sensors are identical, that is all sensors have identical capabilities for sensing, communication, computation, and mobility. Let $\boldsymbol{s} = (\boldsymbol{s}_1, ..., \boldsymbol{s}_N)$, $\boldsymbol{s}_i \in \mathbb{R}^2$ be the location of the N identical robots/sensors moving in the region $\mathcal{Q}$. The kinematic model of the sensors are given by

$$\dot{\boldsymbol{s}}_i = \boldsymbol{u}_i \tag{6.1}$$

where $\boldsymbol{u}_i$ is the control input for the position of sensor i.

The sensor is assumed to have a limited sensing range defined as

Sensor Model 1 Each sensor has a limited sensory domain $\mathcal{Q}_i$ with the maximum sensing range R given by

$$\mathcal{Q}_i = \{\boldsymbol{q} \in \mathcal{Q} : d_i \leq R\} \tag{6.2}$$

where $d_i = \|\boldsymbol{q} - \boldsymbol{s}_i\|$.

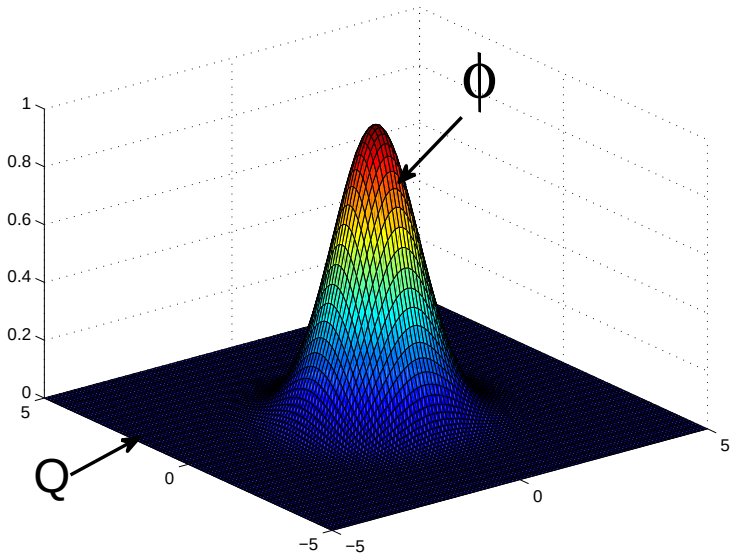

Figure 6.1: The region of interest $\mathcal{Q}$ and its density function $\phi(\boldsymbol{q})$. Regions with a high value of ϕ are regions of higher chances of finding a point of interest. In general, there are some regions in $\mathcal{Q}$ where $\phi(\boldsymbol{q}) = 0$.

When an event occurs at point $\boldsymbol{q}$, it emits a signal and this signal is observed by sensor i at location $\boldsymbol{s}_i$. The received signal strength, i.e, the sensing performance of the sensor is assumed to be decayed with the distance d_i from the sensor i. The degradation of the sensor performance is represented by a monotonically decreasing differentiable function $p_i(\boldsymbol{q}, \boldsymbol{s}_i) : \mathbb{R}_+ \to \mathbb{R}_+$ which expresses the probability that sensor i detects the event occurring at $\boldsymbol{q}$ or indicates how poor the sensing performance is. Lower value of $p_i(\boldsymbol{q}, \boldsymbol{s}_i)$ means that the point $\boldsymbol{q}$ is sensed poorly by sensor i and vice versa. Moreover, we make the following assumption on the sensing performance of the sensor.

Assumption 2

$$p_i(\boldsymbol{q}, \boldsymbol{s}_i) = 0, \frac{\partial p_i(\boldsymbol{q}, \boldsymbol{s}_i)}{\partial d_i(\boldsymbol{q}, \boldsymbol{s}_i)} = 0 \text{ if } \boldsymbol{q} \notin \mathcal{Q}_i. \tag{6.3}$$

The assumption tells us that the sensor i can only sense the point inside its region of sensing $\mathcal{Q}_i$. An example of the sensing performance is given for example by

$$p_i(\boldsymbol{q}, \boldsymbol{s}_i) = \begin{cases} \left(\frac{d_i - R}{R}\right)^2 & \text{if } \boldsymbol{q} \in \mathcal{Q}_i \\ 0 & \text{otherwise.} \end{cases} \tag{6.4}$$

Next we introduce the *information value* of each sensor, that is $I_i : \mathbb{R}_+ \to \mathbb{R}_+$ defined as

Definition 6.1.1 The information value of sensor i is defined as the total received signal

strength inside its sensory domain Q_i. Mathematically, it is formulated as

$$I_i(\boldsymbol{s}_i) = \int_{\mathcal{Q}_i} \phi(\boldsymbol{q}) p_i(\boldsymbol{q}, \boldsymbol{s}_i) d\boldsymbol{q}. \tag{6.5}$$

6.1.3 Communication Graph

Let R_c denote the communication radius of the sensor. The communication topology is described by an undirected graph $\mathcal{G} = (\mathcal{V}, \mathcal{E})$ where the set of vertices $\mathcal{V}$ represents the set of sensors and the set of edges $\mathcal{E}$ denotes all communication connection:

$$\mathcal{E} = \{(i, j) \in \mathcal{V} \times \mathcal{V} | i \in \mathcal{N}_j, j \in \mathcal{N}_i, j \neq i\}$$

where $\mathcal{N}_i$ denotes the neighbors of sensor i, i.e. the set of sensors whom sensor i can communicate with and defined as

$$\mathcal{N}_i = \{j | h_{ij} \leq R_c, j \neq i\} \tag{6.6}$$

where $h_{ij} = \|\boldsymbol{s}_i - \boldsymbol{s}_j\|$. The connectivity of the graph can be checked via the second smallest eigenvalue, i.e. the algebraic connectivity of the Laplacian matrix of the graph $\mathcal{G}$ which represents the communication topology between the mobile sensors [118], see Fig. 6.2. Briefly speaking, a graph is connected if and only if its algebraic connectivity is larger than 0.

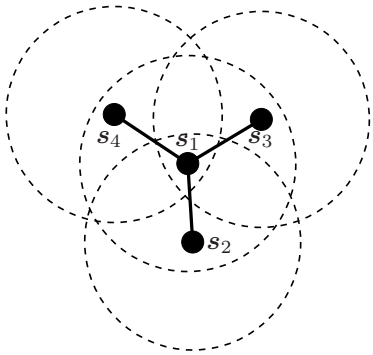

Figure 6.2: Example of communication graph of the sensor networks. The dashed circles represent the communication range and the solid lines represent the communication links.

6.1.4 Optimal Coverage Formulation

Optimal coverage is achieved by deploying the sensors into the region of interest so that the probability of events detected is maximized. In this chapter, sensors are assumed to make observations independently. When an event at $\boldsymbol{q}$ is observed by the sensors, the joint

probability that this event is detected can be written as

$$P(\boldsymbol{q}, \boldsymbol{s}) = 1 - \prod_{i=1}^{N} [1 - p_i(\boldsymbol{q}, \boldsymbol{s}_i)]. \tag{6.7}$$

The optimal coverage problem can then be formulated as an optimization problem which maximizes the objective function defined as

$$F(\boldsymbol{s}) = \int_{\mathcal{Q}} \phi(\boldsymbol{q}) P(\boldsymbol{q}, \boldsymbol{s}) d\boldsymbol{q} \tag{6.8}$$

which is the expected event detection probability by the sensors over the region of interest.

6.1.5 Distributed Coverage Algorithm

The control input for the kinematics of sensor i based on a gradient-based approach that maximizes (6.8) is given by [84]

$$\boldsymbol{u}_i = \boldsymbol{u}_i^{\text{cov}} = \beta \frac{\partial F}{\partial \boldsymbol{s}_i} \tag{6.9}$$

where $\frac{\partial F}{\partial \boldsymbol{s}_i}$ is defined under Assumption 2 as

$$\frac{\partial F}{\partial \boldsymbol{s}_i} = \int_{\mathcal{Q}} \phi(\boldsymbol{q}) \frac{\partial P(\boldsymbol{q}, \boldsymbol{s})}{\partial \boldsymbol{s}_i} d\boldsymbol{q} = \int_{\mathcal{Q}_i} \phi(\boldsymbol{q}) \prod_{k \in \bar{\mathcal{N}}_i} [1 - p_k(\boldsymbol{q}, \boldsymbol{s}_k)] \frac{\partial p_i}{\partial d_i} \frac{\partial d_i}{\partial \boldsymbol{s}_i} d\boldsymbol{q} \tag{6.10}$$

where $\bar{\mathcal{N}}_i$ is the neighbors of sensor i. The algorithm is distributed since each sensor only requires the information of other sensors within the distance of $2R$ from it in order to compute the distributed control law (6.9) and drives the sensors into the region of interest. However, since the control law (6.9) is based on a gradient-based approach and due to the limited sensing range of the sensor, there exists a condition at the initial deployment where the information gained by some agents are zero, that is $I_i(\boldsymbol{s}_i) = 0$, for example sensors located in the area with $\phi(\boldsymbol{q}) = 0$ as shown in Fig. 6.1. This results in that the control input of the sensor $\boldsymbol{u}_i^{\text{cov}}(k) = \boldsymbol{0}$, i.e. the sensor could not participate in the coverage task and the corresponding local optima is called by undesired local optima. Formally, we call such a sensor as an *isolated* sensor defined as

Definition 6.1.2 Sensor i is called an isolated sensor if it collects no information so that it has no ability to move, i.e. $I_i = 0$.

The goal of this chapter is to develop a novel distributed control law in order to improve the coverage performance by guaranteeing the participation of all sensors in the coverage task, that is there will be no isolated sensors exist in the final configuration of the sensors.

6.2 Proposed Coverage Algorithm

The solution to the above problem is not trivial since each sensor only knows the density function inside its own sensing range, i.e. the sensors only have partial information on the environment. In addition, in a typical dynamic deployment application, the mobile sensors start with the same copy of an estimated density function ϕ at the beginning of the deployment. As the sensors deployed and data are collected, each node updates its local map by merging new observations from its sensor into its perception and also by exchanging information with its neighbors [23]. However, since the isolated sensors do not sense any information, they will not be able to update their local maps, i.e. cannot participate in the coverage. Furthermore, promising solution that executes a random movement such as exploration [140] for the isolated sensors do not guarantee the participation of those sensors in the coverage task and would result in a large amount of energy consumption which is not desired.

In this section, a new distributed control law is proposed by combining the standard coverage algorithm and a leader-following algorithm. Since the isolated sensors have no information, that is do not sense any events, they cannot participate in the coverage task. Therefore, they need to be guided in order to move into the region of interest to perform the coverage task. However, no external supervisor is allowed in order to keep the algorithm to be distributed. In this section, as a strategy virtual supervisors termed as leaders are assigned between the sensors. The rest of the sensors then act as followers and will follow their leaders based on the leader-following algorithm until they gain sufficient information to switch to performing a coverage task. In this chapter, we introduce two types of leader: a *global* leader elected among all sensors and *local* leader(s) elected between each sensor and its neighbors. Before proceeding we introduce the following assumption.

Assumption 3 There exists at least one non-isolated sensor in the network, that is $\exists i, I_i \neq 0$.

6.2.1 Global Leader based Algorithm

The first distributed algorithm is based on a global leader where the leader is elected at the initial deployment among all sensors. Furthermore, we assume the following:

Assumption 4 The communication topology $\mathcal{G}$ is static and connected.

Assumption 4 results in that the communication range of the sensor is unlimited, i.e. $R_c \to \infty$. Therefore, the communication graph $\mathcal{G}$ becomes fully connected.

Global Leader Election

At the initial deployment, a sensor with the most information among all sensors in the network is elected using a voting algorithm as a leader. Formally, the leader sensor is defined as

Definition 6.2.1 A leader sensor l^g is a sensor which has the most information on the region of interest. Mathematically,

$$l^g = \underset{i}{\text{argmax}} \ I_i(\boldsymbol{s}_i(0)). \tag{6.11}$$

Since the leader is elected among all sensors, we call such leader as *global* leader.

Remark 20 When more than one sensor have the most information, the leader is selected randomly among those sensors.

The goal of a leader voting algorithm is to choose the sensor with the most information value I_i and broadcast the result all over the network based on a simple implementation of broadcast algorithm called *flooding* [104] using the multi-hop communication capability. The algorithm is initialized by sensor i sending a message I_i to each of its neighbors. Each sensor $j \in \mathcal{N}_i$ receiving one or more such messages compares the best received information value to its currently stored one. If the received information value is higher, its own information value is deleted and the new received one is stored. The message is then forwarded to all of its neighbors except to the sender of the best information value. If the received value is lower, then the sensor sends its own election value to all its neighbors. In the end, a global leader l^g will be elected.

Proposed Distributed Algorithm

Next, a distributed algorithm with a global leader that guarantees the participation of all sensors in the coverage task is proposed. Mathematically, we would like to design $\boldsymbol{u}_i$ that solve the following optimization problem:

$$\begin{aligned} \underset{\boldsymbol{s}}{\text{maximize}} \quad & F \\ \text{subject to} \quad & I_i > 0, \forall i. \end{aligned} \tag{6.12}$$

The proposed distributed control law is given by

$$\boldsymbol{u}_i = {\boldsymbol{u}_i}^{\text{cov}} + \alpha_i {\boldsymbol{u}_i}^{\text{gl}} \tag{6.13}$$

where $\alpha_i = 0$ if $I_i > \eta_i I_{l^g}$. Otherwise $\alpha_i = 1$, where $0 < \eta_i < 1$ is a tunning variable. Depending on the value of α_i, sensor i will be in one of the following modes:

$$\text{sensor } i \text{ is in } \begin{cases} \text{following mode} & \text{if } \alpha_i = 1, i \notin l^g \\ \text{autonomous deployment mode} & \text{if } \alpha_i = 0 \text{ or } i = l^g. \end{cases}$$

Physically, it means that when a sensor has gathered sufficient information, then it will stop following the leader and only performs the coverage, i.e. switch from the following mode into the autonomous deployment mode.

The ${\boldsymbol{u}_i}^{\text{cov}}$ in (6.13) is given by (6.9) and ${\boldsymbol{u}_i}^{\text{gl}}$ is given by

$$\boldsymbol{u}_i^{\text{gl}} = \zeta_i^{\text{gl}}(\boldsymbol{s}_{l^g} - \boldsymbol{s}_i) \tag{6.14}$$

where $\zeta_i^{\text{gl}} > 0$. Formally, the proposed distributed algorithm can be written as Algorithm 3.

Algorithm 3 Proposed distributed algorithm with a global leader

Require: $\mathcal{N}_i, I_i$
  Elect a global leader l^g
  For sensor $i \in \{1, \cdots, N\}$
  loop
    if $I_i > \eta_i I_{l^g}$ **then**
      $\alpha_i \Leftarrow 0$ (autonomous deployment mode)
      $\boldsymbol{u}_i = \boldsymbol{u}_i^{\text{cov}}$
    else
      $\alpha_i \Leftarrow 1$ (following mode)
      $\boldsymbol{u}_i = \boldsymbol{u}_i{}^{\text{cov}} + \boldsymbol{u}_i{}^{\text{gl}}$
    end if
  end loop

Remark 21 Even though each sensor only needs the information from the sensors within the distance of $2R$ in order to compute the standard coverage control law (6.9), it needs the information from the rest of the sensors in order to elect the global leader.

Using the proposed control law (6.13), it is guaranteed that in the end of the deployment all sensors participate in the coverage task as shown in the following.

Theorem 6.2.2 Consider mobile sensors whose kinematic given by (6.1) and the control input is given by (6.13). Therefore, under Assumptions 2- 4, there will be no isolated sensors, i.e. all sensors participate in the coverage.

Proof: From Assumption 3, there will always be a global leader in the network. Moreover, since the graph is fully connected, then by implementing the control law (6.13), the other sensors will approach the global leader until they have a sufficient information, i.e. $I_i > \eta_i I_{l^g} \gg 0$. Thus it is guaranteed that in the end of the deployment, there is no isolated sensors, that is $I_i > 0, \forall i$. ■

6.2.2 Local Leader based Algorithm

Next, a computationally non-expensive, robust distributed control law with more realistic assumption is proposed. A new leader concept called *local* leaders is introduced in order to reduce the complexity of the algorithm with a global leader and is re-elected at every time step to increase the robustness w.r.t. sensor failures. For the local leader case we constrain ourselves to the case given by the following assumption.

Assumption 5 The density function ϕ only consists of a single maxima.

Furthermore, it is assumed that each sensor has a *limited communication range*, thus $2R \leq R_c < \infty$ so that the each sensor can compute the standard coverage control law (6.9). Note that $\mathcal{N}_i$ may change due to the movement of the mobile sensors, that is the graph $\mathcal{G} = (\mathcal{V}, \mathcal{E}) = \mathcal{G}(t)$ is time-varying. Moreover, let us denote the set of connected graphs by $\mathcal{C}$.

Table 6.1: Comparison between global leader and local leader(s)

	global leader	local leader
number of leaders in the network	one	more than one
time of voting	at the initial deployment	at every time step
voters for leader	all sensors in the network	sensor i and its neighbors

Local Leader Election

First, each agent assigned himself either as a *local leader* or a *follower* to the other agents by comparing its information value with its neighbors. Formally, the local leader and the follower are defined as follows.

Definition 6.2.3 Sensor i is a local leader at time t if it has the most information value compared to its neighbors or mathematically

$$I_i(\boldsymbol{s}_i(t)) > I_j(\boldsymbol{s}_j(t)), \forall j \in \mathcal{N}_i. \tag{6.15}$$

Definition 6.2.4 The set of local leader sensor(s) of sensor i, i.e. sensor l is a sensor(s) which has the most information on the region of interest. Mathematically,

$$l(t) \in \underset{j \in \mathcal{N}_i}{\operatorname{argmax}} \; I_j(\boldsymbol{s}_j(t)) \text{ and } I_l > I_i, i \neq l. \tag{6.16}$$

Therefore, at each time step sensor i computes its information value I_i and then compares it with its neighbors to decide whether it is a local leader of follower. Note that when sensor i and j have the same amount of information, i.e. $I_i = I_j > I_m$, $m, j \in \mathcal{N}_i$, the following rule is used in order to decide whether sensor i acts as a leader or a follower:

- if sensor j is a follower to sensor k where $k \in \mathcal{N}_j, k \neq i$, then sensor j is the leader of sensor i,
- otherwise, sensor i itself is the leader.

The similar rule can also be applied in the case of more than two sensors have the same amount of information. Note that an agent which is a follower can at the same time be a local leader to the other agent, for example sensor 4 in Fig. 6.3(b) is a local leader of sensor 3, sensor 5 and at the same time a follower to sensor 1. The comparison between the global and local leader is summarized in Table 6.1.

Connectivity Maintenance

Let us first introduce the following assumption.

Assumption 6 The initial graph of the sensors is connected, i.e. $\mathcal{G}(0) \subseteq \mathcal{C}$ and $\|\boldsymbol{s}_i(0) - \boldsymbol{s}_j(0)\| < \delta$, $\forall i$ and $j \in \mathcal{N}_i$ where δ is a value approaching but less than R_c.

Since the communication range of the sensor is limited, there is a possibility that the network becomes disconnected. Therefore, first we discuss the connectivity maintenance between the sensors using the idea of a potential function. The potential function V_{ij}^c is selected which satisfies the following conditions:

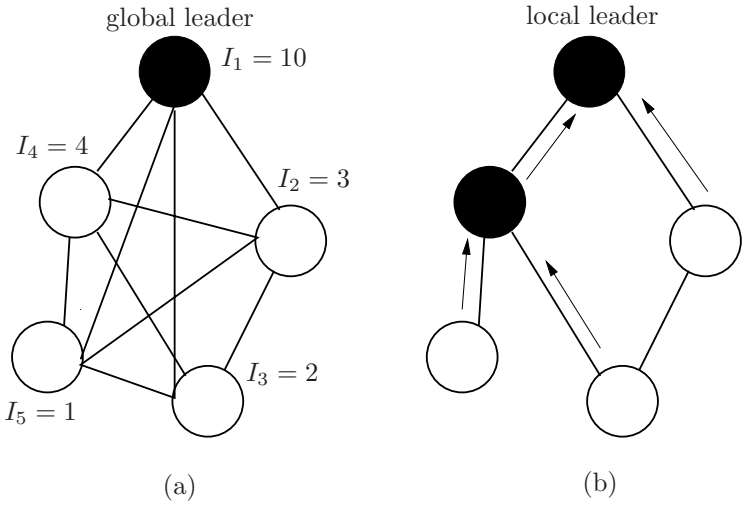

Figure 6.3: Example of (a) global leader and (b) local leaders case. For the global leader case, a leader is elected among all sensors in the network while for the local leader case, each sensor assigned himself either as a leader of follower to the other by comparing its information value with its neighbors. The sensor with outgoing arrow is a follower to its local leader, that is the sensor with ingoing arrow as shown in (b). Moreover, as can be seen from (b), sensor 4 acts as a follower and also a local leader for sensor 3 and sensor 5.

- $V_{ij}^c \geq 0$ and is differentiable. Moreover, $\frac{\partial V_{ij}^c}{\partial h_{ij}} \geq 0$,
- $V_{ij}^c = 0$ when $h_{ij} \leq \delta$,
- $V_{ij}^c \to \infty$ if $h_{ij} \to R_c$.

One example of the potential function which will be used in this chapter is

$$V_{ij}^c(\boldsymbol{s}_i, \boldsymbol{s}_j) = \begin{cases} \frac{(h_{ij}-\delta)^a}{(R_c-h_{ij})^b} & \delta \leq h_{ij} \leq R_c \\ 0 & h_{ij} < \delta \end{cases} \tag{6.17}$$

where $a \geq 2, b \geq 1$. The collective potential function is given by

$$V^c(\boldsymbol{s}) = \frac{1}{2} \sum_{i=1}^{N} \sum_{j \in \mathcal{N}_i} V_{ij}^c(\boldsymbol{s}_i, \boldsymbol{s}_j). \tag{6.18}$$

Remark 22 The potential function employed in this chapter is similar to the one used in [86].

Note that the potential function described above makes the sensors which are connected at time t_0 to be kept connected for $t > t_0$. This may degrade the coverage performance of the sensors, for example when the initial graph is fully connected. In order to deal with this, the connectivity maintenance should only be performed within the core structure which gives a sufficient degree of freedom or produces the least impediment for the sensors to achieve the optimal sensing coverage. Furthermore, the core structure should also keep

the connectivity between the mobile sensors. As stated in [86], the spanning tree [1] is the sparsest connected subgraph for a given connected graph $\mathcal{G}$ which can retain the degree of freedom as large as possible for the sensors as shown in Fig. 6.4. Therefore, similar to [86], in this section the spanning tree is taken as the core structure whose connectivity needs to be maintained. Let us define the graph of the core structure which a spanning tree by $\mathcal{G}^s = (\mathcal{V}, \mathcal{E}^s)$ where $\mathcal{E}^s \subseteq \mathcal{E}$. The new collective potential function thus can be written as

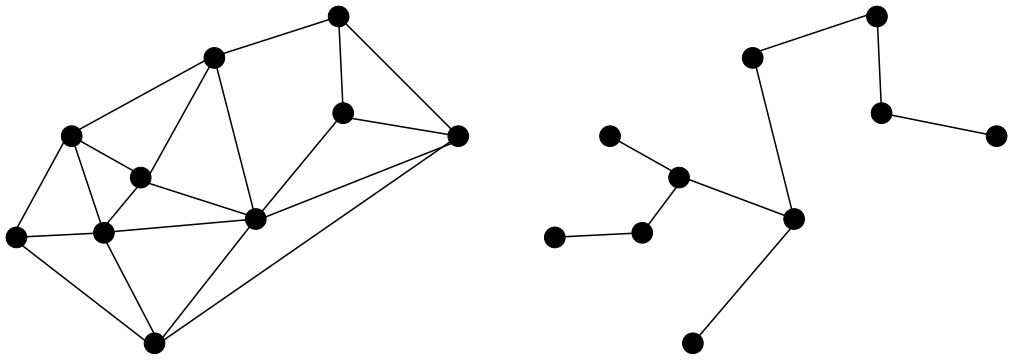

(a) (b)

Figure 6.4: (a) Communication topology of the sensors; (b) Core structure which is a spanning tree whose connectivity needs to be maintained by the mobile sensors.

$$V^{cs}(\boldsymbol{s}) = \frac{1}{2}\sum_{i=1}^{N}\sum_{j\in\mathcal{N}_i(\mathcal{E}^s)} V_{ij}^{c}(\boldsymbol{s}_i, \boldsymbol{s}_j). \tag{6.19}$$

Remark 23 The use of potential function (6.19) instead of (6.18) will also prevent from the discontinuity due to the new agents which join as new neighbors of sensor i during the deployment since the core structure $\mathcal{G}^s$ does not change over the time.

Remark 24 The spanning tree can be constructed in a distributed fashion, for example using the algorithms proposed in [123].

Proposed Distributed Control Law

Next, we propose a novel distributed control law in order to improve the coverage performance by guaranteeing the participation of all sensors in the coverage task while maintaining the connectivity between the sensors. Mathematically, we would like to solve the following optimization problem:

$$\begin{aligned} \underset{\boldsymbol{s}}{\text{maximize}} \quad & F \\ \text{subject to} \quad & I_i > 0, \forall i, \\ & \mathcal{G} \subseteq \mathcal{C}. \end{aligned} \tag{6.20}$$

[1] A spanning tree of a connected graph is a maximal set of edges that contains no cycle, or a minimal set of edges that connect all vertices

Let the set of local leaders of sensor i is given by $\mathcal{N}_i^l$ and $|\mathcal{N}_i^l|$ is its cardinality. The proposed distributed control law is given by

$$\boldsymbol{u}_i = \boldsymbol{u}_i{}^{\text{cov}} + \boldsymbol{u}_i^c + \alpha_i \boldsymbol{u}_i{}^{\text{lf}} \tag{6.21}$$

where $\alpha_i = 0$ if $I_i > \eta_i I_l, l \in \mathcal{N}_i^l$. Otherwise $\alpha_i = 1$, where $0 < \eta_i < 1$ is a tunning variable. Depending on the value of α_i, sensor i will be in one of the following modes:

$$\text{sensor } i \text{ is in } \begin{cases} \text{following mode} & \text{if } \alpha_i = 1 \\ \text{autonomous deployment mode} & \text{if } \alpha_i = 0. \end{cases}$$

Similar to the global leader based algorithm, physically it means that when a sensor has gathered sufficient information, then it will stop following the leader and only performs the coverage, i.e. switch from the following mode into the autonomous deployment mode. Each term of the proposed control law (6.21) is given by

$$\boldsymbol{u}_i^{\text{lf}} = \zeta_i^{\text{lf}} \sum_{l \in \mathcal{N}_i^l} (\boldsymbol{s}_l - \boldsymbol{s}_i), \tag{6.22}$$

$$\boldsymbol{u}_i^c = -\zeta_i^c \frac{\partial V^{cs}(\boldsymbol{s})}{\partial \boldsymbol{s}_i} \tag{6.23}$$

where $\zeta_i^{\text{lf}}, \zeta_i^c > 0$. Formally, the proposed distributed algorithm can be written as Algorithm 4. Thus, by implementing the control law (6.21), the participation of all sensors in the coverage task is guaranteed as shown in the following section.

Algorithm 4 Proposed distributed algorithm for sensor i ($i \in \{1, \cdots, N\}$)

Require: $\mathcal{N}_i, I_i, I_j, j \in \mathcal{N}_i$

```
The network construct the spanning tree graph G^s
loop
  Sensor i decides if it is a local leader or a follower
  if i is a leader or I_i > η_i I_j, j ∈ N_i^l then
    α_i ⇐ 0 (autonomous deployment mode)
    u_i = u_i^cov + u_i^c
  else
    α_i ⇐ 1 (following mode)
    u_i = u_i^cov + u_i^c + u_i^lf
  end if
end loop
```

Analysis

We prove in the following that using the proposed distributed control law above, at the final configuration, there will be no isolated sensors. Furthermore, when the initial graph is connected, the connectivity is always maintained during the deployment.

Theorem 6.2.5 Consider mobile sensors whose kinematics given by (6.1) and the control input is given by (6.21). Under Assumptions 2, 3, 5 and 6, there will be no isolated sensors, that is all sensors participate in the coverage task and the connectivity between the sensors is guaranteed, that is $\mathcal{G}(t) \subseteq \mathcal{C}, t > 0$.

Proof: First, let us assume that there is no isolated sensors in the network, i.e. $\alpha_i = 0, \forall i$, or all sensors are in autonomous deployment mode. The coverage with connectivity maintenance as formulated in (6.20) can be considered as to maximize $V(s) = k_1 F(\boldsymbol{s}) - k_2 V^{cs}(\boldsymbol{s})$ where $k_1 \gg k_2 > 0$ represent the weighting factors for the coverage and connectivity maintenance respectively. First, we prove that for a given initial sensors position $\boldsymbol{s}(0)$ and communication graph $\mathcal{G}(0) \subseteq \mathcal{C}$, the connectivity between the sensors is always maintained during the maneuvers. From Assumption 6, the communication graph is connected at the initial position, i.e. $\mathcal{G}(0) \in \mathcal{C}$, $V_{ij}^c = 0$ which results in $V(\boldsymbol{s}(0)) > 0$. Moreover, the control law (6.21) with $\alpha_i = 0$ can be obtained by taking the partial derivative of $V(\boldsymbol{s})$, i.e. $\frac{\partial V(\boldsymbol{s})}{\partial \boldsymbol{s}_i}$. For mobile sensors steered by the control law (6.21), we have

$$\frac{dV(\boldsymbol{s}(t))}{dt} = \sum_{i=1}^{N} \left[\frac{\partial V(\boldsymbol{s})}{\partial \boldsymbol{s}_i} \dot{\boldsymbol{s}}_i \right] = \sum_{i=1}^{N} \left[\frac{\partial V(\boldsymbol{s})}{\partial \boldsymbol{s}_i} . \left(\frac{\partial V(\boldsymbol{s})}{\partial \boldsymbol{s}_i} \right) \right] = \sum_{i=1}^{N} \left| \frac{\partial V(\boldsymbol{s})}{\partial \boldsymbol{s}_i} \right|^2 \geq 0.$$

Since $\int_{\mathcal{Q}} \phi(\boldsymbol{q}) < \infty$, then $F(\boldsymbol{s})$ is finite, i.e. $F(\boldsymbol{s}) < \infty$. Furthermore, since $V(\boldsymbol{s}(0)) > 0$ and $\frac{dV}{dt} \geq 0$, $V^{cs}(\boldsymbol{s})$ is also finite, that is $V^{cs}(c) < \infty$. Thus, from (6.18), $V_{ij}^c(\boldsymbol{s}_i, \boldsymbol{s}_j)$ is finite, i.e. $V_{ij}^c(\boldsymbol{s}_i, \boldsymbol{s}_j) < \infty$ for each pair of $(i, j) \in \mathcal{E}^s$. According to (6.17), the finite V_{ij}^c implies h_{ij} will never converge to R_c for any $(i, j) \in \mathcal{E}^s$. Hence the connectivity will be preserved all the time. Next, consider the case when $\exists i, \alpha_i = 1$, i.e. there exists at least one sensor which is in the following mode since it does not have sufficient information. Note that the sensor who is a follower will execute the control law $\boldsymbol{u}_i^{\text{lf}} = \zeta_i^{\text{lf}} \sum_{l \in \mathcal{N}_i^l} (\boldsymbol{s}_l - \boldsymbol{s}_i)$ in (6.21), i.e. sensor i will follow its local leader or approach the convex hull spanned by its leaders [118]. Moreover, since all mobile sensors apply the coverage control law $\boldsymbol{u}_i^{\text{cov}}$ whose direction towards the area with higher density function and from Assumption 5 since there is only a single maxima in ϕ, the vectors $\boldsymbol{u}_l$ and $\boldsymbol{u}_{i,i \neq l}$ satisfy the following relation $\boldsymbol{u}_l^T \boldsymbol{u}_i > 0$, i.e. the sensor applying (6.21) does not move in the direction opposite from the movement of its leaders. Therefore, the connectivity will always be maintained.

Next we prove that there exists no isolated sensors in the end of the deployment. In order to prove this and since there is only a single maxima in ϕ as stated in Assumption 5, we consider the worst case scenario as shown in Fig. 6.5. Without loss of generality, we re-order the label of the sensors as shown in Fig. 6.5 and consider the case where $I_1 > 0$ and $I_2 = \cdots = I_N = 0$, i.e. there is only one non-isolated sensor in the network. In addition, it is assumed that the distance between the sensors are closed to the limitation of the communication range R_c, i.e. $h_{ij} = \delta, \forall i, j$. It is clear that using the standard algorithm (6.10), all sensors including sensor 1 at the initial deployment cannot move since the isolated sensors, i.e. sensor $2, \cdots, N$ do not have information, i.e. cannot move while sensor 1 has to keep the connectivity maintenance with the other sensor. Using the proposed approach, at the first time step, sensor 2 chooses sensor 1 as its local leader while sensor $3, \cdots, N$ cannot decide who their local leader is since $I_2 = I_3 = \cdots = I_N = 0$. At the next time step, sensor 3 will choose sensor 2 as its local leader since sensor 2 is the

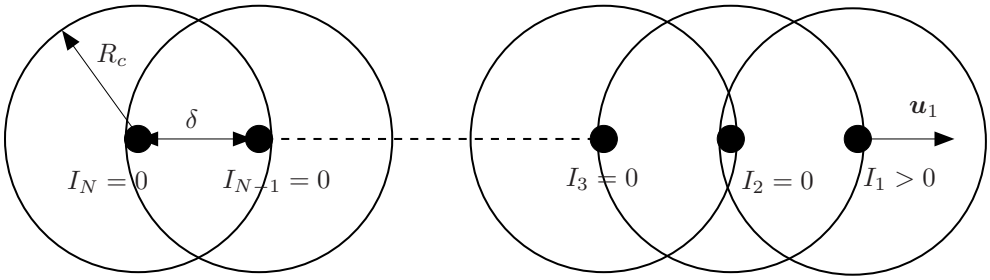

Figure 6.5: Example of worst case scenario. At the initial deployment, the distance between the sensors is closed to the limitation of the communication range R_c of its neighbors. Furthermore, only sensor 1 which is not an isolated sensor, i.e. $I_1 > 0$ while the other sensors are isolated ones, i.e. $I_i = 0, i \neq 1$. Using the standard algorithm [84] no sensors participate in the coverage task.

follower of sensor 1 while sensor $4, \cdots, N$ cannot decide who their local leader is. This process will continue and finally sensor N will select sensor $N-1$ as its local leader. After each sensor assigned its local leader, sensor N will move towards to its local leader, i.e. sensor $N-1$ followed by sensor $N-1, \cdots, 1$. Since the graph is guaranteed to be always connected, then by implementing the leader-following algorithm, all the followers will approach their leaders until they have a sufficient information, i.e. $I_i > \eta_i I_l > 0$ and execute the deployment algorithm (6.10). Thus, it is guaranteed that in the end of the deployment $I_i > 0, \forall i$. This completes the proof. ■

Remark 25 In fact, the connectivity can still be guaranteed even if only the leaders in $\mathcal{G}^s$ who are responsible for maintaining the connectivity while the followers follow their leaders without awareness of maintaining the connectivity. Therefore, in this case the control law (6.21) can be re-written as

$$\boldsymbol{u}_i = \boldsymbol{u}_i{}^{\text{cov}} + (1-\alpha_i)\boldsymbol{u}_i^c + \alpha_i \boldsymbol{u}_i{}^{\text{lf}}.$$

Remark 26 The leader-follower term in the proposed distributed control law (6.13), (6.21) can be seen as a perturbation term that works on the gradient-based control laws which guarantees the agents to avoid the undesired local optimal value in the cost function.

Remark 27 The proposed algorithm based on local leader improves the coverage performance by guaranteeing the participation of the sensors in the coverage task under assumption that there exists only a single maxima in the density function. However, when the density function consists of more than one local maxima, it is not guaranteed that the proposed algorithms could maintain the connectivity and if there is no isolated sensors in the final configuration. This issue is the subject of future work. It should be noted that this situation does not influence the global leader-based approach described in the previous section.

6.2.3 Leader Election's Complexity

One of the main ingredient of the proposed algorithm is the leader election. In this section, the complexity of the global and local leader election in the proposed distributed control law is compared. For the global leader case, the leader is elected among the N sensors by using the broadcast algorithm. Therefore, the complexity of the global leader election algorithm is increased with the number of sensors in the network. On the other hand, the local leader election is conducted by each sensor only between itself and the neighbors. In this case, we consider the worst case complexity which is proportional to $d_{\max}(\mathcal{G})$, that is the maximum degree of the graph $\mathcal{G}$. When the number of sensors in the network increases, the worst case complexity remains constant as long as $d_{\max}(\mathcal{G})$ is not increased. The local leader election is thus more scalable compared to global leader election algorithm. Furthermore, since the leader is re-elected at every time step, the local leader based algorithm is more robust to sensor failures and also the environment changes.

6.3 Evaluation

In this section, the proposed control law is evaluated through numerical simulations. The region of interest $\mathcal{Q}$ is a rectangle of size 800 x 1200 (meter). It is assumed that there are 5 sensors whose sensing performance is given by (6.4) with sensing radius $R = 100$. The initial positions of the sensors are given by $\boldsymbol{s}_1 = [250, 300]$, $\boldsymbol{s}_2 = [120, 210]$, $\boldsymbol{s}_3 = [220, 180]$, $\boldsymbol{s}_4 = [110, 110]$, $\boldsymbol{s}_5 = [200, 100]$. The density function in the region of interest is given by $\phi(q) = 35 - 0.1||\boldsymbol{q} - \boldsymbol{p}_t||$. A Monte Carlo simulation is carried out over different location of the event, that is the value of $\boldsymbol{p}_t$. The value of $\boldsymbol{p}_t$ is chosen randomly between the range $\boldsymbol{p}_t = [(200, 600), (300, 900)]$ and is selected such that Assumption 3 is satisfied and there exists at least one isolated sensor in the network. Moreover, for all simulations we set $\beta = 0.004$, $\zeta_i^{\text{lf}} = \zeta_i^{\text{gl}} = 0.0025$, $\zeta_i^c = 0.004$ and $\eta_i = 0.5$ for $i, l \in \{1, \cdots, 5\}$. We apply the standard coverage algorithm in [84] and the proposed algorithm both with the global and local leader where the communication radius $R_c = 200$ for the similar setup. In addition to the final value of the objective function, the convergence speed of the global and local leader based algorithm are also compared. The comparison is possible since both algorithms guarantee the participation of all sensors in the coverage task, which is not the case for the standard algorithm. The results of the Monte Carlo simulation for 20 different value of $\boldsymbol{p}_t$ are shown in Fig. 6.6. As can be observed from Fig. 6.6(a), both the proposed algorithms improve the coverage performance and outperform the standard algorithm in [84]. The final value of the objective function by the local leader based algorithm is lower than the global leader based one. Moreover, it takes a longer time for the sensors using the local leader based algorithm to converge as can be observed from Fig. 6.6(b). The reason is that for the global leader based algorithm, the sensors are not required to maintain the connectivity among themselves due to the assumption of unlimited communication range. Next, we look into more detail the simulation results for a particular value of $\boldsymbol{p}_t = [400, 600]$. As shown in Fig. 6.7(a), for the given initial position, by using the standard coverage algorithm (6.10), in the end of the deployment there exist four isolated sensors, i.e. sensor 2, sensor 3, sensor 4 and sensor 5 which cannot participate

in the coverage task. Next, we apply the global leader based control law (6.13). At the initial deployment, a voting is conducted among all sensors and as a result sensor 1 with the most information is elected as the global leader. The other sensors follow the leader until their information exceed half of the information of the global leader sensor 1. The snapshot during the deployment using the control law (6.13) is shown in Fig. 6.11. Furthermore, the trajectories and the information gathered by each sensor using the global leader based algorithm are shown in Fig. 6.10. Next, we apply the proposed control law (6.21) based on the local leader. Using the leader election algorithm, at the beginning sensor 1 is selected as the local leader of sensor 2 and sensor 3. After several steps, sensor 3 is selected as the local leader of sensor 4 and sensor 5. The local leader will be re-elected at every step. Thus, the elected local leader may be different at each step. As can be observed from Fig. 6.7(b), all sensors participate in the coverage task which results in a higher coverage performance indicated by a higher value of the objective function as shown in Fig. 6.8. The trajectories and the information gathered by each sensor are shown in Fig. 6.12 while the snapshot during the deployment is shown in Fig. 6.13. As can be observed, sensor 3 switches to the autonomous deployment mode when its information value exceeds half of the information value of its local leader, that is sensor 1 at around step 180. Sensor 2 does the same behavior to sensor 3 as its local leader at around step 240. Both sensor 4 and sensor 5 have sensor 3 as their local leader and switch to autonomous deployment mode around step 300. Moreover, using the proposed algorithm, the connectivity between the sensors is maintained during the deployment indicated by the algebraic connectivity of the Laplacian matrix of the graph always larger than zero while the communication graph will be disconnected, that is the algebraic connectivity is zero when no connectivity maintenance algorithm is applied as shown in Fig. 6.9. Furthermore, As can be observed from Fig. 6.8, the global leader based algorithm results in a better coverage performance value and a faster convergence speed compared to the local leader one since the sensors are not required to maintain the connectivity among them.

6.4 Summary and Discussion

The multi-robot deployment problem generally results in a non-convex optimization problem which makes the gradient-based control laws converge mostly to local optima. It is reported in [125] that the cost function of deployment problem has multiple local optima which all have an equal cost. However, in this chapter it is shown that there exists a condition for which the gradient methods converge to a certain local optima whose value is not as close as the others. We refer to such local optima as the undesired local optima. This local optima occurs in the following condition. When mobile sensors are initially deployed, some sensors may be located far away from the region of interest and due to the sensor's limited sensing of range, some sensors may not be able to participate in the coverage task which results in a degradation of coverage performance of the robotic network. A novel distributed control that avoids the agents to converge to the undesired local optima is then proposed by exploiting the use of information which can be exchanged via the communication network. Specifically, this chapter introduces a novel distributed coverage control law with global and local leader that improves the coverage performance by guaranteeing the

participation of all sensors in the coverage task. At each time step, each sensor executes one of the two modes, namely autonomous deployment mode and following mode, depending on its information value. The innovative idea is that the sensors which have no or less information at their initial deployment follow their neighboring sensors which have higher information value until they gain sufficient information while maintaining the connectivity among them. The leader-follower algorithm in the proposed distributed control law can be viewed as a perturbation influencing the gradient-based control law. Compared to the other non-gradient based approaches, the proposed approach in this chapter is advantageous in the sense that it is more intuitive and guarantees that in the final configuration of the deployment, there is no isolated sensors in the network, which cannot be achieved by other approaches in the related literature. The results obtained in this chapter also indicate that by exchanging more information, in this case the information gained by each sensor, the performance of the overall system can be improved significantly. A similar strategy is also considered in [22] for a consensus problem where it is shown that by using both the current and outdated states in memory, the proposed algorithm converges faster than the standard consensus algorithm while requiring identical maximum control effort if the outdated states are chosen properly.

In this chapter, two different algorithms are proposed, namely global leader and local leader based algorithms. Even though the local leader based algorithm is more robust to environment changes, it relies on the assumption that the density function only consists of a single maxima, which is quite restrictive in reality. Therefore, it is required in the future to relax this assumption and improve the proposed algorithm. In addition, it is also promising to investigate other cases or situations that result in an undesired local optima. One possible situation is the unbalanced coverage of the region of interest by the mobile sensors, for example when there exists area with high density function not covered by the sensors as discussed in [140]. In this situation, exploration-based approach [124, 140] or methods based on deterministic annealing [75] may not guarantee that each important area, i.e. region with high density function is covered by at least one sensor. Therefore, it is necessary to develop distributed control, possibly other than the non-convex optimization-based techniques that guarantee the agents converge to the corresponding local optima.

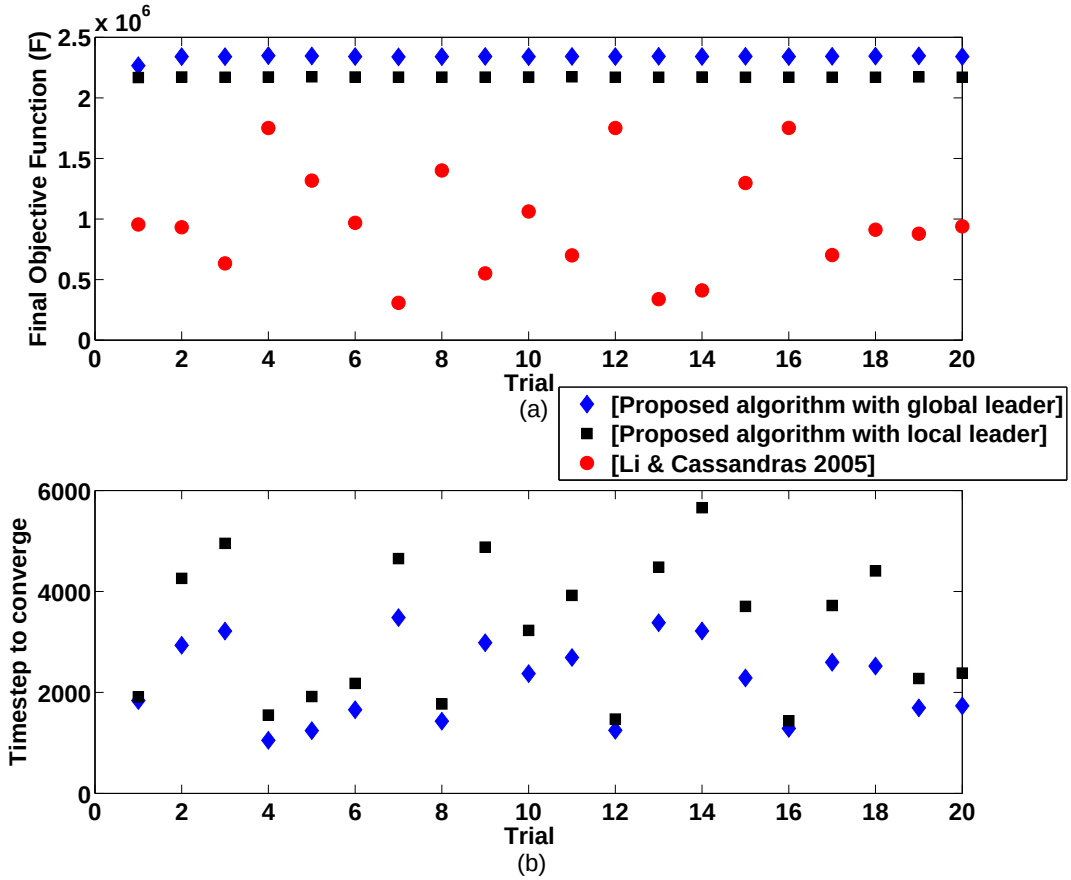

Figure 6.6: Simulation results using the proposed algorithm based on both the global and local leader and the standard algorithm [84] for different value of $\boldsymbol{p}_t$: (a) final value of the objective function. Higher value of F means better coverage performance; (b) time-step until all sensors converge to the final configuration. As can be seen from (a), both the proposed algorithms outperform the standard algorithm. The local leader based algorithm results in a lower final objective function and a slower convergence time compared to one with the global leader.

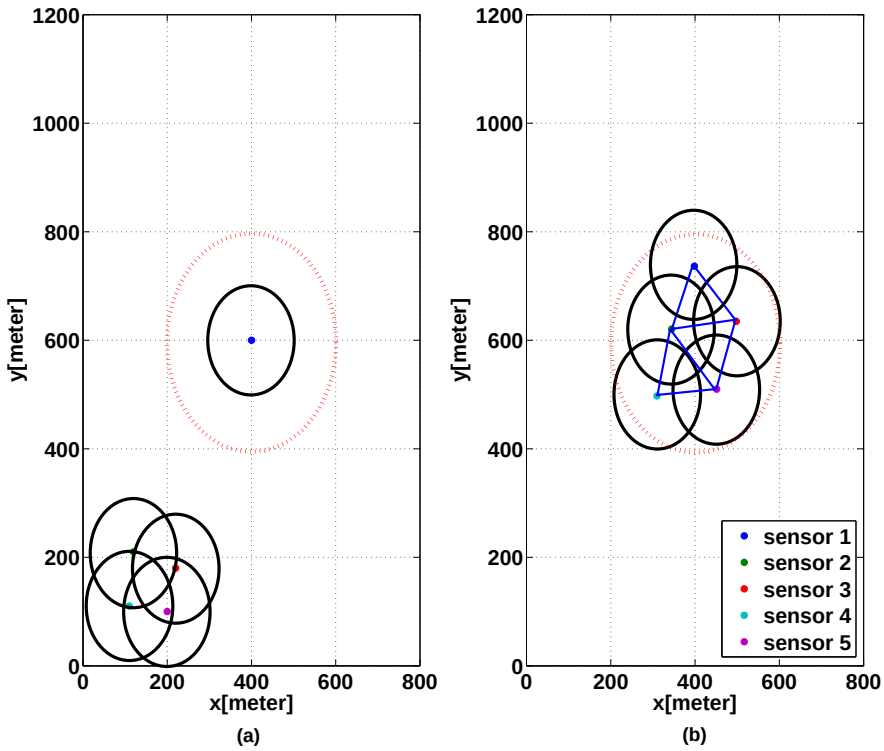

Figure 6.7: Final configuration of the sensors by using (a) the standard algorithm in [84]; (b) the proposed algorithm with local leader. The area inside the dashed circle has higher density function. As can be seen from (a), by using the standard algorithm, only sensor 1 which could participate in the coverage task since the rest do not have sufficient information. Thus in the final configuration, there exists several isolated sensors. Meanwhile, as can be observed from (b), by using the proposed algorithm, all sensors participate in the coverage task, i.e., there is no isolated sensors in the final configuration.

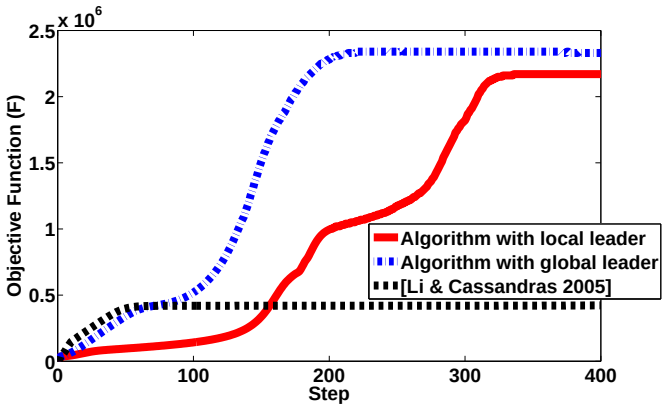

Figure 6.8: Objective function of the coverage problem. The solid, dashed-dot and dashed line represent the evolution of the objective function by using the proposed algorithm with local leader, the proposed algorithm with global leader and the standard algorithm in [84] respectively. As can be seen, both the proposed algorithms result in a better coverage performance compared to the standard coverage algorithm in [84] indicated by a higher value of the objective function. The proposed algorithm with local leader achieves a lower final objective function value and converges slower compared to the algorithm with the global leader. This is due to that for the global leader case, the communication range is assumed to be unlimited so that the sensors do not need to maintain the connectivity among themselves.

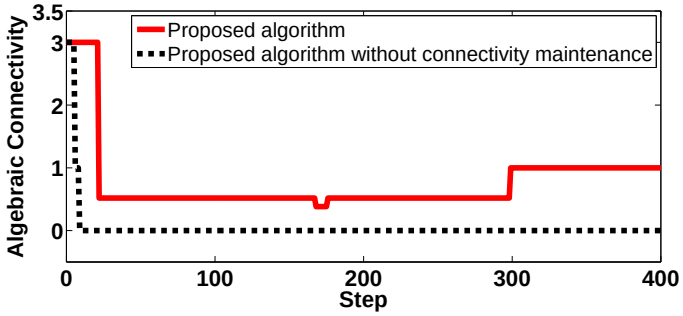

Figure 6.9: Connectivity between the sensors during the deployment. The solid and dashed line represent the connectivity between the mobile sensors with the proposed algorithm and with the proposed algorithm without considering connectivity maintenance. As can be seen, without the connectivity maintenance, the topology between the sensors will be disconnected, indicated by the algebraic connectivity value equals to 0.

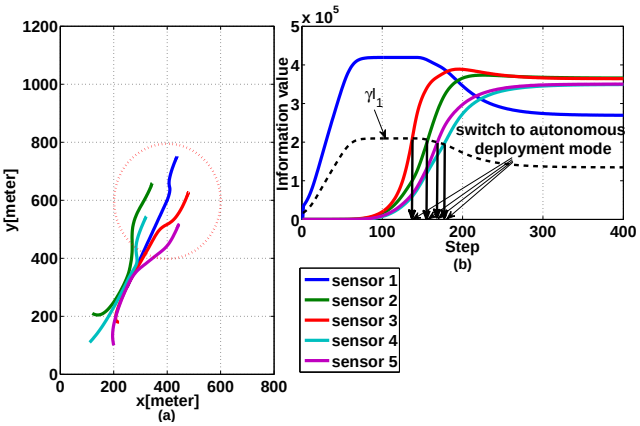

Figure 6.10: (a) Trajectories of the mobile sensors during the deployment using the proposed algorithm with a global leader and (b) The information value of each sensor and the time of switching into a pure coverage algorithm for the followers. The solid line in (b) represents the evolution of the information value of each sensor over the time.

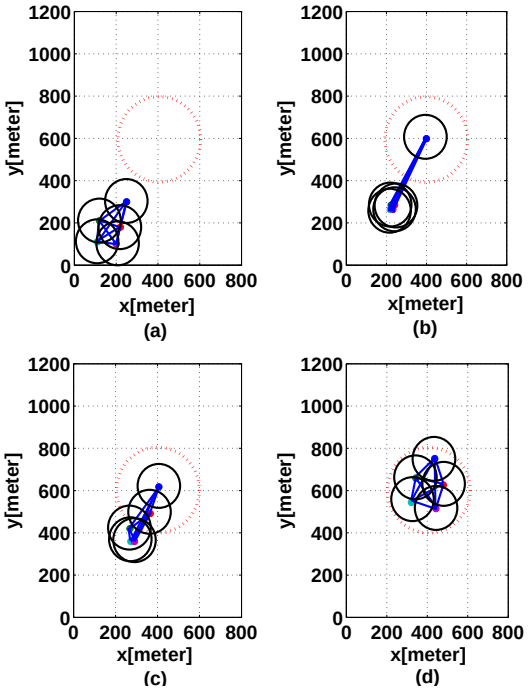

Figure 6.11: Snapshots of the deployment of the sensors with unlimited communication range using the proposed algorithm with a global leader at: (a) Initial Condition; (b) Step = 100; (c) Step = 150; (d) Final Condition. The area inside the dashed circle has higher density function. The lines connecting the sensors represent the communication graph between the sensors.

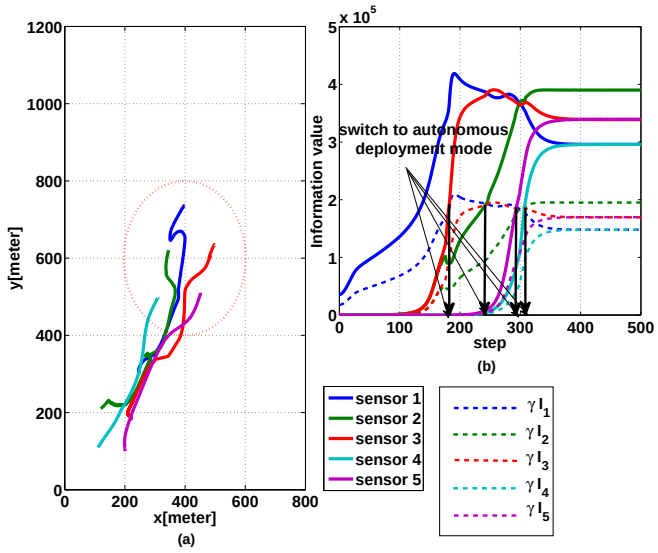

Figure 6.12: (a) Trajectories of the mobile sensors during the deployment using the proposed algorithm with local leader and (b) The information value of each sensor and the time of switching into autonomous deployment mode for the followers. The solid line in (b) represents the evolution of the information value of each sensor over the time.

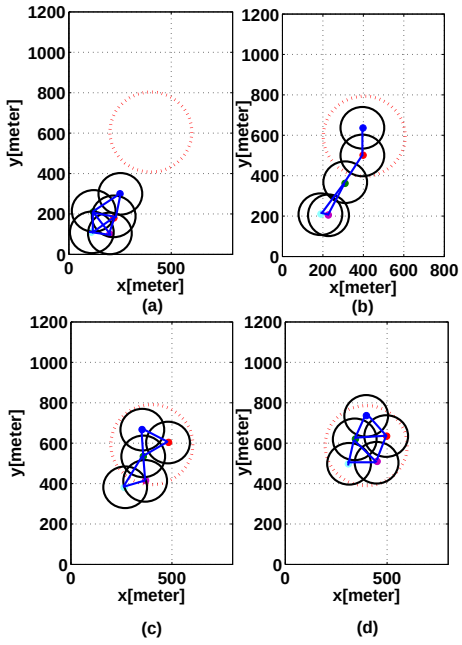

Figure 6.13: Snapshots of the deployment of the sensors using the proposed algorithm with local leader at: (a) Initial Condition; (b) Step = 200; (c) Step = 300; (d) Final Condition. The area inside the dashed circle has higher density function. The lines connecting the sensors represent the communication graph between the sensors. As can be seen, there is no isolated sensors in the final configuration.

7 Conclusions and Future Directions

7.1 Concluding Remarks

The present work focuses on design of performance-oriented distributed control for interconnected systems. So far unique is the exploitation of an additional degree of freedom offered by the introduction of the communication network in the control design. The main approaches along with the corresponding major results are highlighted in the remainder of the section.

While the performance of interconnected systems can be improved by exchanging information between the local controllers of the subsystems via the communication network, the overall system's stability guarantee may be lost under permanent communication link failures. In Chapter 3, a novel two-layer control architecture is proposed in order to guarantee the stability of the system when communication link failures occur while improving at the same time the performance of the overall system. The novel concept is to combine the advantages of decentralized and distributed control. Specifically, the interconnected system is first stabilized by designing the decentralized control without any information exchange between the local controllers. The next step is to improve the system performance by designing the distributed control together with the communication topology under a given communication network constraint. The problem is formulated as a mixed integer optimization problem. The proposed approach is applied to the design of a novel distributed damping control of power systems. Furthermore, it is investigated in-depth for the first time via numerical simulation how the addition of communication links influences the performance improvement of the overall system. It is shown from the simulations that adding more communication links may not always improve the performance of the interconnected system. Finally, the results are extended to the case of non-ideal communication network where it is assumed that identical and constant time delay exists in the communication links.

The design of communication topology results in a combinatorial optimization problem which makes it difficult to have a closed-loop solution which allows for some insights. In Chapter 4, the explicit solutions of the communication topology design for distributed control of interconnected systems with special class of physical interconnection topology, namely ring, star and line structures are presented for the first time. The innovative approach is based on the eigenvalue sensitivity analysis by reformulating the original optimization problem as an optimization problem involving the eigenvector related to the largest eigenvalue of the interconnected system. It is demonstrated that the closed-loop solutions of communication topology design can be obtained for the corresponding physical structure. The analysis starts with identical scalar subsystems and a single communication link. Afterwards, it is investigated how the heterogeneity of the subsystems' local dynamics, the number of subsystems and the strength of the physical interconnection between

these subsystems affect the solutions. The results are further extended by giving class of non-scalar subsystems whose analysis can be reduced to the case of scalar subsystems. Some discussions on how to deal with multiple communication links and some viewpoints on how to extend the results into more complex physical structure are presented. Finally, the eigenvalue sensitivity analysis is applied to the case where identical and constant time delay exists in the communication links which serves as a tool to investigate the influence of the communication topology and time delay on the performance of the system.

The results developed in Chapters 3 and 4 require system-wide information to compute the control law. In reality, however, it is difficult to obtain the whole system model due to, for example, geographical constraints between the subsystems. This issue is investigated in Chapter 5 by proposing a novel coordination algorithm to design the distributed control based only on some local plant model information. As a performance metric, the quadratic infinite horizon cost is considered. The original idea is to distribute the design of the control law among all subsystems. Specifically, first, a sufficient condition is given which enables the designer to decompose the global cost function into the sum of local cost functions. Each subsystem is then assigned a local cost function and, based on the limited plant model information, the optimization problem is iteratively solved by coordinating with the other subsystems. Furthermore, it is demonstrated that the algorithm can be combined with the two-layer control architecture developed in Chapter 3 in order to guarantee the stability of the overall system in the presence of permanent communication link failures. Even though the proposed algorithm can solve the control design in a distributed manner, it suffers from performance degradation compared to the centralized design which comes from the two-layer architecture and also the iterative process in the case of multiple links. The issue of how much the performance degrades compared to the centralized design method is still an open problem.

Finally, Chapter 6 deals with the non-convexity of the objective function for cooperative control problem and specifically the deployment of mobile sensor networks. The objective here is to guarantee that the agents avoid converging to the undesired local optima. The innovative concept is to identify the situation which causes the agents to converge to these local optima and develop a distributed coverage control law which avoids these local optima. It is shown that one possible situation resulting in such local optima is when mobile sensors are initially deployed and some sensors may be located far away from the region of interest and due to the sensor's limited sensing of range, some sensors may not be able to participate in the coverage task which results in a degradation of coverage performance of the robotic network. After characterizing the undesired local optima, a novel distributed coverage control law with global and local leader that guarantees the participation of all sensors in the coverage task is proposed by exploiting the use of information which can be communicated. At each time step, each sensor executes one of the two modes, namely autonomous deployment mode and following mode, depending on its information values. The novel strategy is that the sensors which have no or less information at their initial deployment follow their neighboring sensors which have higher information value until they gain sufficient information while maintaining the connectivity among them. The leader-follower algorithm in the proposed distributed control law is acting as a perturbation which operates on the gradient-based control law. In addition, we show that by using the

proposed control law, it is guaranteed that, in the final configuration of the deployment, there are no isolated sensors in the network which is demonstrated in numerical simulations. It is additionally shown that by exchanging more information gained by each sensor, the performance of the overall system can be significantly improved.

7.2 Outlook

The present dissertation serves as a first step towards designing adaptive and scalable distributed control for interconnected systems. The analysis in this dissertation is performed for the static case. However, in reality, the structure of the interconnected systems may change due to the addition or removal of subsystems or component failures. It is thus necessary to extend the current approach to deal with interconnected systems under dynamic changes. There is a number of exciting research directions emerging from this dissertation and some of them are the following:

- **Self-reconfigurable distributed control**: In general, the structure of the interconnected system may change due to uncertainty, addition of new subsystems or component failures. This occurs, for example, in (smart) power grid where unpredictable interconnection failures and, also, addition/removal of subsystems may result in structural changes of the system. Therefore, it is required to adapt the distributed control together with the communication topology in order to guarantee the stability and performance of the overall system under the structural changes.

- **Exchanged information vs. performance improvement**: While it is well-known, in the consensus problem for example, that exchanging information may improve the performance of the whole system, it is still unclear about the relation between the amount of information exchanged and the improvement of the performance. It is shown in this dissertation via simulations that, starting from a certain point, exchanging more information in the sense of allowing more communication links may not improve the performance significantly. It is thus necessary to develop a rigorous analysis on how the incremental of information exchanged influences the performance. Furthermore, it is significant to investigate the use of a communication network in order to control complex dynamical systems which are originally uncontrollable [91].

- **Combined optimization and feedback control**: Optimization is inherently advantageous with respect to performance and capability of handling constraints. Feedback control mechanisms, on the other hand, can guarantee stability even in the presence of fast dynamic changes and quickly react to disturbances in the system. The combination of optimization-based and feedback control approaches is considered as a powerful and effective way to deal with interconnected systems with different time-scale objectives, as met, for example, in power distribution systems. Therefore, another possible direction is to develop a two-layer architecture by combining distributed optimization and feedback control in order to deal with constraints and uncertainty in the interconnected systems.

A Power systems simulation parameters

Table A.1: Generator parameters

Parameter	G1	G2	G3	G4	G5
M_i	4.6	4.75	4.53	4.04	5
D_i	3.14	3.77	3.45	4.08	3.5
x_{di}	0.1026	0.1026	1.0260	0.1026	1.0260
x'_{di}	0.0339	0.0339	0.3390	0.0339	0.3390
T'_{doi}	5.67	5.67	5.67	5.67	5.67
b_{1i}	$6.66K_A$	$6.66K_A$	$6.66K_A$	$6.66K_A$	$6.66K_A$
b_{0i}	$3.33K_A$	$3.33K_A$	$3.33K_A$	$3.33K_A$	$3.33K_A$
c_{1i}	33.3	33.3	33.3	33.3	33.3
c_{0i}	3.33	3.33	3.33	3.33	3.33
K_A	200	200	200	200	200

Table A.2: Generator operating points

Parameter	G1	G2	G3	G4	G5
V	1.05	1.03	1.025	1.05	1.025
θ	0	0.1051	0.0943	0.0361	0.0907

Table A.3: Parameters of transmission lines [p.u.]

node	node	R	X	B/2
1	7	0.00435	0.01067	0.01536
2	6	0.00213	0.00468	0.00404
3	6	0.02004	0.06244	0.06408
4	8	0.00524	0.01184	0.01756
5	6	0.00711	0.02331	0.02732
6	7	0.04032	0.12785	0.15858
7	8	0.01724	0.04153	0.06014

B Proofs

B.1 Proof of Proposition 4.3.1

With no loss of generality, we re-order the numbering of subsystems in a clockwise direction as $1, 2, \cdots, N$. The overall dynamics of the interconnected system with ring topology can then be written as

$$\boldsymbol{A} = \begin{bmatrix} a & b & 0 & & b \\ b & a & b & & \\ & \ddots & \ddots & \ddots & \\ & & b & a & b \\ b & & 0 & b & a \end{bmatrix} \tag{B.1}$$

which is known as circulant matrix. The eigenvalue of the circulant matrix in (B.1) is given by [80]

$$\lambda_k = a + b\rho_N^k + b\rho_N^{(N-1)k} \tag{B.2}$$

where $\rho_N = e^{\frac{2i\pi}{N}} = \cos\left(\frac{2\pi}{N}\right) + i\sin\left(\frac{2\pi}{N}\right), i^2 = -1$. The eigenvalues can then be computed as

$$\begin{aligned} \lambda_k &= a + b\left(\cos\left(\frac{2\pi k}{N}\right) + i\sin\left(\frac{2\pi k}{N}\right)\right) + \\ &\quad + b\left(\cos\left(\frac{2\pi(N-1)k}{N}\right) + i\sin\left(\frac{2\pi(N-1)k}{N}\right)\right), \\ &= a + b\left(\cos\left(\frac{2\pi k}{N}\right) + \cos\left(\frac{2\pi(N-1)k}{N}\right)\right) + \\ &\quad + ib\underbrace{\left(\sin\left(\frac{2\pi k}{N}\right) + \sin\left(\frac{2\pi(N-1k}{N}\right)\right)}_{=0}, \\ &= a + 2b\cos\left(\frac{2\pi k}{N}\right). \end{aligned}$$

Furthermore, the corresponding eigenvector is given by

$$\boldsymbol{v}_k = [1, \rho_N^k, \rho_N^{2k}, \vdots, \rho_N^{(N-1)k}]^T. \tag{B.3}$$

The largest eigenvalue $\lambda_{\max}$ is achieved at $k = N$. Then the corresponding eigenvector can be computed as

$$\boldsymbol{v}_N = h[1, 1, \cdots, 1]^T, h \in \mathbb{R}. \tag{B.4}$$

The optimal communication link is the solution of (4.8) for $r = N$. However, from (B.4) since $v_{N_1} = \cdots = v_{N_N} = h$, we cannot find the solution of (4.8). Note that from

trace($\bar{\boldsymbol{A}}$) $= \sum \lambda_i(\bar{\boldsymbol{A}})$ we have $\sum \frac{\partial \lambda_i}{\partial K} = 0$. Thus, when $\frac{\partial \lambda_{\max}}{\partial K} < 0$, there exists at least one eigenvalue of $\boldsymbol{A}$ denoted by $\lambda_m(\boldsymbol{A})$ such that $\frac{\partial \lambda_m}{\partial K} > 0$. Therefore in order to find the optimal communication topology, we consider the case where only two eigenvalues affected by the perturbation which is the largest eigenvalue $\lambda_{\max}$ and the second largest eigenvalue λ_m where $m = \{1, N-1\}$. From (4.6), the optimization problem (4.16) can then be reformulated as

$$\begin{aligned} \underset{i,j}{\text{maximize}} \quad & |v_{m_i} v_{m_j}| \\ \text{subject to} \quad & v_{m_i} v_{m_j} < 0 \end{aligned} \tag{B.5}$$

where $\boldsymbol{v}_m$ is the eigenvector corresponding to the second largest eigenvalue λ_m. The eigenvector for $m = 1$ is then given by

$$\boldsymbol{v}_1 = \begin{bmatrix} 1 \\ \cos\left(\frac{2\pi}{N}\right) + i \sin\left(\frac{2\pi}{N}\right) \\ \cos\left(\frac{2\pi.2}{N}\right) + i \sin\left(\frac{2\pi.2}{N}\right) \\ \vdots \\ \cos\left(\frac{2\pi(N-1)}{N}\right) + i \sin\left(\frac{2\pi(N-1)}{N}\right) \end{bmatrix}. \tag{B.6}$$

Since $\left|\cos\left(\frac{2\pi(N-1)}{N}\right) + i \sin\left(\frac{2\pi(N-1)}{N}\right)\right| = 1$, the optimization problem (B.5) is equal to

$$\begin{aligned} \underset{i,j}{\text{maximize}} \quad & |\text{Re}\{v_{1_i}\}\text{Re}\{v_{1_j}\}| \\ \text{subject to} \quad & \text{Re}\{v_{1_i}\}\text{Re}\{v_{1_j}\} < 0. \end{aligned} \tag{B.7}$$

Since $-1 < \cos\left(\frac{2\pi l}{N}\right) < 1$, the solution of (B.7) is achieved at $i^\star = 1$ and

$$\begin{aligned} & \cos\left(\frac{2\pi l}{N}\right) = -1 \\ \Leftrightarrow \quad & \cos\left(\frac{2\pi l}{N}\right) = \cos(\pi) \\ \Leftrightarrow \quad & l = \frac{N}{2}, \end{aligned}$$

or $j^\star = \frac{N}{2} + 1$. In other words, the communication link is added between two local controllers with the largest distance. This completes the proof.

B.2 Proof of Proposition 4.3.2

In order to prove the proposition, instead of computing directly the elements of the corresponding eigenvector, we investigate their changes w.r.t perturbation. In order to do so, we introduce the following Lemmas.

Lemma B.2.1 For the following $N \times N$ matrix:

$$\boldsymbol{A} = \begin{bmatrix} g & b & 0 & & b \\ b & a & b & & \\ & \ddots & \ddots & \ddots & \\ & & b & a & b \\ b & & 0 & b & a \end{bmatrix} \tag{B.8}$$

the elements of the eigenvector corresponding to the largest eigenvalue, i.e. $\boldsymbol{v}_r = [v_{r_1}, \cdots v_{r_N}]$ satisfy

$$v_{r_{i+1}} = v_{r_{N-(i-1)}}$$

where $i = 1, \cdots, \lfloor \frac{N+1}{2} \rfloor$.

Proof: The eigenvector sensitivity analysis is employed in order to prove the Lemma. First, the matrix $\boldsymbol{A}$ in (B.8) can be written as

$$\boldsymbol{A} = \underbrace{\begin{bmatrix} a & b & 0 & & b \\ b & a & b & & \\ & \ddots & \ddots & \ddots & \\ & & b & a & b \\ b & & 0 & b & a \end{bmatrix}}_{\boldsymbol{A}_0} + \underbrace{\begin{bmatrix} \zeta & 0 & 0 & & 0 \\ 0 & 0 & 0 & & \\ & \ddots & \ddots & \ddots & \\ & & 0 & 0 & 0 \\ 0 & & 0 & 0 & 0 \end{bmatrix}}_{\Delta \boldsymbol{A}} \tag{B.9}$$

where $g = a + \zeta$. In other words, the matrix $\boldsymbol{A}$ in (B.8) can be seen as matrix $\boldsymbol{A}_0$ which is perturbed by the matrix $\Delta\boldsymbol{A}$. As shown in (B.4), the eigenvector corresponding to the largest eigenvalue of matrix $\boldsymbol{A}_0$ is $\boldsymbol{v}_r^{\boldsymbol{A}_0} = [1, \cdots, 1]^T$. Thus in order to show that $\boldsymbol{v}_{r_{i+1}}^{\boldsymbol{A}} = \boldsymbol{v}_{r_{N-(i-1)}}^{\boldsymbol{A}}$, we need to show

$$dv_{r_{i+1}}^{\boldsymbol{A}_0} = dv_{r_{N-(i-1)}}^{\boldsymbol{A}_0},$$

i.e. the direction and magnitude of the movement of the $(i+1)$-th and $(N-(i-1))$-th element of the eigenvector corresponding to the largest eigenvalue of the matrix $\boldsymbol{A}_0$ when it is perturbed by the matrix $\Delta\boldsymbol{A}$ are equal.

For the eigenvalue problem which depends on the design variable ζ given as

$$[\boldsymbol{A}(\zeta) - \lambda_i(\zeta)\boldsymbol{I}]\boldsymbol{v}_i(\zeta) = 0, \tag{B.10}$$

the first-order design sensitivities of the eigenvectors with respect to the design ζ represented by $\frac{d\boldsymbol{v}_i}{d\zeta}$ is given by [132]

$$[\boldsymbol{A} - \lambda_i \boldsymbol{I}]\frac{d\boldsymbol{v}_i}{d\zeta} = -\left[\frac{\partial \boldsymbol{A}}{\partial \zeta} - \lambda_i' \boldsymbol{I}\right]\boldsymbol{v}_i \tag{B.11}$$

where $\lambda_i' = \frac{\partial \lambda_i}{\partial \zeta}$ and $\boldsymbol{A}$ is defined in (B.9). For the largest eigenvalue of $\boldsymbol{A}_0$ and its eigenvector, the left-hand-side of (B.11) can be computed as

$$[\boldsymbol{A} - \lambda_r \boldsymbol{I}] \frac{d\boldsymbol{v}_r}{d\zeta} = \begin{bmatrix} \hat{d} & b & 0 & & b \\ b & \hat{a} & b & & \\ & \ddots & \ddots & \ddots & \\ & & b & \hat{a} & b \\ b & & 0 & b & \hat{a} \end{bmatrix} \frac{d\boldsymbol{v}_r}{d\zeta}$$

where $\hat{a} = a - \lambda_r$, $\hat{d} = d - \lambda_r$. The right-hand-side of (B.11) can also be computed as

$$\begin{aligned} \left[\frac{\partial \boldsymbol{A}}{\partial \zeta} - \lambda_r' \boldsymbol{I}\right] \boldsymbol{v}_r &= -\left[\begin{pmatrix} \text{sign}(\zeta) & 0 & \cdots & 0 \\ 0 & 0 & & 0 \\ \vdots & & \ddots & \vdots \\ 0 & \cdots & \cdots & 0 \end{pmatrix} - \lambda_r' \begin{pmatrix} 1 & 0 & \cdots & 0 \\ 0 & 1 & & 0 \\ \vdots & & \ddots & \vdots \\ 0 & \cdots & \cdots & 1 \end{pmatrix} \right] \boldsymbol{v}_r \\ &= \begin{bmatrix} -\text{sign}(\zeta) + \lambda_r' & 0 & 0 & & 0 \\ 0 & & \lambda_r' & 0 & \\ & & \ddots & \ddots & \ddots \\ & & & 0 & \lambda_r' & 0 \\ 0 & & & 0 & 0 & \lambda_r' \end{bmatrix} \boldsymbol{v}_r. \end{aligned}$$

Since from (B.4) it is known that $\boldsymbol{v}_r = [k, \cdots, k]^T$, without loss of generality, taking $k = 1$, Equation (B.11) becomes

$$\begin{bmatrix} \hat{d} & b & 0 & & b \\ b & \hat{a} & b & & \\ & \ddots & \ddots & \ddots & \\ & & b & \hat{a} & b \\ b & & 0 & b & \hat{a} \end{bmatrix} \frac{d\boldsymbol{v}_r}{d\zeta} = \begin{bmatrix} \lambda_r' - \text{sign}(\zeta) \\ \lambda_r' \\ \vdots \\ \lambda_r' \\ \lambda_r' \end{bmatrix}.$$

The above equation can be written by N equations as follows.

$$\begin{aligned} \hat{d}x_1 + bx_2 + bx_N &= \lambda_r' - sign(\zeta) \\ bx_1 + \hat{a}x_2 + bx_3 &= \lambda_r' \\ bx_2 + \hat{a}x_3 + bx_4 &= \lambda_r' \\ &\vdots \\ bx_{N-2} + \hat{a}x_{N-1} + bx_N &= \lambda_r' \\ bx_1 + bx_{N-1} + \hat{a}x_N &= \lambda_r' \end{aligned}$$

where $x_i = \frac{dv_{r_i}}{d\zeta}$. Subtracting the $i-$th and $N-(i-2)$-th equation for $i = 2, \cdots, \lceil \frac{N}{2} \rceil$ gives $\lfloor \frac{N-1}{2} \rfloor$ equations which can be written as

$$\underbrace{\begin{bmatrix} \hat{a} & b & 0 & & 0 \\ b & \hat{a} & b & & \\ & \ddots & \ddots & \ddots & \\ & & b & \hat{a} & b \\ 0 & & 0 & b & \hat{a} \end{bmatrix}}_{\bar{\boldsymbol{R}}} \begin{bmatrix} x_2 & - & x_N \\ x_3 & - & x_{N-1} \\ & \vdots & \\ x_{\lceil \frac{N}{2} \rceil - 1} & - & x_{N-(\lceil \frac{N}{2} \rceil - 3)} \\ x_{\lceil \frac{N}{2} \rceil} & - & x_{N-(\lceil \frac{N}{2} \rceil - 2)} \end{bmatrix} = \begin{bmatrix} 0 \\ 0 \\ \vdots \\ 0 \\ 0 \end{bmatrix}.$$

Note that the matrix $\bar{\boldsymbol{R}}$ is nonsingular. Thus it can be computed

$$\begin{bmatrix} x_2 & - & x_N \\ x_3 & - & x_{N-1} \\ & \vdots & \\ x_{\lceil \frac{N}{2} \rceil - 1} & - & x_{N-(\lceil \frac{N}{2} \rceil - 3)} \\ x_{\lceil \frac{N}{2} \rceil} & - & x_{N-(\lceil \frac{N}{2} \rceil - 2)} \end{bmatrix} = \bar{\boldsymbol{R}}^{-1} \begin{bmatrix} 0 \\ 0 \\ \vdots \\ 0 \\ 0 \end{bmatrix} = \begin{bmatrix} 0 \\ 0 \\ \vdots \\ 0 \\ 0 \end{bmatrix},$$

i.e. $x_{r_{i+1}} = x_{r_{N-(i-1)}}, i = 1, \cdots, \lfloor \frac{N+1}{2} \rfloor$. This completes the proof. ■

Lemma B.2.2 The largest eigenvalue of the $N \times N$ matrix:

$$\boldsymbol{A} = \begin{bmatrix} a+\zeta & b & 0 & & b \\ b & a & b & & \\ & \ddots & \ddots & \ddots & \\ & & b & a & b \\ b & & 0 & b & a \end{bmatrix} \tag{B.12}$$

where $|\zeta| < |a|$ is given by $\lambda_r(\boldsymbol{A}) = \lambda_r(\boldsymbol{A}_0) + \frac{1}{N}\text{sign}(\zeta)$ where $\lambda_r(\boldsymbol{A}_0)$ is the largest eigenvalue of $\boldsymbol{A}$ when $\zeta = 0$.

Proof: The matrix $\boldsymbol{A}$ in (B.12) can be written as

$$\boldsymbol{A} = \underbrace{\begin{bmatrix} a & b & 0 & & b \\ b & a & b & & \\ & \ddots & \ddots & \ddots & \\ & & b & a & b \\ b & & 0 & b & a \end{bmatrix}}_{A_0} + \underbrace{\begin{bmatrix} \zeta & 0 & 0 & & 0 \\ 0 & 0 & 0 & & \\ & \ddots & \ddots & \ddots & \\ & & 0 & 0 & 0 \\ 0 & & 0 & 0 & 0 \end{bmatrix}}_{\bar{\boldsymbol{P}}}$$

where the matrix $\bar{\boldsymbol{P}}$ can be seen as a perturbation matrix working on the matrix $\boldsymbol{A}_0$. From (4.10), the sensitivity of the largest eigenvalue of $\boldsymbol{A}_0$ can be computed as

$$\lambda_r' = \frac{\partial \lambda_r}{\partial \zeta} = v_{r_1}^2 \text{sign}(\zeta).$$

Furthermore, from (B.4) it is known that $\boldsymbol{v}_r = [k, \cdots, k]^T$. The normalized $\boldsymbol{v}_r$ is given by $k = \frac{1}{\sqrt{N}}$. The sensitivity of the largest eigenvalue is then equal to $\lambda_r' = \frac{1}{N}\text{sign}(\zeta)$. Thus the largest eigenvalue of the matrix $\boldsymbol{A}$ is then given by

$$\lambda_r(\boldsymbol{A}) = \lambda_r(\boldsymbol{A}_0) + \lambda_r' = \lambda_r(\boldsymbol{A}_0) + \frac{1}{N}\text{sign}(\zeta).$$

This completes the proof. ■

We are now ready to prove Proposition 4.3.2.

Proof: With no loss of generality, we re-order the numbering of subsystems in a clockwise direction as $1, 2, \cdots, N$ where the susbsystem 1 corresponds to the subsystem m. The overall dynamics of the interconnected system with ring topology can then be written as

$$\boldsymbol{A} = \begin{bmatrix} g & b & 0 & & b \\ b & a & b & & \\ & \ddots & \ddots & \ddots & \\ & & b & a & b \\ b & & 0 & b & a \end{bmatrix}. \tag{B.13}$$

As stated in Lemma B.2.1, the elements of the eigenvector corresponding to the largest eigenvalue of matrix $\boldsymbol{A}$ in (B.13), i.e. $\boldsymbol{v}_r$ has the following pattern: $v_{r_{i+1}} = v_{r_{N-(i-1)}}$. Next we will show that the following relationship between the elements of the eigenvector $\boldsymbol{v}_r$:

$$v_{r_1} \geq v_{r_2} \geq \cdots \geq v_{r_{\lfloor \frac{N+1}{2} \rfloor}} \tag{B.14}$$

or

$$v_{r_1} \leq v_{r_2} \leq \cdots \leq v_{r_{\lfloor \frac{N+1}{2} \rfloor}} \tag{B.15}$$

holds. First, from definition and using Lemma B.2.1, we can write

$$\begin{bmatrix} g & b & 0 & & b \\ b & a & b & & \\ & \ddots & \ddots & \ddots & \\ & & b & a & b \\ b & & 0 & b & a \end{bmatrix} \begin{bmatrix} v_{r_1} \\ v_{r_2} \\ \vdots \\ v_{r_3} \\ v_{r_2} \end{bmatrix} = \lambda_{\max} \begin{bmatrix} v_{r_1} \\ v_{r_2} \\ \vdots \\ v_{r_3} \\ v_{r_2} \end{bmatrix}. \tag{B.16}$$

Equation (B.16) can then be described by $\lfloor \frac{N}{2} \rfloor + 1$ equations where each equation is given by

$$g v_{r_1} + b v_{r_2} + b v_{r_2} = \lambda_r v_{r_1}$$

for $i = 1$ and

$$b v_{r_{i-1}} + a v_{r_i} + b v_{r_{i+1}} = \lambda_r v_{r_i}$$

for $i = 2, \cdots, \lfloor \frac{N}{2} \rfloor + 1$. When $i = 1$ we have

$$v_{r_1} = \frac{2b}{\lambda_r - g} v_{r_2}. \tag{B.17}$$

With no loss of generality, for the remainder of the proof we assume that $|g| < |a|$. From Lemma B.2.2 we have $\lambda_r(\boldsymbol{A}) = \lambda_r(\boldsymbol{A}_0) + \lambda' = 2b + a + \frac{1}{N}$. Equation (B.17) can then be written as

$$v_{r_1} = \frac{2b}{2b + a - g + \frac{1}{N}} v_{r_2}.$$

Since $|g| < |a|$, we have $a - g < 0$. Thus $\frac{2b}{2b+a-g+\frac{1}{N}} \geq 1$, i.e. $v_{r_1} \geq v_{r_2}$. Next, when $i = \lfloor \frac{N}{2} \rfloor + 1$ we have

$$v_{r_{\lfloor \frac{N}{2} \rfloor}} = \frac{\lambda_r - a}{2b} v_{r_{\lfloor \frac{N}{2} \rfloor + 1}} = \frac{2b + \frac{1}{N}}{2b} v_{r_{\lfloor \frac{N}{2} \rfloor + 1}}.$$

Since $\frac{2b+\frac{1}{N}}{2b} \geq 1$, we have $v_{r_{\lfloor \frac{N}{2} \rfloor}} \geq v_{r_{\lfloor \frac{N}{2} \rfloor + 1}}$. In addition, when $i = \lfloor \frac{N}{2} \rfloor$ we have

$$b v_{r_{\lfloor \frac{N}{2} \rfloor - 1}} + a v_{r_{\lfloor \frac{N}{2} \rfloor}} + b v_{r_{\lfloor \frac{N}{2} \rfloor + 1}} = \lambda_r v_{r_{\lfloor \frac{N}{2} \rfloor}}. \tag{B.19}$$

Substituting (B.18), Equation (B.19) can be written as

$$v_{r_{\lfloor \frac{N}{2} \rfloor - 1}} = \underbrace{\frac{1}{b} \left[\lambda_r - a - \frac{2b^2}{\lambda_r - a} \right]}_{= k_{\lfloor \frac{N}{2} \rfloor}} v_{r_{\lfloor \frac{N}{2} \rfloor}}.$$

The term $k_{\lfloor \frac{N}{2} \rfloor} = \frac{1}{b} \left[\lambda_r - a - \frac{2b^2}{\lambda_r - a} \right]$ can be re-written as

$$\begin{aligned} k_{\lfloor \frac{N}{2} \rfloor} &= \frac{1}{b} \left[\lambda_r - a - \frac{2b^2}{\lambda_r - a} \right] \\ &= \frac{1}{b} \left[(2b + a + \frac{1}{N}) - a - \frac{2b^2}{(2b + a + \frac{1}{N}) - a} \right] \\ &= 2 + \frac{1}{bN} - \frac{2b^2}{2b^2 + \frac{b}{N}}. \end{aligned}$$

Taking the derivative of $k_{\lfloor \frac{N}{2} \rfloor}$ w.r.t. N we have

$$\frac{\partial k_{\lfloor \frac{N}{2} \rfloor}}{\partial N} = -\frac{1}{bN^2} - \frac{b}{N^2 \left(2b^2 + \frac{b}{N}\right)^2} < 0, \tag{B.20}$$

i.e. $k_{\lfloor \frac{N}{2} \rfloor}$ is a decreasing function of N. Furthermore, when $N \to \infty$ we have $k_{\lfloor \frac{N}{2} \rfloor} \to 1$. Thus it can be concluded that $k_{\lfloor \frac{N}{2} \rfloor} \geq 1$, i.e. $v_{r_{\lfloor \frac{N}{2} \rfloor - 1}} \geq v_{r_{\lfloor \frac{N}{2} \rfloor}}$. Using the similar procedure

as above, when $i = \left\lfloor \frac{N}{2} \right\rfloor - 1$ we have

$$v_{r_{\left\lfloor \frac{N}{2} \right\rfloor - 2}} = \underbrace{\frac{1}{b}\left[\lambda_r - a - \frac{b}{k_{\left\lfloor \frac{N}{2} \right\rfloor}}\right]}_{=k_{\left\lfloor \frac{N}{2} \right\rfloor - 1}} v_{r_{\left\lfloor \frac{N}{2} \right\rfloor - 1}}. \tag{B.21}$$

The term $k_{\left\lfloor \frac{N}{2} \right\rfloor - 1} = \frac{1}{b}\left[\lambda_r - a - \frac{b}{k_{\left\lfloor \frac{N}{2} \right\rfloor}}\right]$ can be re-written as

$$k_{\left\lfloor \frac{N}{2} \right\rfloor - 1} = 2 + \frac{1}{bN} - \frac{1}{k_{\left\lfloor \frac{N}{2} \right\rfloor}}.$$

Taking the derivative of $k_{\left\lfloor \frac{N}{2} \right\rfloor - 1}$ w.r.t. N we have

$$\frac{\partial k_{\left\lfloor \frac{N}{2} \right\rfloor - 1}}{\partial N} = -\frac{1}{bN^2} - b\frac{\partial\left(\frac{1}{k_{\left\lfloor \frac{N}{2} \right\rfloor}}\right)}{\partial N} < 0.$$

In addition, when $N \to \infty$ we have $k_{\left\lfloor \frac{N}{2} \right\rfloor - 1} \to 1$. Again, it can be concluded that $k_{\left\lfloor \frac{N}{2} \right\rfloor - 1} \geq 1$, i.e. $v_{r_{\left\lfloor \frac{N}{2} \right\rfloor - 2}} \geq v_{r_{\left\lfloor \frac{N}{2} \right\rfloor - 1}}$. Finally, we can write

$$v_{r_{j-1}} = \underbrace{\frac{1}{b}\left[\lambda_r - a - \frac{b}{k_{j+1}}\right]}_{=k_j} v_{r_j} \tag{B.22}$$

for $3 \leq j \leq \left\lfloor \frac{N}{2} \right\rfloor - 2$. Furthermore, it can be proven in the similar way that $k_j \geq 1$ which results in $v_{r_{j-1}} \geq v_{r_j}$. Thus, by collecting all results we can conclude that

$$v_{r_1} \geq v_{r_2} \geq \cdots \geq v_{r_{\left\lfloor \frac{N+1}{2} \right\rfloor}}.$$

The optimal communication link is formulated as the optimization problem (4.8) whose from (B.14), the solution is given by $i^\star = 1 = m$ and $j^\star = 2$ or $j^\star = N$.

For the case $|g| > |a|$, it can also be proven in a similar fashion that

$$v_{r_1} \leq v_{r_2} \leq \cdots \leq v_{r_{\left\lfloor \frac{N+1}{2} \right\rfloor}}.$$

Thus the solution of (4.8) is given by $i^\star = \left\lfloor \frac{N+1}{2} \right\rfloor$ and $j^\star = \left\lfloor \frac{N+1}{2} \right\rfloor - 1$ or $j^\star = \left\lfloor \frac{N+1}{2} \right\rfloor + 1$. This completes the proof. ■

B.3 Proof of Lemma 4.3.4

The eigenvalues of the matrix $\boldsymbol{A}$ in (4.31) are the solution of the following equation

$$|\lambda \boldsymbol{I} - \boldsymbol{A}| = \underbrace{\begin{vmatrix} \lambda - g & -b & -b & \cdots & -b \\ -b & \lambda - a & 0 & & 0 \\ -b & 0 & \lambda - a & & \vdots \\ \vdots & \vdots & & \ddots & 0 \\ -b & 0 & \cdots & 0 & \lambda - a \end{vmatrix}}_{=\hat{L}} = 0.$$

Applying the Laplace's formula, $\hat{L}$ can be written as

$$\hat{L} = (-1)^{1+N}(-b) \underbrace{\begin{vmatrix} -b & -b & -b & \cdots & -b \\ \lambda - a & 0 & 0 & \cdots & 0 \\ 0 & \lambda - a & \ddots & & \vdots \\ \vdots & & \ddots & \ddots & \vdots \\ 0 & \cdots & 0 & \lambda - a & 0 \end{vmatrix}}_{=\bar{L} \in \mathbb{R}^{(N-1)\times(N-1)}}$$
$$+ (-1)^{N+N}(\lambda - a) \underbrace{\begin{vmatrix} \lambda - d & -b & -b & \cdots & -b \\ -b & \lambda - a & 0 & \cdots & 0 \\ -b & 0 & \ddots & & \vdots \\ \vdots & \vdots & & \ddots & 0 \\ -b & 0 & \cdots & 0 & \lambda - a \end{vmatrix}}_{=\tilde{L} \in \mathbb{R}^{(N-1)\times(N-1)}}.$$

Applying the Laplace's formula, $\bar{L}$ can be computed as

$$\bar{L} = (-1)^{1+N}(-b)(-1)^{1+(N-1)}(-b) \underbrace{\begin{vmatrix} \lambda - a & 0 & \cdots & 0 \\ 0 & \lambda - a & & \vdots \\ \vdots & & \ddots & 0 \\ 0 & \cdots & 0 & \lambda - a \end{vmatrix}}_{\in \mathbb{R}^{(N-2)\times(N-2)}}$$
$$= (-1)^{2N+1} b^2 (\lambda - a)^{N-2}$$
$$= -b^2 (\lambda - a)^{N-2}.$$

Next we compute $\tilde{L}$. Again, applying the Laplace's formula results in

$$\tilde{L} = (\lambda - a)(-b)(-1)^{N-1+1} \bar{S}_{N-2} + (\lambda - a)^2 (-1)^{(N-1)+(N-1)} \tilde{S}_{N-2}$$
$$= (\lambda - a)(-b)(-1)^{1+(N-1)} \bar{S}_{N-2} + (\lambda - a)^2 (-b)(-1)^{1+(N-2)} \bar{S}_{N-3}$$
$$+ (\lambda - a)^3 (-1)^{(N-2)+(N-2)} \tilde{S}_{N-3}$$

where

$$\bar{S}_i = \underbrace{\begin{vmatrix} -b & -b & -b & \cdots & -b \\ \lambda-a & 0 & 0 & \cdots & 0 \\ 0 & \lambda-a & \ddots & & \vdots \\ \vdots & & \ddots & \ddots & \vdots \\ 0 & \cdots & 0 & \lambda-a & 0 \end{vmatrix}}_{\in\mathbb{R}^{i\times i}}, \tilde{S}_i = \underbrace{\begin{vmatrix} \lambda-g & -b & -b & \cdots & -b \\ -b & \lambda-a & 0 & \cdots & 0 \\ -b & 0 & \ddots & & \vdots \\ \vdots & \vdots & & \ddots & 0 \\ -b & 0 & \cdots & 0 & \lambda-a \end{vmatrix}}_{\in\mathbb{R}^{i\times i}}.$$

Applying the Laplace's formula iteratively, we have

$$\begin{aligned}\tilde{L} &= (\lambda-a)(-b)(-1)^{1+(N-1)}\bar{S}_{N-2} + (\lambda-a)^2(-b)(-1)^{1+(N-2)}\bar{S}_{N-3} + \cdots + \\ &\quad + (\lambda-a)^{(N-3)-1}(-b)(-1)^{1+[N-((N-3)-1)]}\bar{S}_3 + (\lambda-a)^{N-3}\underbrace{\begin{vmatrix} \lambda-g & -b & -b \\ -b & \lambda-a & 0 \\ -b & 0 & \lambda-a \end{vmatrix}}_{=\tilde{S}_3}.\end{aligned}$$

Computing and substituting $\bar{S}_i$ and $\tilde{S}_3$, we have

$$\begin{aligned}\tilde{L} =& (\lambda-a)(-1)^{1+(N-1)}b^2(-1)^{1+(N-2)}(\lambda-a)^{(N-2)-1} \\ &+ (\lambda-a)^2(-1)^{1+(N-2)}b^2(-1)^{1+(N-3)}(\lambda-a)^{(N-3)-1} + \cdots + \\ &+ (\lambda-a)^{(N-3)-1}(-1)^{1+[N-(N-3-1)]}b^2(-1)^4(\lambda-a)^2 \\ &+ (\lambda-a)^{N-3}(\lambda-a)\left[(\lambda-g)(\lambda-a) - 2b^2\right].\end{aligned}$$

After some straightforward computations we have

$$\begin{aligned}\tilde{L} &= (\lambda-a)^{N-2}b^2(-1)^{2N-1} + (\lambda-a)^{N-2}b^2(-1)^{2N-3} + \cdots + \\ &\quad + (\lambda-a)^{N-2}b^2(-1)^9 + (\lambda-a)^{N-2}\left[(\lambda-g)(\lambda-a) - 2b^2\right] \\ &= \underbrace{-(\lambda-a)^{N-2}b^2 - \cdots - (\lambda-a)^{N-2}b^2}_{N-4} - 2b^2(\lambda-a)^{N-2} + (\lambda-a)^{N-1}(\lambda-g).\end{aligned}$$

Therefore, $\hat{L} = \bar{L} + \tilde{L}$ can be computed as

$$\begin{aligned}\hat{L} &= -b^2(\lambda-a)^{N-2} - (N-4)b^2(\lambda-a)^{N-2} - 2b^2(\lambda-a)^{N-2} + (\lambda-a)^{N-1}(\lambda-g) \\ &= (\lambda-a)^{N-2}\left[(\lambda-a)(\lambda-g) - (N-1)b^2\right].\end{aligned}$$

The eigenvalues of the matrix $\boldsymbol{A}$ in (4.34) are then the solution of

$$\begin{aligned}&(\lambda-a)^{N-2}\left[(\lambda-a)(\lambda-g) - (N-1)b^2\right] = 0, \\ \Leftrightarrow&(\lambda-a)^{N-2}\left[\lambda^2 - (a+g)\lambda + ag - (N-1)b^2\right] = 0\end{aligned}$$

which are given by

$$\begin{aligned}\lambda_1 &= \frac{a+g+\sqrt{(a+g)^2-4\left(ag-(N-1)b^2\right)}}{2}\\ \lambda_2 &= \frac{a+g-\sqrt{(a+g)^2-4\left(ag-(N-1)b^2\right)}}{2}\\ \lambda_3 &= \cdots=\lambda_N=a.\end{aligned}$$

This completes the proof.

B.4 Proof of Proposition 4.4.1

With no loss of generality, we re-order the numbering of subsystems in a clockwise direction as $1,2,\cdots,N$ where the susbsystem 1 corresponds to the subsystem m. Using the similar computation as for the identical subsystems, the matrix $\boldsymbol{A}$ can be written as $\boldsymbol{A}=\boldsymbol{C}\otimes-\hat{\boldsymbol{A}}$ where

$$\boldsymbol{C}=\begin{bmatrix}-\zeta & \bar{l} & \bar{l} & \cdots & \bar{l}\\ \bar{l} & -1 & 0 & & 0\\ \bar{l} & 0 & -1 & & \vdots\\ \vdots & \vdots & & \ddots & 0\\ \bar{l} & 0 & \cdots & 0 & -1\end{bmatrix}$$

where $\bar{l}=-l$. Furthermore, it can also be shown that the sensitivity of the largest eigenvalue of matrix $\boldsymbol{A}$ w.r.t. the control gain k can be written as $\frac{\partial\lambda_{\max}}{\partial k}\sim-2z_{r_i}z_{r_j}$ where $\boldsymbol{z}_r$ is the eigenvector corresponding the largest eigenvalue of $\boldsymbol{C}$. Thus the optimization problem is reduced to the scalar case.

B.5 Proof of Proposition 4.4.2

With no loss of generality, we re-order the numbering of subsystems where the subsystem with the largest degree, i.e. subsystem m as subsystem 1 and the others in clockwise direction as subsystem $2,\cdots,N$. The matrix $\boldsymbol{A}$ can be written as $\boldsymbol{A}=\boldsymbol{C}\otimes-\hat{\boldsymbol{A}}$ where

$$\boldsymbol{C}=\begin{bmatrix}-\zeta & \bar{l} & \bar{l} & & \bar{l}\\ \bar{l} & -1 & \bar{l} & & \\ & \ddots & \ddots & \ddots & \\ & & \bar{l} & -1 & \bar{l}\\ \bar{l} & & 0 & \bar{l} & -1\end{bmatrix}$$

where $\bar{l}=-l$. Furthermore, it can also be shown that the sensitivity of the largest eigenvalue of matrix $\boldsymbol{A}$ w.r.t. the control gain k can be written as $\frac{\partial\lambda_{\max}}{\partial k}\sim-2z_{r_i}z_{r_j}$ where $\boldsymbol{z}_r$ is the eigenvector corresponding the largest eigenvalue of $\boldsymbol{C}$. Thus the optimization problem is reduced to the scalar case.

B.6 Proof of Lemma 4.7.1

Assume that the perturbation K works on $\bar{A}_{ij}$ and $\bar{A}_{ji}$ of $\boldsymbol{A}_{\text{dist}}$. From (4.48) with $\boldsymbol{G}_K(\lambda)$ given by (4.49), the sensitivity of $\lambda_{\max}$ can be written as

$$\lambda'_{\max}(K) = \frac{\boldsymbol{v}_r^* \frac{\partial \boldsymbol{G}_K}{\partial K}(\lambda_{\max})\boldsymbol{w}_r}{\boldsymbol{v}_r^*(\boldsymbol{I}_N - \frac{\partial \boldsymbol{G}_K}{\partial \lambda_{\max}}(\lambda_{\max}))\boldsymbol{w}_r} \tag{B.23}$$

where $\left[\frac{\partial \boldsymbol{G}_K}{\partial K}\right]_{ij} = \left[\frac{\partial \boldsymbol{G}_K}{\partial K}\right]_{ji} = \text{sign}(K)e^{-\tau\lambda_{\max}}$ and zero otherwise, $\left[\frac{\partial \boldsymbol{G}_K}{\partial \lambda_{\max}}\right]_{ij} = \left[\frac{\partial \boldsymbol{G}_K}{\partial \lambda_{\max}}\right]_{ji} = -K\tau e^{-\tau\lambda_{\max}}$ and zero otherwise, $\left[\boldsymbol{I}_N - \frac{\partial \boldsymbol{G}_K}{\partial \lambda_{\max}}\right]_{ij} = \left[\boldsymbol{I}_N - \frac{\partial \boldsymbol{G}_K}{\partial \lambda_{\max}}\right]_{ji} = K\tau e^{-\tau\lambda_{\max}}$ and zero when $i \neq j$ and $\left[\boldsymbol{I}_N - \frac{\partial \boldsymbol{G}_K}{\partial \lambda_{\max}}\right]_{mm} = 1, \forall m$. Thus after some straightforward computation, we have

$$\lambda'_{\max} = \frac{e^{-\tau\lambda_{\max}}(v_{r_i}^* w_{r_j} + v_{r_j}^* w_{r_i})\ \text{sign}(K)}{\sum w_{r_i} v_{r_i}^* + K\tau e^{-\tau\lambda_{\max}}(v_{r_i}^* w_{r_j} + v_{r_j}^* w_{r_i})}. \tag{B.24}$$

Since $\boldsymbol{v}_r^* \boldsymbol{w}_r = 1$ we have

$$\begin{aligned} \lambda'_{\max} &= \frac{e^{-\tau\lambda_{\max}}(v_{r_i}^* w_{r_j} + v_{r_j}^* w_{r_i})\ \text{sign}(K)}{1 + K\tau e^{-\tau\lambda_{\max}}(v_{r_i}^* w_{r_j} + v_{r_j}^* w_{r_i})} \\ &= \frac{(v_{r_i}^* w_{r_j} + v_{r_j}^* w_{r_i})\ \text{sign}(K)}{e^{\tau\lambda_{\max}} + K\tau(v_{r_i}^* w_{r_j} + v_{r_j}^* w_{r_i})}. \end{aligned} \tag{B.25}$$

This completes the proof.

B.7 Proof of Lemma 4.7.3

The sensitivity of $\lambda_{\max}$ w.r.t. time delay τ can be written as

$$\lambda'_{\max}(\tau) = \frac{\boldsymbol{v}_r^* \frac{\partial \boldsymbol{G}_\tau}{\partial \tau}(\lambda_{\max})\boldsymbol{w}_r}{\boldsymbol{v}_r^*(\boldsymbol{I}_N - \frac{\partial \boldsymbol{G}_\tau}{\partial \lambda_{\max}}(\lambda_{\max}))\boldsymbol{w}_r} \tag{B.26}$$

where $\boldsymbol{G}_\tau(\lambda) = \boldsymbol{A}_{\text{dec}} + \boldsymbol{A}_{\text{dist}}(K)e^{-\tau\lambda}$. Computing each term, we have $\left[\frac{\partial \boldsymbol{G}_\tau}{\partial \tau}\right]_{ij} = \left[\frac{\partial \boldsymbol{G}_\tau}{\partial \tau}\right]_{ji} = -K\lambda_{\max}e^{-\tau\lambda_{\max}}$ and zero otherwise, $\left[\frac{\partial \boldsymbol{G}_\tau}{\partial \lambda_{\max}}\right]_{ij} = \left[\frac{\partial \boldsymbol{G}_\tau}{\partial \lambda_{\max}}\right]_{ji} = -K\tau e^{-\tau\lambda_{\max}}$ and zero otherwise, $\left[\boldsymbol{I}_N - \frac{\partial \boldsymbol{G}_\tau}{\partial \lambda_{\max}}\right]_{ij} = \left[\boldsymbol{I}_N - \frac{\partial \boldsymbol{G}_\tau}{\partial \lambda_{\max}}\right]_{ji} = K\tau e^{-\tau\lambda_{\max}}$ and zero when $i \neq j$ and $\left[\boldsymbol{I}_N - \frac{\partial \boldsymbol{G}_\tau}{\partial \lambda_{\max}}\right]_{mm} = 1, \forall m$. Thus after some straightforward computation, we have

$$\lambda'_{\max} = \frac{K\lambda_{\max}e^{-\tau\lambda_{\max}}(v_{r_i}^* w_{r_j} + v_{r_j}^* w_{r_i})}{\sum w_{r_i} v_{r_i}^* + K\tau e^{-\tau\lambda_{\max}}(v_{r_i}^* w_{r_j} + v_{r_j}^* w_{r_i})}. \tag{B.27}$$

Since $\boldsymbol{v}_r^* \boldsymbol{w}_r = 1$ we have

$$\begin{aligned} \lambda'_{\max} &= \frac{K\lambda_{\max} e^{-\tau\lambda_{\max}}(v^*_{r_i} w_{r_j} + v^*_{r_j} w_{r_i})}{1 + K\tau e^{-\tau\lambda_{\max}}(v^*_{r_i} w_{r_j} + v^*_{r_j} w_{r_i})} \\ &= -\frac{\lambda_{\max} K(v^*_{r_i} w_{r_j} + v^*_{r_j} w_{r_i})}{e^{\tau\lambda_{\max}} + K\tau(v^*_{r_i} w_{r_j} + v^*_{r_j} w_{r_i})}. \end{aligned} \tag{B.28}$$

This completes the proof.

Bibliography

[1] Automatica-networked control systems. http://automatica.dei.unipd.it/research/networked-control-systems.html.

[2] Mission & objectives. http://www.car-to-car.org/.

[3] Smart grid-das netz wird intelligent. http://www.abb.com/cawp/seitp202/77a7e74be1ea8904c12577050030ab14.aspx.

[4] Water quality monitoring system enabled by optical mems technology. http://www.memsjournal.com/2010/12/optical-mems-monitoring-system-for-water-quality.html.

[5] Enerfy future: Think efficiency. Technical report, the American Physical Society, September 2008.

[6] M.E. Aboul-Ela, A.A. Sallam, J.D. McCalley, and A.A. Fouad. Damping controller design for power system oscillations using global signals. *IEEE Transactions on Power Systems*, 11(2):767–773, 1996.

[7] Ali Ahmadzadeh, Ali Jadbabaie, and Vijay Kumar. Cooperative coverage using receding horizon control. In *Proceedings of European Control Conference*, pages 2470–2477, 2007.

[8] M. Aldeen and F. Crusca. Multimachine power system stabiliser design based on new lqr approach. *IEE Proceedings in Generation, Transmission and Distribution*, pages 494–502, 2002.

[9] B. Anderson, C. Yu, B. Fidan, and J. Hendrickx. Rigid graph control architectures for autonomous formations. *IEEE Control Systems*, 28(6):48–63, jan. 2008.

[10] J. Baillieul and P. J. Antsaklis. Control and communication challenges in networked real-time systems. *Proceedings of the IEEE*, 95(1):9–28, jan. 2007.

[11] L. Bakule. Decentralized control: An overview. *Annual Reviews in Control*, 32:87–98, aug. 2008.

[12] B. Bamieh, F. Paganini, and M.A. Dahleh. Distributed control of spatially invariant systems. *Automatic Control, IEEE Transactions on*, 47(7):1091–1107, jul 2002.

[13] N. Bamieh and P. G. Voulgaris. A convex characterization of distributed control problems in spatially invariant systems with communication constraints. *Systems Control Letters*, 54:575–583, 2005.

[14] L. D. Baskar, B. De Schutter, J. Hellendoorn, and Z. Papp. Traffic control and intelligent vehicle highway systems: a survey. *IET Intelligent Transport Systems*, 5(1):38–52, jan. 2011.

[15] F. Borrelli and T. Keviczky. Distributed lqr design for identical dynamically decoupled systems. *IEEE Transactions on Automatic Control*, 53(8):1901–1912, aug. 2008.

[16] A. Böttcher and S. Grudsky. *Spectral Properties of Banded Toeplitz Matrices*. SIAM, Philadelphia, PA, 2005.

[17] S. Boyd, L. E. Ghaoui, E. Feron, and V. Balakrishnan. Linear matrix inequalities in systems and control theory. *SIAM Studies in Applied Mathematics*, 15, 1994.

[18] S. Boyd and L. Vandenberghe. *Convex Optimization)*. Cambridge University Press, 2004.

[19] J. Bunch, C. Nielsen, and D. Sorensen. Rank one modification of the symmetric eigenproblem. *Numerical Mathematics*, 31:31–48, 1978.

[20] J. V. Burke, A. S. Lewis, and M. L. Overton. Improved distributed coverage control for robotic visual sensor network under limited energy storage. *Linear Algebra and its Applications*, 351-352:117–145, 2002.

[21] C. Caicedo and M. Zefran. A coverage algorithm for a class of non-convex regions. In *Proceedings of the IEEE Conference on Decision and Control*, pages 4244–4249, dec. 2008.

[22] Y. Cao and W. Ren. Multi-agent consensus using both current and outdated states with fixed and undirected interaction. *Journal of Intelligent and Robotic Systems*, 58(1):95–106, jan. 2010.

[23] C. G. Cassandras and W. Li. Sensor networks and cooperative control. *European Journal of Control*, 11:436–463, 2005.

[24] C.-C. Chen, S. Hirche, and M. Buss. Controller design and experimental validation for networked control systems with time-varying random delay. *Journal of the Society of Instrument and Control Engineers*, 47(8):676–685, 2008.

[25] R. Cogill and S. Lall. Control design for topology-independent stability of interconnected systems. In *Proceedings of American Control Conference*, pages 3717–3722, june 2004.

[26] R. Cogill and S. Lall. Topology independent controller design for networked systems. In *Decision and Control, 2004. CDC. 43rd IEEE Conference on*, pages 1788–1793, dec. 2004.

[27] J. Cortes, S. Martinez, T. Karatas, and F. Bullo. Coverage control for mobile sensing networks. *IEEE Transactions on Robotics and Automation*, 20(2):243–255, april 2004.

[28] Jorge Cortes, Sonia Martinez, and Francesco Bullo. Spatially-distributed coverage optimization and control with limited-range interactions. *ESAIM. Control, Optimisation and Calculus of Variations*, 11:691–719, 2005.

[29] R. Dai and M. Mesbahi. Optimal topology design for dynamic networks. In *Proceedings of the IEEE Conference on Decision and Control and European Control Conference*, pages 1280–1285, dec. 2011.

[30] R. D'Andrea and G.E. Dullerud. Distributed control design for spatially interconnected systems. *Automatic Control, IEEE Transactions on*, 48(9):1478–1495, sept. 2003.

[31] G. A. de Castro and F. Paganini. Convex synthesis of localized controllers for spatially invariant system. *Automatica*, 38:445–456, 2002.

[32] J. De La Ree, V. Centeno, J.S. Thorp, and A.G. Phadke. Synchronized phasor measurement applications in power systems. *IEEE Transactions on Smart Grid*, 1:20–27, 2010.

[33] P. DeLellis, M. di Bernardo, F. Garofalo, and M. Porfiri. Evolution of complex networks via edge snapping. *Circuits and Systems I: Regular Papers, IEEE Transactions on*, 57(8):2132–2143, aug. 2010.

[34] O. Demir and J. Lunze. A decomposition approach to decentralized and distributed control of spatially interconnected systems. In *Proceedings of the 18th IFAC World Congress*, pages 9109–9114, sep. 2011.

[35] Kun Deng, P. Barooah, P.G. Mehta, and S.P. Meyn. Building thermal model reduction via aggregation of states. In *American Control Conference (ACC), 2010*, pages 5118–5123, 2010.

[36] D. Dotta, A.S. e Silva, and I.C. Decker. Wide-area measurements-based two-level control design considering signal transmission delay. *IEEE Transactions on Power Systems*, 24(1):208–216, 2009.

[37] W.B. Dunbar. Distributed receding horizon control of dynamically coupled nonlinear systems. *Automatic Control, IEEE Transactions on*, 52(7):1249–1263, july 2007.

[38] J.W. Durham, R. Carli, and F. Bullo. Pairwise optimal coverage control for robotic networks in discretized environments. In *Proceedings of the IEEE Conference on Decision and Control*, pages 7286–7291, dec. 2010.

[39] I. Eker and T. Kara. Operation and control of a water supply system. *ISA Transactions*, 42:461–473, 2003.

[40] K. Engelborghs. Dde-biftool: a matlab package for bifurcation analysis of delay differential equations. Technical report, Department of Computer Science, Katholieke Universiteit Leuven, Belgium, March, 2000.

[41] M. Fardad, Fu Lin, and M.R. Jovanovic. On the optimal design of structured feedback gains for interconnected systems. In *Proceedings of the 48th IEEE Conference on Decision and Control*, pages 978–983, dec. 2009.

[42] M. Fardad, Fu Lin, and M.R. Jovanovic. Sparsity-promoting optimal control for a class of distributed systems. In *American Control Conference (ACC), 2011*, pages 2050–2055, 2011.

[43] F. Farokhi, C. Lagbort, and K. H. Johansson. Control design with limited model information. In *Proceedings of American Control Conference*, pages 4697–4704, 2011.

[44] Farhad Farokhi and Karl Henrik Johansson. Dynamic control design based on limited model information. In *Proceedings of the 49th Annual Allerton Conference on Communication, Control, and Computing*, 2011.

[45] R. Fraanje, P. Massioni, and M. Verhaegen. A decomposition approach to distributed control of dynamic deformable mirrors. *International Journal of Optimechatronics*, 4(3):269–284, 2010.

[46] Pascal Gahinet and Pierre Apkarian. A linear matrix inequality approach to h_∞ control. *International Journal of Robust and Nonlinear Control*, 4:421–448, 1994.

[47] A. Ghosh and S. Boyd. Growing well-connected graphs. In *Proceedings of the IEEE Conference on Decision and Control*, pages 6605–6611, dec. 2006.

[48] C. Godsil and G. Royle. *Algebraic Graph Theory*. Springer-Verlag, 2001.

[49] K. Gu and S. L. Niculescu. Survey on recent results in the stability and control of time-delay systems. *Journal of Dynamic Systems, Measurement, and Control*, 125(2):158–165, jan. 2003.

[50] A. Gusrialdi, R. Dirza, T. Hatanaka, and M. Fujita. Improved distributed coverage control for robotic visual sensor network under limited energy storage. *International Journal of Imaging and Robotics*, 2012, submitted.

[51] A. Gusrialdi, R. Dirza, and S. Hirche. Information-driven distributed coverage algorithms for mobile sensor networks. In *Networking, Sensing and Control (ICNSC), 2011 IEEE International Conference on*, pages 242–247, april 2011.

[52] A. Gusrialdi, T. Hatanaka, and M. Fujita. Coverage control for mobile networks with limited-range anisotropic sensors. In *Proceedings of the IEEE Conference on Decision and Control*, pages 4263–4268, dec. 2008.

[53] A. Gusrialdi and S. Hirche. Performance-oriented communication topology design for large-scale interconnected systems. In *Proceedings of the IEEE Conference on Decision and Control*, pages 5707–5713, dec. 2010.

[54] A. Gusrialdi and S. Hirche. Communication topology design for large-scale interconnected systems with time delay. In *American Control Conference (ACC), 2011*, pages 4508–4513, 2011.

[55] A. Gusrialdi and S. Hirche. On the explicit solution of communication topology design for distributed control of large-scale interconnected systems. In *Proceedings of American Control Conference*, june 2012, to appear.

[56] A. Gusrialdi, S. Hirche, D. Asikin, T. Hatanaka, and M. Fujita. Voronoi based coverage control with anisotropic sensors and experimental case study. *Intelligent Service Robotics*, 2(4):195–204, june 2009.

[57] A. Gusrialdi and Lu Zeng. Distributed deployment algorithms for robotic visual sensor networks in non-convex environment. In *Networking, Sensing and Control (ICNSC), 2011 IEEE International Conference on*, pages 445–450, april 2011.

[58] B. Hardekopf, K. Kwiat, and S. Upadhyaya. A decentralized voting algorithm for increasing dependability in distributed systems. In *Proceedings of the 5th World Conference on Systemic, Cybernetics and Informatics*, sep. 2001.

[59] A.A. Hashmani and I. Erlich. Power system stabilizer by using supplementary remote signals. *16th Power Systems Computation Conference, July 2008 Glasgow, Scotland*, 2008.

[60] T. Hatanaka, T. Ibuki, A. Gusrialdi, and M. Fujita. Coverage control for camera sensor networks: Its implementation and experimental verification. In *Proceedings of the 17th Mediterranean Conference on Control and Automation*, pages 446–451, june 2009.

[61] Y-C. Ho and K-C. Chu. Team decision theory and information structures in optimal control problems - part i. *Automatic Control, IEEE Transactions on*, 17(1):15–22, 1972.

[62] R. Horn and C. R. Johnson. *Matrix Analysis*. Cambridge University Press, New York, 2009.

[63] Andrew Howard, Maja J Mataric, and Gaurav S Sukhatme. Mobile sensor network deployment using potential fields: A distributed, scalable solution to the area coverage problem. In *Proceedings of the 6th International Symposium on Distributed Autonomous Robotics Systems*, pages 299–308, 2002.

[64] Bin Huang. *Stability of Distribution Systems with a Large Penetration of Distributed Generation*. PhD thesis, Universität of Dortmund, 2006.

[65] H. Huang, C. Yu, A. Gusrialdi, and S. Hirche. Topology design for distributed formation control towards optimal convergence rate. In *Proceedings of American Control Conference*, june 2012, to appear.

[66] Huang Huang, Changbin Yu, and Qinghe Wu. Distributed lqr design for multi-agent formations. In *Proceedings of the 49th IEEE Conference on Decision and Control*, pages 4535–4540, dec. 2010.

[67] E. Jarlebring. *The spectrum of delay-differential equations: numerical methods, stability and perturbation*. PhD thesis, Technische Universität Carolo-Wilhelmina zu Braunschweig, 2008.

[68] M. R. Jovanović. On the optimality of localized distributed controllers. *Int. J. Systems, Control and Communications*, 2(1/2/3):82–99, 2010. Special issue on Information Processing and Decision Making in Distributed Control Systems.

[69] I. Kamwa, R. Grondin, and Y. Hbert. Wide-area measurement based stabilizing control of large power systemsa decentralized/hierarchical approach. *IEEE Transactions on Power Systems*, 16(1):136–153, 2001.

[70] D. Kempe and F. McSherry. A decentralized algorithm for spectral analysis. *Journal of Computer and System Science*, 74(1):70–83, 2008.

[71] O. Khorsand and A. Gattami. A decentralized stabilization scheme for a class of large-scale interconnected systems. In *Proceedings of the 18th IFAC World Congress*, pages 1404–1409, sep. 2011.

[72] R. S. Komali and A. B. MacKenzie. Distributed topology control in ad-hoc networks: a game theoretic perspective. In *Proceedings of IEEE Consumer Coomunication and Network Conference*, pages 563–568, dec. 2007.

[73] B. H. Korte and J. Vygen. *Combinatorial optimization: theory and algorithms.* Berlin: Springer-Verlag, 2000.

[74] A. Kwok and S. Martinez. Deployment algorithms for a power-constrained mobile sensor network. *International Journal of Robust and Nonlinear Control*, 20(7):725–842, dec. 2010.

[75] A. Kwok and S. Martinez. A distributed deterministic annealing algorithm for limited-range sensor coverage. *Control Systems Technology, IEEE Transactions on*, 19(4):792–804, july 2011.

[76] C. Langbort, R.S. Chandra, and R. D'Andrea. Distributed control design for systems interconnected over an arbitrary graph. *Automatic Control, IEEE Transactions on*, 49(9):1502–1519, sept. 2004.

[77] C. Langbort and J. Delvenne. Distributed design methods for linear quadratic control and their limitations. *Automatic Control, IEEE Transactions on*, 55(9):2085–2093, sept. 2010.

[78] C. Langbort and V. Gupta. Minimal interconnection topology in distributed control design. *SIAM Journal on Control and Optimization*, 48(1):397–413, 2009.

[79] A. J. Laub. *Matrix Analysis for Scientists and Engineers*. SIAM, 2005.

[80] S-L. Lee and Y-L. Luo. Eigenvector and eigenvalues of some special graphs. iv. multilevel circulants. *International Journal of Quantum Chemistry*, 41:105–116, 1992.

[81] S. Leirens, C. Zamora, R.R. Negenborn, and B. De Schutter. Coordination in urban water supply networks using distributed model predictive control. In *American Control Conference*, pages 3957–3962, 2010.

[82] N.E. Leonard, D.A. Paley, F. Lekien, R. Sepulchre, D.M. Fratantoni, and R.E. Davis. Collective motion, sensor networks, and ocean sampling. *Proceedings of the IEEE*, 95(1):48–74, jan. 2007.

[83] I. Lestas and G. Vinnicombe. Scalable decentralized robust stability certificates for networks of interconnected heterogeneous dynamical systems. *Automatic Control, IEEE Transactions on*, 51(10):1613–1625, oct. 2006.

[84] Wei Li and C.G. Cassandras. Distributed cooperative coverage control of sensor networks. In *Proceedings of the IEEE Conference on Decision and Control*, pages 2542–2547, dec. 2005.

[85] X. Li, A. Nayak, D. Simplot-Ryl, and I. Stojmenovic. *Sensor Placement in Sensor and Actuator Networks, in Wireless Sensor and Actuator Networks: Algorithms and Protocols for Scalable Coordination and Data Communication (eds A. Nayak and I. Stojmenovic).* John Wiley Sons, Inc., 2010.

[86] Xiaoli Li and Yugeng Xi. Distributed cooperative coverage and connectivity maintenance for mobile sensing devices. In *Proceedings of the IEEE Conference on Decision and Control*, pages 7891–7896, dec. 2009.

[87] J. Liu, A. Gusrialdi, S. Hirche, and A. Monti. Joint controller-communication topology design for distributed wide-area damping control of power systems. In *Proceedings of the 18th IFAC World Congress*, sep. 2011.

[88] J. Liu, A. Gusrialdi, D. Obradovic, and S. Hirche. Study on the effect of time delay on the performance of distributed power grids with networked cooperative control. *1st IFAC Workshop on Estimation and Control of Networked Systems*, pages 168–173, 2009.

[89] P.-L. Liu. Exponential stability for linear time-delay systems with delay dependence. *Journal of the Franklin Institute*, 340(6):481–488, 2003.

[90] T. Liu, D. J. Hill, and J. Zhao. Synchronization of dynamical networks by network control. In *Proceedings of the IEEE Conference on Decision and Control*, pages 1684–1689, dec. 2009.

[91] Y-Y. Liu, J-J. Slotine, and A-L. Barabasi. Controllability of complex networks. *Nature*, 473:167–173, 2011.

[92] J. Lofberg. Yalmip: A toolbox for modelling and optimization in matlab. In *Proceedings of the CACSD*, pages 284–289, dec. 2004.

[93] J. Ma, Z. Y. Dong, and P. Zhang. Eigenvalue sensitivity analysis for dynamic power system. In *International Conference on Power System Technology*, pages 1–7, dec. 2006.

[94] Mehdi Maasoumy Haghighi. Modeling and optimal control algorithm design for hvac systems in energy efficient buildings. Master's thesis, EECS Department, University of California, Berkeley, Feb 2011.

[95] J. Machowski, J. Bialek, and Jim Dr Bumby. *Power System Dynamics : Stability and Control*. Wiley, 2008.

[96] K. Martensson and A. Rantzer. Gradient methods for iterative distributed control synthesis. In *Proceedings of the IEEE Conference on Decision and Control*, pages 549–554, dec. 2009.

[97] S. Martinez, J. Cortes, and F. Bullo. Motion coordination with distributed information. *IEEE Control Systems Magazine*, 27(4):75–88, aug. 2007.

[98] J. M. McQuade. A system approach to high performance buildings. Technical report, United Technologies Corporation, February 2009.

[99] W. Michiels and S. L. Niculescu. *Stability and stabilization of time-delay systems: an eigenvalue-based approach*. Philadelphia, PA: SIAM, 2007.

[100] Petru-Daniel Morosan, Romain Bourdais, Didier Dumur, and Jean Buisson. Buildingtemperatureregulation using adistributed model predictive control. *Energy and Buildings*, 42(9):1445–1452, 2010.

[101] Petru-Daniel Morosan, Romain Bourdais, Didier Dumur, and Jean Buisson. A dynamic horizon distributed predictive control approach for temperature regulation in multi-zone buildings. In *Control Automation (MED), 2010 18th Mediterranean Conference on*, pages 622–627, june 2010.

[102] N. Motee and A. Jadbabaie. Optimal control of spatially distributed systems. *Automatic Control, IEEE Transactions on*, 53(7):1616–1629, aug. 2008.

[103] H. Mukaidani, S. Sakaguchi, Y. Ishii, and T. Tsuji. Bmi-based neurocontroller for state-feedback guaranteed cost control of discrete-time uncertain system. In *Proceedings of the IEEE International Symposium on Circuits and Systems*, pages 3055–3058, sep. 2005.

[104] S. Mullender. *Distributed Systems*. Addison-Wesley, 1993.

[105] R. R. Nagenborn, P. J. Overloop, T. Keviczky, and B. De Schutter. Distributed model predictive control of irrigation canals. *Networks and Heterigeneous Media*, 4(2):359–380, jan. 2009.

[106] T. Namerikawa and T. Kato. Distributed load frequency control of electrical power networks via iterative gradient methods. In *Proceedings of the IEEE Conference on Decision and Control and European Control Conference*, pages 7723–7728, dec. 2011.

[107] H. Ni, G. Heydt, and L. Mili. Power system stability agents using robust wide area control. *IEEE Transactions on Power Systems*, 17(4):1123–1131, 2002.

[108] R. Olfati-Saber and R. M. Murray. Consensus and cooperation in networked multi-agent systems. *Proceedings of the IEEE*, 95(1):215–233, jan. 2007.

[109] Singh. L. P. *Advanced Power System Analysis and Dynamics*. New Age International, 1983.

[110] P. R. Pagilla, N. B. Siraskar, and R. V. Dwivedula. Decentralized control of web processing lines. *IEEE Transactions on Control Systems Technology*, 15(1):106–117, 2007.

[111] D.A. Paley, F. Zhang, and N.E. Leonard. Cooperative control for ocean sampling: The glider coordinated control system. *IEEE Transactions on Control Systems Technology*, 16(4):735–744, july 2008.

[112] A.G. Phadke and J.S. Thorp. *Synchronized Phasor Measurements and Their Applications*. Springer, 2008.

[113] L. Pimenta, V. Kumar, R.C. Mesquita, and G. Pereira. Sensing and coverage for a network of heterogeneous robots. In *Proceedings of the IEEE Conference on Decision and Control*, pages 3947–3952, dec. 2008.

[114] S. Poduri and G.S. Sukhatme. Constrained coverage for mobile sensor networks. In *Proceedings of the IEEE International Conference on Robotics and Automation*, pages 165–171, 2004.

[115] M. Rafiee and A. M. Bayen. Optimal network topology design in multi-agent systems for efficient average consensus. In *Proceedings of the IEEE Conference on Decision and Control*, pages 3877–3883, dec. 2010.

[116] A. Rantzer. Dynamic dual decomposition for distributed control. In *Proceedings of American Control Conference*, pages 884–888, june 2009.

[117] A. Rantzer. Distributed control of positive systems. *ArXiv e-prints*, February 2012.

[118] Wei Ren, R.W. Beard, and E.M. Atkins. Information consensus in multivehicle cooperative control. *IEEE Control Systems Magazine*, 27(2):71–82, april 2007.

[119] N. Rostamkolai, A.G. Phadke, W.F. Long, and J.S. Thorp. An adaptive optimal control strategy for dynamic stability enhancement of ac/dc power systems. *IEEE Transactions on Power Systems*, 3(3):1139–1145, 1988.

[120] M. Rotkowitz and S. Lall. A characterization of convex problems in decentralized control. *IEEE Transactions on Automatic Control*, 51(2):1984–1996, 2006.

[121] S Schuler, P. Li, and F. Allgöwer. Design of structured dynamic output-feedback controllers for interconnected systems. *International Journal of Control*, 84(12):2081–2091, 2011.

[122] S. Schuler, W. Zhou, U. Munz, and F. Allgower. Controller structure design for decentralized control of coupled higher order subsystems. In *2nd IFAC Workshop on Estimation and Control of Networked Systems*, pages 269–274, dec. 2010.

[123] Michael Schuresko and Jorge Cortés. Distributed tree rearrangements for reachability and robust connectivity. In *Proceedings of the 12th International Conference on Hybrid Systems: Computation and Control*, HSCC '09, pages 470–474, Berlin, Heidelberg, 2009. Springer-Verlag.

[124] M. Schwager, F. Bullo, D. Skelly, and D. Rus. A ladybug exploration strategy for distributed adaptive coverage control. In *Proceedings of the International Conference on Robotics an Automation (ICRA 08)*, pages 2346–2353, May 19–23 2008.

[125] Mac Schwager, Daniela Rus, and Jean-Jacques Slotine. Unifying geometric, probabilistic, and potential field approaches to multi-robot deployment. *The International Journal of Robotics Research*, 30(3):371–383, 2011.

[126] S. P. Sethi and Q. Zhang. Near optimization of dynamic systems by decomposition and aggregation. *J. Optim. Theory Appl.*, 99:1–22, October 1998.

[127] M. E. Sezer and D. D. Silijak. Nested ϵ-decompositions and clustering of complex systems. *Automatica*, 22:321–332, May 1986.

[128] S.Y. Shafi, M. Arcak, and L. El Ghaoui. Designing node and edge weights of a graph to meet laplacian eigenvalue constraints. In *Communication, Control, and Computing (Allerton), 2010 48th Annual Allerton Conference on*, pages 1016–1023, 29 2010-oct. 1 2010.

[129] P. Shah and P.A. Parrilo. A partial order approach to decentralized control. In *Proceedings of the 47th IEEE Conference on Decision and Control*, pages 4351–4356, dec. 2008.

[130] P. Shah and P.A. Parrilo. h_2-optimal decentralized control over posets: A state space solution for state-feedback. In *Proceedings of the 49th IEEE Conference on Decision and Control*, pages 6722–6727, dec. 2010.

[131] I. Shames and A. Bishop. Link operations for slowing the spread of disease in complex networks. *Europhysics Letters*, 95:18005, 2011.

[132] Vijendra Siddhi. A generalized approach for calculation of the eigenvector sensitivity for various eigenvector normalizations. Master's thesis, University of Missouri, Columbia, USA, 2005.

[133] A.F. Snyder, D. Ivanescu, N. HadjSaid, D. Georges, and T. Margotin. Delayed-input wide-area stability control with synchronized phasor measurements and linear matrix inequalities. *IEEE Power Engineering Society Summer Meeting*, 2:1009–1014, 2000.

[134] S. Sojoudi and A. G. Aghdam. Overlapping control systems with optimal information exchange. *Automatica*, 45:1176–1181, 2009.

[135] H. Sun and J. Zhao. Decentralized hybrid feedback stabilization for a class of switched composite system. *Acta Automatica Sinica*, 29(1):149–153, 2003.

[136] J. Swigart and S. Lall. A graph-theoretic approach to distributed control over networks. In *Proceedings of the 48th IEEE Conference on Decision and Control and the 28th Chinese Control Conference*, pages 5409–5414, 2009.

[137] A.S.M. Vamsi and N. Elia. Design of distributed controllers realizable over arbitrary directed networks. In *Proceedings of the 49th IEEE Conference on Decision and Control*, pages 4795–4800, dec. 2010.

[138] N. P. Van Der AA, H. G. ter Morsche, and R. R. M. Mattheij. Computation of eigenvalue and eigenvector derivatives for a general complex-valued eigensystem. *Electric Journal of Linear Algebra*, 16:300–314, 2007.

[139] P. G. Voulgaris, G. Bianchini, and B. Bamieh. Optimal h_2 controllers for spatially invariant systems with delayed communication requirements. *Systems Control Letters*, 50:347–361, 2003.

[140] J. Wagenpfeil, A. Trachte, T. Hatanaka, M. Fujita, and O. Sawodny. Distributed decision making for task switching via a consensus-like algorithm. In *Proceedings of American Control Conference*, pages 5761–5766, june 2009.

[141] Yue Wang and I.I. Hussein. Cooperative vision-based multi-vehicle dynamic coverage control for underwater applications. In *Proceedings of the IEEE International Conference on Control Applications*, pages 82–87, oct. 2007.

[142] H. S. Witsenhausen. A counterexample in stochastic optimum control. *SIAM Journal of Control*, 6(1):131–147, 1968.

[143] B. Wu and Om P. Malik. Multivariable adaptive control of synchronous machines in a multimachine power system. *IEEE Transactions on Power Systems*, 21(4):1772–1781, 2006.

[144] H. Wu, K. Tsakalis, and G. Heydt. Evaluation of time delay effects to wide-area power system stabilizer design. *IEEE Transactions on Power Systems*, 19(4):1935–1941, 2004.

[145] H. Xin, Z. Qu, J. Seuss, and A. Maknouninejad. A self-organizing strategy for power flow control of photovoltaic generators in a distribution network. *IEEE Transactions on Power Systems*, 26(3):1462–1473, aug. 2011.

[146] M. F. Younis and K. Akkaya. Strategies and techniques for node placement in wireless sensor networks:a survey. *Ad Hoc Networks*, 6(4):621–655, jan. 2009.

[147] A. Zecevic and D. D. Siljak. *Control of Complex Systems: Structural Constraints and Uncertainty (Communication and Control Engineering)*. Springer, 2010.

[148] D. Zelazo and M. Mesbahi. H_2 analysis and synthesis of networked dynamic systems. In *Proceedings of American Control Conference*, pages 2966–2971, june 2009.

[149] D. Zelazo and M. Mesbahi. Edge agreement: Graph-theoretic performance bounds and passivity analysis. *Automatic Control, IEEE Transactions on*, 56(3):544–555, march 2011.

[150] Y. Zhang and A. Bose. Design of wide-area damping controllers for interarea oscillations. *IEEE Transactions on Power Systems*, 23(3):1136–1143, 2008.

[151] M. Zhong and C. G. Cassandras. Distributed coverage control and data collection with mobile sensor networks. *IEEE Transactions on Automatic Control*, 56(10):2445–2455, 2011.

[152] G. Zhu and J. Hu. Link resource allocation for maximizing the rigidity of multi-agent formations. In *Proceedings of the IEEE Conference on Decision and Control and European Control Conference*, pages 2920–2925, dec. 2011.